A mathematical and numerical study of some generalizations of the Cahn–Hilliard equation with applications to images and biology.

Hussein Fakih

THÈSE

Pour l'obtention du grade de
DOCTEUR DE L'UNIVERSITÉ DE POITIERS
UFR des sciences fondamentales et appliquées
Laboratoire de mathématiques et applications - LMA (Poitiers)
(Diplôme National - Arrêté du 7 août 2006)

École doctorale : Sciences et ingénierie pour l'information, mathématiques - S2IM (Poitiers)
Secteur de recherche : Mathématiques et leur interactions

Présentée par :
Hussein Fakih

Étude mathématique et numérique de quelques généralisations de l'équation de Cahn-Hilliard : applications à la retouche d'images et à la biologie

Directeur(s) de Thèse :
Alain Miranville, Laurence Cherfils

Soutenue le 02 octobre 2015 devant le jury

Jury :

Président	**Danielle Hilhorst**	Directrice de recherche CNRS, Université Paris-Sud, Orsay
Rapporteur	**Maurizio Grasselli**	Professore, Politecnique di Milano, Italie
Rapporteur	**Andrea L. Bertozzi**	Professor, University of California, Los Angeles
Membre	**Alain Miranville**	Professeur des Universités, Université de Poitiers
Membre	**Laurence Cherfils**	Maître de conférences, Université de La Rochelle
Membre	**Morgan Pierre**	Maître de conférences, Université de Poitiers
Membre	**Jean-Paul Chehab**	Professeur des Universités, Université de Picardie Jules Vernes
Membre	**Zakaria Belhachmi**	Professeur des Universités, Université de Haute Alsace

Pour citer cette thèse :
Hussein Fakih. *Étude mathématique et numérique de quelques généralisations de l'équation de Cahn-Hilliard : applications à la retouche d'images et à la biologie* [En ligne]. Thèse Mathématiques et leur interactions. Poitiers : Université de Poitiers, 2015. Disponible sur Internet <http://theses.univ-poitiers.fr>

THESE

Pour l'obtention du grade de
DOCTEUR DE L'UNIVERSITE DE POITIERS

École Doctorale Sciences et Ingénierie pour l'Information, Mathématiques

Diplôme National - Arrêté du 6 Août 2006
SPECIALITE : Mathématique

Présentée par

Hussein FAKIH

Étude mathématique et numérique de quelques généralisations de l'équation de Cahn-Hilliard : Applications à la retouche d'images et à la biologie

Directeur de Thèse : **Alain MIRANVILLE**

Co-Directrice : **Laurence CHERFILS**

Présentée et soutenue publiquement le
02 Octobre 2015

COMPOSITION DU JURY

Rapporteurs :	Andrea L. Bertozzi	Professeur, University of California Los Angeles
	Maurizio Grasselli	Professeur, Politecnico di Milano
Examinateurs :	Zakaria Belhachmi	Professeur, Université de Haute Alsace
	Jean-Paul Chehab	Professeur, Universite de Picardie Jules Verne
	Laurence Cherfils	Maître de conférence, Université de La Rochelle (Co-Directrice)
	Danielle Hilhorst	Directrice de recherche CNRS, Université Paris-Sud, Orsay
	Alain Miranville	Professeur, Université de Poitiers (Directeur)
	Morgan Pierre	Maître de conférence, Université de Poitiers

Thèse préparée au sein du Laboratoire de Mathématiques et Applications

Remerciements

Je remercie la Région Poitou-Charentes pour avoir financé cette thèse dans le cadre d'un contrat doctoral.

Mes remerciement sont, bien entendu, déstinés à Alain Miranville et Laurence Cherfils. Ils m'ont proposé un très bon sujet de thèse, intéressant tant du point de vue mathématique que de celui des applications, et m'ont donné une grande liberté dans la façon de l'aborder. Je leur en suis extrêmement reconnaissant.

En outre, ils ont toujours été disponibles pour répondre à mes questions, m'aider ou me réconforter et me destresser. Par ailleurs, il est très rare dans la vie de rencontrer des personnes ayant la gentillesse que l'on trouve chez Alain et Laurence. Ainsi, j'ai eu la chance, l'honneur et la fierté d'être encadré par eux. Je vous remercie chaleureusement pour tout.

Je voudrais aussi remercier les Professeurs Andrea Bertozzi et Maurizo Grasselli pour avoir eu l'extrême gentillesse d'être rapporteurs de cette thèse. Je suis en particulier très heureux que le Professeur Andrea Bertozzi ait accepté de rapporter ce travail, qui fait, en partie, suite à ses travaux pionniers sur les applications de l'équation de Cahn–Hilliard en retouche d'images. Son avis sur cette thèse m'est très précieux. Je remercie également Zakaria Belhachmi, Jean-Paul Chehab, Danielle Hilhorst, et Morgan Pierre pour avoir accepté de faire partie de mon jury.

Je tiens à remercier tous les membres du Laboratoire de Mathématiques et Applications qui ont contribué à créer une ambiance conviviale et un cadre de travail agréable. Je remercie en particulier le directeur du laboratoire Pol Vanhaecke, le directeur de l'école doctorale Samuel Boissière, l'ancien directeur de l'école doctorale Pierre Torasso et le Professeur Abderrazak Bouaziz pour leur excellent accueil et leur écoute.

J'en profite également pour remercier tous mes enseignants de l'université Libanaise. Je remercie en particulier le Professeur Raafat Talhouk, le directeur du laboratoire de mathématiques à l'université Libanaise ; il m'a été d'un excellent conseil afin d'éffectuer cette thèse.

Je souhaite également remercier les personnels dont la bonne humeur constante est un plaisir quotidien : Brigitte Brault au secrétariat, Nathalie Mongin à la comptabilité, Nathalie Marlet à la bibliothèque, Jocelyne Attab à la bibliothèque et à l'infographie et Benoît Métrot au service informatique.

Je tiens aussi à remercier Mme Barbara Mérigeault, Mme Sylvie Perez, Mme Alicia Lecesve, Mme Nathalie Fofana et Mme Marie-Thérèse Péguin pour tous les services rendus.

À tous mes amis Docteurs ou futurs docteurs du laboratoire, je vous dit également merci.

Enfin, je remercie mes parents pour leur amour et pour avoir toujours été présents en me donnant tous le soutien et les encouragements nécessaires. Merci également à mon frère et mes soeurs pour leur affection. Je termine en remerciant tous les autres membres de ma famille et mes proches pour leurs encouragements.

Résumé : Cette thèse se situe dans le cadre de l'analyse théorique et numérique de quelques généralisations de l'équation de Cahn–Hilliard. On étudie l'existence, l'unicité et la régularité de la solution de ces modèles ainsi que son comportement asymptotique en terme d'existence d'un attracteur global de dimension fractale finie. La première partie de la thèse concerne des modèles appliqués à la retouche d'images. D'abord, on étudie la dynamique de l'équation de Bertozzi–Esedoglu–Gillette–Cahn–Hilliard avec des conditions de type Neumann sur le bord et une nonlinéarité régulière de type polynomial et on propose un schéma numérique avec une méthode de seuil efficace pour le problème de la retouche et très rapide en terme de temps de convergence. Ensuite, on étudie ce modèle avec des conditions de type Neumann sur le bord et une nonlinéarité singulière de type logarithmique et on donne des simulations numériques avec seuil qui confirment que les résultats obtenus avec une nonlinéarité de type logarithmique sont meilleurs que ceux obtenus avec une nonlinéarité de type polynomial. Finalement, on propose un modèle basé sur le système de Cahn–Hilliard pour la retouche d'images colorées. La deuxième partie de la thèse est consacrée à des applications en biologie et en chimie. On étudie la convergence de la solution d'une généralisation de l'équation de Cahn–Hilliard avec un terme de prolifération, associée à des conditions aux limites de type Neumann et une nonlinéarité régulière. Dans ce cas, on démontre que soit la solution explose en temps fini soit elle existe globalement en temps. Par ailleurs, on donne des simulations numériques qui confirment les résultats théoriques obtenus. On termine par l'étude de l'équation de Cahn–Hilliard avec un terme source et une nonlinéarité régulière. Dans cette étude, on considère le modèle à la fois avec des conditions aux limites de type Neumann et de type Dirichlet.
Mots clés : Equation de Cahn–Hilliard, retouche d'images, croissance tumorale, problème bien posé, explosion en temps fini, attracteur global, attracteur exponentiel, simulations.

Abstract : This thesis is situated in the context of the theoretical and numerical analysis of some generalizations of the Cahn–Hilliard equation. We study the well-possedness of these models, as well as the asymptotic behavior in terms of the existence of finite-dimenstional (in the sense of the fractal dimension) attractors. The first part of this thesis is devoted to some models which, in particular, have applications in image inpainting. We start by the study of the dynamics of the Bertozzi–Esedoglu–Gillette–Cahn–Hilliard equation with Neumann boundary conditions and a regular nonlinearity. We give numerical simulations with a fast numerical scheme with threshold which is sufficient to obtain good inpainting results. Furthermore, we study this model with Neumann boundary conditions and a logarithmic nonlinearity and we also give numerical simulations which confirm that the results obtained with a logarithmic nonlinearity are better than the ones obtained with a polynomial nonlinearity. Finally, we propose a model based on the Cahn–Hilliard system which has applications in color image inpainting. The second part of this thesis is devoted to some models which, in particular, have applications in biologie and chemistry. We study the convergence of the solution of a Cahn–Hilliard equation with a proliferation term and associated with Neumann boundary conditions and a regular nonlinearity. In that case, we prove that the solutions blow up in finite time or exist globally in time. Furthermore, we give numericial simulations which confirm the theoritical results. We end with the study of the Cahn–Hilliard equation with a mass source and a regular nonlinearity. In this study, we consider both Neumann and Dirichlet boundary conditions.
Keywords : Cahn–Hilliard equation, image inpainting, tumor growth, well-possedness, blow up, global attractor, exponential attractor, simulations.

Table des matières

Table des matières v

Introduction générale 1

1 Sur l'équation de Cahn–Hilliard . . . 3
1.1 Origine . . . 3
1.2 Conditions aux limites et conservation de la masse . . . 5
1.3 Potentiel . . . 6
2 Problématique . . . 8
2.1 Le cas $g(x,u) = 0$: . . . 8
2.2 Le cas $g(x,u) = \varepsilon u$ ($\varepsilon > 0$) : . . . 9
2.3 Le cas $g(x,u) = \lambda_0 \chi_{\Omega\setminus D}(x)(u-h)$ ($\lambda_0 > 0$) : . . . 9
2.4 Le cas $g(x,u) = \alpha u(u-1)$ ($\alpha > 0$) : . . . 10
2.5 Le cas $g(x,u) = g(u)$: . . . 10
3 Contributions . . . 10
3.1 Première partie : la retouche d'images . . . 10
3.2 Deuxième partie : applications à la biologie et à la chimie . . . 14

I Généralisation de l'équation de Cahn–Hilliard en retouche d'images 19

1 Finite-dimensional attractors for the Bertozzi–Esedoglu–Gillette–Cahn–Hilliard equation in image inpainting 21
1.1 Introduction . . . 24
1.2 Setting of the problem . . . 25
1.3 A priori estimates . . . 27
1.4 Further a priori estimates . . . 30
1.5 Existence of the global attractor . . . 34
1.6 Existence of exponential attractors . . . 36
1.7 Numerical simulations . . . 40
1.7.1 Inpainting of a triangle . . . 41
1.7.2 Inpainting of four 3/4 circles . . . 42

2 On the Bertozzi–Esedoglu–Gillette–Cahn–Hilliard equation with logarithmic nonlinear terms **45**
2.1 Introduction . . . 47
2.2 Setting of the problem . . . 49
2.3 A priori estimates . . . 52
2.4 A local existence result . . . 57
2.5 Numerical simulations . . . 59
2.5.1 Inpainting of a triangle . . . 59
2.5.2 Inpainting of a bar . . . 60
2.5.3 Inpainting of a four circles . . . 60

3 A Cahn–Hilliard system with a fidelity term for color image inpainting **67**
3.1 Introduction . . . 69
3.2 Proposed model and setting of the problem . . . 71
3.3 A priori estimates . . . 77
3.4 Well-posedness and existence of the global attractor . . . 80
3.5 Existence of exponential attractors . . . 84
3.6 Algebraic consistency with the two-phase model . . . 87
3.7 Numerical simulations . . . 88
3.7.1 Three colors inpainting . . . 89
3.7.2 Nine colors inpainting . . . 89
3.7.3 Text inpainting . . . 89
3.7.4 Consistency with the two-phase model example . . . 90

II Généralisations de l'équation de Cahn–Hilliard en biologie et en chimie **93**

4 A Cahn–Hilliard equation with a proliferation term for biological and chemical applications **95**
4.1 Introduction . . . 97
4.2 A chemisorbed overlayer and tumor growth model . . . 100
4.3 A general tumor growth model . . . 110
4.4 Numerical results . . . 119
4.4.1 The case when $g(s) = \alpha s^2 + \beta s + \gamma$. . . . 119
4.4.2 The case when $g(s) = 2\beta s - \beta s^2(s-1)^2$. . . . 120

5 Asymptotic behavior of a generalized Cahn–Hilliard equation with a mass source **127**
5.1 Introduction . . . 129
5.2 Neumann boundary conditions . . . 131
5.2.1 A priori estimates . . . 133

5.2.2 The dissipative semigroup . . . 139
5.2.3 Existence of exponential attractors . . . 141
5.3 Dirichlet boundary conditions . . . 147
5.4 Numerical simulations . . . 150
5.4.1 Dirichlet case . . . 151
5.4.2 Neumann case . . . 151

Conclusion générale et perspectives **155**

Annexes **156**

A Modèles pour la retouche d'images **157**
A.1 Définition et origine de la retouche d'images . . . 157
A.2 Travail pionnier en retouche images . . . 158
A.3 Quelques modèles appliqués à la retouche d'images . . . 160
A.3.1 Applications de l'équation de Navier–Stokes à la retouche d'images 160
A.3.2 Retouche d'images par la variation totale de la diffusion anisotrope : diffusion axée sur la courbure . . . 162
A.3.3 Modèles en retouche basés sur l'énergie de Mumford–Shah . . . 165
A.3.4 Modèles en retouche basés sur l'énergie de Ginzburg–Landau . . . 168

B The Cahn–Hilliard equation as a gradient flow **175**
B.1 Some definitions and properties of the dual of H^1 with Neumann boundary conditions . . . 175
B.2 Gradient Flow in $\dot{H}^{-1}(\Omega)$ . . . 177

C Full proofs of Theorems 7 and 8 in Chapter 5 **181**
C.1 A priori estimates . . . 182
C.2 The dissipative semigroup . . . 187
C.3 Existence of exponential attractors . . . 188
C.4 More regular exponential attractors . . . 192

D Numerical Algorithms and results in image inpainting **199**
D.1 Operator splitting scheme with threshold . . . 199
D.2 Convexity splitting scheme . . . 200
D.3 Comparison between Scheme 1 and Scheme 3 . . . 202
D.4 Comparison between regular nonlinearities and singular nonlinearities . . . 205
D.5 Dynamics of solutions with different values of λ_0 . . . 208
D.6 Inpainting in 3D with scheme 1 . . . 209
D.7 Comparison between binary inpainting results with Scheme 1 and Scheme 2 ($n = 2$) . . . 210
D.8 Binary inpainting image applications with Scheme 2 ($n = 2$) . . . 210
D.9 Numerical results with mesh adaptation for color image inpainting . . . 211
D.10 Consistency with three and four phase-model examples . . . 211

Bibliographie **221**

Introduction générale

1 Sur l'équation de Cahn–Hilliard

1.1 Origine

La décomposition spinodale est un phénomène qui décrit la séparation de deux alliages métalliques. En effet, quand on chauffe un mélange de deux métaux (par exemple, Or et Nickel) à une température très élevée et qu'on le refroidit à une température faible, une séparation de l'alliage peut se produire. Cette séparation de l'alliage métallique est appelée décomposition spinodale.

Par ailleurs, la décomposition spinodale est un processus par lequel un mélange de deux constituants ou plus peut être séparé en régions distinctes avec des concentrations des matériaux différentes. Ce processus diffère de la nucléation puisque la séparation de phase, qui est due à la décomposition spinodale, se produit à travers tout le matériau, et non seulement au niveau des sites de nucléation.

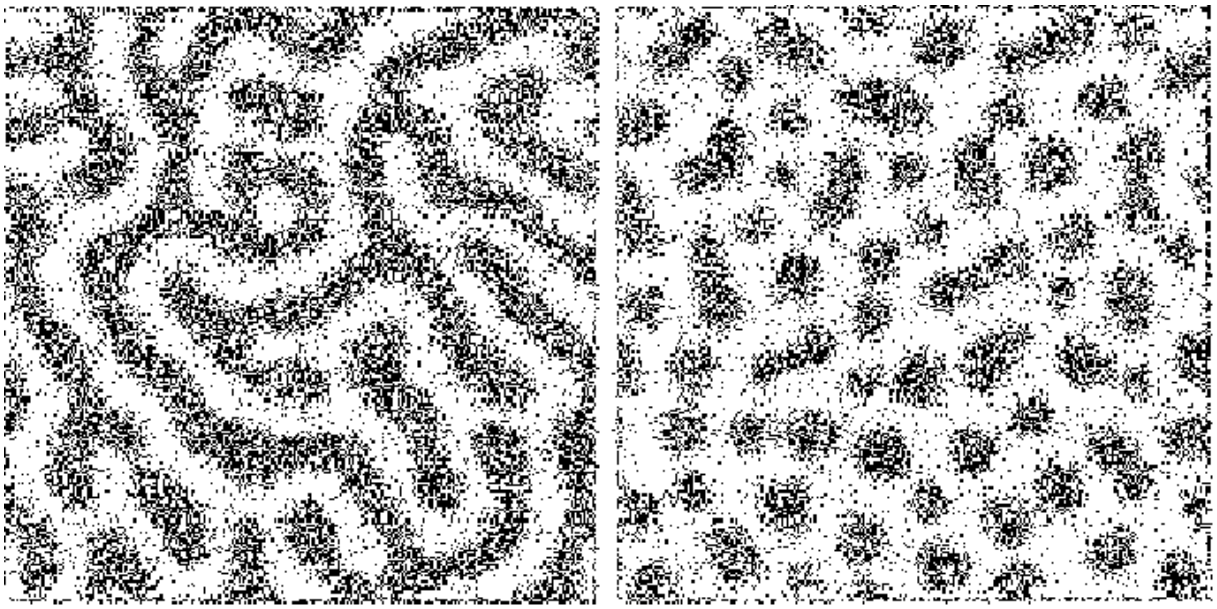

FIGURE 1 – Cet exemple montre la différence entre décomposition spinodale (à gauche) et nucléation (à droite). Figure de [71].

John Cahn et John Hilliard ont proposé en 1958 dans [27] un modèle chimique de la séparation d'un alliage métallique donné par l'énergie suivante :

$$\mathcal{F}(c) = \int_\Omega (F(c) + \frac{\varepsilon^2}{2}|\nabla c|^2)dx, \tag{1}$$

où c est la concentration du matériau, $F(c)$ est la densité d'énergie libre du matériau, $\varepsilon|\nabla c|^2$ est la densité d'énergie libre additionnelle si le matériau est en gradient de composition (c'est-à-dire,

dans une transition entre deux états stables C_A et C_B) et ε représente l'épaisseur de l'interface diffuse. L'énergie (1) est appelée énergie de Ginzburg–Landau ou énergie de Cahn–Hilliard.

La variation formelle de l'énergie (1) par rapport à un champ c qui s'annule sur le bord $\partial\Omega$ est donnée par

$$\partial\mathcal{F}(c) = \int_\Omega [f(c) - \varepsilon^2\Delta c]dcdv, \tag{2}$$

où $f(c) = F'(c)$ et $\Omega \subset \mathbb{R}^N,\ N \leq 3$, est le domaine occupé par le matériau. On obtient l'expression suivante :

$$\frac{\partial\mathcal{F}}{\partial c} = f(c) - \varepsilon^2\Delta c, \tag{3}$$

pour la dérivée variationnelle, sachant que l'équilibre est obtenu lorsque (3) disparaît (c'est-à-dire, $\frac{\partial\mathcal{F}}{\partial c} = 0$) ; l'hypothèse sur laquelle repose la dérivation standard est que la relaxation vers l'équilibre est régie, à l'aide d'un paramètre $\alpha > 0$, par la relation

$$\alpha\frac{\partial c}{\partial t} = -\frac{\partial\mathcal{F}}{\partial c}. \tag{4}$$

Ainsi, en combinant les équations (3) et (4), on obtient l'équation de Ginzburg–Landau ou l'équation de Allen–Cahn :

$$\alpha\frac{\partial c}{\partial t} - \varepsilon^2\Delta c + f(c) = 0. \tag{5}$$

Pour plus de détails, le lecteur peut consulter les références [3, 95].

D'autre part, on a la relation

$$h = -M\nabla\Big(\frac{\partial\mathcal{F}}{\partial c}\Big) = -M\nabla\mu, \tag{6}$$

où h est le flux de masse et M représente la mobilité (on suppose ici que M est une constante strictement positive). En outre, $\mu = \frac{\partial\mathcal{F}}{\partial c}$ est appelé potentiel chimique. Enfin, le bilan de masse est donné par

$$\frac{\partial c}{\partial t} = -\nabla.h. \tag{7}$$

Par conséquent, la combinaison des équations (3), (6), et (7) permet d'aboutir à l'équation de Cahn–Hilliard :

$$\frac{\partial c}{\partial t} = M\Delta\mu = M\Delta(-\varepsilon^2\Delta c + f(c)). \tag{8}$$

Pour plus de détails, voir [26, 85] et voir aussi [27, 41, 56, 92, 96, 99, 100, 117].

L'équation de Cahn–Hilliard s'acrère pertinentepour la modèlisation de nombreux phénomènes pour lesquels la séparation de phase et des processus d'agrégation et de coalescence peuvent être observés. On peut citer, par exemple, la dynamique de populations (voir [45]), les films bactériens (voir [91]), la cicatrisation de plaies et la croissance tumorale (voir [42], [88], [104] et [64]), les films minces (voir [123] et [138]), le traitement d'images et la retouche d'images (voir [16], [17], [25], [29], [38], [39], [40] et [51]), les anneaux de Saturne (voir [139]) et même l'agrégation de moules (voir [98]).

1.2 Conditions aux limites et conservation de la masse

L'équation de Cahn–Hilliard est en général associée à des conditions aux limites de type Neumann homogène ou périodiques. Les conditions au bord de type Neumann homogène de l'équation de Cahn–Hilliard sont données par

$$\frac{\partial c}{\partial \nu} = 0, \quad \text{sur } \Gamma, \tag{9}$$

$$\frac{\partial \mu}{\partial \nu} = 0, \quad \text{sur } \Gamma, \tag{10}$$

où ν est la normale unitaire extérieure.

En supposant que $\Omega = \prod_{i=1}^{n}]0, L_i[$, $L_i > 0$, les conditions aux limites périodiques au bord pour l'équation de Cahn–Hilliard s'écrivent sous la forme suivante :

$$\varphi|_{x_i=0} = \varphi|_{x_i=L_i}, \quad i = 1, ..., n, \tag{11}$$

pour c et les dérivées de c jusqu'à l'ordre 3.
La condition aux limites (9) est appelée condition aux limites variationelle et la condition aux limites (10) est appelée condition aux limites de non-flux (d'après l'équation (6)). Enfin, (9)–(10) s'écrivent de manière équivalente

$$\frac{\partial c}{\partial \nu} = \frac{\partial \Delta c}{\partial \nu} = 0, \quad \text{sur } \Gamma. \tag{12}$$

L'intérêt d'utiliser les conditions aux limites (12) (ou (11)) réside non seulement dans la décroissance de l'énergie $\mathcal{F}$ mais aussi dans la conservation totale de la masse, c'est-à-dire

$$\frac{d}{dt} \int_\Omega c dx = 0, \tag{13}$$

ce qui signifie que

$$\int_\Omega c(t) dx = \int_\Omega c(0) dx = \xi \qquad \forall t \geq 0, \tag{14}$$

où ξ est une constante et $c(0)$ représente la concentration initiale à $t = 0$.

Par ailleurs, l'équation de Cahn–Hilliard peut être associée dans certains cas à des conditions aux limites de type Dirichlet,

$$c = c_b, \quad \text{sur } \Gamma, \tag{15}$$

$$\mu = \mu_b, \quad \text{sur } \Gamma, \tag{16}$$

où c_b et μ_b sont des constantes. Pour plus de détails, le lecteur peut consulter les références [8] et [12].

Un autre type de conditions aux limites consiste en des conditions dynamiques au bord. Dans ce cas, on considère l'énergie libre surfacique

$$\mathcal{F}_\Gamma(c) = \int_\Omega \Big(G(c) + \frac{\varepsilon_\Gamma^2}{2} |\nabla_\Gamma c|^2 \Big) dx, \tag{17}$$

où $\varepsilon_\Gamma > 0$, ∇_Γ est le gradient surfacique, et $G(c)$ est le potentiel surfacique. On obtient alors

$$\frac{\partial c}{\partial t} = \varepsilon_\Gamma^2 \Delta_\Gamma c - g(c) - \frac{\partial c}{\partial \nu}, \quad \text{sur } \Gamma, \tag{18}$$

où Δ_Γ est l'opérateur de Laplace–Beltrami sur le bord Γ et $g = G'$. L'équation de Cahn–Hilliard avec des conditions aux limites dynamiques est utilisée pour :

- L'influence des parois pour les systèmes confinés ;
- Les mélanges de polymères ;
- Des application technologiques.

Pour plus de détails, voir [41, 44, 69, 109, 110, 126, 127, 146].

1.3 Potentiel

Dans le traitement mathématique du problème, on utilise habituellement la variable $c(x) = c_A(x) - c_B(x)$ appelée paramètre d'ordre, de sorte que $c : \Omega \to [-1, 1]$ (A et B sont les 2 constituants).

Tout d'abord, on rappelle que la fonction F (définie dans l'énergie (1)) est une fonction positive qui admet deux puits correspondant aux phases du matériau. Un potentiel thermodynamique F est la fonction logarithmique suivante :

$$F(s) = K_B T_c (1 - s^2) + K_B T \Big[(1 - s) \ln\Big(\frac{1 - s}{2}\Big) + (1 + s) \ln\Big(\frac{1 + s}{2}\Big) \Big], \quad s \in]-1, 1[,$$

où K_B est la constante de Boltzmann, T est la température absolue et T_c une température critique. A partir de cette description, on remarque que T_c joue un rôle essentiel dans le processus :

- Si $T \geq T_c$, le comportement est trivial puisque F présente un minimum global pour $c = 0$, et donc la minimisation de (1) est obtenue avec une distribution homogène $c(x) = 0, \ \forall x \in \Omega$.
- Si $T < T_c$, F a deux minimas (double-puits).

On peut facilement montrer que remplacer F par λF, $\lambda > 0$ constante, n'influence pas la description du problème. Ainsi, l'équation (1) reste inchangée si F est exprimée comme suit :

$$F(s) = \frac{\theta_c}{2}(1 - s^2) + \frac{\theta}{2} \Big[(1 - s) \ln\Big(\frac{1 - s}{2}\Big) + (1 + s) \ln\Big(\frac{1 + s}{2}\Big) \Big], \quad s \in]-1, 1[, \ \ 0 < \theta < \theta_c, \tag{19}$$

c'est-à-dire

$$f(s) := F'(s) = -\theta_c s + \frac{\theta}{2} \ln \frac{1 + s}{1 - s}. \tag{20}$$

En général, l'étude de l'équation de Cahn–Hilliard avec un potentiel F singulier (défini dans (19)) est difficile. Par conséquent, ce potentiel est souvent approché par un potentiel régulier (de type polynomial) qui permet d'éviter le fait que $\lim_{|s| \to 1} F(s) = +\infty$,

$$F(s) = \sum_{k=0}^{2p} a_k s^k, \quad a_{2p} > 0, \ p \in \mathbb{N}, \ p \geq 2, \tag{21}$$

c'est-à-dire

$$f(s) = \sum_{i=0}^{2p-1} (i+1) a_{i+1} s^i, \quad a_{2p} > 0. \tag{22}$$

Par exemple, le choix le plus fréquent est

$$F(s) = \frac{1}{4}(s^2 - 1)^2, \tag{23}$$

les minimas -1 et 1 correspondant aux états purs, c'est-à-dire

$$f(s) = s^3 - s. \tag{24}$$

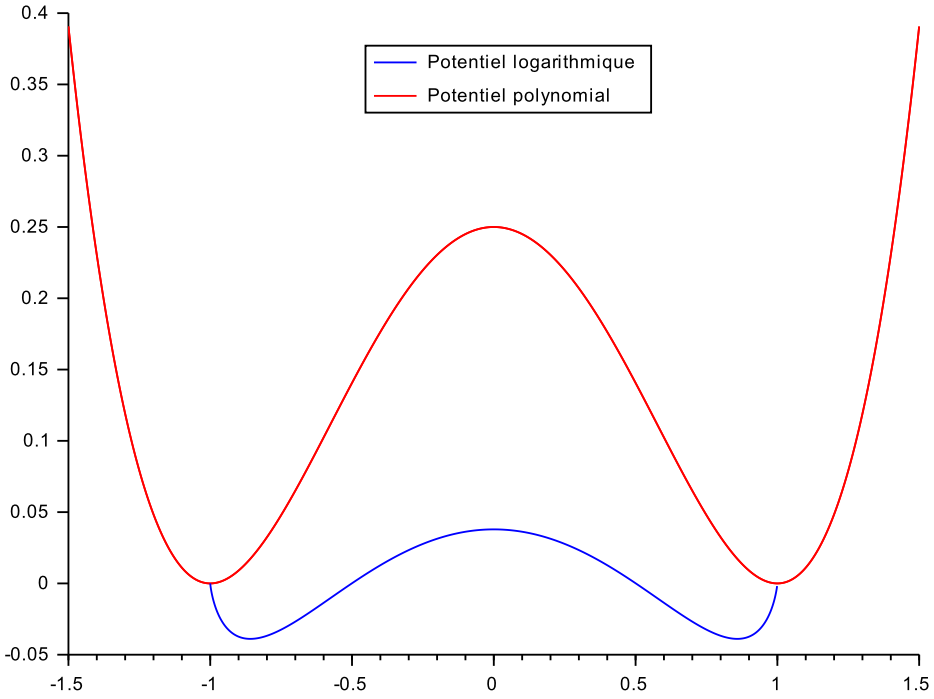

FIGURE 2 – Cet exemple montre la différence entre un potentiel logarithmique (en bleu) et le potentiel polynomial $F(s) = \frac{1}{4}(s^2 - 1)^2$(en rouge).

D'un point de vue physique, le choix de la fonction f pour l'équation de Cahn–Hilliard proposée pour la séparation de phases consiste à avoir trois racines (réelles) a, b, et une valeur intermédiaire $c = \frac{a+b}{2}$. Plus précisément, f doit vérifier

(i) $f(s) = 0$ si et seulement si $s = a, b, c$.

(ii) $f'(s) > 0, \quad s < a^*$ ou $s > b^*$,

(iii) $f'(s) < 0, \quad s \in (a^*, b^*),$

où $a < a^* < c < b^* < b$. Ces trois intervalles intermédiaires sont :
- l'intervalle métastable 1 (a, a^*) ;
- l'intervalle spinodal (a^*, b^*) ;
- l'intervalle métastable 2 (b, b^*).

Finalement, plusieurs auteurs ont considéré l'équation de Cahn–Hilliard avec un potentiel à double obstacle,

$$F(s) = \begin{cases} \frac{1}{2}(1 - s^2) & \text{si } |s| \leq 1, \\ +\infty & \text{si } |s| > 1, \end{cases} \tag{25}$$

qui est équivalent à

$$F(s) = F_0(s) + I_{[-1,1]}(s), \tag{26}$$

où $F_0(s) = \frac{1}{2}(1 - s^2)$ et $I_{[-1,1]}$ représente la fonction indicatrice convexe de $[-1, 1]$ définie par

$$I_{[-1,1]} = \begin{cases} 0 & \text{si } |s| \leq 1, \\ +\infty & \text{si } |s| > 1, \end{cases}$$

d'où

$$f(s) = F_0'(s) + \omega, \qquad \omega \in \partial\vartheta_{[-1,1]}(s), \tag{27}$$

où $\partial\vartheta_{[-1,1]}(s)$ désigne le sous-différentiel de la partie non régulière de F et $\vartheta_{[-1,1]}(s) := \int_\Omega I_{[-1,1]}(s)ds$. Pour plus de détails, voir [120, 121] ; voir également [18, 19].

2 Problématique

On s'intéresse à des modèles en biologie, en chimie, et en retouche d'images qui peuvent s'écrire sous la forme suivante :

$$\frac{\partial u}{\partial t} + \Delta^2 u - \Delta f(u) + g(x, u) = 0. \tag{28}$$

2.1 Le cas $g(x, u) = 0$:

L'équation (28) est l'équation de Cahn–Hilliard introduite dans le premier paragraphe. Cette équation a été beaucoup étudiée, en particulier, l'existence et l'unicité de la solution, l'existence d'un attracteur global de dimension fractale finie, et la convergence vers un état d'équilibre. Quelques travaux traitent le problème avec différents types de conditions aux limites et différents types de nonlinéarités, telles que des conditions aux limites de type Neumann et un potentiel régulier (voir [137] et [114]), des conditions aux limites de type périodique et un potentiel régulier (voir [137]), des conditions aux limites de type Neumann et un potentiel logarithmique (voir [41, 107]), des conditions aux limites de type dynamique et un potentiel logarithmique (voir [41, 76, 109]) et une nonlinéarité de type logarithmique (convergence vers un état d'équilibre) (voir [1]).

2.2 Le cas $g(x,u) = \varepsilon u$ ($\varepsilon > 0$) :

Cette équation est connue comme l'équation de Oono (voir [143]) et a été introduite pour modéliser les interactions longues (non locales). En fait, elle a aussi été introduite pour simplifier les simulations numériques (voir [122]).

Les interactions courtes tendent à homogénéiser le système, tandis que les longues interdisent la formation de grandes structures ; la compétition entre ces deux effets se traduit par la formation d'un état micro-séparé (appelé aussi "super-cristal") avec un paramètre d'ordre modulé spatialement, définissant des structures de taille uniforme.

Par ailleurs, cette équation est un cas particulier du modèle de Cahn–Hilliard non-local (voir [70], [74], et [75]). En effet, le modèle de Cahn–Hilliard non-local est obtenu à partir de l'énergie totale suivante :

$$\mathcal{E}(u) = \int_\Omega \Big[\frac{1}{2}|\nabla u|^2 + F(u)\Big]dx + \int_\Omega \int_\Omega G(x,y)(u(x)-m)(u(y)-m)dxdy,$$

où $m \in \mathbb{R}$ et G est la fonction de Green de l'opérateur "moins Laplacien" $(-\Delta)$ avec la condition de flux nul, c'est-à-dire,

$$-\Delta G(x,y) = \delta(x-y), \quad \text{dans } \Omega.$$

En particulier, l'énergie totale du modèle de Oono (énergie de Cahn–Hilliard–Oono) est donnée par l'énergie suivante :

$$\mathcal{E}(u) = \int_\Omega \Big[\frac{1}{2}|\nabla u|^2 + F(u)\Big]dx + 4\pi\varepsilon \int_\Omega \frac{u(y)u(x)}{|y-x|}dy, \quad \varepsilon > 0.$$

Dans ce cas, si $u(y)$ et $u(x)$ sont de signes opposés, les interactions longues sont répulsives, et la formation d'interfaces est favorisée (voir, par exemple, [143]).

Cette équation est associée aux conditions aux limites de type Neumann. L'existence, l'unicité et la régularité de la solution de cette équation ainsi que l'existence d'un attracteur global de dimension fractale finie, avec un potentiel régulier de type polynomial ont été étudiées dans [103]. Récemment, les auteurs dans [49] ont démontré l'existence globale de la version non-locale de cette équation. Finalement, les auteurs dans [102] ont montré l'existence, l'unicité et les propriétés de séparation de cette équation non-locale avec un potentiel singulier de type logarithmique.

2.3 Le cas $g(x,u) = \lambda_0 \chi_{\Omega\setminus D}(x)(u-h)$ ($\lambda_0 > 0$) :

Cette équation a été proposée par Bertozzi, Esedoglu et Gillette dans [16, 17] pour la retouche d'images binaires (voir l'annexe A). La fonction $h(x)$ représente l'image originale donnée et D un domaine régulier dans Ω ($D \Subset \Omega$) qui représente le domaine à retoucher. L'équation a été proposée dans [16] avec les conditions aux limites de type Neumann. Les auteurs dans [16] ont étudié l'existence, l'unicité et la régularité de la solution de cette équation. De plus, ils ont démontré que pour λ_0 et t très grand ($\lambda_0 \to \infty$), les vecteurs isophotes ($\nabla^\perp$) de u et h sont très proches (et de même direction) sur le bord du domaine à retoucher ∂D (ce dernier résultat est démontré sous les hypothèses $h \in C^2(\Omega)$ et $\partial\Omega \in C^{2,\alpha}$), c'est à dire, pour $\lambda_0 \to \infty$, la solution de l'équation stationnaire de (28) converge vers la solution de l'équation suivante :

$$\Delta\Big(\varepsilon\Delta u - \frac{1}{\varepsilon}f(u)\Big) = 0, \quad \text{dans } D,$$

$$u = h, \quad \text{sur } \partial D,$$
$$\nabla u = \nabla h, \quad \text{sur } \partial D.$$

En outre, l'étude de l'équation stationnaire de (28) a été faite dans [25]. Les auteurs dans [16] et [17] ont introduit un schéma numérique pour ce modèle basé sur la décomposition convexe de l'énergie (voir [60], [61]). Ce schéma s'effectue en deux étapes par rapport à l'épaisseur de l'interface diffuse ε. Tout d'abord, les arêtes se connectent avec une large valeur de ε et ensuite, en remplaçant ε par une valeur très petite, on obtient le résultat final de la retouche. L'analyse numérique de ce schéma a été fait dans [131]. En particulier, le schéma est inconditionnellement stable pour tout pas de temps (sous des conditions sur les constantes ajoutées à l'énergie afin de garder l'énergie comme somme de deux parties telles qu'une partie est convexe et l'autre est concave) et on a la convergence de l'énergie pour ce schéma. Finalement, l'existence globale de ce modèle avec des conditions aux limites de type Dirichlet et un potentiel logarithmique est démontré dans [105].

2.4 Le cas $g(x, u) = \alpha u(u - 1)$ $(\alpha > 0)$:

Cette équation a été proposée dans [88] pour des applications en biologie ; plus précisément, le modèle décrit la cicatrisation de plaies ou la croissance tumorale. Dans ce cas α est la vitesse de prolifération et g est appelé terme de prolifération.

Les auteurs dans [42] ont étudié la convergence de la solution de cette équation quand t tend vers l'infini. En outre, ils ont démontré que soit la solution explose en temps fini, soit elle existe globalement en temps.

2.5 Le cas $g(x, u) = g(u)$:

Cette équation est appliquée en particulier en biologie. Dans le cas où g est régulier de classe C^1 dans un domaine régulier Ω, ce problème avec des conditions aux limites de type Dirichlet a été étudié dans [104], notamment, l'existence, l'unicité et la régularité de la solution ainsi que le comportement asymptotique en termes d'existence de l'attracteur global de dimension fractale finie.

3 Contributions

Les résultats principaux présentés dans cette thèse sont basés sur les articles [38], [39], [40], [63] et [64]. Dans les articles [38], [39] et [40], on étudie des modèles appliqués à la retouche d'images tandis que dans les articles [63] et [64], on étudie des modèles appliqués à la biologie et à la chimie.

3.1 Première partie : la retouche d'images

1. Tout d'abord, on considère le modèle défini sur un domaine borné $\Omega \subset R^N$, $N \leq 3$, suivant :
$$\frac{\partial u}{\partial t} + \varepsilon \Delta^2 u - \frac{1}{\varepsilon} \Delta f(u) + \lambda_0 \chi_{\Omega \setminus D}(x)(u - h) = 0, \tag{29}$$

où $D \Subset \Omega$ représente le domaine à retoucher, $\varepsilon, \lambda_0 > 0$ sont des constantes et $h(x)$ est l'image endommagée. Le terme $\lambda_0 \chi_{\Omega\backslash D}(x)(u-h)$ est appelé terme de fidélité qui est ajouté au modèle afin de garantir que la solution calculée u reste très proche de l'image originale h hors du domaine à retoucher (dans $\Omega\backslash D$). On rappelle que le modèle (29) est proposé par Bertozzi, Esedoglu et Gillette dans [16] et [17].

On associe l'équation (29) à des conditions aux limites de type Neumann de la forme

$$\frac{\partial u}{\partial \nu} = \frac{\partial \Delta u}{\partial \nu} = 0, \quad \text{sur } \Gamma.$$

La nonlinéarité f est la fonction cubique

$$f(s) = s^3 - s,$$

mais, les résultats obtenus restent valables pour toute nonlinéarité polynomiale de dégré impair

$$f(s) = \sum_{i=1}^{2p+1} a_i s^i, \quad a_{2p+1} > 0, \ p \geq 1.$$

On suppose que $h \in L^2(\Omega)$.

La difficulté principale dans ce travail est qu'il n'y a pas la conservation de la masse, (c'est à dire de la moyenne spatiale du paramètre d'ordre), comme c'est le cas dans l'équation originale de Cahn–Hilliard. Afin de remédier à cela, on démontre que la moyenne spatiale de u est dissipative.

On complète les résultats de [16] en montrant que la solution de l'équation (29) est en fait maintenant globale en temps (c'est à dire, on a l'existence de la solution à $t = +\infty$) pour tout $\lambda_0 < +\infty$. On note que pour $\lambda_0 = +\infty$, on a $u = h$ dans $\Omega\backslash D$ et l'équation (29) sur D sera identique à l'équation de Cahn–Hilliard avec des conditions aux limites de type Dirichlet (voir [16]).

De plus, on démontre l'existence d'un attracteur global de dimension finie, c'est à dire, l'existence d'ensembles invariants et compacts qui caractérisent la dynamique globale du problème. Plus précisément, ces ensembles fournissent des informations sur toutes les dynamiques possibles du problème et sont supposées avoir une géométrie complexe ; en particulier, ils contiennent tous les états stationnaires et les orbites hétéroclines. Par ailleurs, la dimension finie signifie, en gros, que même si l'espace de phase initial est de dimension infinie, la dynamique réduite peut être caractérisée par un nombre fini de paramètres.

Finalement, on donne des simulations numériques qui montrent que, dans certaines situations, un schéma à un pas avec seuil par rapport à l'épaisseur de l'interface diffuse ε nous permet de connecter des régions à travers de relativement grands domaines à retoucher. L'idée consiste à choisir une valeur intermédiaire de ε qui est suffisante pour obtenir de bons résultats après le seuillage. Ces simulations sont programmées avec le logiciel FreeFem++ [67, 84]. Elles confirment celles déjà effectuées dans [16] et [17] sur l'efficacité du modèle.

2. Ensuite, on considère la même équation

$$\frac{\partial u}{\partial t} + \varepsilon\Delta^2 u - \frac{1}{\varepsilon}\Delta f(u) + \lambda_0\chi_{\Omega\setminus D}(x)(u-h) = 0, \quad \varepsilon > 0, \ \ \lambda_0 > 0, \tag{30}$$

mais avec une nonlinéarité logarithmique. On note que l'équation originale de Cahn–Hilliard a été proposée avec des termes non linéaire logarithmiques dérivant d'un modèle de champ moyen ; les potentiels non linéaires réguliers sont des approximations de ces termes non linéaires logarithmiques.

On suppose que $h \in L^2(\Omega)$ et

$$\int_{\Omega\setminus D} h dx = 0.$$

De plus, on suppose que

$$f(s) = -\lambda_1 s + \frac{\lambda_2}{2}\ln\frac{1+s}{1-s}, \quad s \in (-1,1).$$

L'équation de Bertozzi–Esedoglu–Gillette–Cahn–Hilliard (30), avec une nonlinéarité logarithmique et des conditions aux limites de type Neumann, semble être bien plus compliquée, du point de vue mathématique, que l'équation de Cahn–Hilliard classique. Nous avons seulement pu démontrer l'existence locale (en temps) de solutions pour une condition initiale u_0 dans $H^1(\Omega)$.

Notons que la difficulté pour montrer l'existence globale du problème est dans le passage à la limite du terme non linéaire $f_N(u^N)$ pour un problème approché. En effet, du fait de la non conservation de la masse, on a besoin d'une estimation sur $\|f_N(u^N) - \langle f_N(u^N)\rangle\|$ et d'une estimation sur $|\langle f_N(u^N)\rangle|$ (pour obtenir une estimation sur $\|f_N(u^N)\|$), tandis que dans ce travail, malheureusement, on ne sait pas démontrer l'estimation sur $|\langle f_N(u^N)\rangle|$ pour tous temps.

En fait, en ce qui concerne les temps des calculs, on obtient de meilleurs résultats en utilisant le terme non linéaire logarithmique plutôt que polynomial. On donne aussi des simulations numériques qui confirment que l'algorithme à un pas avec seuil proposé dans le premier chapitre est efficace. On donne également un exemple pour lequel l'algorithme à un pas donne des résultats qualitativement meilleurs, quand on considère une nonlinéarité logarithmique.

3. Sachant que les articles [16, 17, 20, 38, 39] traitent seulement de la retouche d'images binaires (c'est à dire, noir et blanc ; voir cependant [25] pour la retouche d'images en niveaux de gris), il est naturel et important de traiter aussi la retouche d'images en couleur. L'idée est d'étendre l'approche de [16] à des systèmes de Cahn–Hilliard à n composants, chaque phase correspondant à une couleur donnée. Les systèmes de Cahn–Hilliard ont été proposés et étudiés dans, par exemple, [46], [57], [62], [72] et [97]. L'idée principale dans ce travail est de proposer un modèle pour la retouche en couleur, basé sur le terme de fidélité proposé dans [16].

Finalement, on considère le modèle suivant :

$$\frac{\partial c_i}{\partial t} = \Delta\mu_i + \lambda_0\chi_{\Omega\setminus D}(x)(h_i - c_i), \quad i = 1, ..., n, \tag{31}$$

$$\mu_i = \frac{\partial F(c)}{\partial c_i} - \varepsilon^2 \Delta c_i - \frac{1}{n} \sum_{i=1}^{n} \frac{\partial F}{\partial c_i}, \quad i = 1, ..., n, \tag{32}$$

où $D \Subset \Omega$ est le domaine à retoucher, $h = (h_1, ..., h_n) \in (L^2(\Omega)^n$, n est le nombre de couleurs dans l'image h et $F(s) = \frac{1}{n} c^2 (1 - c)^2$.
Le problème (31)–(32) est associé à des conditions aux limites de type Neumann

$$\frac{\partial c_i}{\partial \nu} = \frac{\partial \Delta c_i}{\partial \nu} = 0, \quad \text{sur } \Gamma, \quad i = 1, ..., n.$$

On suppose qu'une solution $c = (c_1, ..., c_n)$ de (31)–(32) doit satisfaire $\sum_{i=1}^{n} c_i = 1$ en tous points x de Ω. Par ailleurs, on suppose que $h = (h_1, ..., h_n)$ satisfait cette contrainte, c'est-à-dire, $\sum_{i=1}^{n} h_i = 1$.
On définit alors l'hyperplan suivant :

$$S := \{c \in \mathbb{R}^n \text{ tel que } \sum_{i=1}^{n} c_i = 1\}$$

et son espace tangent

$$TS := \{\phi = (\phi_i) \in \mathbb{R}^n \text{ tel que } \sum_{i=1}^{n} \phi_i = 0\}.$$

Le terme $-\frac{1}{n} \sum_{i=1}^{n} \frac{\partial F}{\partial c_i}$ est le multiplicateur de Lagrange qui est ajouté au problème afin de garantir la contrainte $c \in S$.
En ce qui concerne le traitement mathématique du problème, on rencontre deux difficultés essentielles. La première déjà rencontrée dans le modèle binaire dans [38], est que, du fait de la présence du terme de fidélité, on n'a plus la conservation de la masse. Cette difficulté est surmontée en montrant la dissipativité du paramètre d'ordre $c = (c_1, ..., c_n)$; en particulier, une étape clé est d'obtenir une telle estimation sur la moyenne spatiale du paramètre d'ordre. On note que cette estimation est une estimation cruciale, déjà pour obtenir l'existence de la solution. La seconde est que le paramètre d'ordre doit être dans S. Par conséquent, on doit faire attention aux choix des espaces fonctionnels et à la formulation faible du problème.
En particulier, on démontre que, pour toute condition initiale $c_0 \in (L^2(\Omega))^n \cap S$, il existe une solution unique du problème (31)–(32) telle que $c \in L^\infty([0, T], (L^2(\Omega))^n \cap S) \cap L^2([0, T], (H^2(\Omega)) \cap S)^n \cap L^4([0, T], (L^4(\Omega))^n \cap S)$ (on utilise dans la démonstration de l'existence de solutions un schéma de Galerkin). Ensuite, on démontre l'existence d'un attracteur global qui est compact dans $(L^2(\Omega))^n \cap S$ et borné dans $(H^2(\Omega))^n \cap S$. Finalement, on démontre l'existence d'un attracteur exponentiel, si bien que l'attracteur global est maintenant de dimension fractale finie.
Par ailleurs, on démontre la consistance algébrique du modèle avec le modèle à deux phases. Bien sûr, le modèle devrait être aussi consistant avec le modèle à k phases, $k < n$, mais on n'a pas pu démontrer cette propriété générale ici.

Finalement, on présente des simulations numériques confirmant que l'algorithme à un pas avec seuil est efficace, également dans le contexte de la retouche en couleur. Ici, la méthode de seuil consiste à remplacer $\max_{i=1,\dots,n} c_i$ par 1 et $c_j \neq \max_{i=1,\dots,n} c_i$ par 0 pour tout j et à chaque point $(x, y) \in \Omega$; cela signifie qu'on remplace la phase (couleur) dominante par 1 à chaque point de Ω et les autres phases (couleurs) par 0 pour obtenir le résultat final.

3.2 Deuxième partie : applications à la biologie et à la chimie

1. Tout d'abord, on considère le modèle suivant :

$$\frac{\partial u}{\partial t} + \Delta^2 u - \Delta f(u) + g(u) = 0, \tag{33}$$

où g est le terme de prolifération.

– Dans un premier temps, on prend

$$g(s) = \alpha s^2 + \beta s + \gamma, \quad \alpha > 0, \beta, \gamma \in \mathbb{R}.$$

En particulier, pour Ω bidimensionnel, $\beta = -\alpha$, $\gamma = 0$ et pout $\alpha > 0$, on obtient le modèle proposé dans [88] qui modélise par exemple, l'agrégation de cellules tumorales malignes du cerveau (voir [42]) ; dans ce cas, α représente la vitesse de prolifération. Ensuite, pour $\alpha = 1$ et $\beta = -\gamma = P$, le modèle proposé dans [141] modélise en deux dimensions, par exemple, des phénomènes liés à des interactions liquide-gaz ; dans ce cas, P est une constante qui représente la pression réduite de la phase gaz.
De plus, on prend

$$f(s) = s^3 - s, \quad \forall s \in \mathbb{R}.$$

Cependant, les résultats théoriques obtenus restent vrais pour tout f de la forme

$$f(s) = \sum_{i=1}^{2p+1} a_i s^i, \quad a_{2p+1} > 0, \ p \geq 1.$$

Soit $\Theta = \beta^2 - 4\alpha\gamma$ le discriminant de g.
On associe le problème (33) à des conditions aux limites de type Neumann

$$\frac{\partial u}{\partial \nu} = \frac{\partial \Delta u}{\partial \nu} = 0 \quad \text{sur } \Gamma.$$

On note que les conditions aux limites de type Neumann sont cruciales ici ; on a l'existence globale en temps des solutions du même problème avec les conditions Dirichlet aux limites (voir, par exemple, [104] et voir aussi l'annexe C).
On démontre que la moyenne spatiale du paramètre d'ordre peut exploser en temps fini en général. Par ailleurs, quand la moyenne spatiale du paramètre d'ordre est bornée, la solution existe globalement en temps et elle est dissipative.
Ensuite, on démontre entre autres, que, pour $\Theta > 0$, si u est une solution telle que $u(t) \in [\frac{-\beta - \sqrt{\Theta}}{2\alpha}, \frac{-\beta + \sqrt{\Theta}}{2\alpha}]$ ou $u(t) \in [\frac{-\beta + \sqrt{\Theta}}{2\alpha}, a]$, $\forall t \geq 0$, où $a > \frac{-\beta + \sqrt{\Theta}}{2\alpha}$ est arbitraire, alors la solution converge vers $\frac{-\beta + \sqrt{\Theta}}{2\alpha}$ quand t tend vers l'infini.

D'autre part, on démontre que, si $\Theta > 0$, et $\langle u(T)\rangle < \frac{-\beta-\sqrt{\Theta}}{2\alpha}$, pour un certain $T \geq 0$ (et, en particulier, si $\langle u_0\rangle < \frac{-\beta-\sqrt{\Theta}}{2\alpha}$, où $u_0 = u(0)$ est la condition initiale à $t = 0$), alors la solution du problème (33) explose en temps fini. Par ailleurs, le temps d'existence T^+ satisfait

$$T^+ \leq T + \frac{1}{2\alpha z_1} \ln\Big(\frac{z(T) - z_1}{z(T) + z_1}\Big),$$

où $z_1 = \frac{\sqrt{\Theta}}{2\alpha}$ et $z(T) = \langle u(T)\rangle + \frac{\beta}{2\alpha}$.
On obtient également un résultat similaire dans le cas $\Theta = 0$.
Finalement, on donne des simulations numériques qui confirment ces résultats. Elles montrent en particulier que même si la condition initiale est dans l'intervalle physique pertinent $[\frac{-\beta-\sqrt{\Theta}}{2\alpha}, \frac{-\beta+\sqrt{\Theta}}{2\alpha}]$, on peut trouver des solutions qui explosent en temps fini. Ces simulations sont effectuées avec FreeFem++.

– Dans un second temps, on prend

$$g(s) = \alpha s - \beta s^q (s-1)^q, \quad q > 1,\ \alpha, \beta \in \mathbb{R},\ \forall s \in \mathbb{R}.$$

En particulier, pour $q = 2$, le modèle décrit la croissance tumorale incontrôlée de cellules anormales, ce qui se traduit souvent par un cancer (voir [5]) ; dans ce cas, α et β sont deux constantes qui représentent le coefficient de mort et de la croissance, respectivement. On note que les paramètres α et β peuvent aussi dépendre de la variable spatiale et du temps.
De plus, on prend

$$f(s) = \sum_{i=1}^{2p+1} a_i s^i, \quad a_{2p+1} > 0,\ p \geq 1.$$

On associe toujours le problème (33) à des conditions aux limites de type Neumann

$$\frac{\partial u}{\partial \nu} = \frac{\partial \Delta u}{\partial \nu} = 0 \quad \text{sur } \Gamma.$$

On démontre que, si $p = 2q-1$ alors la solution ayant une moyenne nulle est dissipative dans $L^2(\Omega)$. De plus, si $\langle u\rangle$ est dissipative alors la solution est dissipative dans $L^2(\Omega)$.
Par ailleurs, si $\alpha = 0$, q pair et $u(t) \in [0, 1]$, $\forall t \geq 0$ alors, pour $\beta > 0$, la solution u tend vers 1 quand t tend vers l'infini et, pour $\beta < 0$, la solution u tend vers 0 quand t tend vers l'infini.
Ensuite, si $\alpha = 0$, q impair et $u(t) \in [0, 1]$, $\forall t \geq 0$ alors, pour $\beta > 0$, la solution u tend vers 0 quand t tend vers l'infini et, pour $\beta < 0$, la solution u tend vers 1 quand t tend vers l'infini.
On suppose maintenant que $q = 2$ et $\alpha = 2\beta$. Si $\beta > 0$ et $u(t) > 2$, $\forall t \geq 0$, alors la solution u explose en temps fini. En outre, le temps d'existence T^+ satisfait

$$T^+ \leq T + \frac{1}{2\beta} \ln\Big(\frac{y(T)}{y(T) - 2}\Big),$$

où $y(T) = \langle u(T)\rangle$.

De même, on suppose maintenant que $q = 2$ et $\alpha = 2\beta$. Si $\beta < 0$ et $u(t) < 0$, $\forall t \geq 0$, alors la solution u explose en temps fini. En outre, le temps d'existence T^+ satisfait

$$T^+ \leq T + \frac{1}{2\beta} \ln\Big(\frac{y(T)}{y(T) - 2}\Big).$$

Puis, on démontre que, pour $q = 2$ et $\alpha = 2\beta$, si $\beta > 0$ et $u(t) \leq 2$, $\forall t \geq 0$, ou bien $\beta < 0$ et $u(t) \geq 0$, $\forall t \geq 0$, alors la solution u tend vers 0 quand t tend vers l'infini.
Finalement, on donne des simulations numériques qui confirment ces résultats.

2. Ensuite, on considère le modèle suivant :

$$\frac{\partial u}{\partial t} + \Delta^2 u - \Delta f(u) + g(x, u) = 0, \tag{34}$$

où g est un terme de source. L'équation (34) peut être utilisée comme un modèle pour la croissance cancéreuse et d'autres entités biologiques.
Typiquement, g peut être une fonction linéaire, $g(x, s) = \alpha s$, $\alpha > 0$; dans ce cas (34) est l'équation de Cahn–Hilliard–Oono (pour plus de détails, voir le paragraphe précédent). Une seconde possibilité est la fonction quadratique $g(x, s) = \alpha s(s - 1)$, $\alpha > 0$; ici (34) a des applications en biologie et plus précisément, elle modélise la cicatrisation de plaies et la croissance tumorale (pour plus de détails, voir le paragraphe précédent). Une troisième possibilité, avec des applications en biologie et plus précisément à la croissance tumorale [5], est la fonction $g(x, s) = \frac{\alpha}{2}(s + 1) - \beta(1 - s)^2(1 + s)^2 + s(x, t)$, où α et β sont les coefficient de mort et de croissance, respectivement. Une quatrième possibilité est la fonction $g(x, u) = \chi_{\Omega\setminus D}(x)u$ (où $D \Subset \Omega$). Dans ce cas, l'équation (34) est appliquée à la retouche d'images.

– Dans un premier temps, on associe l'équation (34) avec des conditions aux limites de type Dirichlet

$$u = \Delta u = 0 \quad \text{sur } \Gamma.$$

On démontre que, si la condition initiale $u_0 \in H^2(\Omega) \cap H_0^1(\Omega)$, alors il existe une solution unique u telle que $u \in H^2(\Omega) \cap H_0^1(\Omega)$. Par ailleurs, on démontre que la solution est dissipative dans $H^2(\Omega)$.
Ensuite, on démontre l'existence d'un attracteur exponentiel pour la topologie de H^{-1}. Par conséquent, on a l'existence d'un attracteur global de dimension finie. En outre, on démontre l'existence d'un autre attracteur exponentiel plus régulier pour la topologie de H^2.

– Dans un second temps, on associe l'équation (34) avec des conditions aux limites de type Neumann

$$\frac{\partial u}{\partial \nu} = \frac{\partial \Delta u}{\partial \nu} = 0 \quad \text{sur } \Gamma.$$

On note que, dans le cas où g est un polynôme de degré pair, le problème avec les conditions aux limites de type Neumann peut ne pas avoir l'existence globale de solutions (voir [42, 64]).
On prend g de la forme

$$g(s) = \sum_{j=0}^{2q-1} b_j s^j, \quad b_{2q-1} > 0, \ q \geq 1.$$

Par ailleurs, la nonlinéarité est donnée par

$$f(s) = \sum_{i=0}^{2p-1} c_i s^i, \quad c_{2p-1} > 0.$$

On démontre que, si la condition initiale $u_0 \in H^2(\Omega)$, alors il existe une solution unique u telle que $u(t) \in H^2(\Omega),\ \forall t \geq 0$. Par ailleurs, on démontre que la solution est dissipative dans $H^2(\Omega)$.
Ensuite, on démontre l'existence d'un attracteur exponentiel pour la topologie de H^{-1}. Par conséquent, on a l'existence d'un attracteur global de dimension finie.
On note aussi que les résultats obtenus dans ce cas demeurent dans le cas où le terme de source g est donné par

$$g(x, s) = h(x)L(u), \quad h \in L^\infty(\Omega), \quad L(s) = \sum_{j=0}^{2q-1} b_j s^j,$$

sachant que $p = 2q - 1$ et

$$\langle g(x, u)\rangle\langle u\rangle \geq \xi\langle u^{2q-1}\rangle\langle u\rangle + c\langle u\rangle, \quad \xi > 0.$$

Finalement, on donne des simulations numériques qui confirment la dissipativité de la solution du modèle associé à des conditions aux limites de type Dirichlet et avec un terme source de degré pair. Cependant, avec le même terme source la solution du modèle associé à des conditions aux limites de type Neumann explose en temps fini.

Première partie

Généralisation de l'équation de Cahn–Hilliard en retouche d'images

Chapitre 1

Finite-dimensional attractors for the Bertozzi–Esedoglu–Gillette–Cahn–Hilliard equation in image inpainting

Attracteurs de dimension-finie pour l'équation de Bertozzi–Esedoglu–Gillette–Cahn–Hilliard en retouche d'images

Ce chapitre est constitué de l'article **Finite-dimensional attractors for the Bertozzi–Esedoglu–Gillette–Cahn–Hilliard equation in image inpainting**, Inv. Prob. Imag. 9 (2015), 105–125. Cet article est écrit en collaboration avec **Laurence Cherfils** et **Alain Miranville**.

Inverse Problems and Imaging
Volume 9, No. 1, 2015, 105–125

Finite-dimensional attractors for the Bertozzi–Esedoglu–Gillette–Cahn–Hilliard equation in image inpainting

LAURENCE CHERFILS

Laboratoire Mathématiques, Image et Applications
Université de la Rochelle
Avenue Michel Crépeau
F-17042 La Rochelle Cedex, France

HUSSEIN FAKIH AND ALAIN MIRANVILLE

Laboratoire de Mathématiques et Applications
Université de Poitiers
UMR CNRS 7348 - SP2MI
Boulevard Marie et Pierre Curie - Téléport 2
F-86962 Chasseneuil Futuroscope Cedex, France

Dedicated to M. Chipot on the occasion of his 65*th birthday*

(Communicated by Selim Esedoglu)

ABSTRACT : In this article, we are interested in the study of the asymptotic behavior, in terms of finite-dimensional attractors, of a generalization of the Cahn-Hilliard equation with a fidelity term (integrated over $\Omega\backslash D$ instead of the entire domain Ω, $D \subset\subset \Omega$). Such a model has, in particular, applications in image inpainting. The difficulty here is that we no longer have the conservation of mass, i.e. of the spatial average of the order parameter u, as in the Cahn-Hilliard equation. Instead, we prove that the spatial average of u is dissipative. We finally give some numerical simulations which confirm previous ones on the efficiency of the model.

Keys words and phrases : Cahn–Hilliard equation, fidelity term, inpainting image, exponential attractor, global attractor.
2010 Mathematics Subject Classification : 35K55, 35B40

1.1 Introduction

The Cahn–Hilliard equation,

$$\frac{\partial u}{\partial t} + \Delta^2 u - \Delta f(u) = 0, \tag{1.1}$$

is very important in materials science. This equation is a simple model for phase separation processes of a binary alloy at a fixed temperature. We refer the reader to [26, 27] for more details. The function $f : \mathbb{R} \to \mathbb{R}$ is of "bistable type" with three simple zeros and is the derivative of a double-well potential F whose wells correspond to the phases of the material. A typical model nonlinearity is given by

$$F(s) = \frac{1}{4}(s^2 - 1)^2,$$

i.e.

$$f(s) = s^3 - s.$$

The function $u(x, t)$ represents the concentration of one of the metallic components of the alloy.

It is interesting to note that the Cahn–Hilliard equation is also relevant in other phenomena than phase separation. We can mention, for instance, population dynamics [45], bacterial films [91], biology [108, 88, 104], thin films [123, 138], image processing [29], shape recovery in computer vision [51], and even the rings of Saturn [139].

We are interested in this article in the following generalization of the Cahn–Hilliard equation introduced in [16] in view of applications in image inpainting :

$$\frac{\partial u}{\partial t} + \varepsilon\Delta^2 u - \frac{1}{\varepsilon}\Delta f(u) + \lambda_0 1_{\Omega\setminus D}(x)(u - h) = 0, \qquad \varepsilon, \lambda_0 > 0, \tag{1.2}$$

where $h(x)$ is a given binary image, $D \subset\subset \Omega$ is the inpainting domain, and the last term on the left-hand side is added to keep the solution constructed close to the given image $h(x)$ in the complement of the inpainting domain ($\Omega\setminus D$), where there is image information available. The idea here is to solve the equation up to equilibrium to have an inpainted version $u(x)$ of $h(x)$.

Image inpainting involves filling in parts of an image or video using information from the surrounding area. Its applications include restoration of old paintings by museum artists [58], removing scratches from old photographs [24], altering scenes in photographs [89], and restoration of motion pictures [93].

Well-posedness results for (1.2) have been obtained in [16] (see also [25] for the study of the stationary problem).

Equation (1.1) is usually endowed with Neumann boundary conditions,

$$\frac{\partial u}{\partial \nu} = \frac{\partial \Delta u}{\partial \nu} = 0 \qquad \text{on } \partial\Omega.$$

In particular, this yields the conservation of mass, i.e. of the spatial average of the order parameter u,

$$\langle u(t)\rangle = \langle u(0)\rangle, \quad \forall t \geq 0,$$

where

$$\langle . \rangle = \frac{1}{|\Omega|} \int_{\Omega} . dx.$$

Then assuming that $|\langle u(0) \rangle|$ is bounded, we can prove the existence of finite-dimensional global attractors (see, e.g., [114] and [137]) , i.e., the existence of compact invariant sets which characterize the global dynamics of the problem. More precisely, these sets provide information on all the possible dynamics of the system and are expected to have a rich geometric structure ; they contain in particular all steady states and heteroclinic orbits. Furthermore, the finite-dimensionality means, roughly speaking, that, even though the initial phase space is infinite-dimensional, the reduced dynamics can be characterized by a finite number of parameters. We refer the readers to, e.g., [52], [108] and [137] for discussions on this subject.

On the contrary, equation (1.2), which is also endowed with Neumann boundary conditions, does not satisfy this conservation property. We prove instead that $\langle u \rangle$ is dissipative, which then allows us to prove the existence of finite-dimensional attractors. As mentioned above, these sets give information on the global dynamics of the system. To have more precise information on the asymptotic behavior of the problem, it would be important to prove the convergence of single trajectories to steady states, but this seems to be a particularly difficult problem here.

We also give numerical simulations which show that, in some situations, a dynamic one step scheme with a threshold involving the diffuse interface thickness ε (we note that, in [16] and [17], the authors first consider a large value of ε and then a smaller one in order to obtain their numerical simulations) allows us to connect regions across large inpainting domains. More precisely, the idea is to look for an intermediate value of ε which is sufficient to obtain good results (the final inpainting result is obtained by considering a threshold ; see Section 1.7). This one step algorithm is not always applicable (see Remark 1.7.1 below). In that case, we also need the two steps algorithm involving the interface thickness ε in order to connect the edges. We finally note that, while the simulations in [16] and [17] are programmed in MATLAB, we use FreeFem++. These simulations confirm the ones performed in [16] and [17] on the efficiency of the model.

1.2 Setting of the problem

Let Ω be an open bounded domain of $\mathbb{R}^n$, $n = 1,\ 2,$ or 3, with a smooth boundary Γ, and D be an open bounded subset of Ω with a smooth boundary ∂D such that $D \subset\subset \Omega$. The unknown function is a scalar $u = u(x,t)$, $x \in \Omega$, $t \in \mathbb{R}$, and the equation reads (for simplicity, we set ε equal to 1)

$$\frac{\partial u}{\partial t} + \Delta^2 u - \Delta f(u) + \lambda_0 1_{\Omega \setminus D}(x)(u - h) = 0, \tag{1.3}$$

where f is the cubic function

$$f(s) = s^3 - s \tag{1.4}$$

and $h \in L^2(\Omega)$.

We denote by F the antiderivative of f vanishing at $s = 0$,

$$F(s) = \frac{1}{4}s^4 - \frac{1}{2}s^2. \tag{1.5}$$

The equation is associated with the Neumann boundary conditions

$$\frac{\partial u}{\partial \nu} = \frac{\partial \Delta u}{\partial \nu} = 0 \qquad \text{on } \Gamma. \tag{1.6}$$

We finally supplement the equation with the initial condition

$$u(x,0) = u_0(x), \qquad x \in \Omega. \tag{1.7}$$

We denote by $\|.\|$ the L^2-norm (with associated scalar product $((.,.))$) and set

$$V = \left\{\phi \in H^2(\Omega), \quad \frac{\partial \phi}{\partial \nu} = 0 \quad \text{on } \Gamma\right\}. \tag{1.8}$$

The space V in (1.8) makes sense by the trace theorem. Furthermore, V is a closed subspace of $H^2(\Omega)$ and is equipped with the norm induced by $H^2(\Omega)$ denoted by $\|.\|_2$.

We denote by $\langle\phi\rangle$ the average over Ω of a function ϕ in $L^1(\Omega)$,

$$\langle\phi\rangle = \frac{1}{|\Omega|}\int_\Omega \phi(x)dx, \tag{1.9}$$

and we write $\bar{\phi} = \phi - \langle\phi\rangle$.

We set $\dot{L}^2(\Omega) = \{\phi \in L^2(\Omega), \ \langle\phi\rangle = 0\}$.

For ϕ given in $\dot{L}^2(\Omega)$, we denote by $\Psi = N(\phi)$ the solution to the poisson equation

$$-\Delta\Psi = \phi$$

associated with the Neumann boundary condition

$$\frac{\partial \Psi}{\partial \nu} = 0 \quad \text{on } \Gamma.$$

It is easily seen that $\{((N(\phi),\phi))\}^{1/2}$ is a continuous norm on $\dot{L}^2(\Omega)$; we denote it by $\|\phi\|_{-1}$. Similarly, $((\phi_1,\phi_2))_{-1} = ((N(\phi_1),\phi_2)) = ((\phi_1,N(\phi_2)))$ is a (pre-Hilbertian) continuous scalar product on $\dot{L}^2(\Omega)$.

We note that

$$v \to (\|v - \langle v\rangle\|_{-1}^2 + \langle v\rangle^2)^{\frac{1}{2}},$$
$$v \to (\|v - \langle v\rangle\|^2 + \langle v\rangle^2)^{\frac{1}{2}},$$
$$v \to (\|\nabla v\|^2 + \langle v\rangle^2)^{\frac{1}{2}}$$

and

$$v \to (\|\Delta v\|^2 + \langle v\rangle^2)^{\frac{1}{2}},$$

are norms in $H^{-1}(\Omega)$, $L^2(\Omega)$, $H^1(\Omega)$ and $H^2(\Omega)$, respectively, which are equivalent to the usual ones.

We finally set $\dot{H}^{-1}(\Omega) = \{\phi \in H^{-1}(\Omega), \ \langle\phi,1\rangle_{H^{-1}(\Omega),H^1(\Omega)} = 0\}$.

Throughout this article, the same letter c (and, sometimes, c' and c'') denotes constants which may vary from line to line, or even in a same line. Similarly, the same letter Q denotes monotone increasing functions which may vary from line to line, or even in a same line.

1.3 A priori estimates

The weak formulation of the problem is obtained by multiplying (1.3) by a test function $v \in V$, integrating over Ω, and using the Green formula and the boundary conditions. We find

$$\begin{aligned}\frac{d}{dt}((u,v)) + ((\Delta u, \Delta v)) + ((f'(u)\nabla u, \nabla v)) + \lambda_0((1_{\Omega\setminus D}(x)(u-h), v)) \\ = 0, \quad \forall v \in V.\end{aligned} \tag{1.10}$$

Now, we replace v by 1 in (1.10) to have

$$\frac{d}{dt}\int_\Omega u(x,t)dx = -\lambda_0 \int_\Omega 1_{\Omega\setminus D}(x)(u(x,t) - h(x))dx, \tag{1.11}$$

hence

$$\frac{d}{dt}\langle u\rangle = -\frac{\lambda_0}{|\Omega|}\int_\Omega 1_{\Omega\setminus D}(x)(u(x,t) - h(x))dx. \tag{1.12}$$

Owing to (1.12), we can rewrite (1.3) in the form

$$\frac{\partial \bar{u}}{\partial t} + \Delta^2 u - \Delta f(u) + \lambda_0 1_{\Omega\setminus D}(x)(u-h) - \frac{\lambda_0}{|\Omega|}\int_\Omega 1_{\Omega\setminus D}(x)(u-h)dx = 0. \tag{1.13}$$

Recalling that $u = \bar{u} + \langle u\rangle$, we have

$$\frac{\partial \bar{u}}{\partial t} + \Delta^2 \bar{u} - \Delta f(\bar{u} + \langle u\rangle) + \lambda_0 1_{\Omega\setminus D}(x)(u-h) - \frac{\lambda_0}{|\Omega|}\int_\Omega 1_{\Omega\setminus D}(x)(u-h)dx = 0, \tag{1.14}$$

which is equivalent to

$$\begin{aligned}\frac{\partial}{\partial t}N(\bar{u}) - \Delta\bar{u} + f(\bar{u} + \langle u\rangle) - \langle f(\bar{u} + \langle u\rangle)\rangle + N\Big(\lambda_0 1_{\Omega\setminus D}(x)(u-h) \\ - \frac{\lambda_0}{|\Omega|}\int_\Omega 1_{\Omega\setminus D}(x)(u-h)dx\Big) = 0.\end{aligned} \tag{1.15}$$

We take the scalar product of this equation by $\bar{u}$ in $L^2(\Omega)$ and obtain

$$\begin{aligned}\frac{1}{2}\frac{d}{dt}\|\bar{u}\|^2_{-1} - ((\Delta\bar{u}, \bar{u})) + ((f(\bar{u} + \langle u\rangle) - f(\langle u\rangle), \bar{u})) \\ + ((\lambda_0 1_{\Omega\setminus D}(x)(u-h) - \frac{\lambda_0}{|\Omega|}\int_\Omega 1_{\Omega\setminus D}(x)(u-h)dx, N(\bar{u}))) = 0.\end{aligned} \tag{1.16}$$

We have

$$\begin{aligned}&((f(\bar{u} + \langle u\rangle) - f(\langle u\rangle), \bar{u})) \\ &\qquad = \int_\Omega (\bar{u}^4 + 3\bar{u}^3\langle u\rangle + 3\bar{u}^2\langle u\rangle^2)dx - \|\bar{u}\|^2 \\ &\qquad \geq \int_\Omega (\bar{u}^4 + 3\bar{u}^2\langle u\rangle^2)dx - 3\int_\Omega |\bar{u}|^3|\langle u\rangle|dx - \|\bar{u}\|^2 \\ &\qquad \geq c_0\int_\Omega (\bar{u}^4 + \bar{u}^2\langle u\rangle^2)dx - \|\bar{u}\|^2, \;\; c_0 > 0,\end{aligned} \tag{1.17}$$

owing to Young's inequality (e.g., $3ab \le \frac{7}{8}a^2 + \frac{18}{7}b^2$, $a, b \ge 0$; here, $a = \bar{u}^2$ and $b = |\bar{u}\langle u\rangle|$), and

$$\begin{aligned}|((\lambda_0\overline{1_{\Omega\setminus D}(x)(u(x,t)-h(x))},N(\bar{u})))| &\le c\|u-h\|\|\bar{u}\| \\ &\le c(\|\bar{u}\|^2 + |\langle u\rangle|\|\bar{u}\|) + c'\|h\|^2 \\ &\le \frac{c_0}{4}\int_\Omega(\bar{u}^4 + \bar{u}^2\langle u\rangle^2)dx + c(\|h\|^2+1).\end{aligned} \tag{1.18}$$

It follows from (1.16), (1.17) and (1.18) that

$$\begin{aligned}\frac{1}{2}\frac{d}{dt}\|\bar{u}\|_{-1}^2 + \|\nabla\bar{u}\|^2 + c_0\int_\Omega(\bar{u}^4 + \bar{u}^2\langle u\rangle^2)dx \le &\frac{c_0}{4}\int_\Omega(\bar{u}^4 + \bar{u}^2\langle u\rangle^2)dx \\ &+ \|\bar{u}\|^2 + c(\|h\|^2+1),\end{aligned}$$

hence

$$\frac{d}{dt}\|\bar{u}\|_{-1}^2 + \|\nabla\bar{u}\|^2 + c_0\int_\Omega(\bar{u}^4 + \bar{u}^2\langle u\rangle^2)dx \le c. \tag{1.19}$$

It thus follows from (1.19) that

$$\frac{1}{2}\frac{d}{dt}\|\bar{u}\|_{-1}^2 + c\|\bar{u}\|_{-1}^2 \le c', \quad c > 0. \tag{1.20}$$

By Gronwall's lemma, we find

$$\|\bar{u}(t)\|_{-1}^2 \le e^{-ct}\|\bar{u}_0\|_{-1}^2 + c', \quad c > 0, \quad t \ge 0. \tag{1.21}$$

Let B be a bounded subset of $\dot{H}^{-1}(\Omega)$ and t_0 be such that $\bar{u}_0 \in B$ and $t \ge t_0$ implies $\bar{u}(t) \in \mathcal{B}_0$, where $\mathcal{B}_0 = \{\phi \in \dot{H}^{-1}(\Omega),\ \|\phi\|_{-1}^2 \le 2c'\}$, c' being the constant in (1.21). We then deduce from (1.19) that, for $t \ge t_0$,

$$\int_t^{t+r}\|\nabla\bar{u}\|^2 ds \le c(r), \quad \int_t^{t+r} ds\int_\Omega(\bar{u}^4 + \bar{u}^2\langle u\rangle^2)dx \le c(r), \tag{1.22}$$

for $r > 0$ fixed.

We then multiply (1.14) by $\bar{u}$ and find, noting that

$$f' \ge -c_1, \quad c_1 > 0, \tag{1.23}$$

the inequality

$$\begin{aligned}\frac{1}{2}\frac{d}{dt}\|\bar{u}\|^2 + \|\Delta\bar{u}\|^2 + ((\lambda_0 1_{\Omega\setminus D}(x)(u-h) - \frac{\lambda_0}{|\Omega|}\int_\Omega 1_{\Omega\setminus D}(x)(u-h)dx, \bar{u})) \\ \le c_1\|\nabla\bar{u}\|^2.\end{aligned} \tag{1.24}$$

We have

$$\begin{aligned}|((\lambda_0 1_{\Omega\setminus D}(x)(u(x,t)-h(x)) - \frac{\lambda_0}{|\Omega|}\int_\Omega 1_{\Omega\setminus D}(x)(u(x,t)-h(x))dx, \bar{u}))| \\ = \lambda_0|((1_{\Omega\setminus D}(u-h), \bar{u}))| \\ \le c\|u-h\|\|\bar{u}\| \\ \le c(\|\bar{u}\|^2 + |\langle u\rangle|\|\bar{u}\|) + c'\|h\|^2 \\ \le c\Big(\int_\Omega(\bar{u}^4 + \bar{u}^2\langle u\rangle^2)dx + \|h\|^2 + 1\Big).\end{aligned} \tag{1.25}$$

Therefore, we obtain

$$\frac{d}{dt}\|\bar{u}\|^2 + \|\Delta\bar{u}\|^2 \le c\|\nabla u\|^2 + c'\Big(\int_\Omega (\bar{u}^4 + \bar{u}^2\langle u\rangle^2)dx + \|h\|^2 + 1\Big). \tag{1.26}$$

We finally deduce from (1.22), (1.26) and the uniform Gronwall's lemma that

$$\|\bar{u}(t)\|^2 \le c, \quad t \ge t_0 + r, \tag{1.27}$$

where the constant c is independent of $\bar{u}_0$ and t, hence, employing (1.27) and integrating (1.19) and (1.26) between 0 and $t_0 + r$,

$$\|\bar{u}(t)\|^2 \le Q(\|\bar{u}_0\|), \quad t \ge 0, \tag{1.28}$$

for some monotone increasing function Q.

Now, setting $u = \langle u\rangle + \bar{u}$ in (1.11), we have

$$\frac{d}{dt}\langle u\rangle + \frac{\lambda_0}{|\Omega|}\int_{\Omega\setminus D}(\langle u\rangle + \bar{u} - h)dx = 0.$$

Therefore,

$$\frac{d}{dt}\langle u\rangle + c\langle u\rangle = -\frac{\lambda_0}{|\Omega|}\int_{\Omega\setminus D}(\bar{u} - h)dx,$$

where $c = \frac{\lambda_0|\Omega\setminus D|}{|\Omega|}$, hence

$$\frac{d}{dt}(e^{ct}\langle u\rangle) = -\frac{\lambda_0}{|\Omega|}e^{ct}\int_{\Omega\setminus D}(\bar{u} - h)dx$$

and

$$\langle u\rangle = e^{-ct}\langle u_0\rangle - \frac{\lambda_0}{|\Omega|}e^{-ct}\int_0^t e^{cs}\int_{\Omega\setminus D}(\bar{u} - h)dxds.$$

Thus,

$$|\langle u\rangle| \le e^{-ct}|\langle u_0\rangle| + c'e^{-ct}\int_0^t e^{cs}(\|\bar{u}\| + \|h\|)ds, \qquad \forall t \ge 0,$$

where $c' = \frac{\lambda_0}{|\Omega|^{\frac{1}{2}}}$. Here,

$$\begin{aligned} c'e^{-ct}\int_0^t e^{cs}\|h\|ds &\le c'e^{-ct}\|h\|e^{ct} \\ &\le c'\|h\| \\ &\le c''. \end{aligned}$$

Furthermore, for $t \ge t_0 + r$,

$$\begin{aligned} c'e^{-ct}\int_0^t e^{cs}\|\bar{u}\|ds &= c'e^{-ct}\int_0^{t_0+r} e^{cs}\|\bar{u}\|ds + c'e^{-ct}\int_{t_0+r}^t e^{cs}\|\bar{u}\|ds \\ &\le Q(\|\bar{u}_0\|)e^{-ct}e^{c(t_0+r)} + c'e^{-ct}\int_{t_0+r}^t e^{cs}\|\bar{u}\|ds \\ &\le Q(\|\bar{u}_0\|)e^{-ct} + c'e^{-ct}\int_{t_0+r}^t e^{cs}\|\bar{u}\|ds \\ &\le Q(\|\bar{u}_0\|)e^{-ct} + c''e^{-ct}(e^{ct} - e^{c(t_0+r)}) \\ &\le Q(\|\bar{u}_0\|)e^{-ct} + c'', \end{aligned}$$

where we have used (1.28) (resp., (1.27)) to estimate the first (resp., the second) integral in the right-hand side of the first equality. Finally, we obtain

$$|\langle u\rangle| \leq (Q(\|\bar{u}_0\|) + |\langle u_0\rangle|)e^{-ct} + c'', \qquad \forall t \geq 0, \tag{1.29}$$

where c and c'' are two constants which are nonnegative and independent of t and u_0.

1.4 Further a priori estimates

We multiply (1.3) by $\Delta^2 u$ and have

$$\frac{1}{2}\frac{d}{dt}\|\Delta u\|^2 + \|\Delta^2 u\|^2 - ((\Delta f(u), \Delta^2 u)) + ((\lambda_0 1_{\Omega\setminus D}(x)(u-h), \Delta^2 u)) = 0. \tag{1.30}$$

Noting that

$$\begin{aligned} |((\lambda_0 1_{\Omega\setminus D}(x)(u-h), \Delta^2 u))| &\leq c\|u-h\|\|\Delta^2 u\| \\ &\leq c'\|u-h\|^2 + \frac{1}{4}\|\Delta^2 u\|^2 \\ &\leq c'\|u\|^2 + c'\|h\|^2 + \frac{1}{4}\|\Delta^2 u\|^2, \end{aligned} \tag{1.31}$$

we find

$$\frac{1}{2}\frac{d}{dt}\|\Delta u\|^2 + \|\Delta^2 u\|^2 \leq ((\Delta f(u), \Delta^2 u)) + c'\|u\|^2 + c'\|h\|^2 + \frac{1}{4}\|\Delta^2 u\|^2, \tag{1.32}$$

where

$$\begin{aligned} ((\Delta f(u), \Delta^2 u)) &\leq \|\Delta f(u)\|\|\Delta^2 u\| \\ &\leq c\|\Delta f(u)\|^2 + \frac{1}{8}\|\Delta^2 u\|^2. \end{aligned} \tag{1.33}$$

We further have (see, e.g., [137])

$$\|\Delta f(u)\|^2 \leq \frac{1}{8}\|\Delta^2 u\|^2 + c'',$$

hence, owing to (1.32) and (1.33),

$$\frac{d}{dt}\|\Delta u\|^2 + \|\Delta^2 u\|^2 \leq c\|u\|^2 + c' \qquad \forall t \geq 0. \tag{1.34}$$

Noting that

$$\begin{aligned} \frac{d}{dt}|\langle u\rangle|^2 &\leq 2|\langle u\rangle|\left|\frac{d}{dt}\langle u\rangle\right| \\ &\leq c|\langle u\rangle|\left|\int_{\Omega\setminus D}(u-h)dx\right| \\ &\leq c'(|\langle u\rangle|^2 + \|u\|^2 + 1), \end{aligned}$$

owing to (1.12), we find

$$\frac{d}{dt}(\|\Delta u\|^2 + |\langle u\rangle|^2) + \|\Delta^2 u\|^2 \leq c(\|u\|^2 + |\langle u\rangle|^2) + c' \qquad \forall t \geq 0, \tag{1.35}$$

and, owing to (1.27) and (1.29), $\exists t_0'$ such that, $\forall t \geq t_0'$, we have

$$|\langle u(t)\rangle| \leq c \quad \text{and} \quad \|\bar{u}(t)\|^2 \leq c, \tag{1.36}$$

where the constant c is independent of u_0 and t, hence

$$\frac{d}{dt}(\|\Delta u\|^2 + |\langle u\rangle|^2) + \|\Delta^2 u\|^2 \leq c \qquad \forall t \geq t_0'. \tag{1.37}$$

We note that, integrating (1.26) over $(t, t+r)$, for $0 < r < 1$ fixed and owing to (1.22), we have, for $t \geq t_0'$,

$$\int_t^{t+r} \|\Delta u\|^2 ds \leq c(r).$$

Finally, using the uniform Gronwall's lemma in (1.37), we deduce that

$$\|u(t)\|^2_{H^2(\Omega)} \leq c \qquad \forall t \geq t_0' + r, \tag{1.38}$$

where c is independent of u_0 and t, for $0 < r < 1$ fixed.

Multiplying (1.14) by $\frac{\partial \bar{u}}{\partial t}$, we have, for $t \geq t_0' + 1$,

$$\left\|\frac{\partial \bar{u}}{\partial t}\right\|^2 + \frac{1}{2}\frac{d}{dt}\|\Delta u\|^2 \leq \left|\left(\left(\Delta f(u), \frac{\partial \bar{u}}{\partial t}\right)\right)\right| + \left|\lambda_0\left(\left(\overline{1_{\Omega\setminus D}(x)(u-h)}, \frac{\partial \bar{u}}{\partial t}\right)\right)\right|. \tag{1.39}$$

Here,

$$\begin{aligned}\left|\lambda_0\left(\left(\overline{1_{\Omega\setminus D}(x)(u-h)}, \frac{\partial \bar{u}}{\partial t}\right)\right)\right| &= \left|\lambda_0\left(\left(1_{\Omega\setminus D}(x)(u-h), \frac{\partial \bar{u}}{\partial t}\right)\right)\right| \\ &\leq c\|u-h\|\left\|\frac{\partial \bar{u}}{\partial t}\right\| \\ &\leq c(\|u\|^2 + \|h\|^2) + \frac{1}{4}\left\|\frac{\partial \bar{u}}{\partial t}\right\|^2.\end{aligned}$$

Furthermore,

$$\begin{aligned}\left|\left(\left(\Delta f(u), \frac{\partial \bar{u}}{\partial t}\right)\right)\right| &\leq \|\Delta f(u)\|\left\|\frac{\partial \bar{u}}{\partial t}\right\| \\ &\leq c\|\Delta f(u)\|^2 + \frac{1}{4}\left\|\frac{\partial \bar{u}}{\partial t}\right\|^2,\end{aligned}$$

and, owing to (1.38), we note that (see, e.g., [132])

$$\|\Delta f(u)\|^2 \leq c\|u\|^2_{H^2(\Omega)}.$$

Thus, owing to (1.38), (1.39) and by the above estimate, we have

$$\frac{d}{dt}\|u\|^2_{H^2(\Omega)} + \left\|\frac{\partial \bar{u}}{\partial t}\right\|^2 \leq c\|u\|^2_{H^2(\Omega)} + c', \quad \forall t \geq t_0' + 1, \tag{1.40}$$

and deduce that

$$\int_t^{t+r} \left\|\frac{\partial \bar{u}}{\partial t}\right\|^2 d\tau \leq c, \quad \forall t \geq t_0' + 1. \tag{1.41}$$

Differentiating (1.14) with respect to time, we rewrite the resulting equation as, setting $\theta = \frac{\partial \bar{u}}{\partial t}$,

$$\frac{\partial \theta}{\partial t} + \Delta^2 \theta - \Delta\Big(f'(u)\frac{\partial u}{\partial t}\Big) + \lambda_0 \overline{1_{\Omega\setminus D}(x)\frac{\partial u}{\partial t}} = 0. \tag{1.42}$$

We multiply (1.42) by θ and have, for $t \geq t_0' + 1$,

$$\frac{1}{2}\frac{d}{dt}\|\theta\|^2 + \|\Delta\theta\|^2 \leq \left|\left(\Big(f'(u)\frac{\partial u}{\partial t}, \Delta\theta\Big)\right)\right| + \left|\lambda_0\left(\Big(\overline{1_{\Omega\setminus D}(x)\frac{\partial u}{\partial t}}, \theta\Big)\right)\right|. \tag{1.43}$$

Here,

$$\begin{aligned}
\left|\lambda_0\left(\Big(\overline{1_{\Omega\setminus D}(x)\frac{\partial u}{\partial t}}, \theta\Big)\right)\right| &= \left|\lambda_0\left(\Big(1_{\Omega\setminus D}(x)\frac{\partial u}{\partial t}, \theta\Big)\right)\right| \\
&\leq c\left\|\frac{\partial u}{\partial t}\right\|\|\theta\| \\
&\leq c(\|\theta\| + \left|\langle\frac{\partial u}{\partial t}\rangle\right|)\|\theta\| \\
&\leq c(\|\theta\|^2 + \left|\langle\frac{\partial u}{\partial t}\rangle\right|^2).
\end{aligned}$$

Furthermore, owing to (1.38) and the continuous embedding $H^2(\Omega) \subset C(\bar{\Omega})$,

$$\begin{aligned}
\left|\left(\Big(f'(u)\frac{\partial u}{\partial t}, \Delta\theta\Big)\right)\right| &\leq \left\|f'(u)\frac{\partial u}{\partial t}\right\|\|\Delta\theta\| \\
&\leq c\left\|\frac{\partial u}{\partial t}\right\|\|\Delta\theta\| \\
&\leq c(\|\theta\|^2 + \left|\langle\frac{\partial u}{\partial t}\rangle\right|^2) + \frac{1}{4}\|\Delta\theta\|^2,
\end{aligned}$$

which yields

$$\frac{d}{dt}\|\theta\|^2 + \|\Delta\theta\|^2 \leq c(\|\theta\|^2 + |\langle\frac{\partial u}{\partial t}\rangle|^2), \quad \forall t \geq t_0' + 1. \tag{1.44}$$

Noting that, using (1.12) and owing to (1.38),

$$\begin{aligned}
\left|\langle\frac{\partial u}{\partial t}\rangle\right|^2 &= \left|\frac{d}{dt}\langle u\rangle\right|^2 \\
&\leq c\|u - h\|^2 \\
&\leq c(\|u\|^2 + \|h\|^2) \\
&\leq c,
\end{aligned} \tag{1.45}$$

we have, owing to (1.44),

$$\frac{d}{dt}\|\theta\|^2 + \|\Delta\theta\|^2 \leq c\|\theta\|^2 + c'. \tag{1.46}$$

Thus, by (1.41), (1.46), and the uniform Gronwall's lemma,

$$\left\|\frac{\partial \bar{u}}{\partial t}\right\|^2 \leq c, \qquad \forall t \geq t_0' + 1 + r, \quad 0 < r < 1. \tag{1.47}$$

We now rewrite (1.3) in the form

$$\Delta^2 u = h_u, \quad \frac{\partial u}{\partial \nu} = \frac{\partial \Delta u}{\partial \nu} = 0 \quad \text{on } \Gamma, \tag{1.48}$$

where

$$h_u = -\frac{\partial u}{\partial t} + \Delta f(u) - \lambda_0 1_{\Omega\setminus D}(x)(u-h) \tag{1.49}$$

satisfies, for $t \geq t_0' + 2$,

$$\|h_u\| \leq c. \tag{1.50}$$

It then follows from (1.50) that

$$\|u\|^2_{H^4(\Omega)} \leq c, \quad \forall t \geq t_0' + 2. \tag{1.51}$$

We note that, integrating (1.46) over $(t, t+r)$, for $0 < r < 1$ fixed, we have, for $t \geq t_0' + 2$,

$$\int_t^{t+r} \|\Delta\theta\|^2 ds \leq c(r). \tag{1.52}$$

Differentiating (1.3) with respect to time, we rewrite the resulting equation as, setting $\Psi = \frac{\partial u}{\partial t}$,

$$\frac{\partial \Psi}{\partial t} + \Delta^2 \Psi - \Delta(f'(u)\Psi) + \lambda_0 1_{\Omega\setminus D}(x)\Psi = 0. \tag{1.53}$$

We multiply (1.53) by $\Delta\Psi$ and have, for $t \geq t_0' + 2$,

$$\begin{aligned} \frac{1}{2}\frac{d}{dt}\|\nabla\Psi\|^2 + \|\nabla\Delta\Psi\|^2 \leq & \left|((\Delta(f'(u)\Psi), \Delta\Psi))\right| \\ & + \left|\lambda_0((1_{\Omega\setminus D}(x)\Psi, \Delta\Psi))\right|. \end{aligned} \tag{1.54}$$

Here,

$$\begin{aligned} \left|\lambda_0((1_{\Omega\setminus D}(x)\Psi, \Delta\Psi))\right| &\leq c\|\Psi\|\|\Delta\Psi\| \\ &\leq c\|\Psi\|^2 + \frac{1}{2}\|\Delta\Psi\|^2. \end{aligned}$$

Furthermore,

$$\begin{aligned} \left|((\Delta(f'(u)\Psi), \Delta\Psi))\right| &= \left|((\nabla(f'(u)\Psi), \nabla\Delta\Psi))\right| \\ &\leq \|\nabla(f'(u)\Psi)\|\|\nabla\Delta\Psi\| \\ &\leq c\|\nabla(f'(u)\Psi)\|^2 + \frac{1}{2}\|\nabla\Delta\Psi\|^2, \end{aligned}$$

and, owing to (1.51),

$$\begin{aligned} \|\nabla(f'(u)\Psi)\|^2 &= \|f''(u)\Psi\nabla u + f'(u)\nabla\Psi\|^2 \\ &\leq c\|\Psi\|^2 + c'\|\nabla\Psi\|^2, \end{aligned}$$

which yields

$$\frac{d}{dt}\|\nabla\Psi\|^2 + \|\nabla\Delta\Psi\|^2 \leq c(\|\Psi\|^2 + \|\nabla\Psi\|^2) + \|\Delta\Psi\|^2 + c''. \tag{1.55}$$

Thus, by (1.45), (1.52), (1.55) and the uniform Gronwall's lemma,

$$\left\|\nabla\frac{\partial u}{\partial t}\right\|^2 \leq c, \quad \forall t \geq t_0' + 2 + r, \quad 0 < r < 1. \tag{1.56}$$

1.5 Existence of the global attractor

We first have the

Proposition 1.5.1. *For every $u_0 \in L^2(\Omega)$ and every $T > 0$, the initial-boundary value problem (1.10) has a unique solution u which belongs to $C([0,T], L^2(\Omega)) \cap L^2(0,T,V) \cap L^4(0,T,L^4(\Omega))$.*

Proof. *See [16], [137], and [114].* □

Proposition 1.5.2. *We have the continuous (with respect to the H^{-1}-norm) semigroup $S(t)$ defined as*

$$S(t) : L^2(\Omega) \to L^2(\Omega), \quad u_0 \to u(t), \qquad t \geq 0.$$

Proof. *Let u_1 and u_2 be two solutions to (1.3)–(1.6) with initial data $u_{0,1}$ and $u_{0,2}$, respectively. We set $u = u_1 - u_2$ and $u_0 = u_{0,1} - u_{0,2}$ and have*

$$\frac{\partial u}{\partial t} + \Delta^2 u - \Delta(f(u_1) - f(u_2)) + \lambda_0 1_{\Omega\setminus D}(x) u = 0, \tag{1.57}$$

$$\frac{\partial u}{\partial \nu} = \frac{\partial \Delta u}{\partial \nu} = 0 \quad on\ \Gamma, \tag{1.58}$$

$$u|_{t=0} = u_0. \tag{1.59}$$

Integrating (1.57) over Ω, we have

$$\frac{d}{dt}\langle u \rangle = -\lambda_0 \int_{\Omega\setminus D} u dx,$$

which yields

$$\frac{\partial \bar{u}}{\partial t} + \Delta^2 u - \Delta(f(u_1) - f(u_2)) + \lambda_0 \overline{1_{\Omega\setminus D}(x) u} = 0. \tag{1.60}$$

Thus,

$$\begin{aligned} \frac{\partial}{\partial t} N(\bar{u}) - \Delta u + f(u_1) - f(u_2) - \langle f(u_1) - f(u_2) \rangle \\ + \lambda_0 N(\overline{1_{\Omega\setminus D}(x) u}) = 0. \end{aligned} \tag{1.61}$$

We multiply (1.61) by $\bar{u}$ and have

$$\begin{aligned} \frac{1}{2}\frac{d}{dt}\|\bar{u}\|_{-1}^2 + \|\nabla u\|^2 + ((f(u_1) - f(u_2), u)) - ((f(u_1) - f(u_2), \langle u \rangle)) \\ + \lambda_0((N(\overline{1_{\Omega\setminus D}(x) u}), \bar{u})) = 0. \end{aligned}$$

Here,

$$\begin{aligned} |\lambda_0((N(\overline{1_{\Omega\setminus D}(x) u}), \bar{u}))| &= \lambda_0 |(1_{\Omega\setminus D}(x) u, N(\bar{u}))| \\ &\leq c\|u\|\|\bar{u}\| \\ &\leq c(\|\bar{u}\|^2 + |\langle u \rangle|\|\bar{u}\|) \\ &\leq c\|\bar{u}\|^2 + c'|\langle u \rangle|^2. \end{aligned}$$

Furthermore,

$$((f(u_1) - f(u_2), u)) \geq -c_1\|u\|^2$$

and

$$\begin{aligned}|((f(u_1) - f(u_2), \langle u\rangle))| &= |\langle u\rangle \int_\Omega u \int_0^1 f'(u_1 + s(u_2 - u_1))dsdx| \\ &\leq c|\langle u\rangle| \int_\Omega (|u_1|^2 + |u_2|^2 + 1)|u|dx \\ &\leq c|\langle u\rangle|(\|u_1\|^2_{L^4(\Omega)} + \|u_2\|^2_{L^4(\Omega)} + 1)\|u\| \\ &\leq c(\|u_1\|^2_{L^4(\Omega)} + \|u_2\|^2_{L^4(\Omega)} + 1)(|\langle u\rangle|^2 + \|\bar{u}\|^2),\end{aligned}$$

which yields

$$\frac{d}{dt}\|\bar{u}\|^2_{-1} + \|\nabla u\|^2 \leq c(\|u_1\|^4_{L^4(\Omega)} + \|u_2\|^4_{L^4(\Omega)} + 1)(\|\bar{u}\|^2_{-1} + |\langle u\rangle|^2), \tag{1.62}$$

owing to the interpolation inequality $\|\bar{u}\|^2 \leq c\|\bar{u}\|_{-1}\|\nabla u\|$. *Noting then that*

$$\begin{aligned}\frac{d}{dt}|\langle u\rangle|^2 &\leq 2|\langle u\rangle|\left|\frac{d}{dt}\langle u\rangle\right| \\ &\leq c|\langle u\rangle\| \int_{\Omega\setminus D} udx| \\ &\leq c|\langle u\rangle|\|u\| \\ &\leq c(|\langle u\rangle|^2 + \|\bar{u}\|^2),\end{aligned} \tag{1.63}$$

it follows that

$$\begin{aligned}\frac{d}{dt}(\|\bar{u}\|^2_{-1} + |\langle u\rangle|^2) + \frac{1}{2}\|\nabla u\|^2 \leq c(\|u_1\|^4_{L^4(\Omega)} + \|u_2\|^4_{L^4(\Omega)} \\ +1)(\|\bar{u}\|^2_{-1} + |\langle u\rangle|^2).\end{aligned} \tag{1.64}$$

We deduce from (1.64), Proposition 3.5.1, and Gronwall's lemma that

$$\begin{aligned}\|u_1(t) - u_2(t)\|_{H^{-1}(\Omega)} \leq Q(T, \|u_{0,1}\|, \|u_{0,2}\|)\|u_{0,1} - u_{0,2}\|_{H^{-1}(\Omega)} \\ 0 \leq t \leq T.\end{aligned} \tag{1.65}$$

□

It follows from (1.51) that $S(t)$ possesses a bounded absorbing set $\mathcal{B}_0'$ which is compact in $L^2(\Omega)$ and bounded in $H^4(\Omega)$. We thus deduce from standard results (see, e.g., [108, 137]) the following theorem.

Theorem 1. *The semigroup $S(t)$ possesses the connected global attractor $\mathcal{A}$ such that $\mathcal{A}$ is compact in $L^2(\Omega)$ and bounded in $H^4(\Omega)$.*

Remark 1.5.3. *It is easy to see that we can assume, without loss of generality, that $\mathcal{B}_0'$ is positively invariant by $S(t)$, i.e. $S(t)\mathcal{B}_0' \subset \mathcal{B}_0'$, $\forall t \geq 0$.*

1.6 Existence of exponential attractors

Let u_1 and u_2 be two solutions of (1.3)–(1.6) with initial data $u_{0,1}$ and $u_{0,2}$, respectively. We again set $u = u_1 - u_2$ and $u_0 = u_{0,1} - u_{0,2}$ and have

$$\frac{\partial u}{\partial t} + \Delta^2 u - \Delta(f(u_1) - f(u_2)) + \lambda_0 1_{\Omega\setminus D}(x)u = 0, \tag{1.66}$$

$$\frac{\partial u}{\partial \nu} = \frac{\partial \Delta u}{\partial \nu} = 0 \quad \text{on } \Gamma, \tag{1.67}$$

$$u|_{t=0} = u_0. \tag{1.68}$$

Furthermore, it is sufficient here to take initial data belonging to the bounded absorbing set $\mathcal{B}_0'$ defined in the previous section.

We rewrite (1.66) as

$$\begin{aligned}\frac{\partial}{\partial t}N(\bar{u}) - \Delta u + f(u_1) - f(u_2) - \langle f(u_1) - f(u_2)\rangle \\ + \lambda_0 N(\overline{1_{\Omega\setminus D}(x)u}) = 0.\end{aligned} \tag{1.69}$$

Multiplying (1.69) by $t\frac{\partial \bar{u}}{\partial t}$, we have

$$\begin{aligned}t\left\|\frac{\partial \bar{u}}{\partial t}\right\|_{-1}^2 + \frac{t}{2}\frac{d}{dt}\|\nabla u\|^2 + t\left(\left(f(u_1) - f(u_2), \frac{\partial \bar{u}}{\partial t}\right)\right) \\ + \lambda_0 t\left(\left(N(\overline{1_{\Omega\setminus D}(x)u}), \frac{\partial \bar{u}}{\partial t}\right)\right) = 0.\end{aligned} \tag{1.70}$$

Here,

$$\begin{aligned}\left|\lambda_0\left(\left((N(\overline{1_{\Omega\setminus D}(x)u}), \frac{\partial \bar{u}}{\partial t}\right)\right)\right| &= \left|\lambda_0\left(\left(1_{\Omega\setminus D}(x)u, N(\frac{\partial \bar{u}}{\partial t})\right)\right)\right| \\ &\le c\|u\|\left\|\frac{\partial \bar{u}}{\partial t}\right\|_{-1},\end{aligned}$$

where the constant c depends only on $\mathcal{B}_0'$. Furthermore,

$$\begin{aligned}\left|\left(\left(f(u_1)-f(u_2), \frac{\partial \bar{u}}{\partial t}\right)\right)\right| &\le c\|\nabla(f(u_1) - f(u_2))\|\left\|\frac{\partial \bar{u}}{\partial t}\right\|_{-1} \\ &\le c\left\|\nabla\Big(\int_0^1 f'(u_1 + s(u_2 - u_1))ds u\Big)\right\|\left\|\frac{\partial \bar{u}}{\partial t}\right\|_{-1} \\ &\le c\left\|\int_0^1 f'(u_1 + s(u_2 - u_1))ds\nabla u\right\|\left\|\frac{\partial \bar{u}}{\partial t}\right\|_{-1} \\ &\quad + c\left\|u\int_0^1 f''(u_1 + s(u_2 - u_1))(\nabla u_1 + s(\nabla u_2 - \nabla u_1))ds\right\|\left\|\frac{\partial \bar{u}}{\partial t}\right\|_{-1} \\ &\le c(\|\nabla u\| + \|u\nabla u_1\| + \|u\nabla u_2\|)\left\|\frac{\partial \bar{u}}{\partial t}\right\|_{-1} \\ &\le c\|u\|_{H^1(\Omega)}\left\|\frac{\partial \bar{u}}{\partial t}\right\|_{-1},\end{aligned}$$

where the constant c depends only on $\mathcal{B}_0'$, which yields

$$t\frac{d}{dt}\|\nabla u\|^2 + ct\left\|\frac{\partial \bar{u}}{\partial t}\right\|_{-1}^2 \le c' t\|u\|_{H^1(\Omega)}^2, \tag{1.71}$$

and, owing to (1.63), we find

$$\frac{d}{dt}(t\|\nabla u\|^2 + t|\langle u(t)\rangle|^2) + ct\left\|\frac{\partial \bar{u}}{\partial t}\right\|_{-1}^2 \le c' t(\|u\|_{H^1(\Omega)}^2 + |\langle u(t)\rangle|^2) + c''(\|\nabla u\|^2 + |\langle u(t)\rangle|^2),$$

hence

$$\frac{d}{dt}(t\|u\|_{H^1(\Omega)}^2) + ct\left\|\frac{\partial \bar{u}}{\partial t}\right\|_{-1}^2 \le c' t\|u\|_{H^1(\Omega)}^2 + c''\|u\|_{H^1(\Omega)}^2. \tag{1.72}$$

We note that, integrating (1.64) over $(0, t)$, we have

$$\int_0^t \|\nabla u\|^2 ds \le ce^{\alpha t}\|u_{0,1} - u_{0,2}\|_{H^{-1}(\Omega)}^2, \tag{1.73}$$

where the constant α depends only on $\mathcal{B}_0'$, hence

$$\int_0^t \|u\|_{H^1(\Omega)}^2 ds \le ce^{\alpha t}\|u_{0,1} - u_{0,2}\|_{H^{-1}(\Omega)}^2. \tag{1.74}$$

By (1.72), (1.74), and Gronwall's lemma, we obtain

$$\|u_1 - u_2\|_{H^1(\Omega)}^2 \le \frac{c}{t}e^{\alpha t}\|u_{0,1} - u_{0,2}\|_{H^{-1}(\Omega)}^2 \quad \forall t > 0. \tag{1.75}$$

Now multiplying (1.69) by $\frac{\partial \bar{u}}{\partial t}$, we obtain, proceeding as above,

$$\frac{d}{dt}(\|\nabla u\|^2 + |\langle u\rangle|^2) + \left\|\frac{\partial \bar{u}}{\partial t}\right\|_{-1}^2 \le c(\|\nabla u\|^2 + |\langle u\rangle|^2), \tag{1.76}$$

where the constant c depends only on $\mathcal{B}_0'$. Therefore, integrating (1.76) over $(1, t)$ and owing to (1.75) (for t = 1), we have

$$\int_1^t \left\|\frac{\partial \bar{u}}{\partial t}\right\|_{H^{-1}(\Omega)}^2 d\tau \le ce^{\alpha t}\|u_{0,1} - u_{0,2}\|_{H^{-1}(\Omega)}^2, \tag{1.77}$$

where the constant c depends only on $\mathcal{B}_0'$.

We note that, integrating (1.66) over $(0, t)$, we easily obtain

$$\int_0^t \langle\frac{\partial u}{\partial t}\rangle^2 d\tau \le ce^{\alpha t}\|u_{0,1} - u_{0,2}\|_{H^{-1}(\Omega)}^2, \tag{1.78}$$

where the constant c depends only on $\mathcal{B}_0'$.

Differentiating (1.69) with respect to time, we find

$$\begin{aligned}\frac{\partial}{\partial t}N(\theta) - \Delta\theta + l(t)\frac{\partial u}{\partial t} + l'(t)u - \langle\frac{\partial}{\partial t}l(t)u\rangle \\ + \lambda_0 N\Big(\overline{1_{\Omega\setminus D}(x)\frac{\partial u}{\partial t}}\Big) = 0,\end{aligned} \tag{1.79}$$

where $l(t) = \int_0^1 f'(u_1 + s(u_2 - u_1))ds$ and $\theta = \frac{\partial \bar{u}}{\partial t}$.

We multiply (1.79) by $(t-1)\theta$ and have

$$\begin{aligned}\frac{t-1}{2}\frac{d}{dt}\|\theta\|_{-1}^2 + (t-1)\|\nabla\theta\|^2 + (t-1)((l(t)\frac{\partial u}{\partial t},\theta)) + (t-1)((l'(t)u,\theta)) \\ +\lambda_0(t-1)((N\Big(\overline{1_{\Omega\setminus D}(x)\frac{\partial u}{\partial t}}\Big),\theta)) = 0.\end{aligned} \tag{1.80}$$

Here,

$$\begin{aligned}\Big|\lambda_0((N\Big(\overline{1_{\Omega\setminus D}(x)\frac{\partial u}{\partial t}}\Big),\theta))\Big| &= \Big|\lambda_0((1_{\Omega\setminus D}(x)\frac{\partial u}{\partial t}, N(\theta)))\Big| \\ &\le c\Big\|\frac{\partial u}{\partial t}\Big\|\|\theta\|_{-1} \\ &\le c\Big(\|\theta\|^2 + \Big|\langle\frac{\partial u}{\partial t}\rangle\Big|^2\Big) + c'\|\theta\|_{-1}^2 \\ &\le c\Big(\|\theta\|_{-1}^2 + \Big|\langle\frac{\partial u}{\partial t}\rangle\Big|^2\Big) + c'\|\nabla\theta\|^2,\end{aligned}$$

owing to the above estimates and a proper interpolation inequality. Furthermore, owing to (1.51),

$$\begin{aligned}\Big\|((l(t)\frac{\partial u}{\partial t},\theta))\Big\| &\le c\Big\|\nabla\Big(l(t)\frac{\partial u}{\partial t}\Big)\Big\|\|\theta\|_{-1} \\ &\le c(\|l\|_{L^\infty(\Omega)} + \|\nabla l\|_{L^4(\Omega)})\Big\|\frac{\partial u}{\partial t}\Big\|_{H^1(\Omega)}\|\theta\|_{-1} \\ &\le c\Big(\|\nabla\theta\| + \Big|\langle\frac{\partial u}{\partial t}\rangle\Big|\Big)\|\theta\|_{-1}\end{aligned}$$

and, owing to (1.47) and (1.56),

$$\begin{aligned}\|l'(t)u\| &= \|\int_0^1 f''(u_1 - s(u_2-u_1))(\frac{\partial u_1}{\partial t} + s(\frac{\partial u_2}{\partial t} - \frac{\partial u_1}{\partial t}))dsu\| \\ &\le c(\|\frac{\partial u_1}{\partial t}\|_{L^4(\Omega)} + \|\frac{\partial u_2}{\partial t}\|_{L^4(\Omega)})\|u\|_{L^4(\Omega)} \\ &\le c(\|\frac{\partial u_1}{\partial t}\|_{H^1(\Omega)} + \|\frac{\partial u_2}{\partial t}\|_{H^1(\Omega)})\|u\|_{H^1(\Omega)} \\ &\le c\|u\|_{H^1(\Omega)},\end{aligned}$$

which yields

$$\begin{aligned}\frac{d}{dt}((t-1)(\|\theta\|_{-1}^2 + \Big|\langle\frac{\partial u}{\partial t}\rangle\Big|^2)) + (t-1)\|\theta\|_{H^1(\Omega)}^2 \le c(t-1)(\|\theta\|_{-1}^2 + \\ \Big|\langle\frac{\partial u}{\partial t}\rangle\Big|^2) + \|\theta\|_{-1}^2 + \Big|\langle\frac{\partial u}{\partial t}\rangle\Big|^2 + c'(t-1)\|u\|_{H^1(\Omega)}^2.\end{aligned} \tag{1.81}$$

We thus deduce from (1.74), (1.75), (1.77), (1.78), and Gronwall's lemma that

$$\|\theta(t)\|^2_{H^{-1}(\Omega)} \le \frac{c}{t-1} e^{\alpha t} \|u_0\|^2_{H^{-1}(\Omega)}, \qquad \forall t > 1. \tag{1.82}$$

We finally rewrite (1.69) in the form

$$-\Delta u = \tilde{h}_u, \quad \frac{\partial u}{\partial \nu} = 0 \quad \text{on } \Gamma, \tag{1.83}$$

where

$$\begin{aligned} \tilde{h}_u = -N\Big(\frac{\partial \bar{u}}{\partial t}\Big) - (f(u_1) - f(u_2)) + \langle f(u_1) - f(u_2)\rangle \\ - \lambda_0 N\Big(\overline{1_{\Omega\setminus D}(x) u}\Big) \end{aligned} \tag{1.84}$$

satisfies

$$\|\tilde{h}_u\| \le c\Big(\Big\|\frac{\partial \bar{u}}{\partial t}\Big\|_{-1} + \|u\|_{H^1(\Omega)}\Big), \tag{1.85}$$

where the constant c depends only on $\mathcal{B}'_0$. It then follows from (1.75), (1.82), (1.85), and standard elliptic regularity results that

$$\|u_1(t) - u_2(t)\|_{H^2(\Omega)} \le \frac{c}{\sqrt{t-1}} e^{c' t} \|u_{0,1} - u_{0,2}\|_{H^{-1}(\Omega)}, \quad c, c' \ge 0, \ \ t > 1, \tag{1.86}$$

where the constant c depends only on $\mathcal{B}'_0$.

Next, we derive a Hölder (both with respect to space and time) estimate.
Actually, owing to (1.65), it suffices to prove the Hölder continuity with respect to time. We have

$$\begin{aligned} \|u(t_1) - u(t_2)\|_{H^{-1}(\Omega)} &= \Big\| \int_{t_1}^{t_2} \frac{\partial u}{\partial t} d\tau \Big\|_{H^{-1}(\Omega)} \le \Big| \int_{t_1}^{t_2} \Big\| \frac{\partial u}{\partial t} \Big\|_{H^{-1}(\Omega)} d\tau \Big| \\ &\le |t_1 - t_2|^{\frac{1}{2}} \Big| \int_{t_1}^{t_2} \Big\| \frac{\partial u}{\partial t} \Big\|^2_{H^{-1}(\Omega)} d\tau \Big|^{\frac{1}{2}}, \end{aligned} \tag{1.87}$$

where u is solution of (1.3)–(1.6)–(1.7).

We note that, owing to (1.40),

$$\Big| \int_{t_1}^{t_2} \Big\| \frac{\partial \bar{u}}{\partial t} \Big\|^2_{H^{-1}(\Omega)} d\tau \Big| \le c, \tag{1.88}$$

where the constant c depends only on $\mathcal{B}'_0$ and T such that $t_1, t_2 \in [0, T]$, so that

$$\|u(t_1) - u(t_2)\|_{H^{-1}(\Omega)} \le c|t_1 - t_2|^{\frac{1}{2}}, \tag{1.89}$$

where the constant c depends only on $\mathcal{B}'_0$ and T such that $t_1, t_2 \in [0, T]$.

We finally deduce from (1.65), (1.86), and (1.89) the following result (see, e.g., [53, 52]).

Theorem 2. *The semigroup $S(t)$ possesses an exponential attractor $\mathcal{M} \subset \mathcal{B}'_0$, i.e.*
(i) $\mathcal{M}$ is compact in $H^{-1}(\Omega)$;
(ii) $\mathcal{M}$ is positively invariant, $S(t)\mathcal{M} \subset \mathcal{M}$, $\forall t \ge 0$;
(iii) $\mathcal{M}$ has finite fractal dimension in $H^{-1}(\Omega)$;

(iv) $\mathcal{M}$ *attracts exponentially fast the bounded subsets of* $L^2(\Omega)$*,*

$$\forall B \subset L^2(\Omega) \text{ bounded}, \quad dist_{H^{-1}(\Omega)}(S(t)B, \mathcal{M}) \leq Q(\|B\|_{L^2(\Omega)})e^{-ct}, \quad c > 0, \ \ t \geq 0,$$

where the constant c *is independent of* B *and* $dist_{H^{-1}(\Omega)}$ *denotes the Hausdorff semidistance between sets defined by*

$$dist_{H^{-1}(\Omega)}(A, B) = \sup_{a \in A} \inf_{b \in B} \|a - b\|_{H^{-1}(\Omega)}.$$

Remark 1.6.1. *Setting* $\tilde{\mathcal{M}} = S(1)\mathcal{M}$*, we can prove that* $\tilde{\mathcal{M}}$ *is an exponential attractor for* $S(t)$*, but now in the topology of* $L^2(\Omega)$ *(see, e.g., [54]).*

Since $\mathcal{M}$ (or $\tilde{\mathcal{M}}$) is a compact attracting set, we deduce from Theorem 2 the following corollary.

Corollary 1. *The semigroup* $S(t)$ *possesses the finite-dimensional global attractor* $\mathcal{A} \subset \mathcal{B}_0'$*.*

Remark 1.6.2. *We can more generally consider a nonlinear term* f *of the form*

$$f(s) = \sum_{k=0}^{2p+1} a_k s^k, \ \ a_{2p+1} > 0$$

(see [42]).

Remark 1.6.3. *We studied the (global) dynamics of the system when* λ_0 *is constant and* $\varepsilon = 1$*. More generally, all constants here and in the previous sections depend on* λ_0 *and* ε *and grow as these quantities go to* $+\infty$ *and* 0*, respectively. In particular, the dependence on* λ_0 *is an important issue in view of inpainting applications (see [16]) and a natural question is whether one can have an upper bound on the dimension of the global attractor which is independent of this quantity (here, as already mentioned, the upper bound that we obtain explodes as* λ_0 *goes to* $+\infty$*). A natural (but involved, see, e.g., [137]) problem would be to find a lower bound on this dimension (possibly, in terms of* λ_0*). This will be investigated elsewhere.*

1.7 Numerical simulations

As far as the numerical simulations are concerned, we rewrite the problem in the form

$$\frac{\partial u}{\partial t} + \Delta \mu + \lambda_0 1_{\Omega \setminus D}(x)(u - h) = 0 \quad \text{in } \Omega, \tag{1.90}$$

$$\mu = \varepsilon \Delta u - \frac{1}{\varepsilon} f(u) \quad \text{in } \Omega, \tag{1.91}$$

$$\frac{\partial u}{\partial \nu} = \frac{\partial \mu}{\partial \nu} = 0 \quad \text{on } \Gamma, \tag{1.92}$$

$$u_{|t=0} = u_0, \tag{1.93}$$

which has the advantage of splitting the fourth-order (in space) equation into a system of two second-order ones (see [55] and [43]). Consequently, we use a P1-finite element for the space discretization, together with a semi-implicit Euler time disretization (i.e. implicit for the linear terms and explicit for the nonlinear ones). The numerical simulations are performed with the software Freefem++ [67].

In the numerical results presented below, Ω is a $(0, 0.5) \times (0, 0.5)$-square. The triangulation is obtained by dividing Ω into 120×120 rectangles and by dividing every rectangle along the same diagonal.

1.7.1 Inpainting of a triangle

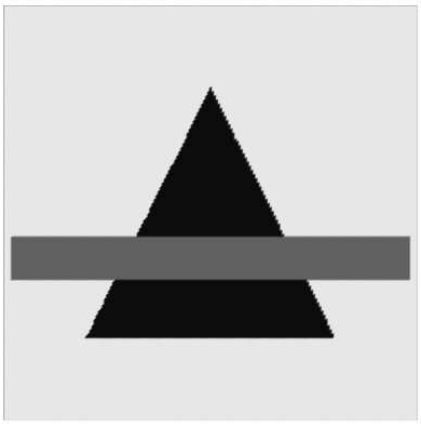

(a)

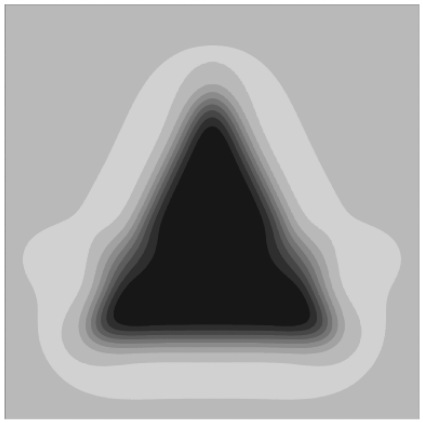

(b)

(c)

FIGURE 1.1 – (a) Inpainting region in gray, random initial datum between 0 and 1 in inpainting region, $\varepsilon = 0.03$, $f(s) = s^3 - s$. (b) Solution at $t = 1$. (c) Replacing the values larger than $\frac{1}{2}$ by 1 and those smaller than $\frac{1}{2}$ by 0.

The gray region in Figure 1.1(a) denotes the inpainting region. We run the modified Cahn-

Hilliard equation with $f(s) = s^3 - s$, $\varepsilon = 0.03$ and, at $t = 1$, we come close to a steady state, shown in Figure 1.1(b). We finally replace all the values larger than $\frac{1}{2}$ by 1 and all those smaller than $\frac{1}{2}$ by 0 to obtain the final inpainting result in Figure 1.1(c). The parameters are $\Delta t = 0.05$, $\lambda_0 = 900000$.

1.7.2 Inpainting of four 3/4 circles

In Figure 1.2(a), the gray region denotes the region to be inpainted. The modified Cahn-Hilliard equation is run close to a steady state with $\varepsilon = 0.05$ and $f(s) = s^3 - s$, resulting in Figure 1.2(b) at $t = 1.25$. We replace all the values larger than $\frac{1}{2}$ by 1 and all those smaller than $\frac{1}{2}$ by 0 to obtain the final inpainting result in Figure 1.2(c).

Furthermore, we run again the modified Cahn–Hilliard equation with the same initial datum as in Figure 1.2(a) and the same $\varepsilon = 0.05$, but we now take $f(s) = 4s^3 - 6s^2 + 2s$. We are close to a steady state at $t = 1.25$, as shown in Figure 1.2(d). As above, we replace all the values larger than $\frac{1}{2}$ by 1 and all those smaller than $\frac{1}{2}$ by 0 to obtain the final inpainting in Figure 1.2(e). We finally deduce that, in the inpainting of a circle, the result obtained is better when considering the function $f(s) = 4s^3 - 6s^2 + 2s$ than $f(s) = s^3 - s$. In this test, $\Delta t = 0.05$, $\lambda_0 = 900000$.

Remark 1.7.1. *As mentioned in the introduction, the one step algorithm is not always relevant. To illustrate this, we take in Figure 3.3 an example of a broken bar for which we obtain good results with the one step algorithm with* $\varepsilon = 0.05$. *Here,* $\lambda_0 = 100000$ *and* $\Delta t = 0.05$. *Then, we enlarge the inpainting region and see that, for the same parameters, the one step algorithm fails.*

Acknowledgments

The authors wish to thank S. Zelik for several useful comments. They also wish to thank the anonymous referee for her/his careful reading of the manuscript and useful suggestions.

Received August 2013 ; revised May 2014.
E-mail address : Laurence.Cherfils@univ-lr.fr
E-mail address : Hussein.Fakih@math.univ-poitiers.fr
E-mail address : Alain.Miranville@math.univ-poitiers.fr

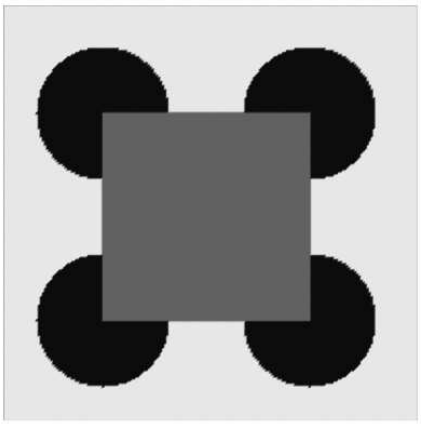

(a)

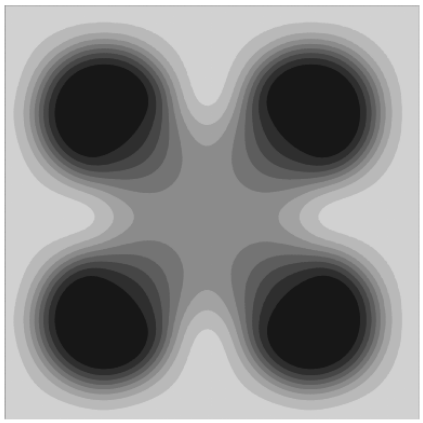

(b)

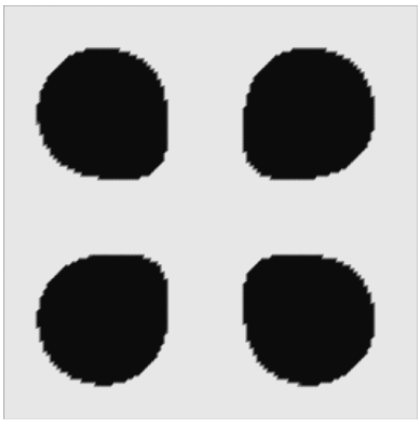

(c)

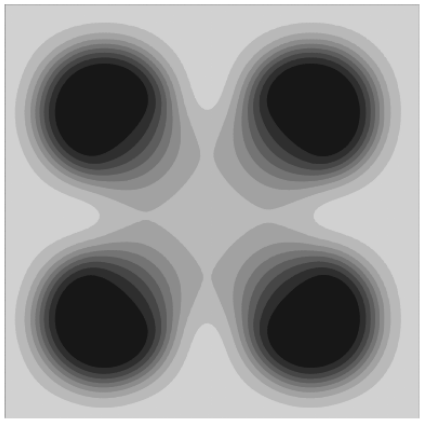

(d)

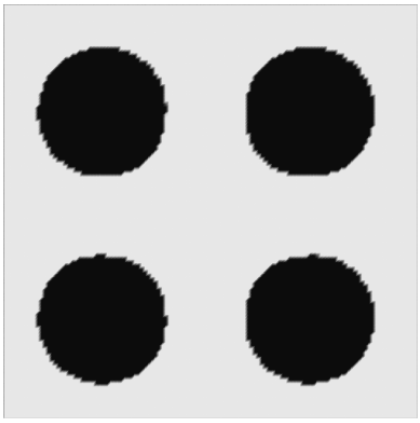

(e)

FIGURE 1.2 – (a) Inpainting region in gray, random initial datum between 0 and 1 in inpainting region, $\varepsilon = 0.05$, $f(s) = s^3 - s$. (b) Solution at $t = 1.25$. (c) Replacing the values larger than $\frac{1}{2}$ by 1 and those smaller than $\frac{1}{2}$ by 0. (d) Solution at $t = 1.25$ when $f(s) = 4s^3 - 6s^2 + 2s$. (e) Replacing the values larger than $\frac{1}{2}$ by 1 and those smaller than $\frac{1}{2}$ by 0.

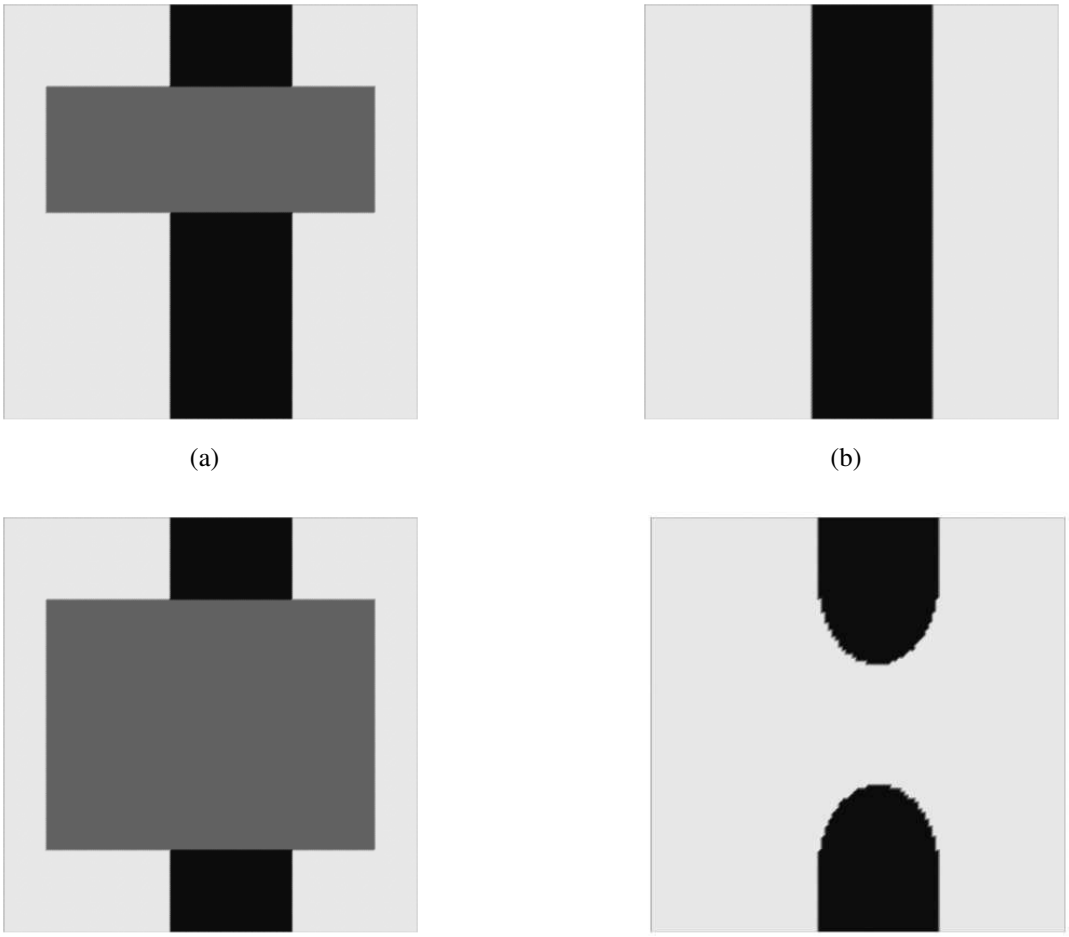

(a) (b)

(c) (d)

FIGURE 1.3 – (a) Inpainting region in gray, random initial datum between 0 and 1 in inpainting region. (b) Solution (close to a steady state) at $t = 2$ with $\Delta t = 0.05$ and $\varepsilon = 0.05$. Here, $f(s) = 4s^3 - 6s^2 + 2s$. (c) Larger inpainting region in gray, random initial datum between 0 and 1 in inpainting region. (d) Solution (close to a steady state) at $t = 10.2$ with $\Delta t = 0.05$ and $\varepsilon = 0.05$. Here, $f(s) = 4s^3 - 6s^2 + 2s$.

Chapitre 2

On the Bertozzi–Esedoglu–Gillette–Cahn–Hilliard equation with logarithmic nonlinear terms

Sur l'équation de Bertozzi–Esedoglu–Gillette–Cahn–Hilliard avec un terme non linéaire logarithmique

Ce chapitre est constitué de l'article **On the Bertozzi–Esedoglu–Gillette–Cahn–Hilliard equation with logarithmic nonlinear terms**, SIAM J. Imag. Sci. 8 (2015), 1123–1140. Cet article est écrit en collaboration avec **Laurence Cherfils** et **Alain Miranville**.

SIAM J. Imaging Sciences
Volume 8, No. 2, pp. 1123–1140

On the Bertozzi–Esedoglu–Gillette–Cahn–Hilliard equation with logarithmic nonlinear terms

LAURENCE CHERFILS[1], HUSSEIN FAKIH[2] AND ALAIN MIRANVILLE[2]

[1] Université de la Rochelle
Laboratoire Mathématiques, Image et Applications
Avenue Michel Crépeau
F-17042 La Rochelle Cedex, France
E-mail address : lcherfil@univ-lr.fr

[2] Université de Poitiers
Laboratoire de Mathématiques et Applications
UMR CNRS 7348 - SP2MI
Boulevard Marie et Pierre Curie - Téléport 2
F-86962 Chasseneuil Futuroscope Cedex, France
E-mail address : Hussein.Fakih@math.univ-poitiers.fr
E-mail address : Alain.Miranville@math.univ-poitiers.fr

Abstract : Our aim in this paper is to study the existence of local (in time) solutions for the Bertozzi-Esedoglu-Gillette-Cahn-Hilliard equation with logarithmic nonlinear terms. This equation was proposed in view of applications to binary image inpainting. We also give some numerical simulations which show the efficiency of the model.

Keywords : Bertozzi-Esedoglu-Gillette-Cahn-Hilliard equation, logarithmic nonlinear term, local existence, simulations.
AMS Subject Classification : 35B45, 35K55

2.1 Introduction

The Cahn-Hilliard equation plays an important role in materials science and describes phase separation processes. This can be observed, e.g., when a binary alloy is cooled down sufficiently. One then observes a partial nucleation (i.e., the apparition of nucleides in the material) or a total nucleation, the so-called spinodal decomposition : the material quickly becomes inhomogeneous, forming a fine-grained structure in which each of the two components appears more or

less alternatively. In a second stage, which is called coarsening and occurs at a slower time scale, these microstructures coarsen. Such phenomena play an essential role in the mechanical properties of the material, e.g., strength. We refer the reader to, e.g., [26], [27], [41], [56], [92], [96], [99], [100], [116] and [117] for more details.

It is also interesting to note that the Cahn-Hilliard equation, or some of its variants, is relevant in other contexts, in which phase separation and coarsening/clustering processes can be observed or come into play. We can mention, for instance, population dynamics (see [45]), bacterial films (see [91]), wound healing and tumor growth (see [42], [88] and [104]), thin films (see [123] and [138]), image processing and inpainting (see [16], [17], [25], [29], [38] and [51]) and even the rings of Saturn (see [139]) and the clustering of mussels (see [98]).

In particular, in [16] and [17], the authors proposed the following variant of the Cahn-Hilliard equation :

$$\frac{\partial u}{\partial t} + \epsilon\Delta^2 u - \frac{1}{\epsilon}\Delta f(u) + \lambda_0\chi_{\Omega\setminus D}(u-h) = 0,\ \epsilon > 0,\ \lambda_0 > 0, \tag{2.1}$$

in view of applications to binary image inpainting. Here, $h = h(x)$ is a given (damaged) image and $D \subset \Omega$ is the inpainting region (Ω is the total region). Furthermore, the term $\lambda_0\chi_{\Omega\setminus D}(u-h)$, called fidelity term, is added in order to keep the solution u close to the image h outside the damaged region (χ denotes the indicator function). Finally, the nonlinear term f is regular and cubic, typically, $f(s) = 4s^3 - 6s^2 + 2s$. The idea in this model is to solve (2.1) up to steady state in order to obtain an inpainted version $u(x)$ of $h(x)$.

This equation was studied, endowed with Neumann boundary conditions, in [16], [25] and [38]. In particular, one has well-posedness and regularity results, as well as the existence of finite-dimensional attractors. Furthermore, numerical simulations were given. In particular, the simulations in [38] show that, in some situations, a dynamic one step scheme with threshold involving the diffuse interface thickness ϵ (we note that, in [16] and [17], the authors first considered a large value of ϵ and then a smaller one in order to obtain their numerical simulations) allows to connect regions across large inpainting domains.

Our aim in this paper is to consider (2.1) now with logarithmic nonlinear terms f (note indeed that the original Cahn-Hilliard equation was actually proposed with thermodynamically relevant logarithmic nonlinear terms which follow from a mean-field model ; regular (and, in particular, cubic) nonlinear terms are approximations of such logarithmic nonlinear terms).

The Bertozzi–Esedoglu–Gillette–Cahn–Hilliard equation, with logarithmic nonlinearities and Neumann boundary conditions, appears to be much more complicated, from a mathematical point of view, than the Cahn-Hilliard equation. Consequently, we are only able to prove the local (in time) existence of solutions.

We also give some numerical simulations which confirm that the one step algorithm with threshold proposed in [38] is efficient. Actually, in that case, we can obtain better results, when using logarithmic nonlinear terms, than those obtained with polynomial nonlinear terms, as far as the convergence time is concerned. Furthermore, we give an example for which the one step algorithm gives much better results when considering a logarithmic nonlinearity.

Notation : We denote by $((\cdot,\cdot))$ the usual L^2-scalar product, with associated norm $\|\cdot\|$. We further set $\|\cdot\|_{-1} = \|(-\Delta)^{-\frac{1}{2}}\cdot\|$, where $(-\Delta)^{-1}$ denotes the inverse minus Laplace operator associated with Neumann boundary conditions and acting on functions with null spatial average.

More generally, $\|\cdot\|_X$ denotes the norm on the Banach space X.

Throughout the paper, the same letters c and c' denote (generally positive) constants which may vary from line to line.

2.2 Setting of the problem

We consider the following initial and boundary value problem in a bounded and regular domain $\Omega \subset \mathbb{R}^n$, $n = 1, 2$ or 3, with boundary Γ :

$$\frac{\partial u}{\partial t} + \Delta^2 u - \Delta f(u) + \chi_{\Omega\setminus D}(x)(u - h) = 0, \tag{2.2}$$

$$\frac{\partial u}{\partial \nu} = \frac{\partial \Delta u}{\partial \nu} = 0 \text{ on } \Gamma, \tag{2.3}$$

$$u|_{t=0} = u_0, \tag{2.4}$$

where $D \Subset \Omega$ (for simplicity, we have set all constants in (2.1) equal to one).

We assume that $h \in L^2(\Omega)$ and

$$\int_{\Omega\setminus D} h\, dx = 0. \tag{2.5}$$

Remark 2.2.1. *We need* (2.5) *in view of the mathematical analysis of the problem. However, this condition is not necessary for the numerical simulations below.*

Furthermore, as far as the nonlinear term f is concerned, we assume that

$$f = F', \text{ where } F(s) = \frac{\lambda_1}{2}(1 - s^2) + \frac{\lambda_2}{2}((1 - s)\ln\frac{1 - s}{2} + (1 + s)\ln\frac{1 + s}{2}), \tag{2.6}$$

$$0 < \lambda_2 < \lambda_1,\ s \in (-1, 1),$$

$$\text{hence } f(s) = -\lambda_1 s + \frac{\lambda_2}{2}\ln\frac{1 + s}{1 - s},\ s \in (-1, 1).$$

Moreover, there holds

$$f' \geq -\lambda_1. \tag{2.7}$$

Writing $F(s) = \frac{\lambda_1}{2}(1 - s^2) + F_1(s)$ and $f_1 = F_1'$, we introduce, following [68] and for $N \in \mathbb{N}$, the approximated function $F_{1,N} \in C^4(\mathbb{R})$ defined by

$$F_{1,N}^{(4)}(s) = \begin{cases} F_1^{(4)}(1 - \frac{1}{N}),\ s \geq 1 - \frac{1}{N}, \\ F_1^{(4)}(s),\ |s| \leq 1 - \frac{1}{N}, \\ F_1^{(4)}(-1 + \frac{1}{N}),\ s \leq -1 + \frac{1}{N}, \end{cases} \tag{2.8}$$

$$F_{1,N}^{(k)}(0) = F_1^{(k)}(0),\ k = 0,\ 1,\ 2,\ 3, \tag{2.9}$$

so that

$$F_{1,N}(s) = \begin{cases} \sum_{k=0}^{4} \frac{1}{k!} F_1^{(k)}(1-\frac{1}{N})(s-1+\frac{1}{N})^k, \ s \geq 1-\frac{1}{N}, \\ F_1(s), \ |s| \leq 1-\frac{1}{N}, \\ \sum_{k=0}^{4} \frac{1}{k!} F_1^{(k)}(-1+\frac{1}{N})(s+1-\frac{1}{N})^k, \ s \leq -1+\frac{1}{N}. \end{cases} \tag{2.10}$$

Setting $F_N(s) = \frac{\lambda_1}{2}(1-s^2) + F_{1,N}(s)$, $f_{1,N} = F'_{1,N}$ and $f_N = F'_N$, there holds

$$f'_{1,N} \geq 0, \ f'_N \geq -\lambda_1, \tag{2.11}$$

$$F_N \geq -c_1, \ c_1 \geq 0, \tag{2.12}$$

and (see [68] and [109])

$$f_N(s)s \geq c_2(F_N(s) + |f_N(s)|) - c_3, \ c_2 > 0, \ c_3 \geq 0, \ s \in \mathbb{R}, \tag{2.13}$$

where the constants c_i, $i = 1$, 2 and 3, are independent of N, for N large enough. We further have the

Proposition 2.2.2. *There holds, for N large enough,*

$$(f_N(s+a) - f_N(a))s \geq c_4(s^4 + a^2 s^2) - c_5, \ c_4 > 0, \ c_5 \geq 0, \ s, \ a \in \mathbb{R}, \tag{2.14}$$

where the constants c_4 and c_5 are independent of N.

Proof. *Note that it suffices to prove* (2.14) *for $f_{1,N}$. Furthermore, all constants below are independent of N.*

Case 1 : $s + a \geq 1 - \frac{1}{N}$, $a \geq 1 - \frac{1}{N}$.

We have, in that case and for N large enough,

$$(f_{1,N}(s+a) - f_{1,N}(a))s = s\sum_{k=0}^{3} \frac{1}{k!} f_1^{(k)}(1-\frac{1}{N})((s+a-1+\frac{1}{N})^k - (a-1+\frac{1}{N})^k)$$

$$\geq \frac{1}{6}((s+a-1+\frac{1}{N})^3 - (a-1+\frac{1}{N})^3)s.$$

Here and below, we use the facts that $f_1^{(k)}(1-\frac{1}{N}) \geq 0$, $k = 0, ..., 3$, and $\lim_{N\to+\infty} f_1'''(1-\frac{1}{N}) = +\infty$. It then follows from [38] that

$$(f_{1,N}(s+a) - f_{1,N}(a))s \geq c(s^4 + s^2(a-1+\frac{1}{N})^2) - c'$$

$$\geq c(s^4 + a^2 s^2) - c', \ c > 0,$$

noting that $|1 - \frac{1}{N}| \leq 1$.

Case 2 : $s + a \geq 1 - \frac{1}{N}$, $|a| \leq 1 - \frac{1}{N}$.

Note that, in that case, $s \geq 1 - \frac{1}{N} - a \geq 0$. *Furthermore,*

$$(f_{1,N}(s+a) - f_{1,N}(a))s = (\sum_{k=0}^{3} \frac{1}{k!} f_1^{(k)}(1 - \frac{1}{N})(s + a - 1 + \frac{1}{N})^k - f_1(a))s.$$

Noting that $f_1(1 - \frac{1}{N}) \geq f_1(a)$ *and that* $|a| \leq 1$, *we obtain, for N large enough,*

$$(f_{1,N}(s+a) - f_{1,N}(a))s \geq \frac{1}{6}(s + a - 1 + \frac{1}{N})^3 s$$

$$\geq \frac{1}{6}(s-2)^3 s \geq cs^4 - c'$$

$$\geq c(s^4 + a^2 s^2) - c',\ c > 0.$$

Case 3 : $s + a \geq 1 - \frac{1}{N}$, $a \leq -1 + \frac{1}{N}$.

Noting that $f_1(-s) = -f_1(s)$, *we have*

$$(f_{1,N}(s+a) - f_{1,N}(a))s = (2f_1(1 - \frac{1}{N}) + f_1'(1 - \frac{1}{N})(s - 2 + \frac{2}{N})$$

$$+\frac{1}{2}f_1''(1 - \frac{1}{N})((s + a - 1 + \frac{1}{N})^2 + (a + 1 - \frac{1}{N})^2) + \frac{1}{6}f_1'''(1 - \frac{1}{N})(s + a - 1 + \frac{1}{N})^3 - (a + 1 - \frac{1}{N})^3)s.$$

Therefore, noting that $s \geq 1 - \frac{1}{N} - a \geq 2 - \frac{2}{N}$ *and* $a \leq 0$, *we find, owing again to [38] and for N large enough,*

$$(f_{1,N}(s+a) - f_{1,N}(a))s \geq \frac{1}{6}((s + a - 1 + \frac{1}{N})^3 - (a + 1 - \frac{1}{N})^3)s$$

$$\geq \frac{1}{12}((s+a)^3 - a^3)s - cs$$

$$\geq c(s^4 + a^2 s^2) - c',\ c > 0.$$

Case 4 : $|s + a| \leq 1 - \frac{1}{N}$, $|a| \leq 1 - \frac{1}{N}$.

In that case, we have, noting that $f_1' \geq 0$,

$$(f_{1,N}(s+a) - f_{1,N}(a))s \geq 0 \geq K(s^4 + a^2 s^2) - c_K,\ \forall K > 0,$$

since $|a| \leq 1$ *and* $|s| \leq 2$.

Case 5 : $|s + a| \leq 1 - \frac{1}{N}$, $a \geq 1 - \frac{1}{N}$.

Note that, in that case, $s \leq 1 - \frac{1}{N} - a \leq 0$ *and, as* $s \to -\infty$, $a \sim -s$. *Furthermore, for N large enough,*

$$(f_{1,N}(s+a) - f_{1,N}(a))s = (f_1(s+a) - f_1(1 - \frac{1}{N}) - f_1'(1 - \frac{1}{N})(a - 1 + \frac{1}{N})$$

$$-\frac{1}{2}f_1''(1-\frac{1}{N})(a-1+\frac{1}{N})^2-\frac{1}{6}f_1'''(1-\frac{1}{N})(a-1+\frac{1}{N})^3)s$$

$$\geq -\frac{1}{6}(a-1+\frac{1}{N})^3 s \geq -\frac{1}{12}a^3 s + cs.$$

Therefore, since, as $s \to -\infty$,

$$-\frac{1}{12}a^3 s + cs \sim \frac{1}{12}s^4 \sim \frac{1}{24}(s^4 + a^2 s^2),$$

we deduce that, for $s \leq -s_0$ *and* $a \geq s_0$ *(with* $|s+a| \leq 1 - \frac{1}{N}$*),* $s_0 > 0$ *independent of* N,

$$(f_{1,N}(s+a) - f_{1,N}(a))s \geq \frac{1}{48}(s^4 + a^2 s^2)$$

and the result follows.

The remaining cases can be treated in a similar way.

□

2.3 A priori estimates

In this section, all constants are independent of N.
We consider, for $N \in \mathbb{N}$, the approximated problem

$$\frac{\partial u^N}{\partial t} + \Delta^2 u^N - \Delta f_N(u^N) + \chi_{\Omega\setminus D}(x)(u^N - h) = 0, \tag{2.15}$$

$$\frac{\partial u^N}{\partial \nu} = \frac{\partial \Delta u^N}{\partial \nu} = 0 \text{ on } \Gamma, \tag{2.16}$$

$$u^N|_{t=0} = u_0. \tag{2.17}$$

First, integrating (2.15) over Ω, we have, owing to (2.5),

$$\frac{d\langle u^N\rangle}{dt} + \frac{1}{\mathrm{Vol}(\Omega)}\int_{\Omega\setminus D} u^N\,dx = 0, \tag{2.18}$$

where $\langle\cdot\rangle = \frac{1}{\mathrm{Vol}(\Omega)}\int_\Omega \cdot\,dx$. Setting $u^N = \langle u^N\rangle + v^N$ (so that $\langle v^N\rangle = 0$), we can rewrite (2.18) as

$$\frac{d\langle u^N\rangle}{dt} + c_0\langle u^N\rangle = -\frac{1}{\mathrm{Vol}(\Omega)}\int_{\Omega\setminus D} v^N\,dx, \tag{2.19}$$

where $c_0 = \frac{\mathrm{Vol}(\Omega\setminus D)}{\mathrm{Vol}(\Omega)}$ and v^N is solution to

$$\frac{\partial v^N}{\partial t} + \Delta^2 v^N - \Delta(f_N(u^N) - \langle f_N(u^N)\rangle) + \chi_{\Omega\setminus D}(x)(u^N - h) - \langle\chi_{\Omega\setminus D}(x)(u^N - h)\rangle = 0, \tag{2.20}$$

$$\frac{\partial v^N}{\partial \nu} = \frac{\partial \Delta v^N}{\partial \nu} = 0 \text{ on } \Gamma, \tag{2.21}$$

$$v^N|_{t=0} = v_0 = u_0 - \langle u_0 \rangle. \tag{2.22}$$

We rewrite (2.20)-(2.21) in the equivalent form

$$(-\Delta)^{-1}\frac{\partial v^N}{\partial t} - \Delta v^N + f_N(u^N) - \langle f_N(u^N)\rangle \tag{2.23}$$

$$+(-\Delta)^{-1}(\chi_{\Omega\setminus D}(x)(u^N - h) - \langle \chi_{\Omega\setminus D}(x)(u^N - h)\rangle) = 0,$$

$$\frac{\partial v^N}{\partial \nu} = 0 \text{ on } \Gamma. \tag{2.24}$$

We multiply (2.23) by v^N to obtain

$$\frac{1}{2}\frac{d}{dt}\|v^N\|^2_{-1} + \|\nabla v^N\|^2 \tag{2.25}$$

$$+((f_N(u^N) - \langle f_N(u^N)\rangle, v^N)) + ((\chi_{\Omega\setminus D}(x)(u^N - h), (-\Delta)^{-1}v^N)) = 0.$$

Noting that

$$((f_N(u^N) - \langle f_N(u^N)\rangle, v^N)) = ((f_N(u^N) - f_N(\langle u^N\rangle), v^N)),$$

it follows from (2.14) that

$$((f_N(u^N) - \langle f_N(u^N)\rangle, v^N)) \geq c_4(\|v^N\|^4_{L^4(\Omega)} + \langle u^N\rangle^2\|v^N\|^2) - c. \tag{2.26}$$

Furthermore,

$$|((\chi_{\Omega\setminus D}(x)(u^N - h), (-\Delta)^{-1}v^N))| \leq c(\|v^N\|^2 + |\langle u^N\rangle|\|v^N\| + \|h\|^2) \tag{2.27}$$

$$\leq \frac{c_4}{2}(\|v^N\|^4_{L^4(\Omega)} + \langle u^N\rangle^2\|v^N\|^2) + c(\|h\|^2 + 1).$$

We thus deduce from (2.25)-(2.27) that

$$\frac{d}{dt}\|v^N\|^2_{-1} + \|\nabla v^N\|^2 + c_4(\|v^N\|^4_{L^4(\Omega)} + \langle u^N\rangle^2\|v^N\|^2) \leq c(\|h\|^2 + 1). \tag{2.28}$$

Next, it follows from (2.19) that

$$\frac{d\langle u^N\rangle^2}{dt} + c_0\langle u^N\rangle^2 \leq c\|v^N\|^2,$$

hence

$$\frac{d\langle u^N\rangle^2}{dt} + c_0\langle u^N\rangle^2 \leq \frac{c_4}{2}(\|v^N\|^4_{L^4(\Omega)} + \langle u^N\rangle^2\|v^N\|^2) + c. \tag{2.29}$$

Summing (2.28) and (2.29), we find a differential inequality of the form

$$\frac{dE_{1,N}}{dt} + c(\|u^N\|^2_{H^1(\Omega)} + \|v^N\|^4_{L^4(\Omega)} + \langle u^N\rangle^2\|v^N\|^2) \leq c(\|h\|^2 + 1),\ c > 0, \tag{2.30}$$

where

$$E_{1,N} = \langle u^N\rangle^2 + \|v^N\|^2_{-1}$$

satisfies

$$E_{1,N} \geq c\|u^N\|^2_{H^{-1}(\Omega)},\ c > 0, \tag{2.31}$$

where $H^{-1}(\Omega)$ is the topological dual of $H^1(\Omega)$. Here, we have used the fact that $v \mapsto (\langle v\rangle^2 + \|v - \langle v\rangle\|^2_{-1})^{\frac{1}{2}}$ (resp., $v \mapsto (\langle v\rangle^2 + \|\nabla v\|^2)^{\frac{1}{2}}$) is a norm on $H^{-1}(\Omega)$ (resp., $H^1(\Omega)$) which is equivalent to the usual one (being understood that, for $v \in H^{-1}(\Omega)$, then $\langle v\rangle = \frac{1}{\mathrm{Vol}(\Omega)}\langle v, 1\rangle_{H^{-1}(\Omega),H^1(\Omega)}$).

We then multiply (2.15) by u^N and have, owing to (2.11),

$$\frac{d}{dt}\|u^N\|^2 + \|\Delta u^N\|^2 \leq 2\lambda_1\|\nabla u^N\|^2 + c(\|u^N\|^2 + \|h\|^2). \tag{2.32}$$

Summing (2.30) and (2.32) multiplied by δ_1, where $\delta_1 > 0$ is chosen small enough, we obtain a differential inequality of the form

$$\frac{dE_{2,N}}{dt} + c(\|u^N\|^2_{H^2(\Omega)} + \|v^N\|^4_{L^4(\Omega)} + \langle u^N\rangle^2\|v^N\|^2) \leq c(\|h\|^2 + 1),\ c > 0, \tag{2.33}$$

where

$$E_{2,N} = \delta_1\|u^N\|^2 + E_{1,N}$$

satisfies

$$E_{2,N} \geq c\|u^N\|^2,\ c > 0. \tag{2.34}$$

We now rewrite (2.15)-(2.16) in the equivalent form

$$\frac{\partial u^N}{\partial t} + \chi_{\Omega\setminus D}(x)(u_N - h) = \Delta\mu^N, \tag{2.35}$$

$$\mu^N = -\Delta u^N + f_N(u^N), \tag{2.36}$$

$$\frac{\partial u^N}{\partial \nu} = \frac{\partial \mu^N}{\partial \nu} = 0 \text{ on } \Gamma, \tag{2.37}$$

where, by analogy with the original Cahn-Hilliard equation, μ^N is called chemical potential.

We multiply (2.35) by μ^N and (2.36) by $\frac{\partial u^N}{\partial t}$ to find

$$\frac{1}{2}\frac{d}{dt}(\|\nabla u^N\|^2 + 2\int_\Omega F_N(u^N)\,dx) + \|\nabla\mu^N\|^2 = -((u^N - h, \chi_{\Omega\setminus D}(x)\mu^N)). \tag{2.38}$$

Furthermore, multiplying (2.36) by $\chi_{\Omega\setminus D}(x)u^N$, we have

$$((u^N,\chi_{\Omega\setminus D}(x)\mu^N)) = -((\Delta u^N,\chi_{\Omega\setminus D}(x)u^N)) + \int_{\Omega\setminus D} f_N(u^N)u^N\,dx. \tag{2.39}$$

Finally, it follows from (2.5) that

$$((h,\chi_{\Omega\setminus D}(x)\mu^N)) = ((\chi_{\Omega\setminus D}(x)h,\mu^N - \langle\mu^N\rangle)),$$

hence

$$|((h,\chi_{\Omega\setminus D}(x)\mu^N))| \le c\|h\|\|\nabla\mu^N\|. \tag{2.40}$$

We deduce from (2.13) and (2.38)-(2.40) that

$$\frac{d}{dt}(\|\nabla u^N\|^2 + 2\int_\Omega F_N(u^N)\,dx) \tag{2.41}$$

$$+c(\|\nabla\mu^N\|^2 + \int_{\Omega\setminus D}|f_N(u^N)|\,dx + \int_{\Omega\setminus D} F_N(u^N)\,dx) \le c'(\|u^N\|^2_{H^2(\Omega)} + \|h\|^2),\ c>0.$$

Summing (2.33) and (2.41) multiplied by δ_2, where $\delta_2 > 0$ is chosen small enough, we obtain a differential inequality of the form

$$\frac{dE_{3,N}}{dt} + c(\|u^N\|^2_{H^2(\Omega)} + \|v^N\|^4_{L^4(\Omega)} + \langle u^N\rangle^2\|v^N\|^2 \tag{2.42}$$

$$+\int_{\Omega\setminus D}|f_N(u^N)|\,dx + \int_{\Omega\setminus D} F_N(u^N)\,dx + \|\nabla\mu^N\|^2) \le c(\|h\|^2+1),\ c>0,$$

where

$$E_{3,N} = \delta_2(\|\nabla u^N\|^2 + 2\int_\Omega F_N(u^N)\,dx) + E_{2,N}$$

satisfies

$$E_{3,N} \ge c\|u^N\|^2_{H^1(\Omega)} - c',\ c>0. \tag{2.43}$$

Rewriting (2.35)-(2.36) in the equivalent form

$$(-\Delta)^{-1}\frac{\partial v^N}{\partial t} + (-\Delta)^{-1}(\chi_{\Omega\setminus D}(x)(u_N - h) - \langle\chi_{\Omega\setminus D}(x)(u_N-h)\rangle) = -(\mu^N - \langle\mu^N\rangle), \tag{2.44}$$

$$\mu^N - \langle\mu^N\rangle = -\Delta v^N + f_N(u^N) - \langle f_N(u^N)\rangle, \tag{2.45}$$

we deduce from (2.44) that

$$\|\frac{\partial v^N}{\partial t}\|_{-1} \le c(\|u^N\| + \|\nabla\mu^N\| + \|h\|),$$

hence, owing to (2.19),

$$\|\frac{\partial u^N}{\partial t}\|_{H^{-1}(\Omega)} \leq c(\|u^N\| + \|\nabla \mu^N\| + \|h\|). \tag{2.46}$$

Furthermore, (2.45) yields

$$\|f_N(u^N) - \langle f_N(u^N)\rangle\| \leq c(\|u^N\|_{H^2(\Omega)} + \|\nabla \mu^N\|). \tag{2.47}$$

It thus follows from (2.42) and (2.46)-(2.47) that

$$\frac{dE_{3,N}}{dt} + c(\|u^N\|^2_{H^2(\Omega)} + \|v^N\|^4_{L^4(\Omega)} + \langle u^N\rangle^2\|v^N\|^2 \tag{2.48}$$

$$+\|\frac{\partial u^N}{\partial t}\|^2_{H^{-1}(\Omega)} + \|f_N(u^N) - \langle f_N(u^N)\rangle\|^2$$

$$+ \int_{\Omega\setminus D} |f_N(u^N)|\,dx + \int_{\Omega\setminus D} F_N(u^N)\,dx + \|\nabla \mu^N\|^2) \leq c(\|h\|^2 + 1),\ c > 0.$$

We can note that (2.48) is not sufficient to pass to the limit in the nonlinear term $f_N(u^N)$ (say, in a variational formulation). To do so, we also need an estimate on $|\langle f_N(u^N)\rangle|$ (in order to have an estimate on $\|f_N(u^N)\|$). This could be done if we were able to prove that $|\langle u^N(t)\rangle| \leq 1 - \delta$, $t \geq 0$, $\delta \in (0, 1)$ (see [107] ; see also below). Unfortunately, we are not able to prove such a result and, therefore, we will only be able to obtain a local (in time) result.

We now assume that $|\langle u_0\rangle| < 1$. Then, there exists $\delta \in (0, 1)$ such that $|\langle u_0\rangle| \leq 1 - 2\delta$. Therefore, since the function $t \mapsto \langle u^N(t)\rangle$ is continuous, there exists $T_0 = T_0(\delta, N)$ such that, if $t \in [0, T_0]$, then $|\langle u^N(t)\rangle| \leq 1 - \delta$.

Actually, we can note that it follows from (2.19) that

$$\langle u^N(t)\rangle = e^{-c_0 t}\langle u_0\rangle - e^{-c_0 t}\int_0^t e^{c_0 s}\,ds \int_{\Omega\setminus D} v^N\,dx,$$

so that

$$|\langle u^N(t)\rangle| \leq |\langle u_0\rangle| + ce^{-c_0 t}\int_0^t e^{c_0 s}\|u^N\|\,ds \tag{2.49}$$

$$\leq 1 - 2\delta + c(1 - e^{-c_0 t}),$$

where we emphasize that $c = c(u_0)$ is independent of N (note indeed that it follows from (2.33)-(2.34) and Gronwall's lemma that $\|u^N\|$ is bounded uniformly with respect to time and N). We can thus find $T_0 = T_0(\delta, u_0)$ independent of N such that, if $t \in [0, T_0]$, then $|\langle u^N(t)\rangle| \leq 1 - \delta$.

Then, noting that we have a similar result for f (see [107]), it is not difficult to prove that, for N large enough,

$$f_N(s + m)s \geq c_m|f_N(s + m)| - c'_m,\ c_m > 0,\ c'_m \geq 0,\ s \in \mathbb{R},\ m \in (-1, 1), \tag{2.50}$$

where the constants c_m and c'_m depend continuously on m (see also [109]).

Remark 2.3.1. *When $|m| > 1$, then we cannot expect to have such a result. Indeed, if, e.g., $m = 3$, then, as $s \to -2^-$, $f(s + 3)s$ tends to $-\infty$, while $|f(s + 3)|$ tends to $+\infty$.*

Having (2.50), we obtain, proceeding as in [107], Proposition A.2,

$$|\langle f_N(v)\rangle| \leq c_\delta \|v - \langle v\rangle\| \|f_N(v) - \langle f_N(v)\rangle\| + c'_\delta, \tag{2.51}$$

$$c_\delta > 0,\ c'_\delta \geq 0,\ v \in L^2(\Omega),\ |\langle v\rangle| \leq 1 - \delta,\ \delta \in (0,1),$$

for $N \geq N_0 = N_0(\delta)$.

It then follows from (2.51) (taking $v = u^N$) that

$$|\langle f_N(u^N)\rangle| \leq c_\delta \|v^N\| \|f_N(u^N) - \langle f_N(u^N)\rangle\| + c'_\delta,\ t \in [0, T_0],$$

hence

$$\int_0^{T_0} |\langle f_N(u^N)\rangle|^2\, ds \leq c_\delta \|v^N\|^2_{L^\infty(0,T_0;L^2(\Omega))} \|f_N(u^N) - \langle f_N(u^N)\rangle\|^2_{L^2((0,T_0)\times\Omega)} + c'_\delta. \tag{2.52}$$

Therefore, noting that $v \mapsto (|\langle v\rangle|^2 + \|v - \langle v\rangle\|^2)^{\frac{1}{2}}$ is a norm on $L^2(\Omega)$ which is equivalent to the usual L^2-norm, (2.47) and (2.52) yield that

$$\|f_N(u^N)\|_{L^2((0,T_0)\times\Omega)} \tag{2.53}$$

$$\leq c_\delta(\|u^N\|_{L^\infty(0,T_0;L^2(\Omega))} + 1)(\|u^N\|_{L^2(0,T_0;H^2(\Omega))} + \|\nabla\mu^N\|_{L^2((0,T_0)\times\Omega)^n}) + c'_\delta.$$

Noting finally that $\langle\mu^N\rangle = \langle f_N(u^N)\rangle$, we deduce that

$$\|\mu^N\|_{L^2(0,T_0;H^1(\Omega))} \tag{2.54}$$

$$\leq c_\delta(\|u^N\|_{L^\infty(0,T_0;L^2(\Omega))} + 1)(\|u^N\|_{L^2(0,T_0;H^2(\Omega))} + \|\nabla\mu^N\|_{L^2((0,T_0)\times\Omega)^n}) + c'_\delta.$$

2.4 A local existence result

We have the

Theorem 3. *We assume that $u_0 \in H^1(\Omega)$, $|\langle u_0\rangle| < 1$ and $-1 < u_0(x) < 1$ a.e. $x \in \Omega$. Then, there exists $T_0 = T_0(u_0)$ and a solution to* (2.2)-(2.4) *on $[0, T_0]$ such that $u \in C([0,T_0]; H^{-1}(\Omega)) \cap L^\infty(0,T_0;H^1(\Omega)) \cap L^2(0,T_0;H^2(\Omega))$ and $\frac{\partial u}{\partial t} \in L^2(0,T_0;H^{-1}(\Omega))$. Furthermore, $-1 < u(t,x) < 1$ a.e. $(t,x) \in (0,T_0)\times\Omega$.*

Proof. *We consider the solution u^N to the approximated problem* (2.15)-(2.17) *(the proof of existence, uniqueness and regularity of such a solution can be adapted from the results in [38], owing to* (2.14)*). Then, it follows from the a priori estimates derived in the previous section that, up to a subsequence, this solution converges to a limit function u such that*

$$u^N \to u \text{ in } L^\infty(0,T_0;H^1(\Omega)) \text{ weak}-\star \text{ and in } L^2(0,T_0;H^2(\Omega)) \text{ weak},$$

$$u^N \to u \text{ a.e. } (t,x) \in (0,T_0)\times\Omega,$$

$$\frac{\partial u^N}{\partial t} \to \frac{\partial u}{\partial t} \text{ in } L^2(0,T_0;H^{-1}(\Omega)) \text{ weak.}$$

The only difficulty here is to pass to the limit in the nonlinear term $f_N(u^N)$.

First, it follows from (2.53) *that $f_N(u^N)$ is bounded, independently of N, in $L^1((0,T_0)\times\Omega)$. Then, it follows from the explicit expression of f_N that*

$$\text{meas}(E_{N,M}) \le c\varphi(\frac{1}{N}),\ N \le M,$$

where

$$E_{N,M} = \{(t,x) \in (0,T_0)\times\Omega,\ |u^M(t,x)| > 1 - \frac{1}{N}\}$$

and

$$\varphi(s) = \frac{1}{|f(1-s)|},$$

the constant c being independent of N and M. Note indeed that there holds

$$\int_0^{T_0}\int_\Omega |f_M(u^M)|\,dx\,dt \ge \int_{E_{N,M}} |f_M(u^M)|\,dx\,dt \ge c'\text{meas}(E_{N,M})|f(1-\frac{1}{N})|, \tag{2.55}$$

where the constant c' is independent of N and M (recall that $f(-s) = -f(s)$). We can pass to the limit $M \to +\infty$ (employing Fatou's lemma, see (2.55)*) and then $N \to +\infty$ (noting that $\lim_{s\to 0}\varphi(s) = 0$) to find*

$$\text{meas}\{(t,x) \in (0,T_0)\times\Omega,\ |u(t,x)| \ge 1\} = 0,$$

so that

$$-1 < u(t,x) < 1 \text{ a.e. } (t,x) \in (0,T_0)\times\Omega.$$

Next, it follows from the above almost everywhere convergence of u^N to u (and also from the explicit expression of f_N) that

$$f_N(u^N) \to f(u) \text{ a.e. } (t,x) \in (0,T_0)\times\Omega. \tag{2.56}$$

Finally, since, owing to (2.53)*, $f_N(u^N)$ is bounded, independently of N, in $L^2((0,T_0)\times\Omega)$, it follows from* (2.56) *that $f_N(u^N) \to f(u)$ in $L^2((0,T_0)\times\Omega)$ weak, which finishes the proof of the passage to the limit.*

□

Remark 2.4.1. *We assume that* $|u_0(x)| \leq 1 - \delta$ *a.e.,* $\delta \in (0,1)$*. Then, recalling that* $f_N(s) = f(s)$ *when* $|s| \leq 1 - \frac{1}{N}$*, we can also obtain a local (in time) existence result. However, the local existence given by Theorem 3 is more general.*

Remark 2.4.2. *a) When the positive constant c (which depends on* Ω*, D, h and, for the more general equation* (2.1)*, on* ϵ *and* λ_0*) in* (2.49) *is small (namely,* $c \leq \delta$*), then one actually has a global (in time) existence result. Note however that, in concrete applications,* λ_0 *is large, while* ϵ *can be small, so that this condition should be too restrictive.*

b) When $D = \emptyset$*, in which case one obtains the so-called Oono equation (for* $h = 0$*; see [103], [122] and [143]), one has a global well-posedness result (see [?]). One also has a global well-posedness result, for the Bertozzi–Esedoglu–Gillette–Cahn–Hilliard equation, when considering Dirichlet boundary conditions (see [105]).*

2.5 Numerical simulations

As far as the numerical simulations are concerned, we rewrite the problem in the form

$$\frac{\partial u}{\partial t} + \Delta \mu + \lambda_0 \chi_{\Omega \setminus D}(x)(u - h) = 0, \tag{2.57}$$

$$\mu = \epsilon \Delta u - \frac{1}{\epsilon} f(u), \tag{2.58}$$

$$\frac{\partial u}{\partial \nu} = \frac{\partial \mu}{\partial \nu} = 0 \text{ on } \Gamma, \tag{2.59}$$

$$u_{|t=0} = u_0, \tag{2.60}$$

which has the advantage of splitting the fourth-order (in space) equation into a system of two second-order ones (see [55], [80] and [86]). Consequently, we use a P1-finite element for the space discretization, together with a semi-implicit Euler time discretization (i.e., implicit for the linear terms and explicit for the nonlinear ones). The numerical simulations are performed with the software Freefem++ (see [67]).

In the numerical results presented below, Ω is a $(0, 0.5) \times (0, 0.5)$-square. The triangulation is obtained by dividing Ω into 200×200 rectangles and by dividing each rectangle along the same diagonal.

In order to obtain the final inpainting results, we use a dynamic one step algorithm with threshold involving the diffuse interface thickness ϵ (see [38]).

2.5.1 Inpainting of a triangle

The gray region in Figure 2.1(a) corresponds to the inpainting region. We run the modified Cahn-Hilliard equation with $f(s) = -2\ln(3)s + \ln\left(\frac{1+s}{1-s}\right)$ (note that f vanishes at -0.5 and 0.5), $\epsilon = 0.03$, $\lambda_0 = 900000$ and $\Delta t = 0.05$. Furthermore, we take the initial datum u_0 in $[0, 0.5]$ (random in the inpainting region), so that $|\langle u_0 \rangle| < 1$. We observe that the solution remains in $(-1, 1)$ when considering an intermediate value of the diffuse interface thickness ϵ. We are close

to a steady state at $t = 0.45$, as shown in Figure 2.1(b), and we replace all values larger than $\frac{1}{4}$ by $\frac{1}{2}$ and all those smaller than $\frac{1}{4}$ by 0 to obtain the final inpainting in Figure 2.1(c).

Then, we run again the modified Cahn-Hilliard equation with the same $\epsilon = 0.03$, $\Delta t = 0.05$ and $\lambda_0 = 900000$, but we now take $f(s) = 4s^3 - 6s^2 + 2s$ and the initial datum in $[0, 1]$ instead of $[0, 0.5]$ in order to have comparable inpainting results (note that the solution does not remain in the relevant interval $[0, 1]$). We are close to a steady state at $t = 1.2$, as shown in Figure 2.1(d), and we replace all values larger than $\frac{1}{2}$ by 1 and all those smaller than $\frac{1}{2}$ by 0 to obtain the final inpainting in Figure 2.1(e).

2.5.2 Inpainting of a bar

Here and in the other simulations below, the initial datum is taken as above.

In Figure 2.2(a), the gray region corresponds to the inpainting region. We run the modified Cahn-Hilliard equation with $f(s) = -2\ln(3)s + \ln\left(\frac{1+s}{1-s}\right)$, $\epsilon = 0.05$, $\Delta t = 0.05$ and $\lambda_0 = 900000$. We are close to a steady state at $t = 0.4$, as shown in Figure 2.2(b), and we replace all values larger than $\frac{1}{4}$ by $\frac{1}{2}$ and all those smaller than $\frac{1}{4}$ by 0 to obtain the final inpainting in Figure 2.2(c).

Furthermore, we run again the modified Cahn-Hilliard equation with the same $\epsilon = 0.05$ and $\Delta t = 0.05$, but we now take $f(s) = 4s^3 - 6s^2 + 2s$ and $\lambda_0 = 500000$ (note that, contrary to the next example below, a smaller value of λ_0 allows to have comparable inpainting results). We are close to a steady state at $t = 0.75$, as shown in Figure 2.2(d), and we replace all values larger than $\frac{1}{2}$ by 1 and all those smaller than $\frac{1}{2}$ by 0 to obtain the final inpainting in Figure 2.2(e).

2.5.3 Inpainting of a four circles

The gray region in Figure 2.3(a) corresponds to the inpainting region. We run the modified Cahn-Hilliard equation with $f(s) = -2\ln(3)s + \ln\left(\frac{1+s}{1-s}\right)$, $\epsilon = 0.05$, $\Delta t = 0.05$ and $\lambda_0 = 300000$. We are close to a steady state at $t = 0.4$, as shown in Figure 2.3(b), and we replace all values larger than $\frac{1}{4}$ by $\frac{1}{2}$ and all those smaller than $\frac{1}{4}$ by 0 to obtain the final inpainting in Figure 2.3(c).

Furthermore, we run again the modified Cahn-Hilliard equation with the same $\epsilon = 0.05$ and $\Delta t = 0.05$, but we now take $f(s) = 4s^3 - 6s^2 + 2s$ and $\lambda_0 = 900000$. We are close to a steady state at $t = 1.2$, as shown in Figure 2.3(d), and we replace all values larger than $\frac{1}{2}$ by 1 and all those smaller than $\frac{1}{2}$ by 0 to obtain the final inpainting in Figure 2.3(e).

Remark 2.5.1. *We noticed in [38] that the one step algorithm does not always work when the inpainting region is too large. We take here the same counterexample as in [38] of the broken bar illustrated in Figure 2.4(a). We run the modified Cahn-Hilliard equation with* $f(s) = -2\ln(3)s + \ln\left(\frac{1+s}{1-s}\right)$, $\Delta t = 0.05$, $\lambda_0 = 300000$ *and* $\epsilon = 0.05$. *We are close to a steady state at* $t = 0.4$ *and we replace all values larger than* $\frac{1}{4}$ *by* $\frac{1}{2}$ *and all those smaller than* $\frac{1}{4}$ *by* 0 *to obtain the final inpainting in Figure 2.4(b). Furthermore, we run again the modified Cahn-Hilliard equation with* $f(s) = 4s^3 - 6s^2 + 2s$, $\Delta t = 0.05$, $\lambda_0 = 300000$ *and* $\epsilon = 0.05$. *We are close to a steady state at* $t = 5.6$ *and we replace all values larger than* $\frac{1}{2}$ *by* 1 *and all those smaller than* $\frac{1}{2}$ *by* 0 *to obtain the final inpainting in Figure 2.4(c). We thus observe that the one step algorithm gives better results for this example when taking a logarithmic nonlinear term. Actually, for a smaller value of* λ_0 *(namely,* $\lambda_0 = 100000$*), we observed in [38] that the algorithm fails*

for the polynomial nonlinear term ; however, we again obtain good inpainting results for the logarithmic one.

Conclusion : We considered in this paper the Bertozzi–Esedoglu–Cahn–Hilliard equation with a logarithmic nonlinear term. Compared to the same equation with a polynomial nonlinear term, the mathematical analysis of the problem is much more involved and we could only prove a local well-posedness result. However, as far as the numerical simulations are concerned, we observed that, for the one-step algorithm with threshold proposed in [38], we can obtain better results. In particular, a logarithmic nonlinear term allows one to treat cases when the one-step algorithm fails for a polynomial nonlinear term.

Acknowledgments : The authors wish to thank the referees for their careful reading of the paper and useful comments.

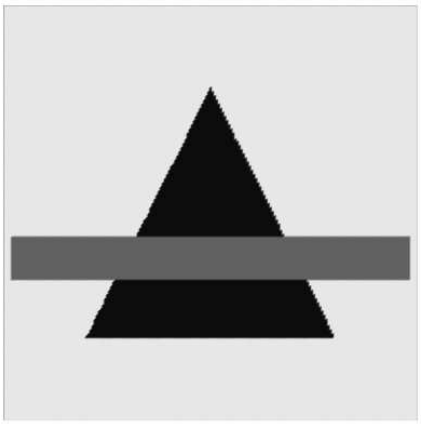

(a)

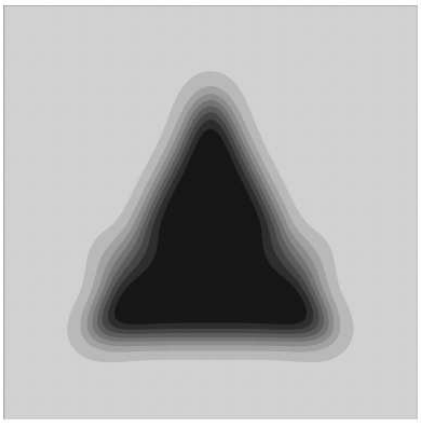

(b)

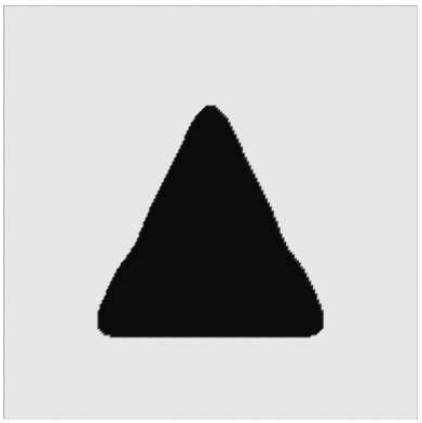

(c)

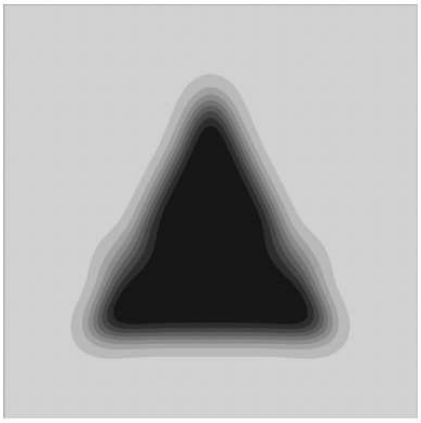

(d)

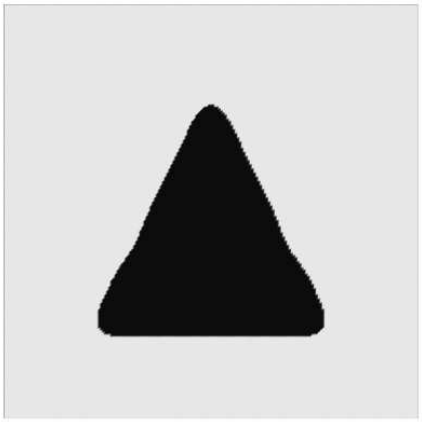

(e)

FIGURE 2.1 – (a) Inpainting region in gray, $\epsilon = 0.03$. (b) Solution at $t = 0.45$, $f(s) = -2\ln(3)s + \ln\left(\frac{1+s}{1-s}\right)$. (c) Replacing the values larger than $\frac{1}{4}$ by $\frac{1}{2}$ and those smaller than $\frac{1}{4}$ by 0. (d) Solution at $t = 1.2$, $f(s) = 4s^3 - 6s^2 + 2s$. (e) Replacing the values larger than $\frac{1}{2}$ by 1 and those smaller than $\frac{1}{2}$ by 0.

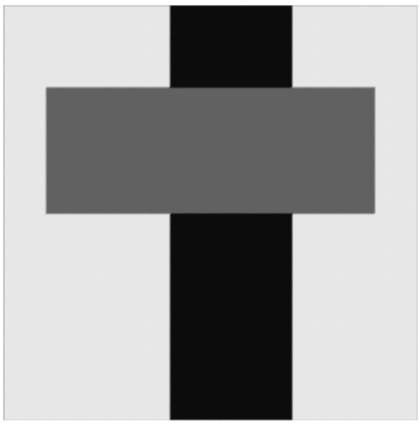

(a)

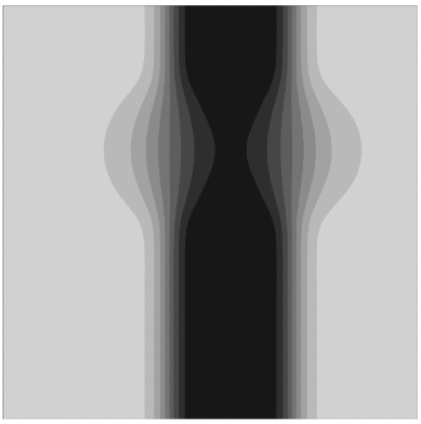

(b)

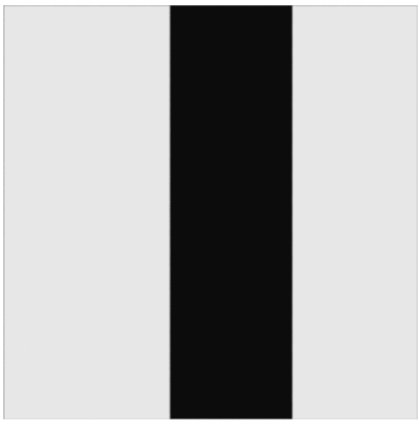

(c)

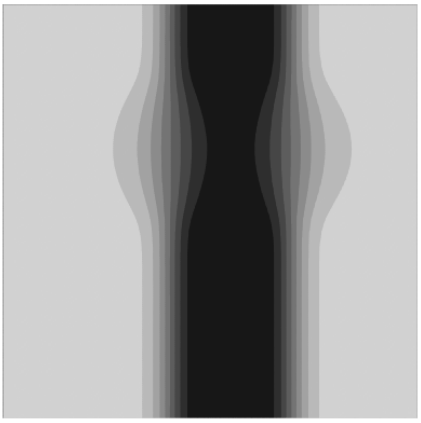

(d)

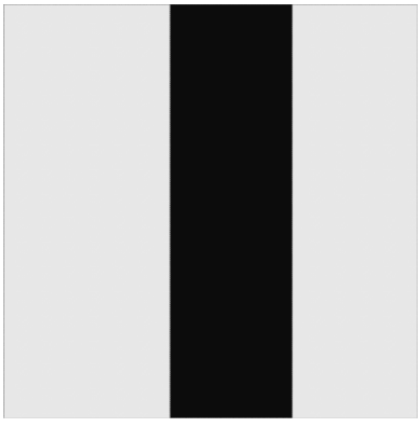

(e)

FIGURE 2.2 – (a) Inpainting region in gray, $\epsilon = 0.05$. (b) Solution at $t = 0.4$, $f(s) = -2\ln(3)s + \ln\left(\frac{1+s}{1-s}\right)$. (c)Replacing the values larger than $\frac{1}{4}$ by $\frac{1}{2}$ and those smaller than $\frac{1}{4}$ by 0. (d) Solution at $t = 0.75$, $f(s) = 4s^3 - 6s^2 + 2s$. (e) Replacing the values larger than $\frac{1}{2}$ by 1 and those smaller than $\frac{1}{2}$ by 0.

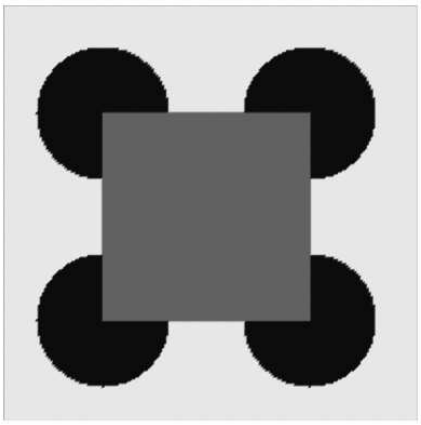

(a)

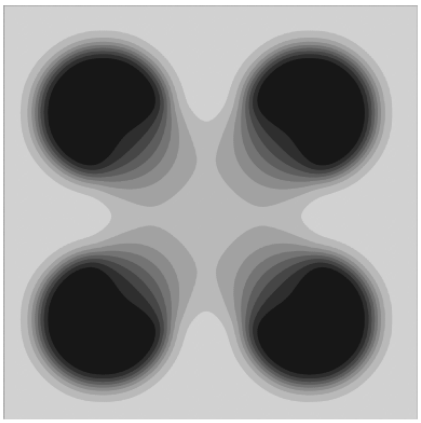

(b)

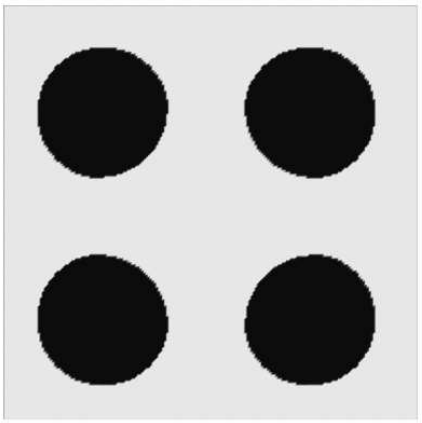

(c)

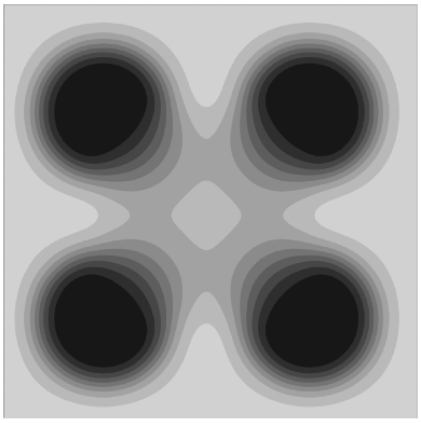

(d)

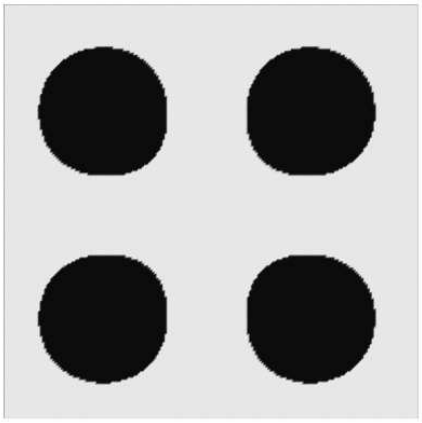

(e)

FIGURE 2.3 – (a) Inpainting region in gray, $\epsilon = 0.05$. (b) Solution at $t = 0.4$, $f(s) = -2\ln(3)s + \ln\left(\frac{1+s}{1-s}\right)$. (c) Replacing the values larger than $\frac{1}{4}$ by $\frac{1}{2}$ and those smaller than $\frac{1}{4}$ by 0. (d) Solution at $t = 0.65$, $f(s) = 4s^3 - 6s^2 + 2s$. (e) Replacing the values larger than $\frac{1}{2}$ by 1 and those smaller than $\frac{1}{2}$ by 0.

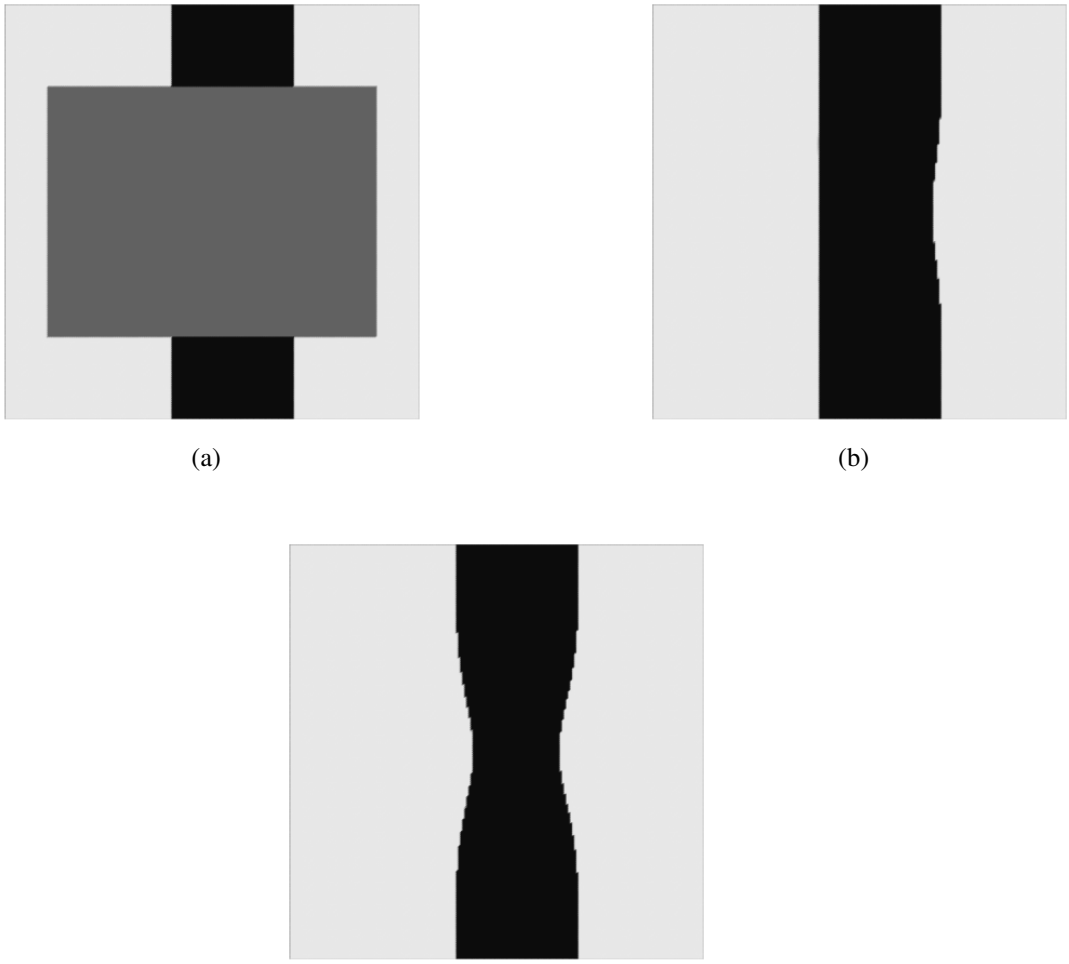

(a) (b)

(c)

FIGURE 2.4 – (a) Larger inpainting region in gray, $\epsilon = 0.05$. (b) Final inpainting result (solution close to a steady state at $t = 0.4$ with $\Delta t = 0.05$). Here, $f(s) = -2\ln(3)s + \ln\left(\frac{1+s}{1-s}\right)$. (c) Final inpainting result (solution close to a steady state at $t = 5.6$ with $\Delta t = 0.05$). Here, $f(s) = 4s^3 - 6s^2 + 2s$.

Chapitre 3

A Cahn–Hilliard system with a fidelity term for color image inpainting

Un système de Cahn–Hilliard avec un terme de fidélité pour la retouche en couleur

Ce chapitre est constitué de l'article **A Cahn–Hilliard system with a fidelity term for color image inpainting**, J. Math. Imag. Vision, 2015. Cet article est écrit en collaboration avec **Laurence Cherfils** et **Alain Miranville**.

J. Math. Imag. Vision
DOI 10.1007/s10851-015-0593-9

A Cahn–Hilliard system with a fidelity term for color image inpainting

LAURENCE CHERFILS[1], HUSSEIN FAKIH[2] AND ALAIN MIRANVILLE[2]

[1] Université de la Rochelle
Laboratoire Mathématiques, Image et Applications
Avenue Michel Crépeau
F-17042 La Rochelle Cedex, France
E-mail address : lcherfil@univ-lr.fr

[2] Université de Poitiers
Laboratoire de Mathématiques et Applications
UMR CNRS 7348 - SP2MI
Boulevard Marie et Pierre Curie - Téléport 2
F-86962 Chasseneuil Futuroscope Cedex, France
E-mail address : Hussein.Fakih@math.univ-poitiers.fr
E-mail address : Alain.Miranville@math.univ-poitiers.fr

Abstract : In this paper, we propose a model for multi-color image inpainting composed of n colors. In particular, as in the binary model, i.e., the Bertozzi–Esedoglu–Gillette–Cahn–Hilliard equation [16], we add a fidelity term to the corresponding Cahn–Hilliard system. We are interested in the study of the asymptotic behavior, in terms of finite-dimensional attractors, of the dynamical system associated with the problem. The main difficulty here is that we no longer have the conservation of mass, i.e., of the spatial average of the order parameter c, as in the Cahn–Hilliard system. Instead, we prove that the spatial average of c is dissipative. We finally give numerical simulations which confirm and extend previous ones on the efficiency of the binary model.

Keywords : Cahn–Hilliard system, fidelity term, color image inpainting, well-posedness, exponential attractor, simulations.
AMS Subject Classification : 35B40 ; 35K55 ; 68M07 ; 80A23

3.1 Introduction

Image inpainting involves filling in part of an image or video from the surrounding area. It is essentially some kind of interpolation. Its applications include restoration of old paintings by

museum artists [58], removing scratches from old photographs [24], altering scenes in photographs [89], and restoration of motion pictures [93].

The authors in [15] introduced image inpainting for digital image processing. Their model is based on nonlinear PDE's. A large number of PDE's and variational approaches have been considered in view of such applications, such as the total variation model [34, 32, 33, 51, 129, 130, 133], the Euler elastica model [31, 37, 101], the active contour model based on the Mumford and Shah segmentation [140], the inpainting scheme based on the Mumford-Shah-Euler image model [59], inpainting with the Navier-Stokes equations [14], or wavelet-based inpainting [37, 50].

The authors of [16] introduced the following Cahn–Hilliard model for binary image inpainting :

$$\frac{\partial c}{\partial t} = -\Delta(\varepsilon\Delta c - \frac{1}{\varepsilon}f(c)) + \lambda(x)(h - c), \tag{3.1}$$

where

$$\lambda(x) = \begin{cases} 0 & \text{if} \quad x \in D, \\ \lambda_0 & \text{if} \quad x \in \Omega\backslash D, \end{cases}$$

$h(x)$ is a given binary image, and $D \Subset \Omega$ is the inpainting domain. Here, c satisfies the Neumann boundary conditions

$$\frac{\partial c}{\partial \nu} = \frac{\partial \Delta c}{\partial \nu} = 0, \quad \text{on } \partial\Omega,$$

and F is the antiderivative of f such that

$$F(s) = s^2(s-1)^2.$$

Equation (3.1) is identical to the standard Cahn–Hilliard equation [11, 119], except for the second term on the right-hand side. This term is added to keep the solution constructed close to the given image $h(x)$ in the complement of the inpainting domain, where image information is available.

Well-posedness results for (3.1) have been obtained in [16] (see also [25] for the study of the stationary problem).

Furthermore, the asymptotic behavior, in terms of finite-dimensional attractors, of (3.1) has been studied in [38]. More precisely, such sets provide information on all the possible dynamics of the system and are expected to have a rich geometric structure ; they contain in particular all steady states and heteroclinic orbits. Moreover, the finite-dimensionality means, roughly speaking, that, even though the initial phase space is infinite-dimensional, the reduced dynamics can be characterized by a finite number of parameters. We refer the reader to, e.g., [54, 108, 137] for discussions on this subject.

Finally, the existence of local (in time) solutions to (3.1) with logarithmic nonlinear terms has been studied in [39] (note indeed that the original Cahn–Hilliard equation was actually proposed with thermodynamically relevant logarithmic nonlinear terms which follow from a mean-field model ; regular (and, in particular, cubic) nonlinear terms are approximations of such logarithmic nonlinear terms). In that case, we can obtain better results than those obtained with polynomial nonlinear terms in [38], as far as the convergence time is concerned, in particular. We also note that double obstacle nonlinear terms give better results than those obtained with polynomial nonlinear terms, see [20].

While the articles mentioned above only deal with binary images (i.e., black and white ; see however [25] for grayvalue images), it is natural and important to also address color images. In particular, one idea in this direction is to extend the approach of [16] to multi-component Cahn–Hilliard systems, each phase corresponding to a given color. Multi-component Cahn–Hilliard systems have been proposed and studied in, e.g., [46, 57, 62, 72, 97]. Our main aim in this article is to propose such a model for color image inpainting, based on a fidelity term as in [16].

As far as the mathematical treatment of the problem is concerned, we have to face two essential difficulties. The first one, which we already encountered in the binary model in [38], is that, due to the presence of the fidelity term, we no longer have the conservation of mass, i.e., of the spatial average of the order parameter, contrary to the original Cahn–Hilliard system. This is overcome by deriving a global (in time) and dissipative (i.e., independent of time and bounded sets of initial data, at least for large times) estimate on the order parameter ; in particular, a key step is to obtain such an estimate on the spatial average of the order parameter. We can note that this estimate is a crucial one, already in order to prove the existence of a solution. The second difficulty is that the order parameter has to satisfy some constraint, namely, the sum of the phases must be equal to one. As a consequence, we have to be careful in the choice of the functional spaces and in the (weak) formulation of the problem.

This article is organized as follows. In Section 3.2, we present the model constructed from the multi-phase Cahn–Hilliard system by adding a fidelity term. Furthermore, we give the assumptions on the nonlinear term. Then, in Section 3.3, we derive a priori estimates which allow us to prove, in Section 3.4, the existence and uniqueness of solutions, as well as the existence of the global attractor. In Section 3.5, we construct finite-dimensional attractors and, in Section 3.6, we prove that the model is algebraically consistent with the diphasic one. Finally, in Section 3.7, we give some numerical simulations which confirm that the one step algorithm with threshold proposed in [38] (see also [39]) is efficient, also in the context of multi-color inpainting.

Remark 3.1.1. *After this work was completed, we discovered the recent preprint [21] in which a similar model is considered for grayvalue inpainting. Note however that, there, the mathematical analysis of the problem is not addressed.*

3.2 Proposed model and setting of the problem

Let $c = (c_1, c_2, ..., c_n)$ be the phase variable and Ω be a bounded domain of $\mathbb{R}^N$ $(N = 2, 3)$ with a regular boundary Γ. We assume that $\sum_{i=1}^{n} c_i = 1$ and $0 \leq c_i \leq 1, \;\; i = 1, ..., n$. We define the hyperplane

$$S := \{c \in \mathbb{R}^n \text{ such that } \sum_{i=1}^{n} c_i = 1\}. \tag{3.2}$$

We postulate that the free energy can be written as follows :

$$\mathcal{F} = \int_\Omega \Big[F(c) + \frac{\varepsilon^2}{2} \sum_{i=1}^{n} |\nabla c_i|^2\Big] dx, \tag{3.3}$$

where $F(c) = \frac{1}{n}\sum_{i=1}^{n} c_i^2(1-c_i)^2$. The time evolution of c is governed by the gradient of the energy with respect to the $H^{-1}-$inner product under the additional constraint (3.2). This constraint has to hold everywhere and at every time. In order to ensure this constraint, we use a variable Lagrangian multiplier $\beta(c)$ [72]. The time dependence of c_i is given by the following system of Cahn–Hilliard equations describing each phase :

$$\frac{\partial c_i}{\partial t} = \Delta\mu_i, \quad i = 1, ..., n, \tag{3.4}$$

$$\mu_i = \frac{\partial F(c)}{\partial c_i} - \varepsilon^2\Delta c_i + \beta(c), \quad i = 1, ..., n. \tag{3.5}$$

To compute $\beta(c)$, we write the equation satisfied by $C = c_1 + c_2 + ... + c_n$ and we want $C = 1$ to be solution to this equation,

$$\frac{\partial C}{\partial t} = \Delta\Big(\sum_{i=1}^{n}\frac{\partial F}{\partial c_i} - \varepsilon^2\Delta C + n\beta(c)\Big). \tag{3.6}$$

Therefore, $\beta(c) = -\frac{1}{n}\sum_{i=1}^{n}\frac{\partial F}{\partial c_i}$ and we obtain

$$\frac{\partial c_i}{\partial t} = \Delta\mu_i, \quad i = 1, ..., n, \tag{3.7}$$

$$\mu_i = \frac{\partial F(c)}{\partial c_i} - \varepsilon^2\Delta c_i - \frac{1}{n}\sum_{i=1}^{n}\frac{\partial F}{\partial c_i}, \quad i = 1, ..., n. \tag{3.8}$$

Finally, we need to add the fidelity term $\lambda(x)(h_i - c_i)$ to each equation to keep the solution constructed close to the given image $h_i(x)$ as in the Bertozzi–Esedoglu–Gillette–Cahn–Hilliard model for binary image inpainting ; more precisely, $h_i(x)$ is a part of the original image corresponding to the color representing the phase c_i. We thus have the following model :

$$\frac{\partial c_i}{\partial t} = \Delta\mu_i + \lambda(x)(h_i - c_i), \quad i = 1, ..., n, \tag{3.9}$$

$$\mu_i = \frac{\partial F(c)}{\partial c_i} - \varepsilon^2\Delta c_i - \frac{1}{n}\sum_{i=1}^{n}\frac{\partial F}{\partial c_i}, \quad i = 1, ..., n, \tag{3.10}$$

where

$$\lambda(x) = \begin{cases} 0 & \text{if} \quad x \in D, \\ \lambda_0 & \text{if} \quad x \in \Omega\backslash D, \end{cases}$$

$D \Subset \Omega$ is the inpainting domain, and $h = (h_1, ..., h_n) \in (L^2(\Omega))^n$.

Equations (3.9)–(3.10) are endowed with the Neumann boundary conditions

$$\frac{\partial c_i}{\partial \nu} = \frac{\partial \mu_i}{\partial \nu} = 0, \qquad \text{on } \partial\Omega, \ i = 1, ..., n. \tag{3.11}$$

We note that the additional fidelity term in (3.9) can be derived from a gradient flow under the L^2-inner product for the energy

$$\frac{\lambda_0}{2}\sum_{i=1}^{n}\int_{\Omega\setminus D}(c_i-h_i)^2dx. \tag{3.12}$$

Our proposed model (3.9)–(3.10) can thus be thought of as the superposition of a gradient descent with respect to the $H^{-1}-$inner product for (3.3) and a gradient descent with respect to the L^2-inner product for (3.12). However, it is not the gradient descent, neither in the $H^{-1}-$ nor the L^2-inner product, for the sum of the energies (3.3) and (3.12).

We again assume that $\sum_{i=1}^{n} c_i = 1$, so that the additional fidelity term in (3.9) must also satisfy the constraint (3.2) everywhere and at every time,

$$\sum_{i=1}^{n} h_i = 1,$$

hence

$$\lambda(x)\sum_{i=1}^{n}(c_i-h_i)=0, \qquad \forall t\geq 0.$$

We rewrite (3.9)–(3.11) in the form

$$\frac{\partial c}{\partial t} = \Delta\mu + \lambda_0\chi_{\Omega\setminus D}(x)(h-c), \tag{3.13}$$

$$\mu = f(c) - \varepsilon^2\Delta c, \tag{3.14}$$

$$\frac{\partial c}{\partial \nu} = \frac{\partial \mu}{\partial \nu} = 0, \tag{3.15}$$

where $c=(c_i)_i$, $\mu=(\mu_i)_i$, $h=(h_i)_i$, and $f(c)=(f_i(c))_i$,

$$f_i(c) = \frac{2}{n}[c_i(1-c_i)^2 - c_i^2(1-c_i)] - \frac{1}{n}\sum_{i=1}^{n}\frac{\partial F}{\partial c_i},$$

$i=1,...,n$.

We define the tangent space of S (defined in (3.2)) as

$$TS := \{\phi=(\phi_i)_i\in\mathbb{R}^n \text{ such that } \sum_{i=1}^{n}\phi_i = 0\}. \tag{3.16}$$

Then, we introduce the projection

$$\begin{aligned}\mathbb{P}:\mathbb{R}^n &\to TS\\ \phi &\mapsto \mathbb{P}\phi = \phi - \frac{1}{n}(\phi.e)e,\end{aligned}$$

where $e=(1,...,1)$. Notice that, if $\phi\in S\cap(L^2(\Omega))^n$, then

$$\mathbb{P}\bar{\phi}=\bar{\phi}.$$

We denote by $\langle\phi\rangle$ the spatial average of a function ϕ in $(L^1(\Omega))^n$,

$$\langle\phi\rangle := \frac{1}{\mathrm{Vol}(\Omega)}\int_\Omega \phi(x)dx$$

and set

$$\bar{c} := c - \langle c\rangle,$$

$\bar{c}$ being the mean-free part of c.

We further introduce the following spaces :

$$L = (H^{-1}(\Omega))^n \cap S, \quad H = (L^2(\Omega))^n \cap S,$$

$$V = (H^1(\Omega))^n \cap S,\ W = \left\{v \in (H^2(\Omega))^n \cap S,\ \frac{\partial v}{\partial \nu} = 0 \text{ on } \Gamma\right\},$$

$$\dot{H}^{-1}(\Omega) = \{\phi \in (H^{-1}(\Omega))^n \cap TS,\ \langle\phi, e\rangle_{(H^{-1}(\Omega))^n,(H^1(\Omega))^n} = 0\},$$

$$\dot{H} = \{\phi \in (L^2(\Omega))^n \cap TS,\ \langle\phi\rangle = 0\},$$

$$\dot{V} = \{\phi \in (H^1(\Omega))^n \cap TS,\ \langle\phi\rangle = 0\},$$

and

$$\dot{W} = \{\phi \in (H^2(\Omega))^n \cap TS,\ \langle\phi\rangle = 0\}.$$

We finally introduce the bilinear form

$$a(u, v) = ((\nabla u, \nabla v))$$

which is continuous on V. Here and below, we denote by $\|.\|$ the usual L^2-norm (with associated scalar product $((.,.))$) ; in general, $\|.\|_X$ denotes the norm on the Banach space X. We can associate with a the linear operator A in $\dot{V}$ with domain $D(A) = \dot{W}$. For $u \in D(A)$, Au is defined by

$$((Au, v)) = a(u, v), \qquad \forall v \in \dot{V},$$

which amounts to saying that $Au = -\Delta u$. It is easy to show that A is an isomorphism from $\dot{V}$ onto $\dot{V}'$ (the dual of $\dot{V}$) and from $D(A)$ onto $\dot{H}$. Furthermore, in light of the compact injection of $(H^1(\Omega))^n$ in $(L^2(\Omega))^n$ (and also of $\dot{V}$ in $\dot{H}$), it follows that A^{-1} is self-adjoint and compact. There thus exists an orthonormal basis of $\dot{H}$ associated with the eigenvalues λ_j, $j \geq 1$, of A,

$$\begin{cases} \lambda_1 = \inf\limits_{v\in\dot{V}\setminus\{0\}} \dfrac{\|v\|_V^2}{\|v\|^2}, \\ AN_j = \lambda_j N_j, \quad N_j \in D(A), \quad j \geq 1, \\ 0 < \lambda_1 \leq \lambda_2 ..., \end{cases}$$

The family $\{N_j\}_j$ may be assumed to be normalized in the norm of $\dot{H}$, i.e.,

$$((N_i, N_j)) = \delta_{ij},$$

where

$$\delta_{ij} = \begin{cases} 1 & \text{if } i = j, \\ 0 & \text{otherwise.} \end{cases}$$

We now rewrite problem (3.13)-(3.14) in the form

$$\frac{\partial c}{\partial t} + A\overline{\mathbb{P}\mu} + \lambda_0 \chi_{\Omega\setminus D}(x)(c-h) = 0, \tag{3.17}$$

$$\mathbb{P}\mu = \mathbb{P}f(c) + \varepsilon^2 A\bar{c}. \tag{3.18}$$

For simplicity, we set $\varepsilon = 1$ and have

$$\frac{\partial c}{\partial t} + A\overline{\mathbb{P}\mu} + \lambda_0 \chi_{\Omega\setminus D}(x)(c-h) = 0, \tag{3.19}$$

$$\mathbb{P}\mu = \mathbb{P}f(c) + A\bar{c}. \tag{3.20}$$

Integrating (3.19) over Ω, we obtain

$$\frac{d\langle c\rangle}{dt} = -\lambda_0 \langle \chi_{\Omega\setminus D}(x)(c-h)\rangle \tag{3.21}$$

We can thus rewrite (3.19)-(3.20) in the form

$$\frac{\partial \bar{c}}{\partial t} + A\overline{\mathbb{P}\mu} + \lambda_0 \overline{\chi_{\Omega\setminus D}(x)(c-h)} = 0, \tag{3.22}$$

$$\mathbb{P}\mu = \mathbb{P}f(c) + A\bar{c}. \tag{3.23}$$

Finally, we can reformulate the problem as follows :

$$\frac{\partial A^{-1}\bar{c}}{\partial t} + \overline{\mathbb{P}\mu} + \lambda_0 A^{-1}(\overline{\chi_{\Omega\setminus D}(x)(c-h)}) = 0, \tag{3.24}$$

$$\mathbb{P}\mu = \mathbb{P}f(c) + A\bar{c}. \tag{3.25}$$

As far as the function f is concerned, we assume that $f \in C^2(\mathbb{R}^n)$, f' has at most a quadratic growth, f'' has at most a linear growth, and

$$((f'(c)v, v)) \geq -\xi_0 \|v\|^2, \quad \xi_0 \geq 0, \ \forall c \in \mathbb{R}^n, \ \forall v \in TS, \tag{3.26}$$

$$((\overline{f(c)}, \bar{c})) \geq \alpha \int_\Omega (\bar{c}^2.\bar{c}^2 + \langle c\rangle^2.\bar{c}^2)dx - \xi\|\bar{c}\|^2, \quad \alpha > 0, \ \xi \geq 0, \ \forall c \in S, \tag{3.27}$$

where $\varphi^2 = (\varphi_i^2)_i$, $\varphi = (\varphi_i)_i \in \mathbb{R}^n$, and $f'(c) = (\nabla f_i(c))_i$ denotes the Jacobian matrix of f, $i = 1, ..., n$.

Remark 3.2.1. *In particular, assumptions* (3.26) *and* (3.27) *are satisfied by our proposed model* (3.9)–(3.10). *Indeed, we recall that*

$$f_i(c) = \frac{2}{n}[c_i(1-c_i)^2 - c_i^2(1-c_i)] - \frac{1}{n}\sum_{j=1}^{n}\frac{\partial F}{\partial c_j},$$

$i = 1, ..., n$. *We thus have*

$$\frac{\partial f_i}{\partial c_i}(c) = \frac{2}{n}[6c_i^2 - 6c_i + 1] - \frac{2}{n^2}[6c_i^2 - 6c_i + 1], \quad i = 1, ..., n,$$

and

$$\frac{\partial f_i}{\partial c_j}(c) = -\frac{2}{n^2}[6c_j^2 - 6c_j + 1], \quad i, j = 1, ..., n, \ \ j \neq i.$$

Therefore, the i-th component of $f'(c)v$ reads

$$(f'(c)v)_i = \frac{2}{n}[6c_i^2 - 6c_i + 1]v_i - \frac{2}{n^2}\sum_{j=1}^{n}\Big([6c_j^2 - 6c_j + 1]v_j\Big), \quad i = 1, ..., n,$$

hence

$$\begin{aligned}((f'(c)v, v)) =& \frac{2}{n}\int_\Omega \sum_{i=1}^{n}\Big([6c_i^2 - 6c_i + 1]v_i^2\Big)dx \\ & -\frac{2}{n^2}\int_\Omega \sum_{j=1}^{n}\Big([6c_j^2 - 6c_j + 1]v_j\Big)\sum_{i=1}^{n} v_i dx \\ =& \frac{2}{n}\int_\Omega \sum_{i=1}^{n}\Big([6c_i^2 - 6c_i + 1]v_i^2\Big)dx,\end{aligned}$$

since $v \in TS$. It thus follows that

$$((f'(c)v, v)) \geq -\sum_{i=1}^{n}\xi_i\|v_i\|^2,$$

where $\xi_i > 0$, $i = 1, ..., n$. On the other hand, writing $c = \bar{c} + \langle c\rangle$, we have

$$\begin{aligned}((\overline{f(c)}, \bar{c})) &= ((f(c), \bar{c})) \\ &= \int_\Omega \sum_{i=1}^{n} f_i(c)\bar{c}_i dx \\ &= \frac{2}{n}\int_\Omega \sum_{i=1}^{n}[2c_i^3 - 3c_i^2 + c_i]\bar{c}_i dx - \frac{1}{n}\int_\Omega \sum_{j=1}^{n}\frac{\partial F}{\partial c_j}\sum_{i=1}^{n}\bar{c}_i dx \\ &= \frac{2}{n}\sum_{i=1}^{n}\int_\Omega (2c_i^3 - 3c_i^2 + c_i)\bar{c}_i dx \\ &= \frac{2}{n}\sum_{i=1}^{n}\int_\Omega (2\bar{c}_i^3 + 6\bar{c}_i^2\langle c_i\rangle + 6\bar{c}_i\langle c_i\rangle^2 - 3\bar{c}_i^2 - 6\bar{c}_i\langle c_i\rangle + \bar{c}_i)\bar{c}_i dx \\ &\geq \frac{2}{n}\sum_{i=1}^{n}\Big[\int_\Omega (2\bar{c}_i^4 + 6\bar{c}_i^2\langle c_i\rangle^2 + \bar{c}_i^2)dx - 6\int_\Omega |\bar{c}_i|^3|\langle c_i\rangle|dx \\ &\quad - 3\int_\Omega |\bar{c}_i|^3 dx - 6\int_\Omega \bar{c}_i^2|\langle c_i\rangle|dx\Big],\end{aligned}$$

for all $c \in S$, since $\bar{c} \in TS$. We then deduce from Young's inequality (e.g., $6ab \leq \frac{7}{4}a^2 + \frac{36}{7}b^2$; see [42] for more details) that

$$((\overline{f(c)}, \bar{c})) \geq \alpha\int_\Omega \sum_{i=1}^{n}[\bar{c}_i^4 + \langle c_i\rangle^2\bar{c}_i^2]dx - \xi\sum_{i=1}^{n}\|\bar{c}_i\|^2, \quad \alpha > 0, \ \ \xi \geq 0.$$

We note that, for $v = (v_i)_i \in S$,

$$v \to (\|v - \langle v\rangle\|_{-1}^2 + \langle v\rangle^2)^{\frac{1}{2}},$$
$$v \to (\|v - \langle v\rangle\|^2 + \langle v\rangle^2)^{\frac{1}{2}},$$
$$v \to (\|A^{\frac{1}{2}}\bar{v}\|^2 + \langle v\rangle^2)^{\frac{1}{2}},$$

and

$$v \to (\|A\bar{v}\|^2 + \langle v\rangle^2)^{\frac{1}{2}}$$

are norms in L, H, V, and W, respectively, which are equivalent to the usual ones. Here, $\|\cdot\|_{-1} = \|A^{-\frac{1}{2}}\cdot\|$.

Throughout this article, the same letter ξ (and, sometimes, ζ and η) denotes constants which may vary from line to line, or even in a same line. Similarly, the same letter Q denotes monotone increasing functions which may vary from line to line, or even in a same line.

3.3 A priori estimates

We first multiply (3.24) by $\bar{c}$ and have

$$\begin{aligned}
\frac{1}{2}\frac{d}{dt}\|\bar{c}\|_{-1}^2 &= -((\overline{\mathbb{P}\mu}, \bar{c})) - \lambda_0((A^{-1}\overline{\chi_{\Omega\setminus D}(x)(c-h)}, \bar{c})) \\
&= -\|A^{\frac{1}{2}}\bar{c}\|^2 - ((\overline{f(c)}, \bar{c})) - \lambda_0((\chi_{\Omega\setminus D}(x)(c-h), A^{-1}\bar{c})) \\
&\le -\|A^{\frac{1}{2}}\bar{c}\|^2 - \alpha\int_\Omega (\bar{c}^2.\,\bar{c}^2 + \langle c\rangle^2.\,\bar{c}^2)dx + \lambda_0(\|c\| + \|h\|)\|\bar{c}\| \\
&\le -\|A^{\frac{1}{2}}\bar{c}\|^2 - \alpha\int_\Omega (\bar{c}^2.\,\bar{c}^2 + \langle c\rangle^2.\,\bar{c}^2)dx + \zeta(\|\bar{c}\|^2 + \langle c\rangle^2) + \eta(\|h\|^2 + 1) \\
&\le -\|A^{\frac{1}{2}}\bar{c}\|^2 - \alpha\int_\Omega (\bar{c}^2.\,\bar{c}^2 + \langle c\rangle^2.\,\bar{c}^2)dx + \frac{\alpha}{2}\int_\Omega (\bar{c}^2.\,\bar{c}^2 + \langle c\rangle^2.\,\bar{c}^2)dx + \eta(\|h\|^2 + 1) \\
&\le -\|A^{\frac{1}{2}}\bar{c}\|^2 - \frac{\alpha}{2}\int_\Omega (\bar{c}^2.\,\bar{c}^2 + \langle c\rangle^2.\,\bar{c}^2)dx + \eta(\|h\|^2 + 1),
\end{aligned}$$

owing to (3.25) and (3.27), hence

$$\frac{d}{dt}\|\bar{c}\|_{-1}^2 + \|A^{\frac{1}{2}}\bar{c}\|^2 + \alpha\int_\Omega (\bar{c}^2.\,\bar{c}^2 + \langle c\rangle^2.\,\bar{c}^2)dx \le \xi, \tag{3.28}$$

which yields

$$\frac{d}{dt}\|\bar{c}\|_{-1}^2 + \xi\|\bar{c}\|_{-1}^2 \le \zeta, \qquad \xi > 0. \tag{3.29}$$

It thus follows from (3.29) and Gronwall's lemma that

$$\|\bar{c}\|_{-1}^2 \le e^{-\xi t}\|\bar{c}_0\|_{-1}^2 + \zeta, \qquad \xi > 0, \;\; t \ge 0. \tag{3.30}$$

Let B be a bounded subset of $\dot{H}^{-1}(\Omega)$ and t_0 be such that $\bar{c}_0 \in B$ and $t \ge t_0$ implies $\bar{c}(t) \in \mathcal{B}_0$, where $\mathcal{B}_0 = \{\phi \in \dot{H}^{-1}(\Omega),\ \|\phi\|_{-1}^2 \le 2\zeta\}$, ζ being the constant in (3.30). We then deduce from (3.28) that, for $t \ge t_0$,

$$\int_t^{t+r} \|A^{\frac{1}{2}}\bar{c}\|^2 ds \le \xi(r), \quad \int_t^{t+r} ds\int_\Omega (\bar{c}^2.\,\bar{c}^2 + \langle c\rangle^2.\,\bar{c}^2)dx \le \xi(r), \tag{3.31}$$

for $r > 0$ fixed.

We then multiply (3.24) by $A\bar{c}$ and find

$$\begin{aligned}
\frac{1}{2}\frac{d}{dt}\|\bar{c}\|^2 &= -((\mathbb{P}\mu, A\bar{c})) - \lambda_0((\overline{\chi_{\Omega\setminus D}(x)(c-h)}, \bar{c})) \\
&= -\|A\bar{c}\|^2 - ((f(c), A\bar{c})) - \lambda_0((\chi_{\Omega\setminus D}(x)(c-h), \bar{c})) \\
&\leq -\|A\bar{c}\|^2 - ((f'(c)A^{\frac{1}{2}}\bar{c}, A^{\frac{1}{2}}\bar{c})) + \lambda_0(\|c\| + \|h\|)\|\bar{c}\| \\
&\leq -\|A\bar{c}\|^2 + \xi_0\|A^{\frac{1}{2}}\bar{c}\|^2 + \zeta\int_\Omega(\int_\Omega \bar{c}^2.\,\bar{c}^2 + \langle c\rangle^2.\,\bar{c}^2)dx + \eta\|h\|^2 \\
&\leq -\|A\bar{c}\|^2 + \xi_0\|A^{\frac{1}{2}}\bar{c}\|^2 + \zeta\Big(\int_\Omega(\bar{c}^2.\,\bar{c}^2 + \langle c\rangle^2.\,\bar{c}^2)dx + \|h\|^2 + 1\Big),
\end{aligned}$$

owing to (3.25) and (3.26), hence

$$\frac{d}{dt}\|\bar{c}\|^2 + \|A\bar{c}\|^2 \leq \xi_0\|A^{\frac{1}{2}}\bar{c}\| + \zeta\Big(\int_\Omega(\bar{c}^2.\,\bar{c}^2 + \langle c\rangle^2.\,\bar{c}^2)dx + \|h\|^2 + 1\Big). \tag{3.32}$$

It thus follows from (3.31), (3.32), and the uniform Gronwall's lemma that

$$\|\bar{c}\|^2 \leq \xi, \qquad t \geq t_0 + r, \tag{3.33}$$

where the constant ξ is independent of $\bar{c}_0$ and t, hence, employing (3.33) and integrating (3.28) and (3.32) between 0 and $t_0 + r$,

$$\|\bar{c}(t)\|^2 \leq Q(\|\bar{c}_0\|), \quad t \geq 0. \tag{3.34}$$

Now, writing $c = \langle c\rangle + \bar{c}$ in (3.21), we find

$$\frac{d}{dt}\langle c\rangle + \frac{\lambda_0}{\mathrm{Vol}(\Omega)}\int_{\Omega\setminus D}(\langle c\rangle + \bar{c} - h)dx = 0.$$

Therefore,

$$\frac{d}{dt}\langle c\rangle + \xi\langle c\rangle = -\frac{\lambda_0}{\mathrm{Vol}(\Omega)}\int_{\Omega\setminus D}(\bar{c} - h)dx,$$

where $\xi = \frac{\lambda_0\mathrm{Vol}(\Omega\setminus D)}{\mathrm{Vol}(\Omega)}$, hence

$$\frac{d}{dt}(e^{\xi t}\langle c\rangle) = -\frac{\lambda_0}{\mathrm{Vol}(\Omega)}e^{\xi t}\int_{\Omega\setminus D}(\bar{c} - h)dx$$

and

$$\langle c\rangle = e^{-\xi t}\langle c_0\rangle - \frac{\lambda_0}{\mathrm{Vol}(\Omega)}e^{-\xi t}\int_0^t e^{\xi s}\int_{\Omega\setminus D}(\bar{c} - h)dxds.$$

Thus,

$$|\langle c\rangle| \leq e^{-\xi t}|\langle c_0\rangle| + \zeta e^{-\xi t}\int_0^t e^{\xi s}(\|\bar{c}\| + \|h\|)ds, \qquad \forall t \geq 0,$$

where $\zeta = \frac{\lambda_0}{(\mathrm{Vol}(\Omega))^{\frac{1}{2}}}$. Here,

$$\begin{aligned}\zeta e^{-\xi t}\int_0^t e^{\xi s}\|h\|ds &\le \zeta e^{-\xi t}\|h\|e^{\xi t}\\ &\le \zeta\|h\|\\ &\le \eta.\end{aligned}$$

Furthermore, for $t \ge t_0 + r$,

$$\begin{aligned}\zeta e^{-\xi t}\int_0^t e^{\xi s}\|\bar{c}\|ds &= \zeta e^{-\xi t}\int_0^{t_0+r} e^{\xi s}\|\bar{c}\|ds + \zeta e^{-\xi t}\int_{t_0+r}^t e^{\xi s}\|\bar{c}\|ds\\ &\le Q(\|\bar{c}_0\|)e^{-\xi t}e^{\xi(t_0+r)} + \zeta e^{-\xi t}\int_{t_0+r}^t e^{\xi s}\|\bar{c}\|ds\\ &\le Q(\|\bar{c}_0\|)e^{-\xi t} + \zeta e^{-\xi t}\int_{t_0+r}^t e^{\xi s}\|\bar{c}\|ds\\ &\le Q(\|\bar{c}_0\|)e^{-\xi t} + \eta e^{-\xi t}(e^{\xi t} - e^{\xi(t_0+r)})\\ &\le Q(\|\bar{c}_0\|)e^{-\xi t} + \zeta,\end{aligned}$$

where we have used (3.33) (resp., (3.34)) to estimate the first (resp., the second) integral in the right-hand side of the first equality. Finally, we obtain

$$|\langle c\rangle| \le (Q(\|\bar{c}_0\|) + |\langle c_0\rangle|)e^{-\xi t} + \zeta, \qquad \forall t \ge 0, \tag{3.35}$$

where ξ and ζ are two constants which are nonnegative and independent of t and c_0.

We finally multiply (3.19) by $A^2\bar{c}$ to obtain, noting that

$$((A\overline{\mathbb{P}\mu}, A^2\bar{c})) = ((\mathbb{P}\mu, A^3\bar{c})) = ((\mu, A^3\bar{c})),$$

the differential equalities

$$\begin{aligned}\frac{1}{2}\frac{d}{dt}\|A\bar{c}\|^2 &= -((\mu, A^3\bar{c})) - \lambda_0((\chi_{\Omega\setminus D}(x)(c-h), A^2\bar{c}))\\ &= -\|A^2\bar{c}\|^2 - ((A\overline{f(c)}, A^2\bar{c})) - \lambda_0((\chi_{\Omega\setminus D}(x)(c-h), A^2\bar{c})).\end{aligned} \tag{3.36}$$

Using the fact that

$$\Delta f(c) = f'(c)\Delta c + f''(c)|\nabla c|^2,$$

we have (see, e.g., [137])

$$\begin{aligned}|((A\overline{f(c)}, A^2\bar{c}))| &= |((-\Delta f(c), A^2\bar{c}))|\\ &\le \xi\|\Delta f(c)\|^2 + \frac{1}{4}\|A^2\bar{c}\|^2\\ &\le \frac{1}{2}\|A^2\bar{c}\|^2 + \xi.\end{aligned} \tag{3.37}$$

Furthermore,

$$\begin{aligned}\lambda_0|((\chi_{\Omega\setminus D}(x)(c-h), A^2\bar{c}))| &\le \xi\|c-h\|\|A^2\bar{c}\|\\ &\le \xi(\|\bar{c}\|^2 + \langle c\rangle^2) + \frac{1}{2}\|A^2\bar{c}\|^2 + \zeta\|h\|^2.\end{aligned} \tag{3.38}$$

We finally deduce from (3.36), (3.37), and (3.38) that

$$\frac{d}{dt}\|A\bar{c}\|^2 \leq \xi(\|\bar{c}\|^2 + \langle c\rangle^2) + \zeta. \tag{3.39}$$

Note that, integrating (3.32) over $(t, t+r)$, we have, for $t \geq t_0 + r$,

$$\int_t^{t+r} \|A\bar{c}\|^2 dx \leq \xi(r), \tag{3.40}$$

owing to (3.33). Furthermore, owing to (3.21), we have

$$\begin{aligned} \frac{d}{dt}\langle c\rangle^2 &= 2\langle c\rangle \frac{d}{dt}\langle c\rangle \\ &\leq 2\lambda_0|\langle c\rangle|\Big|\int_{\Omega\setminus D}(c-h)dx\Big| \\ &\leq \xi(\|\bar{c}\|^2 + (\langle c\rangle)^2) + \zeta(\|h\|^2 + 1) \end{aligned} \tag{3.41}$$

and, owing to (3.33) and (3.35), $\exists t_1$ such that, $\forall t \geq t_1$,

$$|\langle c\rangle| \leq \xi \quad \text{and} \quad \|\bar{c}\|^2 \leq \xi. \tag{3.42}$$

We finally deduce from (3.33), (3.35), (3.39), (3.40), (3.41), (3.42), and the uniform Gronwall's lemma that

$$\|c\|_W \leq \xi, \quad t \geq t_1 + r, \tag{3.43}$$

where $r > 0$ is fixed.

3.4 Well-posedness and existence of the global attractor

We have the

Theorem 3.4.1. *We assume that $c_0 \in H$. Then, (3.19)–(3.20) possesses a unique solution c such that*

$$c \in L^\infty([0,T], H) \cap L^2([0,T], W) \cap L^4([0,T], (L^4(\Omega))^n \cap S), \quad \forall T > 0.$$

Proof. *We first denote by E_m the space*

$$E_m = span\{N_1, N_2, ..., N_m\}$$

and by P_m the orthogonal projection from $\dot{V}$ onto E_m,

$$P_m h = \sum_{j=1}^{m} ((h, N_j))N_j.$$

The variational formulation of the problem reads : Find $c_m : [0,T] \to \langle c_m\rangle + E_m$, $c_m(t) = \langle c_m(t)\rangle + \overline{c}_m(t) = \langle c_m(t)\rangle + \sum_{j=1}^{m} c_{m_j}(t)N_j$, such that

$$\begin{aligned} &\frac{d}{dt}\Big(\Big(A^{-1}\sum_{i=1}^{m}\bar{c}_m(t)N_i, N_j\Big)\Big) - \Big(\Big(\sum_{i=1}^{m}\bar{c}_{m_i}(t)A^{\frac{1}{2}}N_i, A^{\frac{1}{2}}N_j\Big)\Big) + ((\overline{\mathbb{P}f(\langle c_m\rangle + \overline{c}_m)}, N_j)) \\ &\quad + \lambda_0((A^{-1}(\overline{\chi_{\Omega\setminus D}(x)(\langle c_m\rangle + \overline{c}_m - h)}), N_j)) = 0, \quad j = 1, ..., m, \end{aligned} \tag{3.44}$$

$$\frac{d}{dt}\langle c_m\rangle + \xi\langle c_m\rangle = -\frac{\lambda_0}{Vol(\Omega)}\int_{\Omega\setminus D}(\bar{c}_m - h)dx, \tag{3.45}$$

$$\bar{c}_m(0) = P_m c_0, \tag{3.46}$$

$$\langle c_m(0)\rangle = \langle c_0\rangle. \tag{3.47}$$

We can rewrite (3.44) and (3.46) as

$$\begin{aligned}\frac{\partial A^{-1}\bar{c}_m}{\partial t} &+ \overline{\mathbb{P}f(\langle c_m\rangle + \overline{c}_m)} + A\bar{c}_m + \lambda_0 A^{-1}(\overline{\chi_{\Omega\setminus D}(x)(\langle c_m\rangle + \overline{c}_m - h)}) \\ &= 0, \quad \text{in } E_m',\end{aligned} \tag{3.48}$$

$$\bar{c}_m(0) = P_m c_0, \tag{3.49}$$

and we finally rewrite equation (3.44) as follows :

$$M^{-1}\frac{dY}{dt} + MY + H(Y) = 0,$$

where $M = ((AN_i, N_j))_{i,j=1,\dots,m}$, $Y = \begin{pmatrix} c_{m_1} \\ . \\ . \\ . \\ c_{m_m} \end{pmatrix}$, *and*

$$H(Y) = \begin{pmatrix} ((\overline{\mathbb{P}f(\langle c_m\rangle + \overline{c}_m)} + \lambda_0 A^{-1}(\overline{\chi_{\Omega\setminus D}(\mathbb{P}(\langle c_m\rangle + \overline{c}_m - h))}), N_1)) \\ . \\ . \\ . \\ ((\overline{\mathbb{P}f(\langle c_m\rangle + \overline{c}_m)} + \lambda_0 A^{-1}(\overline{\chi_{\Omega\setminus D}(\mathbb{P}(\langle c_m\rangle + \overline{c}_m - h))}), N_m)) \end{pmatrix},$$

noting that $\langle c_m\rangle$ *can be expressed as a function of* $\overline{c}_m$ *by solving (3.45). The matrix* M *is invertible and positive definite and* $H(Y)$ *depends continuously on* Y. *Applying Cauchy's theorem, we find that there exists a time* $t_m \in (0, T)$ *and a solution* Y *to*

$$\frac{dY}{dt} + M^2 Y + MH(Y) = 0$$

on the time interval $[0, t_m[$. *Having* $\overline{c}_m$, *we then deduce* $\langle c_m\rangle$ *(from (3.45)).*

It follows from the a priori estimates derived in the previous section for the solution $c_m(t)$ *(*$c(t)$ *being replaced by* $c_m(t)$*) that any local solution to* (3.19)–(3.20) *is actually a global solution defined on the whole interval* $[0, T]$. *It then follows from the a priori estimates that, up to a subsequence which we do not relabel,*

$$c_m \rightharpoonup c \text{ weakly in } L^2(0, T, W), \tag{3.50}$$

$$\frac{\partial c_m}{\partial t} \rightharpoonup \frac{\partial c}{\partial t} \text{ weakly in } L^{\frac{4}{3}}(0, T, W^{-2,\frac{4}{3}}(\Omega)), \tag{3.51}$$

as $m \to \infty$. It follows from (3.50), (3.51), *and the Aubin-Lions compactness theorem that*

$$c_m \to c \text{ strongly in } L^{\frac{4}{3}}(0,T,(L^{\frac{4}{3}}(\Omega))^n \cap S) \tag{3.52}$$

and $c_m(t,x) \to c(x,t)$ a.e. $(t,x) \in [0,T] \times \Omega$. Moreover, since f is a continuous,

$$f(c_m(t,x)) \to f(c(t,x)) \text{ a.e.}$$

and, since $f(c_m)$ is bounded in $L^{\frac{4}{3}}(\Omega_T)$, $\Omega_T = (0,T) \times \Omega$,

$$f(c_m) \rightharpoonup f(c) \text{ weakly in } L^{\frac{4}{3}}(\Omega_T) \cap TS,$$

owing to the weak dominated convergence theorem. Finally, we deduce that $A^{-1}\frac{\partial \bar{c}_m}{\partial t} \rightharpoonup A^{-1}\frac{\partial \bar{c}}{\partial t}$ weakly in $L^{\frac{4}{3}}(\Omega_T)$. Thus, passing to the limit in (3.48), *we obtain*

$$\frac{\partial A^{-1}\bar{c}}{\partial t} + \overline{\mathbb{P}f(c)} + A\bar{c} + \lambda_0 A^{-1}(\overline{\chi_{\Omega\setminus D}(x)(\mathbb{P}c - \mathbb{P}h)}) = 0, \quad \text{in } L^{\frac{4}{3}}(\Omega_T) \cap TS. \tag{3.53}$$

Finally, we easily pass to the limit in (3.45), at least in a weak sense, i.e., solving explicitly this ODE.

Let now c_1 and c_2 be two solutions to (3.19)–(3.20) with initial data $c_{0,1}$ and $c_{0,2}$, respectively. We set $c = c_1 - c_2$, $c_0 = c_{0,1} - c_{0,2}$, and $\mu = \mu_1 - \mu_2$ and have

$$\frac{\partial c}{\partial t} + A\overline{\mathbb{P}\mu} + \lambda_0 \chi_{\Omega\setminus D}(x)c = 0, \tag{3.54}$$

$$\mathbb{P}\mu = \mathbb{P}(f(c_1) - f(c_2)) + A\bar{c}, \tag{3.55}$$

$$c|_{t=0} = c_0 = c_{0,1} - c_{0,2}. \tag{3.56}$$

Integrating (3.54) over Ω, we obtain

$$\frac{d}{dt}\langle c \rangle = -\frac{\lambda_0}{Vol(\Omega)} \int_{\Omega\setminus D} c dx. \tag{3.57}$$

We can thus rewrite the problem as

$$\frac{\partial \bar{c}}{\partial t} + A\overline{\mathbb{P}\mu} + \lambda_0 \overline{\chi_{\Omega\setminus D}(x)c} = 0, \tag{3.58}$$

$$\mathbb{P}\mu = \mathbb{P}(f(c_1) - f(c_2)) + A\bar{c}, \tag{3.59}$$

or else

$$\frac{\partial A^{-1}\bar{c}}{\partial t} + \overline{\mathbb{P}\mu} + \lambda_0 A^{-1}\overline{\chi_{\Omega\setminus D}(x)c} = 0, \tag{3.60}$$

$$\mathbb{P}\mu = \mathbb{P}(f(c_1) - f(c_2)) + A\bar{c}. \tag{3.61}$$

We multiply (3.60) *by* $\bar{c}$ *and find*

$$\begin{aligned}\frac{1}{2}\frac{d}{dt}\|\bar{c}\|_{-1}^2 &= -((\mu,\bar{c})) - \lambda_0((A^{-1}\overline{\chi_{\Omega\setminus D}(x)c},\bar{c}))\\ &= -((f(c_1)-f(c_2),c)) + ((f(c_1)-f(c_2),\langle c\rangle))\\ &\quad - \|A^{\frac{1}{2}}\bar{c}\|^2 - \lambda_0((\overline{\chi_{\Omega\setminus D}(x)c},A^{-1}\bar{c}))\\ &\le \xi_0\|c\|^2 + ((f(c_1)-f(c_2),\langle c\rangle)) - \|A^{\frac{1}{2}}\bar{c}\|^2 - \lambda_0((\chi_{\Omega\setminus D}(x)c,A^{-1}\bar{c}))\\ &\le \xi_0\|c\|^2 + \Big|((f(c_1)-f(c_2),\langle c\rangle))\Big| - \|A^{\frac{1}{2}}\bar{c}\|^2 + \xi\|c\|\|\bar{c}\|_{-1}\\ &\le \xi(\|\bar{c}\|^2+\langle c\rangle^2) + \zeta\|\bar{c}\|_{-1}^2 - \|A^{\frac{1}{2}}\bar{c}\|^2 + \Big|((f(c_1)-f(c_2),\langle c\rangle))\Big|,\end{aligned}$$

owing to (3.26) *and* (3.61). *We note that, owing also to* (3.26),

$$\begin{aligned}\Big|((f(c_1)-f(c_2,\langle c\rangle))\Big| &= \Big|\langle c\rangle\int_\Omega c\int_0^1 f'(c_1+s(c_2-c_1))dsdx\Big|\\ &\le \xi|\langle c\rangle|\int_\Omega(|c_1|^2+|c_2|^2+1)|c|dx\\ &\le \xi|\langle c\rangle|(\|c_1\|^2_{(L^4(\Omega))^n}+\|c_2\|^2_{(L^4(\Omega))^n}+1)\|c\|\\ &\le \xi(\|c_1\|^2_{(L^4(\Omega))^n\cap S}+\|c_2\|^2_{(L^4(\Omega))^n\cap S}+1)(|\langle c\rangle|^2+\|\bar{c}\|^2),\end{aligned}$$

hence

$$\begin{aligned}\frac{1}{2}\frac{d}{dt}\|\bar{c}\|_{-1}^2 + \|A^{\frac{1}{2}}\bar{c}\|^2 \le \xi(\|c_1\|^2_{(L^4(\Omega))^n\cap S}+\|c_2\|^2_{(L^4(\Omega))^n\cap S}\\ +1)(|\langle c\rangle|^2+\|\bar{c}\|^2)+\zeta\|\bar{c}\|_{-1}^2.\end{aligned}\tag{3.62}$$

Noting then that

$$\begin{aligned}\frac{1}{2}\frac{d}{dt}|\langle c\rangle|^2 &\le |\langle c\rangle|\Big|\frac{d}{dt}\langle c\rangle\Big|\\ &\le \xi|\langle c\rangle|\,|\int_{\Omega\setminus D}cdx|\\ &\le \xi|\langle c\rangle|\|c\|\\ &\le \xi(\langle c\rangle^2+\|\bar{c}\|^2)\end{aligned}\tag{3.63}$$

and recalling the interpolation inequality

$$\|\bar{c}\|^2 \le \xi\|\bar{c}\|_{-1}\|A^{\frac{1}{2}}\bar{c}\|,$$

it follows that

$$\begin{aligned}\frac{d}{dt}(\|\bar{c}\|_{-1}^2+|\langle c\rangle|^2)+\|A^{\frac{1}{2}}\bar{c}\|^2 \le \xi(\|c_1\|^4_{(L^4(\Omega))^n\cap S}+\|c_2\|^4_{(L^4(\Omega))^n\cap S}\\ +1)(|\langle c\rangle|^2+\|\bar{c}\|_{-1}^2).\end{aligned}\tag{3.64}$$

We thus deduce from (3.64) and Gronwall's lemma that

$$\|c_1(t)-c_2(t)\|_L \le Q(T,\|c_{0,1}\|,\|c_{0,2}\|)\|c_{0,1}-c_{0,2}\|_L,\qquad 0\le t\le T,\tag{3.65}$$

hence the uniqueness, as well as the continuous dependence with respect to the initial data in the L–norm. □

It follows from Theorem 3.4.1 that we have the continuous (with respect to the L–norm) semigroup

$$S(t) : H \to H, \qquad c_0 \mapsto c(t), \quad t \geq 0$$

(i.e., $S(0) = I,\ S(t+s) = S(t) \circ S(s),\ t,\ s \geq 0$).

It then follows from (3.43) that $S(t)$ possesses a bounded absorbing set $\mathcal{B}_1$ which is compact in H and bounded in W. We thus deduce from standard results (see, e.g., [108, 137]) the following theorem.

Theorem 3.4.2. *The semigroup $S(t)$ possesses the connected global attractor $\mathcal{A}$ such that $\mathcal{A}$ is compact in H and bounded in W.*

3.5 Existence of exponential attractors

Let c_1 and c_2 be two solutions to (3.19)–(3.20) with initial data $c_{0,1}$ and $c_{0,2}$, respectively. We set $c = c_1 - c_2$, $c_0 = c_{0,1} - c_{0,2}$, and $\mu = \mu_1 - \mu_2$ and have

$$\frac{\partial c}{\partial t} + A\overline{\mathbb{P}\mu} + \lambda_0 \chi_{\Omega\setminus D}(x) c = 0, \tag{3.66}$$

$$\mathbb{P}\mu = \mathbb{P}(f(c_1) - f(c_2)) + A\bar{c}, \tag{3.67}$$

$$c|_{t=0} = c_0. \tag{3.68}$$

Furthermore, it is sufficient here to take initial data belonging to the bounded absorbing set $\mathcal{B}_1$ defined in the previous section.

We multiply (3.66) by tc to find, owing to (3.26) and (3.67),

$$\begin{aligned}\frac{1}{2}\frac{d}{dt}(t\|c\|^2) + \lambda_0 t\|\chi_{\Omega\setminus D}(x)c\|^2 &= \frac{1}{2}\|c\|^2 - t\|A\bar{c}\|^2 - t((A^{\frac{1}{2}}(\overline{f(c_1) - f(c_2)}), A^{\frac{1}{2}}\bar{c})) \\ &\leq \frac{1}{2}\|c\|^2 + \xi_0 t\|A^{\frac{1}{2}}\bar{c}\|^2,\end{aligned}$$

which yields

$$\frac{d}{dt}(t\|c\|^2) \leq \|c\|^2 + \xi t\|A^{\frac{1}{2}}\bar{c}\|^2. \tag{3.69}$$

Integrating (3.69) between 0 and t, we obtain

$$\|c\|^2 \leq \xi \frac{1+t}{t} \int_0^t \|c\|_V^2 ds, \quad t > 0. \tag{3.70}$$

Noting that (3.64) is equivalent to

$$\frac{d}{dt}(\|\bar{c}\|_{-1}^2 + |\langle c\rangle|^2) + \|c\|_V^2 \leq \xi(\|c_1\|_{(L^4(\Omega))^n\cap S}^4 + \|c_2\|_{(L^4(\Omega))^n\cap S}^4 + 1)(|\langle c\rangle|^2 + \|\bar{c}\|_{-1}^2), \tag{3.71}$$

it follows from (3.28), (3.65), and (3.71) that

$$\int_0^t \|c\|_V^2 ds \le \xi e^{\zeta t}\|c\|_L^2. \tag{3.72}$$

We then deduce from (3.69) and (3.72) that

$$t\|c\|_H^2 \le \xi e^{\zeta t}\|c\|_L^2, \quad t > 0. \tag{3.73}$$

Next, we derive a Hölder (both with respect to space and time) estimate. Actually, owing to (3.65), it suffices to prove the Hölder continuity with respect to time. We have

$$\begin{aligned} \|c(t_1) - c(t_2)\|_L &= \left\| \int_{t_1}^{t_2} \frac{\partial c}{\partial t} d\tau \right\|_L \le \left| \int_{t_1}^{t_2} \left\| \frac{\partial c}{\partial t} \right\|_L d\tau \right| \\ &\le |t_1 - t_2|^{\frac{1}{2}} \left| \int_{t_1}^{t_2} \left\| \frac{\partial c}{\partial t} \right\|_L^2 d\tau \right|^{\frac{1}{2}}. \end{aligned} \tag{3.74}$$

Multiplying (3.24) by $\frac{\partial \bar{c}}{\partial t}$, we find

$$\begin{aligned} \left\| \frac{\partial \bar{c}}{\partial t} \right\|_{-1}^2 &= -\Big(\Big(f(c), \frac{\partial \bar{c}}{\partial t} \Big) \Big) - \frac{1}{2}\frac{d}{dt}\|A^{\frac{1}{2}}\bar{c}\|^2 + \lambda_0 \Big(\Big(\chi_{\Omega\setminus D}(x)(h-c), A^{-1}\frac{\partial \bar{c}}{\partial t} \Big) \Big) \\ &\le \|A^{\frac{1}{2}}\overline{f(c)}\| \left\| \frac{\partial \bar{c}}{\partial t} \right\|_{-1} - \frac{1}{2}\frac{d}{dt}\|A^{\frac{1}{2}}\bar{c}\|^2 + \lambda_0 \|c-h\| \left\| \frac{\partial \bar{c}}{\partial t} \right\|_{-1}, \end{aligned}$$

owing to (3.25), hence

$$\frac{d}{dt}\|A^{\frac{1}{2}}\bar{c}\|^2 + \left\| \frac{\partial \bar{c}}{\partial t} \right\|_{-1}^2 \le \xi \|c\|_V^2 + \zeta, \tag{3.75}$$

owing to (3.26) and the continuous embedding $H^2(\Omega) \subset C(\overline{\Omega})$. Noting that

$$\langle \frac{\partial c}{\partial t} \rangle^2 \le \xi \|c\|^2 + \zeta, \tag{3.76}$$

owing to (3.21), we then deduce from (3.43), (3.75), and (3.76) that

$$\int_{t_1}^{t_2} \left\| \frac{\partial c}{\partial t} \right\|_L^2 d\tau \le \xi, \tag{3.77}$$

where the constant ξ depends on $\mathcal{B}_1$ and T such that $t_1, t_2 \in [0, T]$, so that

$$\|c(t_1) - c(t_2)\|_L \le \xi |t_1 - t_2|^{\frac{1}{2}}, \tag{3.78}$$

where the constant ξ depends on $\mathcal{B}_1$ and T such that $t_1, t_2 \in [0, T]$.

We finally deduce from (3.65), (3.73), and (3.78) the following result (see, e.g., [52, 53]).

Theorem 3.5.1. *The semigroup $S(t)$ possesses an exponential attractor $\mathcal{M} \subset \mathcal{B}_1$, i.e.,*

(i) $\mathcal{M}$ is compact in L;

(ii) $\mathcal{M}$ is positively invariant, $S(t)\mathcal{M} \subset \mathcal{M}$, $\forall t \ge 0$;

(iii) $\mathcal{M}$ has finite fractal dimension in L;

(iv) $\mathcal{M}$ *attracts exponentially fast the bounded subsets of* H,

$$\forall B \subset H \text{ bounded}, \quad dist_L(S(t)B, \mathcal{M}) \leq Q(\|B\|_H)e^{-\xi t}, \\ \xi > 0, \ \ t \geq 0,$$

where the constant ξ *is independent of* B *and* $dist_L$ *denotes the Hausdorff semidistance between sets defined by*

$$dist_L(A, B) = \sup_{a\in A} \inf_{b\in B} \|a - b\|_L.$$

Remark 3.5.2. *Setting* $\tilde{\mathcal{M}} = S(1)\mathcal{M}$*, we can prove that* $\tilde{\mathcal{M}}$ *is an exponential attractor for* $S(t)$*, but now in the topology of* H *(see, e.g., [54]).*

Since $\mathcal{M}$ (or $\tilde{\mathcal{M}}$) is a compact attracting set, we deduce from Theorem 3.5.1 the following corollary.

Corollary 1. *The semigroup* $S(t)$ *possesses the finite-dimensional global attractor* $\mathcal{A} \subset \mathcal{B}_1$.

Remark 3.5.3. *A more generally a nonlinear term* F *given in the following form :*

$$F(v) = \sum_{i=1}^{n} \sum_{k=0}^{2p+2} a_k v_i^k, \ \ a_{2p+2} > 0, \ \ v = (v_i)_i \in S.$$

We can replace assumption (3.27) *by*

$$((\overline{f(c)}, \bar{c})) \geq \alpha \int_\Omega \sum_{i=1}^{n} \sum_{k=0}^{p} \bar{c}_i^{2p+2-2k} \langle c \rangle^{2k} dx, \quad \alpha > 0, \ c = (c_i)_i \in S.$$

Indeed, since $F(c) = \sum\limits_{i=1}^{n} \sum\limits_{k=0}^{2p+2} a_k c_i^k$, $a_{2p+2} > 0$*, we have*

$$\frac{\partial F(c)}{\partial c_i} = \sum_{k=0}^{2p+1} (k+1) a_{k+1} c_i^k, \quad i = 1, ..., n,$$

hence

$$\frac{\partial^2 F(c)}{\partial c_i^2} \geq -\xi_i, \quad \xi_i \geq 0,$$

$i = 1, ..., n$*, and, owing to Remark 3.2.1,*

$$\begin{aligned} ((f'(c)v, v)) &= \int_\Omega \sum_{i=1}^{n} \frac{\partial^2 F(c)}{\partial c_i^2} v_i^2 dx \\ &\geq -\sum_{i=1}^{n} \xi_i \|v_i\|^2, \quad \xi_i \geq 0, \end{aligned}$$

for all $v \in TS$*. Furthermore, it follows from Remark 2.11 in [42] that*

$$((\overline{\frac{\partial F(c)}{\partial c_i}}, \bar{c}_i)) \geq \alpha \int_\Omega \sum_{k=0}^{p} \bar{c}_i^{2p+2-2k} \langle c \rangle^{2k} dx, \quad \alpha > 0, \ c \in S,$$

$i = 1, ..., n$, and, owing to Remark 3.2.1,

$$((\overline{f(c)}, \bar{c})) = \int_\Omega \sum_{i=1}^{n} \overline{\frac{\partial F(c)}{\partial c_i}} \bar{c}_i dx$$
$$\geq \alpha \int_\Omega \sum_{i=1}^{n} \sum_{k=0}^{p} \bar{c}_i^{2p+2-2k} \langle c \rangle^{2k} dx, \quad \alpha > 0,$$

for all $c \in S$. In that case, we can also obtain the global existence of the problem, as well as the existence of finite-dimensional attractors, of the dynamical system associated with the problem (at least $H^2 - L^2-$attractors) but we lose the uniqueness of the problem.

Remark 3.5.4. *We studied the (global) dynamics of the system when λ_0 is constant and $\varepsilon = 1$. More generally, all constants here and in the previous sections depend on λ_0 and ε and grow as these quantities go to $+\infty$ and 0, respectively. In particular, the dependence on λ_0 is an important issue in view of inpainting applications (see [16]) and a natural question is whether one can have an upper bound on the dimension of the global attractor which is independent of this quantity (here, the upper bound that we obtain explodes as λ_0 goes to $+\infty$). A natural (but involved, see, e.g., [137]) problem would be to find a lower bound on this dimension (possibly, in terms of λ_0). This will be investigated elsewhere.*

3.6 Algebraic consistency with the two-phase model

In order to ensure the "physical" constraints of our proposed model, the model must (at least, see below) satisfy two properties :

(i) When phases $(i_1, i_2, i_3, ..., i_{n-2}) \in \{1, ..., n\}$ are not present, the n-phase free energy is equal to the one of the two-phase model.

(ii) When phases $(i_1, i_2, i_3, ..., i_{n-2}) \in \{1, ..., n\}$ are not present at the initial time (i.e., $c_{i_j}(0) = 0$ and $h_{i_j} = 0$, $j = 1,...,n-2$), these phases do not appear artificially during the evolution of the system.

In that case, we say that the model is algebraically consistent with the two-phase model (see [22]). Of course, the model should also be consistent with the k-phase model, $k < n$, but we have not been able to prove this more general property here.

Theorem 3.6.1. *Model* (3.9)–(3.10) *is algebraically consistent with the diphasic system.*

Proof. *We first recall that the total free energy of* (3.9)–(3.10) *(n-phase model) can be written as follows :*

$$\mathcal{F}_n((c_i)_i) = \int_\Omega \Big[\frac{1}{n} \sum_{i=1}^{n} (c_i^2(1-c_i)^2) + \frac{\varepsilon^2}{2} \sum_{i=1}^{n} |\nabla c_i|^2\Big] dx + \frac{\lambda_0}{2} \sum_{i=1}^{n} \int_{\Omega \setminus D} (c_i - h_i)^2 dx. \tag{3.79}$$

We assume that $c_i = c$, $c_j = 1 - c$, and $c_k = h_k = 0$, for i and j fixed in $\{1, 2, ..., n\}$ and $k = 1, ..., n$, $k \neq i, j$. We set $h_i = h$ (i.e., $h_j = 1 - h$) and $\tilde{c} = (0, ..., 0, c, 0, .., 0, 1 - c, 0, .., 0) \in \mathbb{R}^n$. Then, the total free energy can be rewritten as

$$\mathcal{F}_n(\tilde{c}) = \int_\Omega \Big[\frac{2}{n}(c^2(1-c)^2) + \varepsilon^2 |\nabla c|^2\Big] dx + \lambda_0 \int_{\Omega \setminus D} (c - h)^2 dx \tag{3.80}$$

which is equal, up to a multiplicative constant, which, therefore, does not change anything in the description of the problem, to the total free energy of the two-phase model (3.1)*,*

$$\mathcal{F}(\tilde{c}) = \int_\Omega \Big[\frac{1}{n}(c^2(1-c)^2) + \frac{\varepsilon^2}{2}|\nabla c|^2\Big]dx + \frac{\lambda_0}{2}\int_{\Omega\setminus D}(c-h)^2dx, \tag{3.81}$$

so that the model satisfies (i).

Furthermore, (ii) says that our particular $\tilde{c}$ *has to be solution to* (3.9)–(3.10)*, which is equivalent to*

$$\frac{\partial F}{\partial c_k} - \frac{1}{n}\sum_{l=1}^{n}\frac{\partial F}{\partial c_l}|_{c_k=0, c_j=1-c_i} = 0. \tag{3.82}$$

Moreover, we have

$$\begin{aligned}
&\frac{\partial F}{\partial c_k} - \frac{1}{n}\sum_{l=1}^{n}\frac{\partial F}{\partial c_l}|_{c_k=0, c_i=c, c_j=1-c_i} \\
&= -\frac{2}{n^2}\Big[c(1-c)^2 - c^2(1-c) + (1-c)c^2 - (1-c)^2c\Big] \\
&= 0,
\end{aligned} \tag{3.83}$$

which yields that the model satisfies (3.82) *and then (ii).* □

3.7 Numerical simulations

As far as the numerical simulations are concerned, we rewrite the problem in the form

$$\frac{\partial c_i}{\partial t} + \Delta\mu_i + \lambda_0\chi_{\Omega\setminus D}(x)(c_i - h_i) = 0, \quad i = 1, ..., n, \tag{3.84}$$

$$\mu_i = \epsilon^2\Delta c_i - f_i(c), \quad i = 1, ..., n, \tag{3.85}$$

$$\frac{\partial c_i}{\partial \nu} = \frac{\partial \mu_i}{\partial \nu} = 0 \text{ on } \Gamma, \quad i = 1, ..., n, \tag{3.86}$$

$$c_{|t=0} = c_0, \tag{3.87}$$

where $f_i(c) = \frac{2}{n}[c_i(1-c_i)^2 - c_i^2(1-c_i)] - \frac{1}{n}\sum_{i=1}^{n}\frac{\partial F(c)}{\partial c_i}$, $i = 1, ..., n$. Problem (3.84)–(3.87) has the advantage of splitting the fourth-order (in space) equation into a system of two second-order ones (see [55, 80, 86]). Consequently, we use a P1-finite element for the space discretization, together with a semi-implicit Euler time discretization (i.e., implicit for the linear terms and explicit for the nonlinear ones). The numerical simulations are performed with the software Freefem++ (see [67]).

In the numerical results presented below, Ω is a $(0, 0.5) \times (0, 0.5)$-square. The triangulation is obtained by dividing Ω into 100×100 rectangles and by dividing each rectangle along the same diagonal.

In order to obtain the final inpainting results, we use a dynamic one step algorithm with threshold involving the diffuse interface thickness ε which allows us to connect regions across

large inpainting domains (see [38]). Here, the thresholding consists in replacing $\max_{i=1,\dots,n} c_i$ by 1 and $c_j \neq \max_{i=1,\dots,n} c_i$ by 0 for all j and at every point $(x, y) \in \Omega$ (more generally, at every point $(x, y, z) \in \Omega$) ; this means that we replace the dominant phase (color) by 1 at every point of Ω and the other phases (colors) by 0 to obtain the final inpainting result.

3.7.1 Three colors inpainting

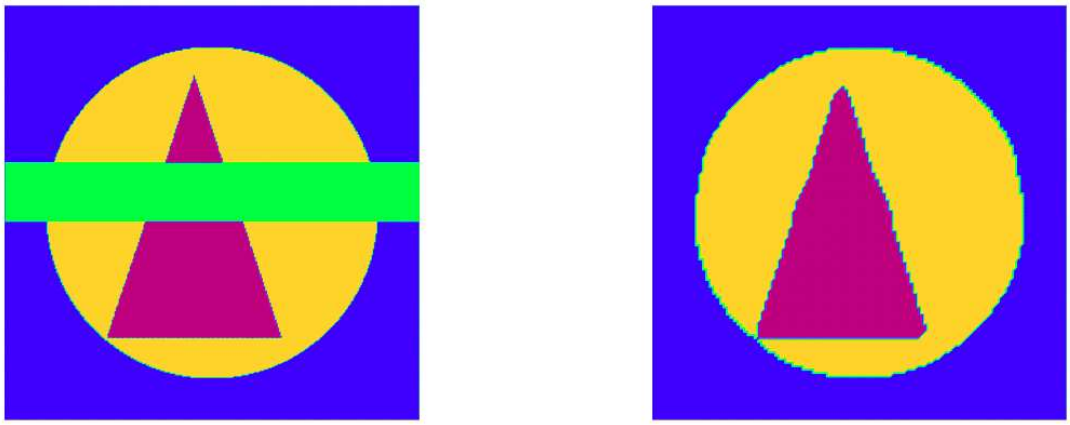

(a) (b)

FIGURE 3.1 – (a) Inpainting region in green, random initial datum between 0 and 1 in inpainting region, $\varepsilon = 0.03$. (b) Solution at $t = 0.006$; replacing the dominant color by 1 and the other colors by 0.

The green region in Figure 3.1(a) corresponds to the inpainting region. We run the modified Cahn–Hilliard system ($n = 3$) with $\varepsilon = 0.03$, $\Delta t = 0.001$, and $\lambda_0 = 500000$. We are close to a steady state at $t = 0.006$ and we replace the dominant color by 1 and the other colors by 0 to obtain the final inpainting in Figure 3.1(b).

3.7.2 Nine colors inpainting

In Figure 3.2(a), the light blue region corresponds to the inpainting region. We run the modified Cahn–Hilliard system ($n = 9$) with $\varepsilon = 0.03$, $\Delta t = 0.05$, and $\lambda_0 = 900000$. We are close to a steady state at $t = 0.2$ and we replace the dominant color by 1 and the other colors by 0 to obtain the final inpainting in Figure 3.2(b).

3.7.3 Text inpainting

The light green region (horizontal bars) in Figure 3.3(a) corresponds to the inpainting region. We run the modified Cahn–Hilliard system ($n = 10$) with $\varepsilon = 0.008$, $\lambda_0 = 3000000$, and $\Delta t = 0.01$. We are close to a steady state at $t = 0.04$ and we replace the dominant color by 1 and the other colors by 0 to obtain the final inpainting in Figure 3.3(b).

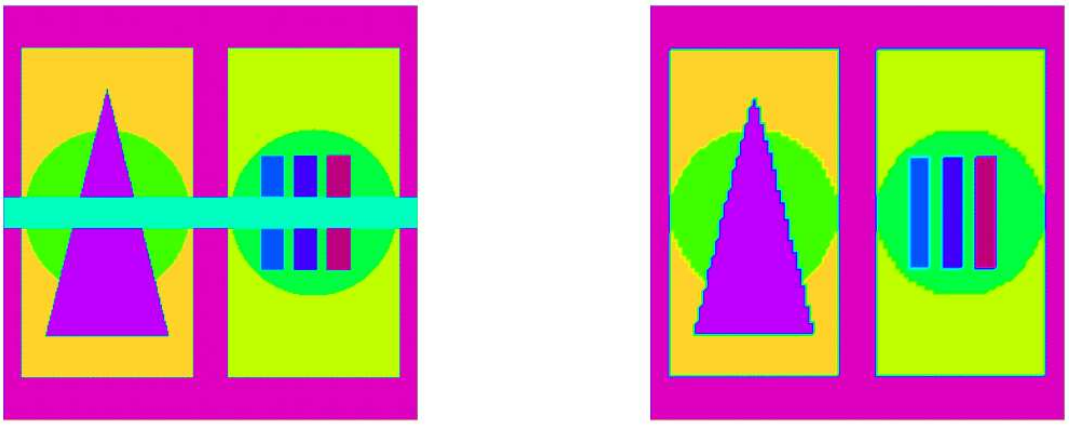

(a) (b)

FIGURE 3.2 – (a) Inpainting region in light blue, random initial datum between 0 and 1 in inpainting region, $\varepsilon = 0.03$. (b) Solution at $t = 0.2$; replacing the dominant color by 1 and the other colors by 0.

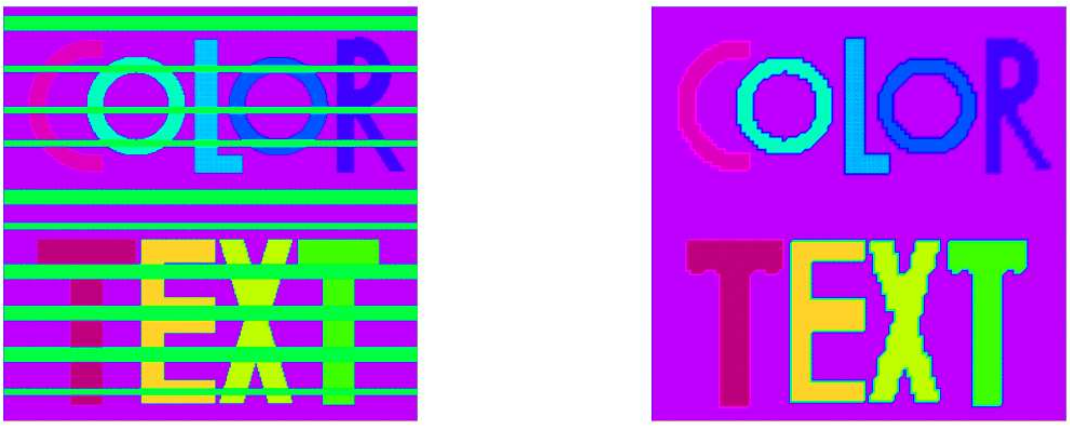

(a) (b)

FIGURE 3.3 – (a) Inpainting region in green (horizontal bars), random initial datum between 0 and 1 in inpainting region, $\varepsilon = 0.008$. (b) Solution at $t = 0.04$; replacing the dominant color by 1 and the other colors by 0.

3.7.4 Consistency with the two-phase model example

In Figure 3.4, we take the same example of nine colors inpainting as in Figure 3.2, but, now, we take $h_i = c_i(0) = 0$, $i = 1, ..., 7$. We run again the modified Cahn–Hilliard system ($n = 9$) with the same parameters as in Figure 3.2. We are close to a steady state at $t = 0.2$ and we replace the dominant color by 1 and the other colors by 0 to obtain the final inpainting in Figure 3.4(b). Note that $|c_i(t)| < 10^{-5}$, $\forall t \geq 0$, $i = 1, ..., 7$.

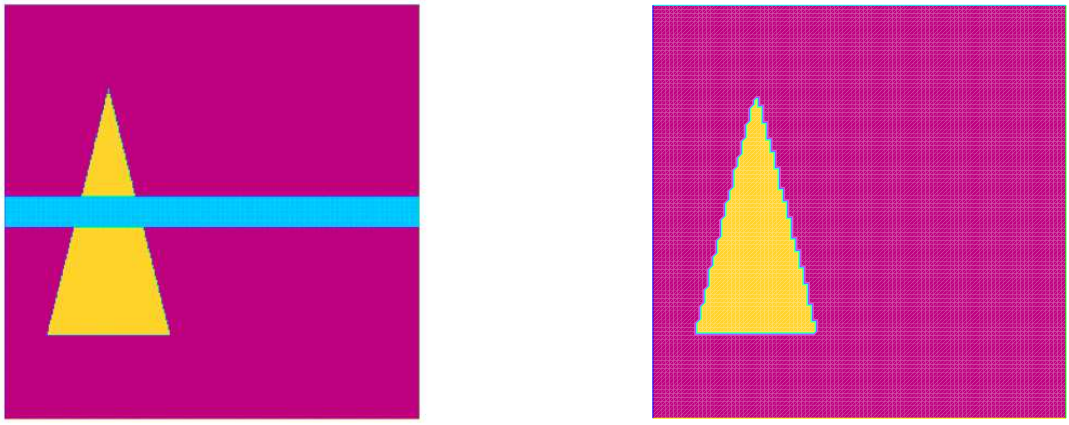

(a) (b)

FIGURE 3.4 – (a) Inpainting region in light blue, random initial datum between 0 and 1 in inpainting region, $\varepsilon = 0.03$. (b) Solution at $t = 0.2$; replacing the dominant color by 1 and the other colors by 0.

Deuxième partie

Généralisations de l'équation de Cahn–Hilliard en biologie et en chimie

Chapitre 4

A Cahn–Hilliard equation with a proliferation term for biological and chemical applications

Une équation de Cahn–Hilliard avec un terme de prolifération pour des applications en biologie et en chimie

Ce chapitre est constitué de l'article **A Cahn–Hilliard equation with a proliferation term for biological and chemical applications**, Asymptotic Analysis 94 (2015), 71–104.

Asymptotic Analysis
Volume 94, No. 1,2, 2015, 71–104

A Cahn–Hilliard equation with a proliferation term for biological and chemical applications

HUSSEIN FAKIH

Université de Poitiers, Laboratoire de Mathématiques et Applications
UMR CNRS 7348 - SP2MI
Boulevard Marie et Pierre Curie - Téléport 2
F-86962 Chasseneuil Futuroscope Cedex, France
E-mail address : Hussein.Fakih@math.univ-poitiers.fr

Abstract : In this paper, we are interested in the study of the solution to a generalization of the Cahn–Hilliard equation endowed with Neumann boundary conditions. This model has, in particular, applications in biology and in chemistry. We show that the solutions blow up in finite time or exist globally in time. We further prove that the relevant, from a biological and a chemical point of view, solutions converge to a constant as time goes to infinity. We finally give some numerical simulations which confirm the theoretical results.

Keywords : Cahn–Hilliard equation, proliferation term, blow up, convergence to a steady state, simulations.
AMS Subject Classification : 35K55 ; 35B40 ; 35B44

4.1 Introduction

The Cahn–Hilliard equation is very important in materials science. It describes important qualitative features of two phase systems, related with phase separation processes. In materials science, this pattern formation is referred to as the microstructures of the material and these microstructures are highly influential in determining many of the properties of the material, such as strength, hardness, and conductivity. The Cahn–Hilliard model is rather broad ranged in its evolutionary scope ; it can serve as a good model for many systems during early times, it can give a reasonable qualitative description for these systems during intermediate times, and it can serve as a good model for even more systems at late times. Often, the late time evolution is so slow that the pattern formation becomes effectively frozen into the system over time scales of interest and, hence, it is the long time behavior of the system which is seen in practice. We refer the reader to, e.g., [26], [27], [41], [56], and [116] for more details.

The Cahn–Hilliard equation also appears in the modeling of many other phenomena. These include population dynamics [45], bacterial films [91], thin films [123, 138], image processing [29, 51], and even the rings of Saturn [139].

In [42], the authors studied the following model proposed in [88] :

$$\frac{\partial u}{\partial t} + \Delta^2 u - \Delta f(u) + g(u) = 0, \tag{4.1}$$

where

$$g(s) = s(s-1) \tag{4.2}$$

and

$$f(s) = (s - \frac{1}{2})^3 - (s - \frac{1}{2}). \tag{4.3}$$

Equation (1) models, e.g., the clustering of malignant brain tumor cells in two space dimensions, see [88].

Furthermore, the authors in [141] proposed the following related equation :

$$\frac{\partial u}{\partial t} + M\Delta(2\kappa\Delta u - f(u)) + u^2 - P(1-u) = 0 \tag{4.4}$$

to model the formation of adsorbate islands on a proposed surface (in the modeling of a two dimensional liquid-gas). Here, u is the distance from the critical coverage $u^* = u - \frac{1}{2}$, M is the surface mobility which is supposed to be constant, $u^2 - P(1-u)$ is the nonlinear reaction rate, $P = \frac{\kappa_{ad} s}{\kappa_{des}} p$ is the reduced pressure of the gas phase, p being the pressure of the gas above the absorbed layer, and s is the stinking coefficient. Furthermore, κ_{ad} and κ_{des} are constants which represent the adsorption rate and the desorption one, respectively. Finally, F is the free energy of the corresponding homogeneous system,

$$f(s) = F'(s) = a_0(\frac{T}{T_c} - 1)(s - \frac{1}{2}) + \frac{4}{3}\frac{T}{T_c}(s - \frac{1}{2})^3, \tag{4.5}$$

where $a_0 = 4\kappa_B T_c$ and $\kappa = \kappa_B T_c \xi_0^2$, ξ_0 is a phenomenological length related to the range of the interactions, and T and T_c are the absolute temperature and a critical one, respectively.

Actually, in what follows, we will, for simplicity, set all physical constants equals to 1 and we will solve the problem in space dimension $N \leq 3$, i.e., we consider in section 2 the generalized Cahn–Hilliard equation

$$\frac{\partial u}{\partial t} + \Delta^2 u - \Delta f(u) + g(u) = 0, \tag{4.6}$$

where

$$g(s) = \alpha s^2 + \beta s + \gamma, \qquad \alpha > 0, \ \ \beta, \gamma \in \mathbb{R}. \tag{4.7}$$

We note that, in two space dimensions, if $\alpha = 1$ and $\gamma = -\beta$ ($\beta \in \mathbb{R}$), the equation models, e.g., the literal attractive interactions between adsorbed molecules which may induce a transition in the chemisorbed overlayer, see [141]. Furthermore, if $\gamma = 0$ and $\beta = -\alpha$ ($\alpha > 0$), the equation models, e.g., the clustering of malignant brain tumor cells, see [88]. Finally, if $\alpha = \gamma = 0$ and $\beta > 0$, the equation (named Cahn–Hilliard–Oono) accounts for long-ranged (nonlocal)

interactions in the phase separation process (see [122, 143] ; see also [103] for the study of the limit dynamics as β goes to zero, [39] for the study of the local existence with a logarithmic nonlinear term and [49] for the study of the global existence of the nonlocal equation with a transport term).

We further take, for simplicity,

$$f(s) = s^3 - s \tag{4.8}$$

and we set

$$\Theta = \beta^2 - 4\alpha\gamma, \tag{4.9}$$

Θ being the discriminant of g (g is defined here as in (4.7)).

A third related model, proposed in [5], reads

$$\frac{\partial u}{\partial t} + \Delta^2 u - \Delta f(u) + g(x,u) = 0, \tag{4.10}$$

where

$$g(x,s) = \frac{\alpha}{2}(s+1) - \beta(1-s)^2(1+s)^2 + \sigma(x,t), \tag{4.11}$$

α and β being constants which represent the growth coefficient and the death one, respectively. Here, the term $\sigma(x,t)$ is used as an artificial growth term which allows us to manufacture a desired PDE solution, but it could also serve to model biologically relevant phenomena. Equation (4.10) has applications in biology and, more specifically, in tumor growth and wound healing. The uncontrolled tumor growth of abnormal cells often results in cancer. The morphological evolution of a growing solid tumor is the result of many factors, including cell-cell and cell-matrix adhesion, mechanical stress, cell motility, and the degree of heterogeneity of cell proliferation.

In that follows, we will, for simplicity, set $\sigma \equiv 0$ and we will solve the problem in space dimension $N \leq 3$, i.e., we consider in section 3 the generalized Cahn–Hilliard equation

$$\frac{\partial u}{\partial t} + \Delta^2 u - \Delta f(u) + g(u) = 0, \tag{4.12}$$

where

$$g(s) = \alpha s - \beta s^q (s-1)^q, \quad q \geq 2. \tag{4.13}$$

We further take

$$f(s) = \sum_{i=0}^{2p+1} a_i s^i, \quad a_{2p+1} > 0, \quad p \geq 1 \tag{4.14}$$

(in particular, we will sometimes need compatibility conditions on p and q).

Problems (4.6) and (4.10), endowed with Dirichlet boundary conditions (and with more general nonlinear terms f and g), are considered in [104] ; see also [63]. There, the well-posedness and the existence of the finite-dimensional global attractor are established. Furthermore, equation (4.6), when the nonlinear term g has odd degree and endowed with Neumann boundary conditions (and with more general nonlinear terms f), is considered in [63]. In that case, we also have the well-posedness and the existence of the finite-dimensional global attractor.

In this paper, equations (4.6) and (4.10) are endowed with Neumann boundary conditions,

$$\frac{\partial u}{\partial \nu} = \frac{\partial \Delta u}{\partial \nu} = 0 \qquad \text{on } \Gamma,$$

where Γ is the boundary of the domain Ω occupied by the system (we assume that it is a bounded and regular domain of $\mathbb{R}^N$) and ν is the unit outer normal vector.

We set

$$v = u - \langle u \rangle, \tag{4.15}$$

where

$$\langle . \rangle = \frac{1}{\mathrm{Vol}(\Omega)} \int_\Omega . dx. \tag{4.16}$$

Then, assuming that g is defined as in (4.7), with $\alpha = -\beta = 1$ and $\gamma = 0$, the authors of [42] proved that v is bounded and $\langle u \rangle$ can blow up in finite time. Furthermore, when $\langle u \rangle$ is bounded, the solution exists globally in time and is dissipative. They finally proved that, if $u(t) \in [0, 1],\ \forall t \geq 0$, then u tends to 1 as time goes to infinity.

We note that Neumann boundary conditions are crucial here and we have global in time existence for the same problem with Dirichlet boundary conditions (see, e.g., [104]).

In section 4.2, we take g as in (4.7) with $\alpha > 0$ and $\beta, \gamma \in \mathbb{R}$. We prove that $\langle u \rangle$ can blow up in finite time in general. Furthermore, when $\langle u \rangle$ is bounded, the solution exists globally in time and is dissipative. We then prove that, if $\Theta > 0$ and u is a solution such that $u(t) \in [\frac{-\beta - \sqrt{\Theta}}{2\alpha}, \frac{-\beta + \sqrt{\Theta}}{2\alpha}]$ or $u(t) \in [\frac{-\beta + \sqrt{\Theta}}{2\alpha}, a],\ \forall t \geq 0$, where $a > \frac{-\beta + \sqrt{\Theta}}{2\alpha}$ is arbitrary, then u tends to $\frac{-\beta + \sqrt{\Theta}}{2\alpha}$ as time goes to infinity. Finally, if $\Theta = 0$ and u is a solution such that $u(t) \in [\frac{-\beta}{2\alpha}, a],\ \forall t \geq 0$, where $a > \frac{-\beta}{2\alpha}$, then u tends to $\frac{-\beta}{2\alpha}$ as time goes to infinity.

In section 4.3, we take g as in (4.13). We prove that, if $\alpha = 2\beta$, $\beta > 0$ (resp., $\beta < 0$) and $q = 2$ and u is a solution such that $u(t) \in [0, 2]$, then u tends to 0 (resp., to 2) as time goes to infinity. Finally, we can again prove that $\langle u \rangle$ can blow up in finite time in general. Note that, if $\beta > 0$ (resp., $\beta < 0$), the blow up solution tends to $+\infty$ (resp., to $-\infty$).

We finally give some numerical simulations which confirm these results. They also show that, for g defined as in (4.7), even when the initial datum belongs to the relevant interval $[\frac{-\beta - \sqrt{\Theta}}{2\alpha}, \frac{-\beta + \sqrt{\Theta}}{2\alpha}]$, we can have blow up in finite time.

Throughout the paper, the same letter c (and, sometimes, c') denotes constants which may vary from line to line.

4.2 A chemisorbed overlayer and tumor growth model

We consider the following initial and boundary value problem :

$$\frac{\partial u}{\partial t} + \Delta^2 u - \Delta f(u) + g(u) = 0, \tag{4.17}$$

$$\frac{\partial u}{\partial \nu} = \frac{\partial \Delta u}{\partial \nu} = 0 \quad \text{on } \Gamma, \tag{4.18}$$

$$u|_{t=0} = u_0, \tag{4.19}$$

where f and g are defined in (4.7) and (4.8), respectively.

Integrating (4.17) over Ω, we have

$$\frac{d}{dt} \int_\Omega u dx + \int_\Omega g(u) dx = 0, \tag{4.20}$$

hence

$$\frac{d}{dt}\langle u\rangle + \langle g(u)\rangle = 0. \tag{4.21}$$

We rewrite (4.21) in the form

$$\frac{d\langle u\rangle}{dt} + g(\langle u\rangle) = g(\langle u\rangle) - \langle g(u)\rangle.$$

Noting that

$$g(\langle u\rangle) - \langle g(u)\rangle = -\alpha\langle v^2\rangle,$$

where $v = u - \langle u\rangle$, we obtain

$$\frac{d\langle u\rangle}{dt} + g(\langle u\rangle) = -\alpha\langle v^2\rangle. \tag{4.22}$$

We first have the

Proposition 4.2.1. *For every $u_0 \in L^2(\Omega)$, there exists $T_0 = T_0(\|u_0\|) > 0$ and a unique solution u to (4.17)-(4.19) such that $u \in C([0, T_0); L^2(\Omega)) \cap L^2(0, T; H^2(\Omega))$, $\forall T < T_0$.*

Proof. *See [114] and [137].* □

Remark 4.2.2. *In the case when g has two distinct zeros, i.e., $\Theta > 0$ (Θ is defined in* (4.9)*), we give below an example which proves that, even if we start in the physically relevant interval, namely $\left[\frac{-\beta-\sqrt{\Theta}}{2\alpha}, \frac{-\beta+\sqrt{\Theta}}{2\alpha}\right]$, the solution can leave this interval. We consider the following equation :*

$$\frac{\partial u}{\partial t} + \frac{\partial^4 u}{\partial x^4} - \frac{\partial^2}{\partial x^2}\Big((u - \frac{1}{2})^3 - (u - \frac{1}{2})\Big) + \alpha u^2 + \beta u + \gamma = 0. \tag{4.23}$$

We assume that $\Theta > 0$, take $u_0(x) = \frac{-\beta+\sqrt{\Theta}}{2\alpha} - \left(x - \frac{1}{2}\right)^4$ in a neighborhood of $\frac{1}{2}$, and extend u_0 by a smooth function defined in $\Omega = (0, 1)$, with values in $\left[\frac{-\beta-\sqrt{\Theta}}{2\alpha}, \frac{-\beta+\sqrt{\Theta}}{2\alpha}\right]$. We note that $u_0'(\frac{1}{2}) = u_0''(\frac{1}{2}) = 0$ and $u_0^{(4)}(\frac{1}{2}) = -24$. Furthermore,

$$\frac{\partial^2}{\partial x^2}\Big((u_0 - \frac{1}{2})^3 - (u_0 - \frac{1}{2})\Big)\Big|_{x=\frac{1}{2}} = 0. \tag{4.24}$$

We thus have

$$\frac{\partial u}{\partial t}\Big(\frac{1}{2}, 0\Big) = 24 > 0. \tag{4.25}$$

Noting finally that

$$\begin{aligned} u\Big(\frac{1}{2}, t\Big) &= u\Big(\frac{1}{2}, 0\Big) + t\frac{\partial u}{\partial t}\Big(\frac{1}{2}, 0\Big) + o(t) \\ &= \frac{-\beta + \sqrt{\Theta}}{2\alpha} + 24t + o(t) \\ &> \frac{-\beta + \sqrt{\Theta}}{2\alpha}, \end{aligned} \tag{4.26}$$

for $t > 0$ small, we see that u cannot stay in $\left[\frac{-\beta-\sqrt{\Theta}}{2\alpha}, \frac{-\beta+\sqrt{\Theta}}{2\alpha}\right]$. Similarly, if we take $u_0(x) = \frac{-\beta-\sqrt{\Theta}}{2\alpha} + \left(x-\frac{1}{2}\right)^4$ in a neighborhood of $\frac{1}{2}$ and extend it as above, we have

$$\frac{\partial u}{\partial t}\Big(\frac{1}{2}, 0\Big) = -24 < 0, \tag{4.27}$$

hence

$$\begin{aligned} u\Big(\frac{1}{2}, t\Big) &= \frac{-\beta-\sqrt{\Theta}}{2\alpha} - 24t + o(t) \\ &< \frac{-\beta-\sqrt{\Theta}}{2\alpha}, \end{aligned} \tag{4.28}$$

for $t > 0$ small, and we see that u cannot stay in $\left[\frac{-\beta-\sqrt{\Theta}}{2\alpha}, \frac{-\beta+\sqrt{\Theta}}{2\alpha}\right]$.

Lemma 4.2.3. *Let u be a solution to (4.17)–(4.19). Then, $\langle u\rangle$ is bounded from above.*

Proof. *If $\beta < 0$, we note that*

$$-2\beta s \le \alpha s^2 + \frac{\beta^2}{\alpha}.$$

It thus follows from (4.22) that

$$\frac{d\langle u\rangle}{dt} - \beta\langle u\rangle \le \frac{\beta^2}{\alpha} - \gamma, \tag{4.29}$$

which yields, owing to Gronwall's lemma,

$$\langle u(t)\rangle \le \Big(\langle u_0\rangle - \frac{\gamma}{\beta}\Big)e^{\beta t} - \frac{\beta}{\alpha} + \frac{\gamma}{\beta}, \quad t \ge 0, \tag{4.30}$$

and $\langle u\rangle$ is bounded from above.

If $\beta = 0$, we further note that

$$2s \le \alpha s^2 + \frac{1}{\alpha}. \tag{4.31}$$

It thus follows from (4.22) that

$$\frac{d}{dt}\langle u\rangle + 2\langle u\rangle \le \frac{1}{\alpha} - \gamma, \tag{4.32}$$

which yields, owing to Gronwall's lemma,

$$\langle u(t)\rangle \le \Big(\langle u_0\rangle + \frac{\gamma}{2} - \frac{1}{2\alpha}\Big)e^{-2t} + \frac{1}{2\alpha} - \frac{\gamma}{2}, \quad t \ge 0, \tag{4.33}$$

and $\langle u\rangle$ is bounded from above.

Finally, if $\beta > 0$, we have, owing to (4.21),

$$\frac{d\langle u\rangle}{dt} + \beta\langle u\rangle + \gamma \le 0 \tag{4.34}$$

and, also by Gronwall's lemma, we obtain

$$\langle u(t)\rangle \le \Big(\langle u_0\rangle + \frac{\gamma}{\beta}\Big)e^{-\beta t} - \frac{\gamma}{\beta}, \quad t \ge 0, \tag{4.35}$$

and $\langle u\rangle$ is bounded from above. □

Lemma 4.2.4. *Let u be a solution to (4.17)–(4.19). Then, if $\beta < 0$ and $\langle u(T)\rangle < -\frac{\gamma}{\beta}$, for some $T > 0$ (and, in particular, if $\langle u_0\rangle < -\frac{\gamma}{\beta}$), there exists $t_0 \geq T$ such that*

$$\langle u(t)\rangle < 0, \qquad \forall t \geq t_0,$$

and, if the solution exists globally in time,

$$\lim_{t\to+\infty} \langle u(t)\rangle = -\infty.$$

Proof. *It follows from (4.21) that*

$$\frac{d\langle u\rangle}{dt} + \beta\langle u\rangle + \gamma \leq 0, \tag{4.36}$$

which yields, owing to Gronwall's lemma,

$$\langle u(t)\rangle \leq e^{-\beta(t-T)}\Big(\langle u(T)\rangle + \frac{\gamma}{\beta}\Big) - \frac{\gamma}{\beta}. \tag{4.37}$$

Therefore, if

$$\langle u(T)\rangle < -\frac{\gamma}{\beta}, \tag{4.38}$$

then $\exists t_0 \geq T$ such that

$$\langle u(t)\rangle < 0, \quad \forall t \geq t_0 \tag{4.39}$$

and, moreover, if the solution exits globally in time,

$$\lim_{t\to+\infty} \langle u(t)\rangle = -\infty. \tag{4.40}$$

□

Lemma 4.2.5. *Let u be a solution to (4.17)–(4.19). We have*

– *If $\Theta < 0$, then, for all u_0, there exists $t_0 \geq 0$ such that*

$$\langle u(t)\rangle < 0, \qquad \forall t \geq t_0,$$

and, if the solution exists globally in time,

$$\lim_{t\to+\infty} \langle u(t)\rangle = -\infty.$$

– *If $\Theta = 0$ and $\langle u_0\rangle < 0$, then*

$$\langle u(t)\rangle < 0, \quad \forall t \geq 0.$$

Proof. *It follows from (4.21) that*

$$\frac{d\langle u\rangle}{dt} + \alpha\langle\Big(u + \frac{\beta}{2\alpha}\Big)^2\rangle - \frac{\Theta}{4\alpha} = 0. \tag{4.41}$$

Setting $w = u + \frac{\beta}{2\alpha}$, we rewrite (4.41) in the form

$$\frac{d\langle w\rangle}{dt} + \alpha\langle w^2\rangle - \frac{\Theta}{4\alpha} = 0. \tag{4.42}$$

It follows from (4.42) that

$$\frac{d\langle w\rangle}{dt} \leq \frac{\Theta}{4\alpha},$$

hence

$$\langle w(t)\rangle \leq \langle w_0\rangle + \frac{\Theta}{4\alpha}t, \tag{4.43}$$

which yields

$$\langle u(t)\rangle \leq \langle u_0\rangle + \frac{\Theta}{4\alpha}t. \tag{4.44}$$

If $\Theta < 0$, then, $\forall u_0$, $\exists t_0$ such that

$$\langle u(t)\rangle < 0, \quad \forall t \geq t_0, \tag{4.45}$$

and, if the solution exists globally in time,

$$\lim_{t\to+\infty} \langle u(t)\rangle = -\infty. \tag{4.46}$$

Now, assuming that $\Theta = 0$, we have, owing to (4.44),

$$\langle u(t)\rangle \leq \langle u_0\rangle, \quad \forall t \geq 0. \tag{4.47}$$

Therefore, if

$$\langle u_0\rangle < 0, \tag{4.48}$$

then

$$\langle u(t)\rangle < 0, \quad \forall t \geq 0. \tag{4.49}$$

□

Proposition 4.2.6. *Let u be a solution to (4.17)–(4.19). Then, there exists a monotone increasing function Q such that*

$$\|u(t) - \langle u(t)\rangle\|^2 \leq Q(\|u_0 - \langle u_0\rangle\|), \qquad \forall t \geq 0.$$

Proof. *Setting $v = u - \langle u\rangle$, we rewrite problem (4.17)–(4.19) in the form*

$$\frac{\partial v}{\partial t} + \Delta^2 v - \Delta f(v + \langle u\rangle) + g(v + \langle u\rangle) - \langle g(v + \langle u\rangle) >= 0, \tag{4.50}$$

$$\frac{\partial v}{\partial \nu} = \frac{\partial \Delta v}{\partial \nu} = 0 \quad on\ \Gamma, \tag{4.51}$$

$$v|_{t=0} = v_0 = u_0 - \langle u_0\rangle. \tag{4.52}$$

We multiply (4.50) by $(-\Delta)^{-1}v$ and have

$$\begin{aligned} &\frac{1}{2}\frac{d}{dt}\|v\|_{-1}^2 + \|\nabla v\|^2 + ((f(v + \langle u\rangle) - f(\langle u\rangle), v)) \\ &\qquad + ((g(v + \langle u\rangle) - g(\langle u\rangle), (-\Delta)^{-1}v)) = 0. \end{aligned} \tag{4.53}$$

Here,

$$\begin{aligned}((f(v+\langle u\rangle)-f(\langle u\rangle),v)) &= \int_\Omega (v^4+3v^3\langle u\rangle+3v^2\langle u\rangle^2)dx-\|v\|^2\\ &\geq \int_\Omega (v^4+3v^2\langle u\rangle^2)dx-3\int_\Omega |v^3\langle u\rangle|dx-\|v\|^2\\ &\geq \frac{1}{8}\int_\Omega (v^4+v^2\langle u\rangle^2)dx-\|v\|^2,\end{aligned}$$

owing to Young's inequality (e.g., $3ab \leq \frac{7}{8}a^2+\frac{18}{7}b^2,\ a,\ b\geq 0$*). Furthermore,*

$$\begin{aligned}|((g(v+\langle u\rangle)-g(\langle u\rangle),(-\Delta)^{-1}v))| &= |((\alpha v^2+2\alpha v\langle u\rangle+\beta v,(-\Delta)^{-1}v))|\\ &\leq \frac{1}{16}\int_\Omega (v^4+v^2\langle u\rangle^2)dx+c\|v\|^2,\end{aligned}$$

which yields

$$\frac{d}{dt}\|v\|_{-1}^2+\|\nabla v\|^2+\frac{1}{8}\int_\Omega (v^4+v^2\langle u\rangle^2)dx\leq c\|v\|^2. \tag{4.54}$$

Therefore,

$$\frac{d}{dt}\|v\|_{-1}^2+\|\nabla v\|^2+\frac{1}{16}\int_\Omega (v^4+v^2\langle u\rangle^2)dx\leq c, \tag{4.55}$$

hence

$$\frac{d}{dt}\|v\|_{-1}^2+c\|v\|_{-1}^2\leq c',\quad c>0. \tag{4.56}$$

It thus follows from Gronwall's lemma that

$$\|v\|_{-1}^2\leq e^{-ct}\|v_0\|_{-1}^2+c',\quad c>0,\ t\geq 0. \tag{4.57}$$

We set $\dot{H}^{-1}(\Omega)=\{\phi\in H^{-1}(\Omega),\ \langle\phi,1\rangle_{H^{-1}(\Omega),H^1(\Omega)}=0\}$.

Let B be a bounded subset of $\dot{H}^{-1}(\Omega)$ *and* t_0 *be such that* $v_0\in B$ *and* $t\geq t_0$ *implies* $v(t)\in\mathcal{B}_0$*, where* $\mathcal{B}_0=\{\phi\in\dot{H}^{-1}(\Omega),\ \|\phi\|_{-1}^2\leq 2c'\}$*,* c' *being the constant in (4.57). We then deduce from (4.55) that, for* $t\geq t_0$*,*

$$\int_t^{t+r}\|\nabla v\|^2ds\leq c(r),\quad \int_t^{t+r}ds\int_\Omega (v^4+v^2\langle u\rangle^2)dx\leq c(r),\quad r>0\ \textit{fixed}.$$

Finally, multiplying (4.50) by v, it is easy to obtain, noting that

$$\begin{aligned}|((g(v+\langle u\rangle)-g(\langle u\rangle),v))| &= |((\alpha v^2+2\alpha v\langle u\rangle+\beta v,v))|\\ &\leq c\int_\Omega (\alpha^2|v|^4+\alpha^2v^2|\langle u\rangle|^2)dx+c'(|\beta|+1)\|v\|^2\\ &\leq c\Big(\int_\Omega (v^4+v^2\langle u\rangle^2)dx+\|v\|^2\Big),\end{aligned}$$

the inequality

$$\frac{d}{dt}\|v\|^2+\|\Delta v\|^2\leq c\Big(\int_\Omega (v^4+v^2\langle u\rangle^2)dx+\|\nabla v\|^2+1\Big). \tag{4.58}$$

It thus follows from (4.58) and the uniform Gronwall's lemma that

$$\|v(t)\|^2 \leq c, \qquad t \geq t_0 + r, \tag{4.59}$$

where r is fixed and the constant c is independent of v_0 and t, hence, owing to (4.59) and integrating (4.55) and (4.58) between 0 and $t_0 + r$,

$$\|v(t)\|^2 \leq Q(\|v_0\|), \qquad t \geq 0, \tag{4.60}$$

where the function Q is monotone increasing. □

Theorem 4.2.7. *If $\Theta > 0$ and $\langle u(T)\rangle < -\frac{\beta+\sqrt{\Theta}}{2\alpha}$, for some $T \geq 0$ (and, in particular, if $\langle u_0\rangle < -\frac{\beta+\sqrt{\Theta}}{2\alpha}$), then the solution to (4.17)–(4.19) blows up in finite time. Furthermore, the blow up time T^+satisfies*

$$T^+ \leq T + \frac{1}{2\alpha z_1} \ln\Big(\frac{z(T) - z_1}{z(T) + z_1}\Big),$$

where $z_1 = \frac{\sqrt{\Theta}}{2\alpha}$ and $z(T) = \langle u(T)\rangle + \frac{\beta}{2\alpha}$.

Proof. *We can rewrite (4.22) in the form*

$$\frac{d}{dt}\langle u\rangle + \alpha\langle u\rangle^2 + \beta\langle u\rangle + \gamma = -\alpha\langle v^2\rangle, \tag{4.61}$$

hence the ODE

$$y' + \alpha y^2 + \beta y + \gamma = -\alpha\langle v^2\rangle, \tag{4.62}$$

where $y = \langle u\rangle$. Thus,

$$y' + \alpha(y + \frac{\beta}{2\alpha})^2 + \frac{4\alpha\gamma - \beta^2}{4\alpha} = -\alpha\langle v^2\rangle. \tag{4.63}$$

We finally set $z = y + \frac{\beta}{2\alpha}$ and have

$$z' + \alpha z^2 - \frac{\Theta}{4\alpha} = -\alpha\langle v^2\rangle. \tag{4.64}$$

Since $\Theta > 0$, we can rewrite (4.64) in the form

$$z' + \alpha z^2 - \frac{\Theta}{4\alpha} = c(t), \tag{4.65}$$

where $c(t) = -\alpha\langle v^2\rangle$ is nonpositive and uniformly bounded. Noting that the solution to the Riccati ODE $z' + \alpha z^2 - \frac{\Theta}{4\alpha} = 0$ reads

$$z(t) = z_1 + \frac{1}{\frac{z(T)+z_1}{2z_1(z(T)-z_1)} e^{2\alpha z_1(t-T)} - \frac{1}{2z_1}}, \quad t \geq T,$$

where $z_1 = \frac{\sqrt{\Theta}}{2\alpha}$, we conclude in view of the comparison principle. Indeed, we note that it follows from (4.60) *that $\|v\|$ is bounded and $\varphi \longmapsto \|\varphi - \langle\varphi\rangle\| + \langle\varphi\rangle$ is a norm in $L^2(\Omega)$ which is equivalent to the usual one.* □

As a consequence of Theorem 4.2.7, (4.30), (4.33), and (4.35), we have the

Corollary 2. *We assume that $\Theta > 0$. Let u be a solution to (4.17)–(4.19). Then, either u blows up in finite time or u exists globally in time and, $\forall t \geq 0$,*

$$-\frac{\beta + \sqrt{\Theta}}{2\alpha} \leq \langle u(t) \rangle \leq \begin{cases} \left| \langle u_0 \rangle - \frac{\gamma}{\beta} \right| - \frac{\beta}{\alpha} + \frac{\gamma}{\beta} & \text{if } \beta < 0, \\ \left| \langle u_0 \rangle + \frac{\gamma}{\beta} \right| - \frac{\gamma}{\beta} & \text{if } \beta > 0, \\ \left| \langle u_0 \rangle + \frac{\gamma}{2} - \frac{1}{2\alpha} \right| - \frac{\gamma}{2} + \frac{1}{2\alpha} & \text{if } \beta = 0. \end{cases}$$

Theorem 4.2.8. *If $\Theta \leq 0$ and $\langle u(T) \rangle < -\frac{\beta}{2\alpha}$, for some $T \geq 0$ (and, in particular, if $\langle u_0 \rangle < -\frac{\beta}{2\alpha}$), then the solution to (4.17)–(4.19) blows up in finite time. Furthermore, the blow up time T^+ satisfies*

$$T^+ \leq T - \frac{1}{\alpha z(T)}.$$

Proof. *Since $\Theta \leq 0$, we can rewrite (4.64) in the form*

$$z' + \alpha z^2 = c(t), \tag{4.66}$$

where $c(t) = -\alpha \langle v^2 \rangle + \frac{\Theta}{4\alpha}$ is nonpositive and uniformly bounded. Noting that the solution to the Riccati ODE $z' + \alpha z^2 = 0$ reads

$$z(t) = \frac{1}{\alpha(t - T) + \frac{1}{z(T)}}, \quad t \geq T,$$

we conclude, owing to the comparison principle. □

As a consequence of Theorem 4.2.8, (4.30), (4.33), and (4.35), we have the

Corollary 3. *We assume that $\Theta = 0$. Let u be a solution to (4.17)–(4.19). Then, either u blows up in finite time or u exists globally in time and, $\forall t \geq 0$,*

$$-\frac{\beta}{2\alpha} \leq \langle u(t) \rangle \leq \begin{cases} \left| \langle u_0 \rangle - \frac{\gamma}{\beta} \right| - \frac{\beta}{\alpha} + \frac{\gamma}{\beta} & \text{if } \beta < 0, \\ \left| \langle u_0 \rangle + \frac{\gamma}{\beta} \right| - \frac{\gamma}{\beta} & \text{if } \beta > 0, \\ \left| \langle u_0 \rangle + \frac{\gamma}{2} - \frac{1}{2\alpha} \right| - \frac{\gamma}{2} + \frac{1}{2\alpha} & \text{if } \beta = 0. \end{cases}$$

Note that, as a consequence of Lemma 4.2.4 and Lemma 4.2.5, we also have the

Corollary 4. *We assume that $\beta < 0$. Let u be a solution to (4.17)–(4.19). If $\langle u_0 \rangle < -\frac{\gamma}{\beta}$, then u blows up in finite time.*

Corollary 5. *We assume that $\Theta < 0$. Let u be a solution to (4.17)–(4.19). Then, for all u_0, u blows up in finite time.*

We finally deduce from (4.30), (4.33), (4.35), (4.59), Corollary 2, and Corollary 3 the

Corollary 6. *Let u be a global in time solution to (4.17)–(4.19). Then, u is dissipative in $L^2(\Omega)$.*

Remark 4.2.9. *It is not difficult to also prove the dissipativity in $H^1(\Omega)$ and $H^2(\Omega)$ (see also [104], [114], and [137]).*

Remark 4.2.10. *We assume that $\Theta > 0$. We saw in Remark 4.2.2 that u can become smaller than $\frac{-\beta-\sqrt{\Theta}}{2\alpha}$ even if $u_0 \in \left[\frac{-\beta-\sqrt{\Theta}}{2\alpha}, \frac{-\beta+\sqrt{\Theta}}{2\alpha}\right]$. Similarly, we can prove that $\langle u\rangle$ can become smaller than $\frac{-\beta-\sqrt{\Theta}}{2\alpha}$ (and blow up) even if $\langle u_0\rangle \in \left[\frac{-\beta-\sqrt{\Theta}}{2\alpha}, \frac{-\beta+\sqrt{\Theta}}{2\alpha}\right]$. Indeed, assume that*

$$\langle u_0\rangle = \frac{-\beta-\sqrt{\Theta}}{2\alpha} \text{ and } u_0 \neq \frac{-\beta-\sqrt{\Theta}}{2\alpha}.$$

Then, it follows from (4.22) that, at $t = 0$,

$$\frac{d}{dt}\langle u\rangle < 0,$$

meaning that $\langle u\rangle$ is smaller than $\frac{-\beta-\sqrt{\Theta}}{2\alpha}$, for $t > 0$, and blows up in finite time. Of course, an interesting question is whether $\langle u\rangle$ can become smaller than $\frac{-\beta-\sqrt{\Theta}}{2\alpha}$ even if $\langle u_0\rangle \in \left]\frac{-\beta-\sqrt{\Theta}}{2\alpha}, \frac{-\beta+\sqrt{\Theta}}{2\alpha}\right]$. As a partial answer in this direction (see also the numerical simulations below), let us consider the Riccati ODE

$$z' + \alpha z^2 - \frac{\Theta}{4\alpha} = c_0. \tag{4.67}$$

Then, when $-\frac{\Theta}{4\alpha} < c_0 < 0$, the solution to this equation reads

$$z(t) = c_1 + \frac{1}{\frac{z_0+c_1}{2c_1(z_0-c_1)}e^{2\alpha c_1 t} - \frac{1}{2c_1}}, \quad c_1^2 = \frac{c_0}{\alpha} + \frac{\Theta}{4\alpha^2}.$$

Therefore, when $\frac{-\sqrt{\Theta}}{2\alpha} \leq z_0 < -c_1$ (i.e., $\frac{-\beta-\sqrt{\Theta}}{2\alpha} \leq y_0 < -c_1 - \frac{\beta}{2\alpha}$), the solution blows up in finite time and becomes smaller than $\frac{-\beta-\sqrt{\Theta}}{2\alpha}$. Furthermore, when $c_0 = -\frac{\Theta}{4\alpha}$, the solution to (4.67) reads

$$z(t) = \frac{1}{\alpha t + \frac{1}{z_0}}$$

and the same holds, for $\frac{-\sqrt{\Theta}}{2\alpha} \leq z_0 < 0$ (i.e., $\frac{-\beta-\sqrt{\Theta}}{2\alpha} \leq y_0 < -\frac{\beta}{2\alpha}$). Finally, when $c_0 < -\frac{\Theta}{4\alpha}$, then

$$z' \leq c_0 + \frac{\Theta}{4\alpha} (< 0),$$

which yields that

$$z(t) \leq z_0 + \left(c_0 + \frac{\Theta}{4\alpha}\right)t, \quad t \geq 0.$$

Therefore,

$$y(t) \leq y_0 + \left(c_0 + \frac{\Theta}{4\alpha}\right)t, \quad t \geq 0,$$

and the solution becomes smaller than $\frac{-\beta-\sqrt{\Theta}}{2\alpha}$, for every initial datum y_0 in $\left[\frac{-\beta-\sqrt{\Theta}}{2\alpha}, \frac{-\beta+\sqrt{\Theta}}{2\alpha}\right]$.

Theorem 4.2.11. *Let $\Theta > 0$, and let u be a solution to (4.17)–(4.19) such that $u(t) \in \left[\frac{-\beta-\sqrt{\Theta}}{2\alpha}, \frac{-\beta+\sqrt{\Theta}}{2\alpha}\right]$, $\forall t \geq 0$. Then, u tends to $\frac{-\beta+\sqrt{\Theta}}{2\alpha}$ in $H^1(\Omega)$ as $t \to +\infty$.*

Proof. *We first note that, if $u_0 \equiv \frac{-\beta-\sqrt{\Theta}}{2\alpha}$, then $u \equiv \frac{-\beta-\sqrt{\Theta}}{2\alpha}$. We thus assume that $u_0 \not\equiv \frac{-\beta-\sqrt{\Theta}}{2\alpha}$.*

Setting again $y = \langle u \rangle$, we have

$$y' = -\langle g(u) \rangle. \tag{4.68}$$

Then, since $u(t) \in \left[\frac{-\beta-\sqrt{\Theta}}{2\alpha}, \frac{-\beta+\sqrt{\Theta}}{2\alpha}\right]$, $\forall t \geq 0$, we note that

$$g(u) \leq 0, \ \forall t \geq 0,$$

hence

$$\langle g(u) \rangle \leq 0, \ \forall t \geq 0,$$

and we can deduce from (1.4) that y is monotone increasing. Since it is bounded from above (by $\frac{-\beta+\sqrt{\Theta}}{2\alpha}$), it follows that y tends to some limit $\bar{y}$ as $t \to +\infty$.

Let now t_n, $n \in \mathbb{N}$, be such that $y'(t_n)$ tends to 0 as $n \to +\infty$ (indeed, note that $y(t+1) - y(t) = y'(\tau)$, for some $\tau \in (t, t+1)$). Then, $\langle u(t_n) \rangle$, $\|u(t_n)\|$, and $\|u(t_n)\|_{H^1(\Omega)}$ (see Remark 4.2.9), and also $g(u(t_n))$, $\langle g(u(t_n)) \rangle$, and $\|g(u(t_n))\|_{L^1(\Omega)}$, are bounded, independently of n, so that, at least for a subsequence which we do not relabel,

$$u(t_n) \to \bar{u} \text{ a.e. and in } L^2(\Omega), \ y(t_n) \to \langle \bar{u} \rangle,$$

as $n \to +\infty$. Thus, passing to the limit $n \to +\infty$ in (4.68), we have

$$\langle g(\bar{u}) \rangle = 0$$

and

$$\|g(\bar{u})\|_{L^1(\Omega)} = 0,$$

hence

$$g(\bar{u}) = 0,$$

which yields that $\bar{u}$ is constant and $\bar{u} \equiv \frac{-\beta+\sqrt{\Theta}}{2\alpha}$ (indeed, $\langle u \rangle$ is monotone increasing and cannot tend to $\frac{-\beta-\sqrt{\Theta}}{2\alpha}$). Finally, we see that y tends to $\frac{-\beta+\sqrt{\Theta}}{2\alpha}$ as $t \to +\infty$.

Now, noting that the trajectory is asymptotically compact in $H^1(\Omega)$ (see again Remark 4.2.9), the ω-limit set of u_0 is nonempty and compact in $H^1(\Omega)$. Then, if $\bar{u}$ belongs to this set, necessarily, $\langle \bar{u} \rangle = \frac{-\beta+\sqrt{\Theta}}{2\alpha}$, whence $\bar{u} \equiv \frac{-\beta+\sqrt{\Theta}}{2\alpha}$. □

We also have the

Theorem 4.2.12. *Let $\Theta \geq 0$, and let u be a solution to (4.17)–(4.19) such that $u(t) \in \left[\frac{-\beta+\sqrt{\Theta}}{2\alpha}, a\right]$, $\forall t \geq 0$, where $a > \frac{-\beta+\sqrt{\Theta}}{2\alpha}$ is arbitrary. Then, u tends to $\frac{-\beta+\sqrt{\Theta}}{2\alpha}$ in $H^1(\Omega)$ as $t \to +\infty$.*

Remark 4.2.13. *The proof of Theorem 4.2.12 is similar to the one of Theorem 4.2.11, but, now, $y = \langle u \rangle$ is monotone decreasing.*

Remark 4.2.14. *The results in Theorem 4.2.11 and Theorem 4.2.12 also hold in the H^2–norm (see Remark 4.2.9).*

Remark 4.2.15. *We can more generally consider a nonlinear term f of the form*

$$f(s) = \sum_{k=0}^{2p+1} a_k s^k, \quad a_{2p+1} > 0$$

(see [42]).

4.3 A general tumor growth model

We consider in this section the following initial and boundary value problem :

$$\frac{\partial u}{\partial t} + \Delta^2 u - \Delta f(u) + g(u) = 0, \tag{4.69}$$

$$\frac{\partial u}{\partial \nu} = \frac{\partial \Delta u}{\partial \nu} = 0 \quad \text{on } \Gamma, \tag{4.70}$$

$$u|_{t=0} = u_0, \tag{4.71}$$

where the nonlinear term f is defined as

$$f(s) = \sum_{i=0}^{2p+1} a_i s^i, \quad a_{2p+1} > 0, \quad p \geq 1, \tag{4.72}$$

and the proliferation term is defined as

$$g(s) = \alpha s - \beta s^q (s-1)^q, \quad q > 1, \tag{4.73}$$

where $\alpha,\ \beta \in \mathbb{R}$.

Remark 4.3.1. *Note that, here, we assume that the parameters α and β are constant but, in general biological applications, they can depend on the spatial variable and on time.*

We set

$$L(s) = s^q (s-1)^q, \quad q > 1. \tag{4.74}$$

We note that it is easy to prove that there exist c_0 and $c_1 \geq 0$ such that

$$f'(s) \geq -c_0 \tag{4.75}$$

and

$$\frac{1}{2} s^{2q} - c_1 \leq L(s) \leq \frac{3}{2} s^{2q} + c_1. \tag{4.76}$$

Integrating (4.69) over Ω, we have

$$\frac{d}{dt}\langle u \rangle + \langle g(u) \rangle = 0, \tag{4.77}$$

hence

$$\frac{d}{dt}\langle u \rangle + \alpha \langle u \rangle - \beta \langle L(u) \rangle = 0. \tag{4.78}$$

We first have the

Proposition 4.3.2. *For every $u_0 \in L^2(\Omega)$, there exists $T_0 = T_0(\|u_0\|) > 0$ and a unique solution u to (4.69)–(4.71) such that $u \in C([0, T_0); L^2(\Omega)) \cap L^2(0, T; H^2(\Omega))$, $\forall T < T_0$.*

Proof. *See [114] and [137].* □

Lemma 4.3.3. *We assume that $\alpha > 0$. Let u be a solution to* (4.69)–(4.71)*. We have*
- *If $\beta \geq 0$, then $\langle u \rangle$ is bounded from below.*
- *If $\beta \leq 0$, then $\langle u \rangle$ is bounded from above.*

Proof. *First, owing to* (4.78)*, we have*

$$\frac{d\langle u \rangle}{dt} + \alpha \langle u \rangle = \beta \langle L(u) \rangle. \tag{4.79}$$

We assume that $\beta \geq 0$. Then, owing to (4.76) *and* (4.79)*,*

$$\frac{d\langle u \rangle}{dt} + \alpha \langle u \rangle \geq \frac{\beta}{2} \langle u^{2q} \rangle - \beta c_1 \geq -\beta c_1, \tag{4.80}$$

hence

$$\frac{d}{dt}(e^{\alpha t} \langle u \rangle) \geq -\beta c_1 e^{\alpha t}. \tag{4.81}$$

It thus follows from (4.81) *that*

$$\langle u(t) \rangle \geq \Big(\langle u_0 \rangle + \frac{\beta c_1}{\alpha} \Big) e^{-\alpha t} - \frac{\beta c_1}{\alpha}, \qquad \forall t \geq 0, \tag{4.82}$$

i.e., $\langle u \rangle$ is bounded from below.

Now, assuming that $\beta \leq 0$, we have, owing to (4.76) *and* (4.79)*,*

$$\frac{d\langle u \rangle}{dt} + \alpha \langle u \rangle \leq \frac{\beta}{2} \langle u^{2q} \rangle - \beta c_1 \leq -\beta c_1, \tag{4.83}$$

hence

$$\frac{d}{dt}(e^{\alpha t} \langle u \rangle) \leq -\beta c_1 e^{\alpha t}. \tag{4.84}$$

It thus follows from (4.84) *that*

$$\langle u(t) \rangle \leq \Big(\langle u_0 \rangle + \frac{\beta c_1}{\alpha} \Big) e^{-\alpha t} - \frac{\beta c_1}{\alpha}, \qquad \forall t \geq 0, \tag{4.85}$$

i.e., $\langle u \rangle$ is bounded from above. □

Lemma 4.3.4. *We assume that $\alpha < 0$. Let u be a solution to* (4.69)–(4.71)*. We have*
- *If $\beta \geq 0$ and $\langle u(T) \rangle > -\frac{\beta c_1}{\alpha}$ (and, in particular, if $\langle u_0 \rangle > -\frac{\beta c_1}{\alpha}$), then there exists $t_0 \geq T$ such that*

$$\langle u(t) \rangle > 0, \quad \forall t \geq t_0,$$

and, if the solution exists globally in time,

$$\lim_{t \to +\infty} \langle u(t) \rangle = +\infty.$$

– *If* $\beta \leq 0$ *and* $\langle u(T)\rangle < -\frac{\beta c_1}{\alpha}$ *(and, in particular, if* $\langle u_0\rangle < -\frac{\beta c_1}{\alpha}$*), then there exists* $t_0 \geq T$ *such that*

$$\langle u(t)\rangle < 0, \quad \forall t \geq t_0,$$

and, if the solution exists globally in time,

$$\lim_{t\to+\infty} \langle u(t)\rangle = -\infty.$$

Proof. *We assume that* $\beta \geq 0$*. It thus follows from* (4.76) *and* (4.78) *that*

$$\frac{d\langle u\rangle}{dt} + \alpha\langle u\rangle \geq -\beta c_1, \tag{4.86}$$

which yields, owing to Gronwall's lemma,

$$\langle u(t)\rangle \geq \Big(\langle u_0\rangle + \frac{\beta c_1}{\alpha}\Big)e^{-\alpha t} - \frac{\beta c_1}{\alpha}. \tag{4.87}$$

Therefore, if

$$\langle u_0\rangle > -\frac{\beta c_1}{\alpha}, \tag{4.88}$$

then there exists $t_0 \geq 0$ *such that*

$$\langle u(t)\rangle > 0, \quad \forall t \geq t_0, \tag{4.89}$$

and, moreover, if the solution exists globally in time,

$$\lim_{t\to+\infty} \langle u(t)\rangle = +\infty. \tag{4.90}$$

Now, assuming that $\beta \leq 0$*, it also follows from* (4.76) *and* (4.78) *that*

$$\frac{d\langle u\rangle}{dt} + \alpha\langle u\rangle \leq -\beta c_1, \tag{4.91}$$

which yields, owing to Gronwall's lemma,

$$\langle u(t)\rangle \leq \Big(\langle u_0\rangle + \frac{\beta c_1}{\alpha}\Big)e^{-\alpha t} - \frac{\beta c_1}{\alpha}. \tag{4.92}$$

Therefore, if

$$\langle u_0\rangle < -\frac{\beta c_1}{\alpha}, \tag{4.93}$$

then there exists $t_0 \geq 0$ *such that*

$$\langle u(t)\rangle < 0, \quad \forall t \geq t_0, \tag{4.94}$$

and, moreover, if the solution exists globally in time,

$$\lim_{t\to+\infty} \langle u(t)\rangle = -\infty. \tag{4.95}$$

□

Lemma 4.3.5. *We assume that $\alpha = 0$ and q is even. Let u be a solution to* (4.69)–(4.71)*. We have*

- *If $\beta \geq 0$, then $\langle u \rangle$ is bounded from below.*
- *If $\beta \leq 0$, then $\langle u \rangle$ is bounded from above.*

Proof. *We assume that $\beta \geq 0$. We have, owing to* (4.79)*,*

$$\frac{d\langle u \rangle}{dt} \geq 0, \tag{4.96}$$

since q is even, hence

$$\langle u(t) \rangle \geq \langle u_0 \rangle, \qquad \forall t \geq 0, \tag{4.97}$$

i.e., $\langle u \rangle$ is bounded from below.

Now, assuming that $\beta \leq 0$, we have, owing to (4.79)*,*

$$\frac{d\langle u \rangle}{dt} \leq 0, \tag{4.98}$$

since q is even, hence,

$$\langle u \rangle \leq \langle u_0 \rangle, \qquad \forall t \geq 0, \tag{4.99}$$

i.e., $\langle u \rangle$ is bounded from above.

□

Proposition 4.3.6. *We assume that $p = 2q - 1$. Let u be a solution to (4.69)–(4.71). Then, there exists a monotone increasing function Q such that*

$$\|u(t) - \langle u(t) \rangle\|^2 \leq Q(\|u_0 - \langle u_0 \rangle\|), \qquad \forall t \geq 0.$$

Proof. *Setting again $v = u - \langle u \rangle$, we rewrite problem (4.69)–(4.71) in the form*

$$\frac{\partial v}{\partial t} + \Delta^2 v - \Delta f(v + \langle u \rangle) + g(v + \langle u \rangle) - \langle g(v + \langle u \rangle) \rangle = 0, \tag{4.100}$$

$$\frac{\partial v}{\partial \nu} = \frac{\partial \Delta v}{\partial \nu} = 0 \quad \text{on } \Gamma, \tag{4.101}$$

$$v|_{t=0} = v_0 = u_0 - \langle u_0 \rangle. \tag{4.102}$$

We multiply (4.100) *by $(-\Delta)^{-1} v$ and have*

$$\begin{aligned} &\frac{1}{2}\frac{d}{dt}\|v\|_{-1}^2 + \|\nabla v\|^2 + ((f(v + \langle u \rangle) - f(\langle u \rangle), v)) + \alpha \|v\|_{-1}^2 \\ &\quad - \beta((L(v + \langle u \rangle) - \langle L(v + \langle u \rangle) \rangle, (-\Delta)^{-1} v)) = 0. \end{aligned} \tag{4.103}$$

Here,

$$((f(v + \langle u \rangle) - f(\langle u \rangle), v)) \geq \xi \int_\Omega \sum_{k=0}^{p} v^{2p+2-2k} \langle u \rangle^{2k} dx,$$

where $\xi > 0$ (see [42]). Furthermore,

$$\begin{aligned}&\Big|\beta((L(v+\langle u\rangle)-\langle L(v+\langle u\rangle)\rangle,(-\Delta)^{-1}v))\Big|\\&\qquad\le c\|L(v+\langle u\rangle)-L(\langle u\rangle)\|\|v\|,\end{aligned}$$

which yields

$$\begin{aligned}&\frac{d}{dt}\|v\|_{-1}^2+2\|\nabla v\|^2+\xi\int_\Omega\sum_{k=0}^{p}v^{2p+2-2k}\langle u\rangle^{2k}dx\\&\le|\alpha|\|v\|_{-1}^2+c(\varepsilon)\|\,v\|^2+\varepsilon\|L(v+\langle u\rangle)-L(\langle u\rangle)\|^2.\end{aligned}\tag{4.104}$$

Actually, it suffices to treat the case $L(s)=s^{2q}$ (see Remark 4.3.8) and we have

$$\begin{aligned}\|L(v+\langle u\rangle)-L(\langle u\rangle\|^2&\le\int_\Omega\Big((v+\langle u\rangle)^{2q}-\langle u\rangle^{2q}\Big)^2dx\\&\le\int_\Omega\Big(\sum_{k=0}^{2q-1}C_{2q}^kv^{2q-k}\langle u\rangle^kdx\Big)^2dx\\&\le c\int_\Omega\sum_{k=0}^{2q-1}v^{4q-2k}\langle u\rangle^{2k}dx+c'\\&\le c\int_\Omega\sum_{k=0}^{p}v^{2p+2-2k}\langle u\rangle^{2k}dx+c',\end{aligned}$$

since $4q=2p+2$. Therefore,

$$\begin{aligned}&\frac{d}{dt}\|v\|_{-1}^2+\|\nabla v\|^2+\xi\int_\Omega\sum_{k=0}^{p}v^{2p+2-2k}\langle u\rangle^{2k}dx\\&\qquad\le c,\end{aligned}\tag{4.105}$$

hence

$$\frac{d}{dt}\|v\|_{-1}^2+c\|v\|_{-1}^2\le c',\quad c>0.\tag{4.106}$$

It thus follows from Gronwall's lemma that

$$\|v(t)\|_{-1}^2\le e^{-ct}\|v_0\|_{-1}^2+c',\quad c>0,\ t\ge0.\tag{4.107}$$

Let B be a bounded subset of $\dot H^{-1}(\Omega)$ and t_0 be such that $v_0\in B$ and $t\ge t_0$ implies $v(t)\in\mathcal{B}_0$, where $\mathcal{B}_0=\{\phi\in\dot H^{-1}(\Omega),\ \|\phi\|_{-1}^2\le 2c'\}$, c' being the constant in (4.107). We then deduce from (4.105) that, for $t\ge t_0$,

$$\int_t^{t+r}\|\nabla v\|^2ds\le c(r),\quad\int_t^{t+r}ds\int_\Omega\sum_{k=0}^{p}v^{2p+2-2k}\langle u\rangle^{2k}dx\le c(r),$$

where $r>0$ is fixed.

Now, multiplying (4.100) by v, it is easy to obtain, noting that

$$|((L(v+\langle u\rangle)-L(\langle u\rangle),v))| \le c\|L(v+\langle u\rangle)\|\|v\| \le c\Big(\int_\Omega \sum_{k=0}^{p} v^{2p+2-2k}\langle u\rangle^{2k}dx + \|v\|^2\Big),$$

the inequality

$$\frac{d}{dt}\|v\|^2 + \|\Delta v\|^2 \le c\Big(\int_\Omega \sum_{k=0}^{p} v^{2p+2-2k}\langle u\rangle^{2k}dx + \|v\|^2_{H^1(\Omega)} + 1\Big). \tag{4.108}$$

It thus follows from (4.108) and Gronwall's lemma that

$$\|v(t)\|^2 \le c, \qquad t \ge t_0 + r, \tag{4.109}$$

where $0 < r < 1$ *is fixed and the constant c is independent of* v_0 *and t, hence, owing to (4.109) and integrating (4.105) and (4.108) between* 0 *and* $t_0 + r$ *(r is fixed in* $(0,1)$*),*

$$\|v(t)\|^2 \le Q(\|v_0\|), \qquad t \ge 0, \tag{4.110}$$

where the function Q is monotone increasing.

□

Corollary 7. *Let u be a global in time solution to (4.69)–(4.71). Then,* $v = u - \langle u\rangle$ *is dissipative in* $L^2(\Omega)$*.*

Remark 4.3.7. *It is not difficult to also prove the dissipativity of v in* $H^1(\Omega)$ *and* $H^2(\Omega)$ *(see also [104], [114], and [137]).*

Remark 4.3.8. *We treated in Proposition 4.3.6 the term* $\|L(v+\langle u\rangle) - L(\langle u\rangle)\|$ *in the particular case* $L(s) = s^{2q}$*, but, in general, we are interested in the case when* $L(s) = s^q(s-1)^q$*. We have, more generally,*

$$\begin{aligned} L(v+\langle u\rangle) - L(\langle u\rangle) &= \Big((v+\langle u\rangle)^2 - (v+\langle u\rangle)\Big)^q - \Big(\langle u\rangle^2 - \langle u\rangle\Big)^q \\ &= \sum_{k=0}^{q} C_k^q(-1)^k(v+\langle u\rangle)^{2q-2k}(v+\langle u\rangle)^k - \sum_{k=0}^{q} C_k^q(-1)^k\langle u\rangle^{2q-2k}\langle u\rangle^k \\ &= \sum_{k=0}^{q} C_k^q(-1)^k\Big((v+\langle u\rangle)^{2q-k} - \langle u\rangle^{2q-k}\Big) \\ &= \sum_{k=0}^{q} C_k^q(-1)^k \sum_{j=0}^{2q-k-1} C_j^{2q-k} v^{2q-k-j}\langle u\rangle^j, \end{aligned}$$

hence

$$\begin{aligned} |L(v+\langle u\rangle) - L(\langle u\rangle)| &\le c\sum_{k=0}^{q}\sum_{j=0}^{2q-k-1} |v|^{2q-k-j}|\langle u\rangle|^j \\ &\le c\sum_{i=q-1}^{2q-1}\sum_{j=0}^{i} |v|^{i+1-j}|\langle u\rangle|^j, \end{aligned}$$

which yields

$$\begin{aligned}\|L(v+\langle u\rangle)-L(\langle u\rangle)\|^2 &\le c\int_\Omega \sum_{i=q-1}^{2q-1}\sum_{j=0}^{i}|v|^{2i+2-2j}|\langle u\rangle|^{2j}\\ &\le c\int_\Omega \sum_{l=0}^{2q-1}|v|^{4q-2l}|\langle u\rangle|^{2l}+c'.\end{aligned}$$

We also have the

Theorem 4.3.9. *Let u be a solution to* (4.69)–(4.70) *(note that the same holds for the solution to* (4.17)–(4.18)*). Then, $v = u - \langle u\rangle$ tends to* 0 *in $H^1(\Omega)$ as $t \to +\infty$.*

Proof. *We note that $\langle v\rangle = 0,\ \forall t \ge 0$. It thus follows from Proposition 4.3.6 that $\|v(t)\|$ and $\|v(t)\|_{H^1(\Omega)}$ (see Remark 4.3.7) are bounded, so that, at least for a subsequence which we do not relabel,*

$$v(t_n) \to \bar v \quad \text{in } L^2(\Omega) \quad n \in \mathbb{N},$$

hence

$$v(t_n) \to \bar v \quad \text{a.e. in } \Omega.$$

Since $\langle v\rangle = 0$, we have

$$\langle \bar v\rangle = 0,$$

whence

$$\bar v \equiv 0.$$

Finally, as a consequence of Remark 4.2.9 and Remark 4.3.7, v tends to 0 *in $H^1(\Omega)$ as $t \to +\infty$.* □

Theorem 4.3.10. *We assume that $\alpha = 0$ and q is even. Let u be a nonvanishing solution to (4.69)–(4.71) such that $u(t) \in [0,1],\ \forall t \ge 0$. Then,*

- *If $\beta > 0$, u tends to* 1 *in $H^1(\Omega)$ as $t \to +\infty$.*
- *If $\beta < 0$, u tends to* 0 *in $H^1(\Omega)$ as $t \to +\infty$.*

Proof. *We first note that, if $u_0 \equiv 0$, then $u \equiv 0$. We thus assume that $u_0 \not\equiv 0$.*

Setting again $y = \langle u\rangle$, we have

$$y' + \langle g(u)\rangle = 0, \tag{4.111}$$

hence

$$y' = \beta\langle L(u)\rangle. \tag{4.112}$$

We note that

$$L(u) \ge 0,\ \forall t \ge 0,$$

hence

$$\langle L(u)\rangle \ge 0,\ \forall t \ge 0,$$

and, if $\beta > 0$, we can deduce from (4.112) that y is monotone increasing. Since it is bounded from above (by 1*), it follows that y tends to some limit $\bar u$ as $t \to +\infty$.*

Let now t_n, $n \in \mathbb{N}$, be such that $y'(t_n)$ tends to 0 as $n \to +\infty$ (indeed, note that $y(t+1)-y(t) = y'(\tau)$, for some $\tau \in (t, t+1)$). Then, $\langle u(t_n)\rangle$, $\|u(t_n)\|$, and $\|u(t_n)\|_{H^1(\Omega)}$ (see Remark 4.3.7), and also $L(u(t_n))$, $\langle L(u(t_n))\rangle$, and $\|L(u(t_n))\|_{L^1(\Omega)}$, are bounded, independently of n, so that, at least for a subsequence which we do not relabel,

$$u(t_n) \to \bar{u} \text{ a.e. and in } L^2(\Omega),\ \ y(t_n) \to \langle \bar{u}\rangle,$$

as $n \to +\infty$. Thus, passing to the limit $n \to +\infty$ in (4.112), we have

$$\langle L(\bar{u})\rangle = 0$$

and

$$\|L(\bar{u})\|_{L^1(\Omega)} = 0,$$

hence

$$L(\bar{u}) = 0,$$

which yields that $\bar{u}$ is constant and that $\bar{u} \equiv 1$ (indeed, $\langle u\rangle$ is monotone increasing and cannot tend to 0). Finally, we see that y tends to 1 as $t \to +\infty$.

Now, noting that the trajectory is asymptotically compact in $H^1(\Omega)$ (see again Remark 4.3.7), the ω-limit set of u_0 is nonempty and compact in $H^1(\Omega)$. Then, since $\bar{u}$ belongs to this set, necessarily, $\langle \bar{u}\rangle = 1$, whence $\bar{u} \equiv 1$.

Similarly, if $\beta < 0$, we can deduce from (4.112) that y is monotone decreasing. Since it is bounded from below (by 0), we can prove that u tends to 0. □

Theorem 4.3.11. *We assume that $\alpha = 0$ and q is odd. Let u be a nonvanishing solution to (4.69)–(4.71) such that $u(t) \in [0,1],\ \forall t \geq 0$. Then,*

- *If $\beta > 0$, u tends to 0 in $H^1(\Omega)$ as $t \to +\infty$.*
- *If $\beta < 0$, u tends to 1 in $H^1(\Omega)$ as $t \to +\infty$.*

Proof. *Since $u(t) \in [0,1],\ \forall t \geq 0$, we note that*

$$L(u) \leq 0, \quad \forall t \geq 0,$$

hence

$$\langle L(u)\rangle \leq 0, \quad \forall t \geq 0,$$

and we deduce that (proceeding as the proof of the previous theorem), if $\beta > 0$, u tends to 0 in $H^1(\Omega)$ as $t \to +\infty$ and, if $\beta < 0$, u tends to 1 in $H^1(\Omega)$ as $t \to +\infty$. □

The particular case $g(s) = 2\beta s - \beta s^2(s-1)^2$.

Theorem 4.3.12. *Let $\beta > 0$, and let u be a solution to (4.69)–(4.71) such that $u(t) > 2,\ \forall t \geq 0$. Then, u blows up in finite time. Furthermore, the blow up time T^+ satisfies*

$$T^+ \leq T + \frac{1}{2\beta} \ln\Big(\frac{y(T)}{y(T)-2}\Big),$$

where $y(T) = \langle u(T)\rangle$.

Proof. *We first note that*

$$g(u) = -\beta u(u-2)(u^2+1),$$

hence, we can rewrite (4.22) in the form

$$\frac{d}{dt}\langle u\rangle = \beta\langle u(u-2)(u^2+1)\rangle. \tag{4.113}$$

We set

$$\vartheta(s) = s^2 + 1$$

and note that

$$\vartheta(s) \geq 1, \quad \forall s \in \mathbb{R}.$$

Therefore,

$$\frac{d}{dt}\langle u\rangle \geq \beta\langle u(u-2)\rangle, \tag{4.114}$$

since, by assumption, $u(u-2) > 0$. It thus follows that

$$\frac{d}{dt}\langle u\rangle - \beta\langle u\rangle^2 + 2\beta\langle u\rangle \geq \beta\langle v^2\rangle, \tag{4.115}$$

hence the ODE

$$y' - \beta y^2 + 2\beta y \geq \beta\langle v^2\rangle, \tag{4.116}$$

where $y = \langle u\rangle$. Thus,

$$y' - \beta y^2 + 2\beta y \geq c(t), \tag{4.117}$$

where $c(t) = \beta\langle v^2\rangle$ is nonnegative and uniformly bounded. Noting that the solution to the Riccati ODE $y' - \beta y^2 + 2\beta y = 0$ reads

$$y(t) = \frac{2y(T)}{e^{2\beta(t-T)}(2 - y(T)) + y(T)}, \quad t \geq T,$$

we conclude, owing to the comparison principle. □

Theorem 4.3.13. *Let $\beta < 0$, and let u be a solution to (4.69)–(4.71) such that $u(t) < 0, \ \forall t \geq 0$. Then, u blows up in finite time. Furthermore, the blow up time T^+satisfies*

$$T^+ \leq T + \frac{1}{2\beta}\ln\Big(\frac{y(T)}{y(T)-2}\Big),$$

where $y(T) = \langle u(T)\rangle$.

Remark 4.3.14. *The proof of Theorem 4.3.13 is similar to the one of Theorem 4.3.12, but, now, the solution tends to $-\infty$.*

We also have the

Theorem 4.3.15. *Let $\beta > 0$, and let u be a solution to (4.69)–(4.71) such that $u(t) \leq 2, \ \forall t \geq 0$. Then, u tends to 0 in $H^1(\Omega)$ as $t \to +\infty$.*

Theorem 4.3.16. *Let $\beta < 0$, and let u be a solution to (4.69)–(4.71) such that $u(t) \geq 0, \ \forall t \geq 0$. Then, u tends to 0 in $H^1(\Omega)$ as $t \to +\infty$.*

Remark 4.3.17. *The proof of Theorem 4.3.15 and Theorem 4.3.16 is similar to the one of Theorem 4.3.10 ; see also Theorem 4.2.11.*

4.4 Numerical results

As far as the numerical simulations are concerned, we rewrite the problem in the form

$$\frac{\partial u}{\partial t} + \Delta\mu + g(u) = 0 \quad \text{in } \Omega, \tag{4.118}$$

$$\mu = \Delta u - f(u) \quad \text{in } \Omega, \tag{4.119}$$

$$\frac{\partial u}{\partial \nu} = \frac{\partial \mu}{\partial \nu} = 0 \quad \text{on } \Gamma, \tag{4.120}$$

$$u_{|t=0} = u_0, \tag{4.121}$$

which has the advantage of splitting the fourth-order (in space) equation into a system of two second-order ones (see [43] and [56]). Consequently, we use a P1-finite element for the space discretization, together with an implicit Euler time disretization. The numerical simulations are performed with the software Freefem++ [67].

In the numerical results presented below, Ω is a $(0,5)\times(0,1)$-rectangle. The triangulation is obtained by dividing Ω into 200×40 rectangles and by dividing each rectangle along the same diagonal. The time step is taken as $\delta t = 0.01$. We further take $f(s) = (s-\frac{1}{2})^3 - (s-\frac{1}{2})$.

The left pictures below represent the evolution of $u_{min} = \min_{x\in\Omega} u(x)$ (green curve), $u_{max} = \max_{x\in\Omega} u(x)$ (blue curve), and $\langle u\rangle$ with respect to time (black curve), u being the numerical solution to (4.118), while the right pictures represent the evolution of $\|u - \langle u\rangle\|$ with respect to t, for different choices of the initial datum u_0.

4.4.1 The case when $g(s) = \alpha s^2 + \beta s + \gamma$.

First case : $\Theta > 0$.

We show in Figure 4.1 that, for $g(s) = \frac{1}{2}s^2 - s - \frac{1}{2}$ with zeros $1-\sqrt{2}$ and $1+\sqrt{2}$ and $u_0 = 1 - \sin^2(x+y)$, leading to $u_0 \in [1-\sqrt{2}, 1+\sqrt{2}]$ and $\langle u_0\rangle = 0.422$, the solution stays between $[1-\sqrt{2}, 1+\sqrt{2}]$ for all $t \geq 0$ and converges to $\bar{u} = 1+\sqrt{2}$.

In Figure 4.2, we take $g(s) = s^2 + s$ with zeros -1 and 0. The solution remains greater than 0 and converges to 0. Here, $u_0 = 1 - \sin^2(x-y)$, leading to $u_0 \geq 0$ and $\langle u_0\rangle = 0.552$.

Figure 4.3 corresponds to the function $g(s) = \frac{3}{4}s^2 + 5s + 3$ with zeros -6 and $-\frac{2}{3}$ and to the initial datum $u_0 = \frac{-5}{(x^6+1)(y^3+1)} - 6$, leading to $\langle u_0\rangle = -6.892 < -6$. The solution blows up in finite time and $\|u - < u >\|$ approaches 0, in agreement with the theoretical results.

In Figure 4.4, we take $u_0 = \frac{1}{5(x^6+1)(y^5+\frac{1}{2})} + \frac{1}{2} \in [\frac{1}{2}, 1]$, leading to $\langle u_0\rangle = 0.569$, and $g(s) = s^2 - \frac{3}{2}s + \frac{1}{2}$ with two zeros $\frac{1}{2}$ and 1. In that case, the solution blows up in finite time, while $\|u - < u >\|$ approaches 0.

Second case : $\Theta = 0$.

In Figure 4.5, the solution blows up in finite time. Here, we take $g(s) = \frac{1}{2}s^2 - s + \frac{1}{2}$ with a double zero 1 and $u_0 = \frac{16(\sin(x-y)+1)}{x^6+5}$, hence $\langle u_0\rangle = 1.043 > 1$.

Finally, we take $g(s) = \frac{1}{2}s^2 + s + \frac{1}{2}$ with a double zero -1. Here, $u_0 = \frac{-4\cos(x-y)}{x^6+1}$ and $\langle u_0\rangle = -0.740$. We emphasize that, at $t = 1.04$, $u > -1$ and the solution does not blow up and converges to -1 as shown in Figure 4.6.

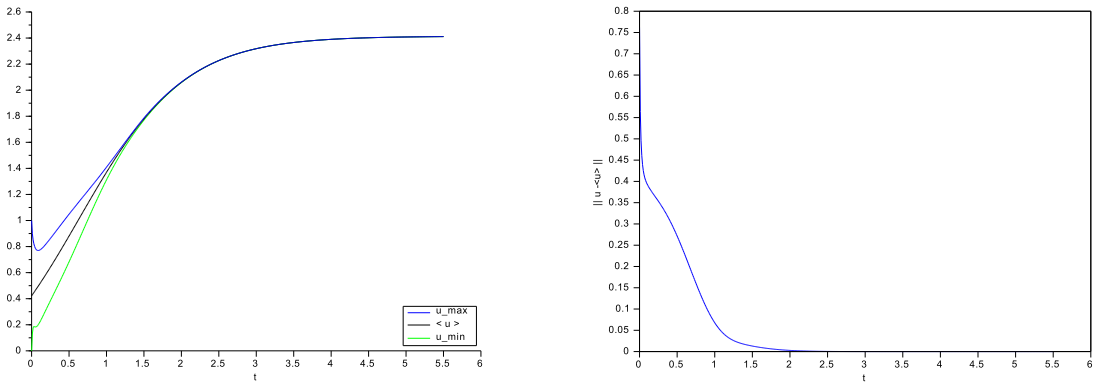

(a) (b)

FIGURE 4.1 – $u_0 \in [1 - \sqrt{2}, 1 + \sqrt{2}]$ and $\langle u_0 \rangle = 0.422$; the solution tends to $1 + \sqrt{2}$.

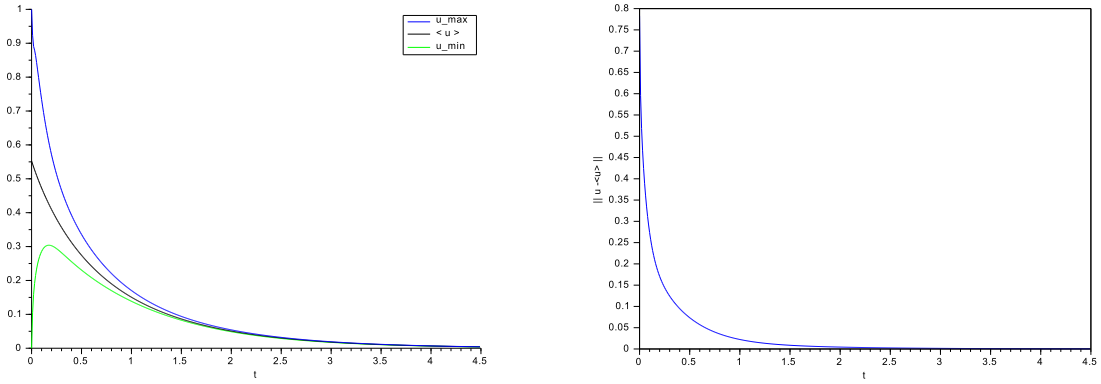

(a) (b)

FIGURE 4.2 – $u_0 \geq 0$ and $\langle u_0 \rangle = 0.552$; the solution tends to 0.

Third case : $\Theta < 0$.

Figure 4.7 corresponds to the case $4\alpha\gamma - \beta^2 > 0$; more precisely, $g(s) = \frac{1}{2}s^2 - s + 1$. The solution blows up in finite time, in agreement with the theoretical results. Here, $u_0 = \frac{8\cos(x-y)}{x^6+1}$, leading to $\langle u_0 \rangle = 1.481$.

4.4.2 The case when $g(s) = 2\beta s - \beta s^2(s-1)^2$.

First case : $\beta > 0$.

In Figure 4.8, we take $g(s) = 0.03s - 0.015s^2(s-1)^2$. Here, $u_0 = 2 + \frac{1}{2(x^6+0.1)} > 2$ and $\langle u_0 \rangle = 2.476$. The solution blows up in finite time and $\|u - \langle u \rangle\|$ tends to 0, in agreement with the theoretical results.

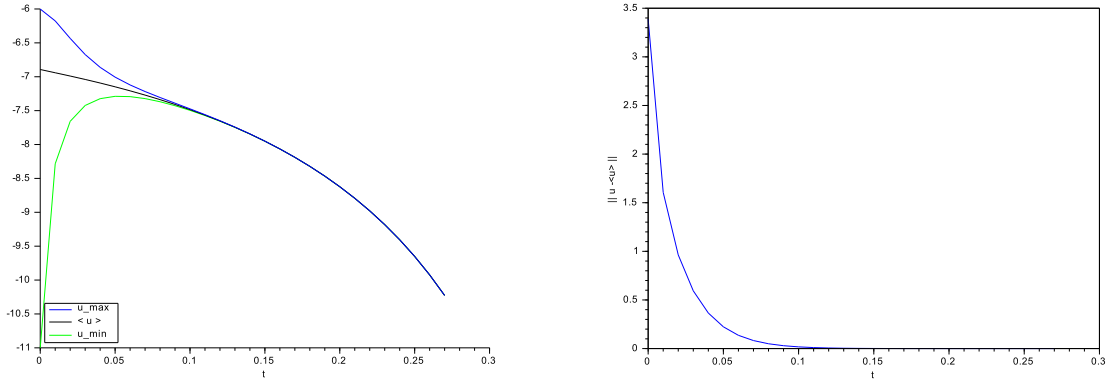

(a) (b)

FIGURE 4.3 – $\langle u_0 \rangle = -0.250 < 1 - \frac{\sqrt{2}}{2}$; the solution blows up, while $\|u - \langle u \rangle\|$ tends to 0.

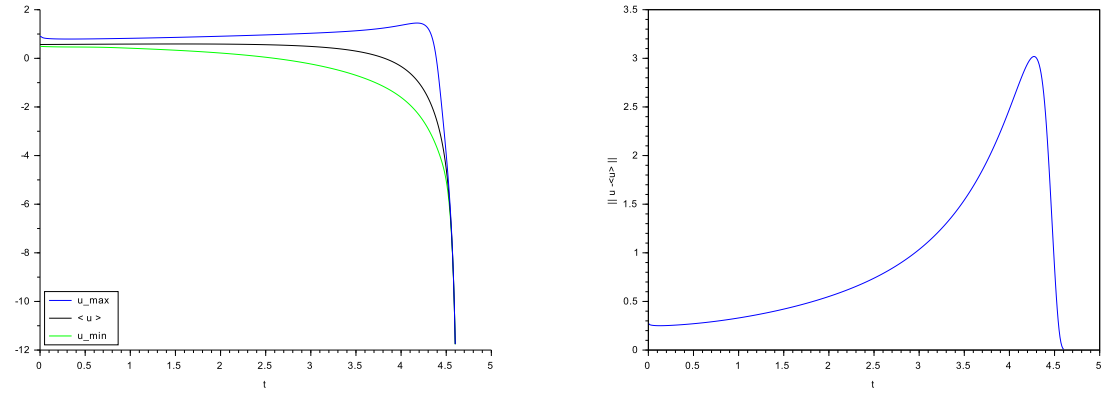

(a) (b)

FIGURE 4.4 – $\langle u_0 \rangle = 0.569$; the solution blows up, while $\|u - \langle u \rangle\|$ tends to 0.

Figure 4.9 corresponds to the function $g(s) = 2s - s^2(s-1)^2$ and to the initial datum $u_0 = -\frac{0.1\cos(x-y)}{x^6+1} + 2 \in [0,2]$, leading to $\langle u_0 \rangle = 1.981$. The solution remains between $[0,2]$ and converges to $\bar{u} = 0$, which confirms the theoretical results.

In Figure 4.10, we take $g(s) = 0.6s - 0.3s^2(s-1)^2$ and the solution remains smaller than 0 and converges to $\bar{u} = 0$, which comfirms the theoretical results. Here, $u_0 = -1 - \cos^2(x+y)$, leading to $u_0 < 0$ and $\langle u_0 \rangle = -1.422 < 0$.

Second case : $\beta < 0$.

In Figure 4.11, we take $u_0 = -\frac{4\cos(x-y)}{(x^6+1)}$, leading to $\langle u_0 \rangle = -0.740$, and $g(s) = -0.04s + 0.02s^2(s-1)^2$. In that case, the solution blows up in finite time, while $\|u - < u > \|$ approaches 0.

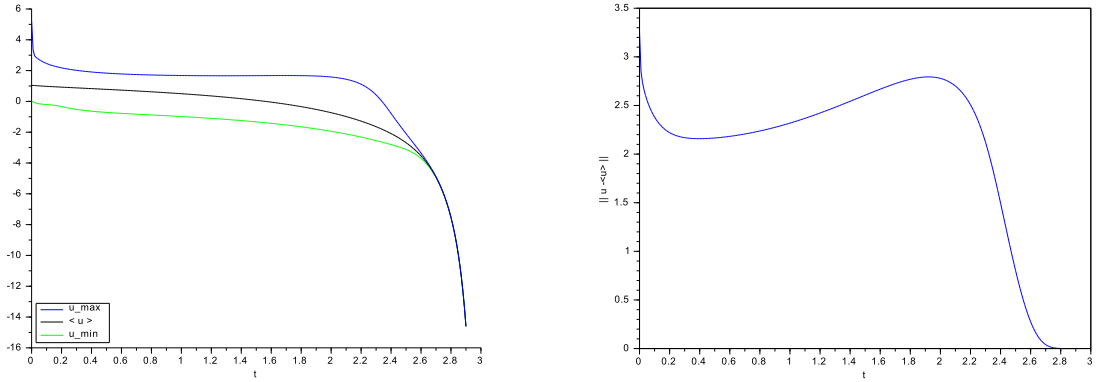

(a) (b)

FIGURE 4.5 – $\langle u_0 \rangle = 1.043 > 1$; the solution blows up, while $\|u - \langle u \rangle\|$ tends to 0.

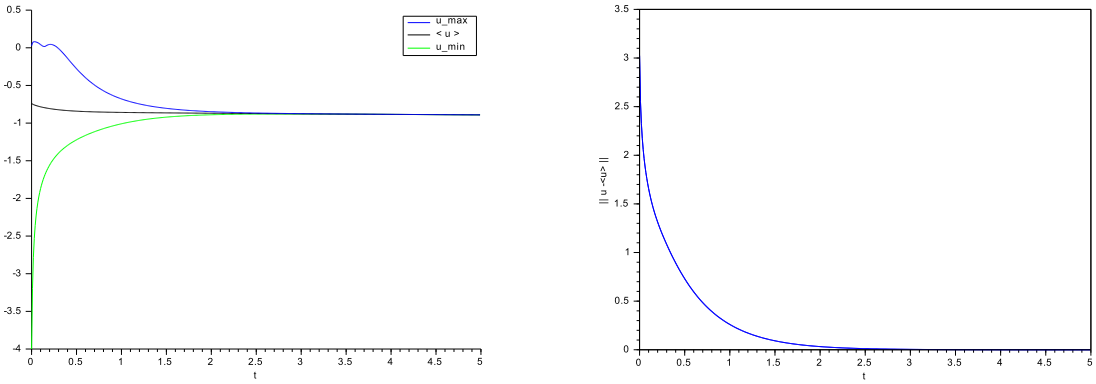

(a) (b)

FIGURE 4.6 – $\langle u_0 \rangle = -0.740$; the solution tends to -1.

Remark 4.4.1. *We come back to the proliferation term considered in subsection 4.4.1. We assume that* $\Theta > 0$. *We saw in Remark 4.2.10 that* $\langle u \rangle$ *can become smaller than* $\frac{-\beta - \sqrt{\Theta}}{2\alpha}$, *for* $t > 0$, *and blow up in finite time (note that the partial answer given in Remark 4.2.10 is independent of the choice of potential* f*). An interesting question is whether the solutions* u *can blow up in finite time even if the initial datum* $u_0 \in \left[\frac{-\beta - \sqrt{\Theta}}{2\alpha}, \frac{-\beta + \sqrt{\Theta}}{2\alpha}\right]$ *and the potential* f *has zeros in this interval, e.g.,*

$$f(s) = \Big(s - \frac{-\beta - \sqrt{\Theta}}{2\alpha}\Big)\Big(s + \frac{\beta}{2\alpha}\Big)\Big(s - \frac{-\beta + \sqrt{\Theta}}{2\alpha}\Big).$$

We give a partial answer via numerical simulations which seem to indicate that there is no blow up. We saw in Figure 4.4 that the solution u *blows up in finite time, even if* u_0 *is chosen between the zeros of* g. *We take* $g(s) = s^2 - \frac{3}{2}s + \frac{1}{2}$, *with zeros* $\frac{1}{2}$ *and* 1, *and* $f(s) = (s - \frac{1}{2})^3 - (s - \frac{1}{2})$ *with three zeros* $-\frac{1}{2}$, $\frac{1}{2}$, *and* $\frac{3}{2}$. *Furthermore,* $u_0 = \frac{1}{5(x^6+1)(y^5+\frac{1}{2})} + \frac{1}{2} \in [\frac{1}{2}, 1]$, *leading to* $\langle u_0 \rangle = 0.569$. *We*

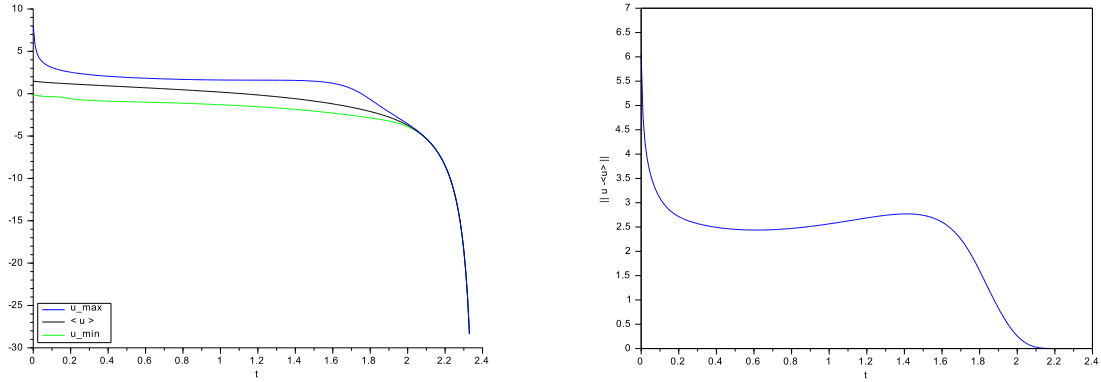

(a) (b)

FIGURE 4.7 – $\langle u_0 \rangle = 1.481$; the solution blows up, while $\|u - \langle u \rangle\|$ tends to 0.

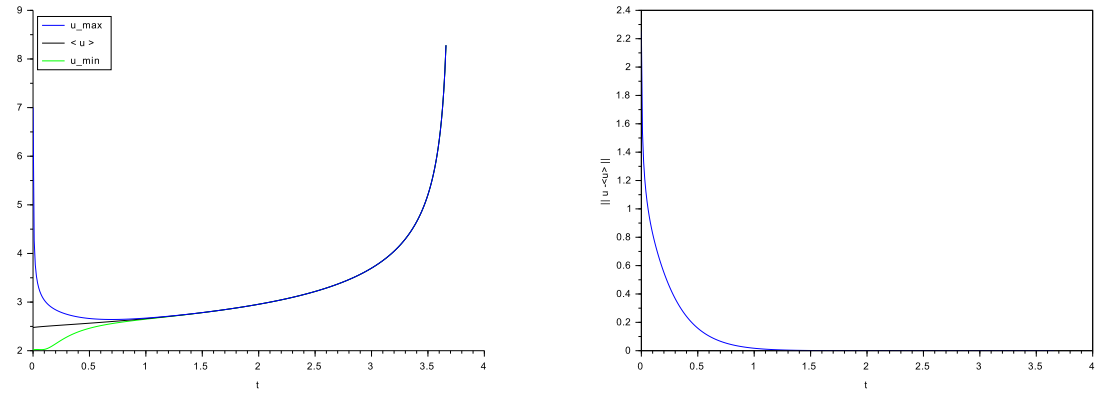

(a) (b)

FIGURE 4.8 – $u_0 > 2$; the solution blows up, while $\|u - \langle u \rangle\|$ tends to 0.

run again the modified Cahn-Hilliard equation (4.118)–(4.121) with the same initial datum as in Figure 4.4 and the same function g, but we now take $f(s) = (s - \frac{1}{2})(s - \frac{3}{4})(s - 1)$. *The solution u remains in* $[\frac{1}{2}, 1]$ *(no blow up) and converges to* 1 *as shown in Figure 4.12.*

Remark 4.4.2. *We come back to the proliferation term considered* (4.11). *We give real tumor growth results as in [5]. We rewrite the problem in the form*

$$\frac{\partial u}{\partial t} + \Delta \mu + \frac{1}{\varepsilon} g(u) = 0 \quad in\ \Omega, \tag{4.122}$$

$$\mu = \varepsilon \Delta u - \frac{1}{\varepsilon} f(u) \quad in\ \Omega, \tag{4.123}$$

$$\frac{\partial u}{\partial \nu} = \frac{\partial \mu}{\partial \nu} = 0 \quad on\ \Gamma, \tag{4.124}$$

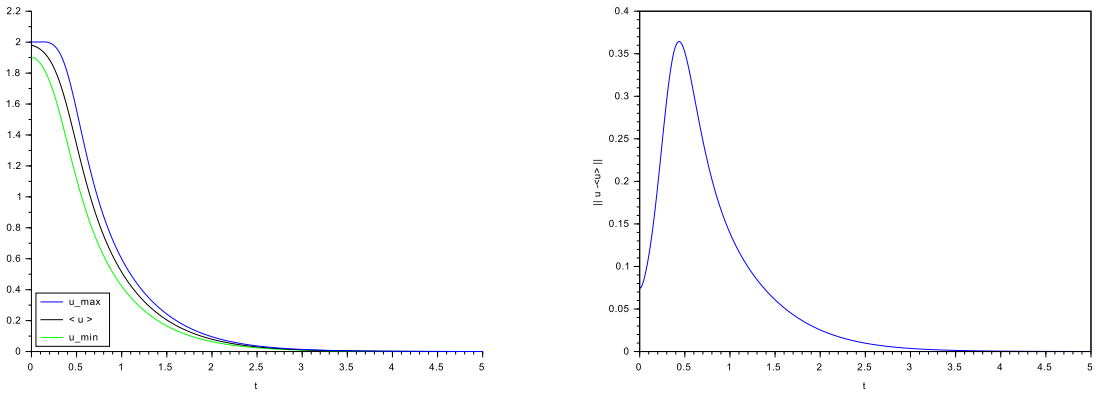

(a) (b)

FIGURE 4.9 – $u_0 \in [0, 2]$; the solution tends to 0.

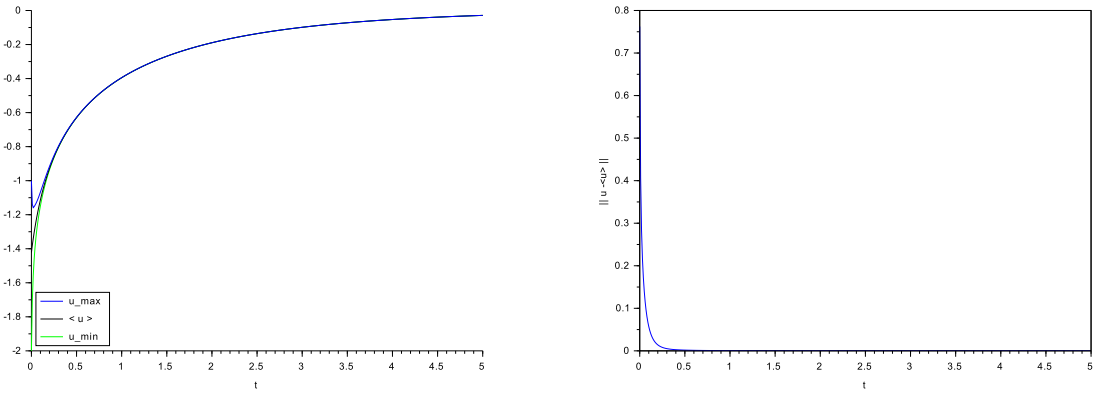

(a) (b)

FIGURE 4.10 – $u_0 < 0$; the solution tends to 0.

$$u_{|t=0} = u_0, \tag{4.125}$$

where Ω *is a circle of radius* 1.2 *centered at* $(0.5, -0.5)$ *and the triangulation is obtained by dividing* Ω *into* 15676 *triangles. The time step is taken as* $\delta t = 10^{-5}$ *and the diffuse interface thickness* $\varepsilon = 0.0125$*. We take* $f(s) = s^3 - s$*. Here,*

$$u_0 = -\tanh\Big(\frac{1}{\sqrt{2}\varepsilon}\sqrt{2(x-0.5)^2 + \frac{1}{4}(y+0.5)^2} - 0.1\Big) \in [-1, 1],$$

leading to $\langle u_0 \rangle = -0.225$*. Furthermore,* $g(s) = 46(u+1) - 280(u-1)^2(u+1)^2$ *and the variation of the solution* u *is shown in Figure 4.13. We note that, without mesh adaptation strategy, it seems too heavy in calculation time to reach a steady state in this example.*

Acknowledgments : I would like to thank L. Cherfils and A. Miranville, my supervisors, for many stimulating discussions and useful comments on the subject of the paper.

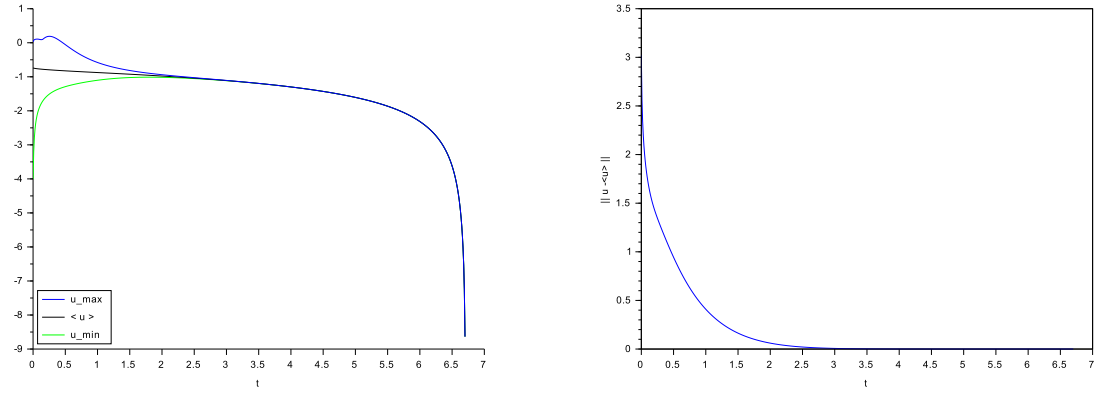

(a) (b)

FIGURE 4.11 – $\langle u_0 \rangle = -0.740$; the solution blows up, while $\|u - \langle u \rangle\|$ tends to 0.

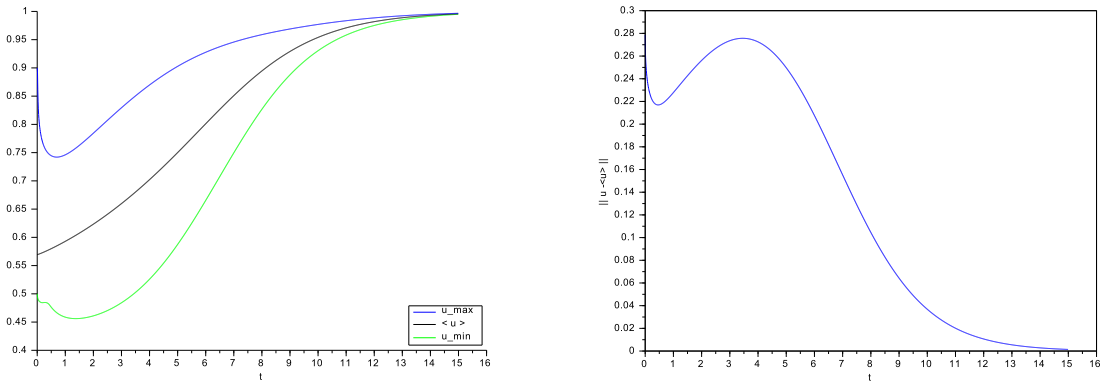

(a) (b)

FIGURE 4.12 – $\langle u_0 \rangle = 0.569$; the solution tends to 1.

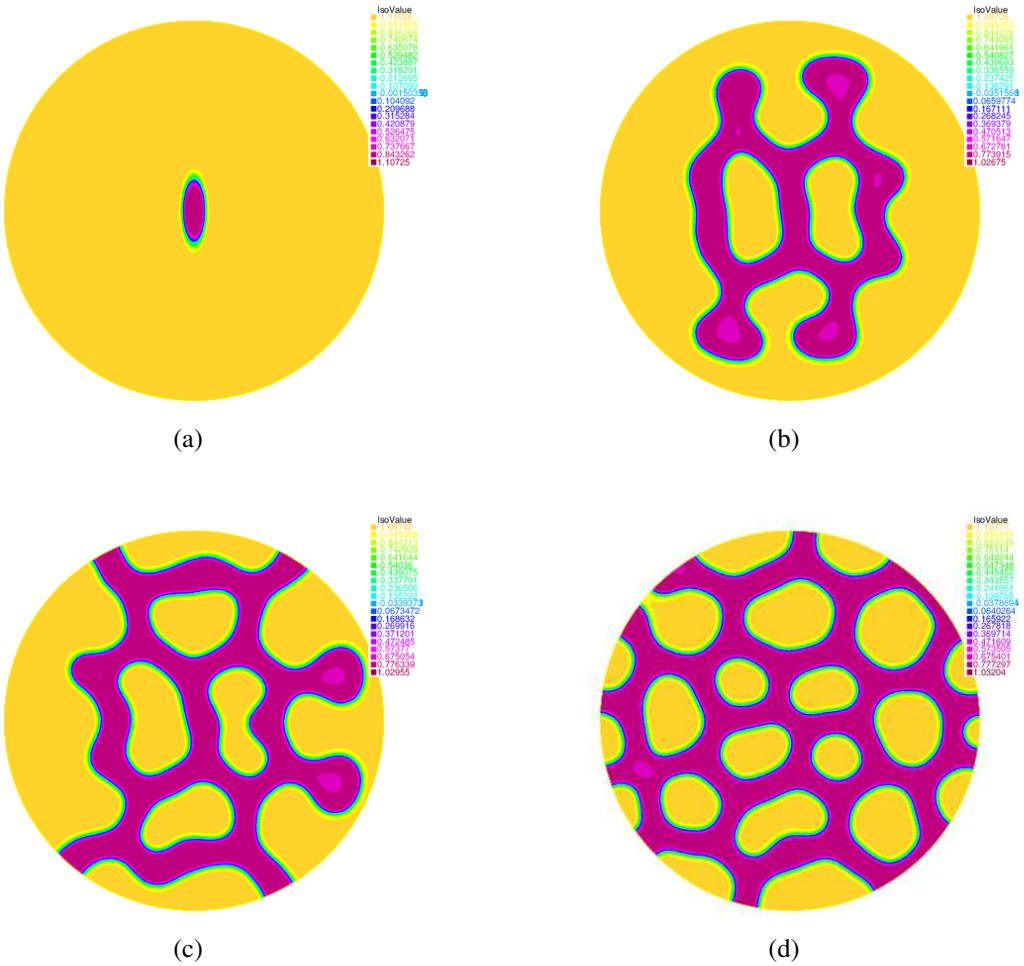

(a) (b)

(c) (d)

FIGURE 4.13 – (a) Initial datum at $t = 0$. (b) Solution after 2300 iterations. (c) Solution after 3500 iterations. (d) Solution after 4500 iterations.

Chapitre 5

Asymptotic behavior of a generalized Cahn–Hilliard equation with a mass source

Comportement asymptotique d'une généralisation de Cahn–Hilliard avec un terme source

Ce chapitre est constitué de l'article **Asymptotic behavior of a generalized Cahn–Hilliard equation with a mass source**, Applicable Analysis, à paraître.

Asymptotic behavior of a generalized Cahn–Hilliard equation with a mass source

HUSSEIN FAKIH

Université de Poitiers, Laboratoire de Mathématiques et Applications
UMR CNRS 7348 - SP2MI
Boulevard Marie et Pierre Curie - Téléport 2
F-86962 Chasseneuil Futuroscope Cedex, France
E-mail address : Hussein.Fakih@math.univ-poitiers.fr

Abstract : We consider in this article a generalized Cahn–Hilliard equation with mass source (nonlinear reaction term) which has applications in biology. We are intersted in the well-posedness and the study of the asymptotic behavior of the solutions (and, more precisely, the existence of finite-dimensional attractors). We first consider the usual Dirichlet boundary conditions and then Neumann boundary conditions. The latter require additional assymptions on the mass source term to obtain the dissipativity. Indeed, otherwise, the order parameter u can blow up in finite time. We also give numerical simulations which confirm the theoretical results.

Keywords : Cahn–Hilliard equation, mass source, tumor growth, well-posedness, global attractor, exponential attractor, simulations.
AMS Subject Classification : 35K55 ; 35B40 ; 35J60

5.1 Introduction

The Cahn–Hilliard equation,

$$\frac{\partial u}{\partial t} + \Delta^2 u - \Delta f(u) = 0, \tag{5.1}$$

plays an essential role in materials science as it describes the phase separation of binary systems in physics and chemistry (see [27] and [119]).

When a binary solution is cooled down sufficiently, phase separation may occur and then proceed in two ways : either by nucleation in which case nuclei of the second phase appear randomly and grow, or the whole solution appears to nucleate at once and then periodic or semiperiodic structures appear in the so-called spinodal decomposition. The pattern formation resulting from phase separation has been observed in alloys, glasses, and polymer solutions.

Here f is the derivative of a double-well potential F whose wells correspond to the phases of the material. A thermodynamically relevant potential F is the following logarithmic function which follows from a mean-field model :

$$F(s) = \frac{\theta_c}{2}(1-s^2) + \frac{\theta}{2}\Big[(1-s)\ln\Big(\frac{1-s}{2}\Big) + (1+s)\ln\Big(\frac{1+s}{2}\Big)\Big]$$
$$s \in]-1,1[, \quad 0 < \theta < \theta_c,$$

i.e.

$$f(s) = -\theta_c s + \frac{\theta}{2} \ln \frac{1+s}{1-s},$$

although such a function is very often approximated by regular ones,

$$F(s) = \sum_{k=0}^{2p} a_k s^k, \quad a_{2p} > 0, \ p \in \mathbb{N}, \ p \geq 2,$$

i.e.

$$f(s) = \sum_{i=0}^{2p-1} (i+1) a_{i+1} s^i, \quad a_{2p} > 0.$$

It is interesting to note that the Cahn–Hilliard equation is also relevant in other phenomena such as population dynamics [45], bacterial films [91], thin films [123, 138], image processing [29, 51] and even the rings of Saturn [139].

Equation (1) is usually endowed with Neumann boundary conditions,

$$\frac{\partial u}{\partial \nu} = \frac{\partial \Delta u}{\partial \nu} = 0 \qquad \text{on } \partial\Omega.$$

In particular, this yields the conservation of mass, i.e. of the spatial average of the order parameter u. Then, we can prove the existence of finite-dimensional global attractors (see, e.g., [119], [113], [47], [114], and [143]).

We are interested in this article in the following generalization of the Cahn–Hilliard equation :

$$\frac{\partial u}{\partial t} + \Delta^2 u - \Delta f(u) + g(x,u) = 0, \tag{5.2}$$

where g is the mass source term. This equation (5.2) can be as used as a model for the growth of cancerous tumors and other biological entities.

Here, g can be a linear function, $g(x,s) = \alpha s$, $\alpha > 0$, in which case (5.2) is known as the Cahn–Hilliard–Oono equation and accounts for long-ranged (nonlocal) interactions in the phase separation process (see [122, 143] ; see also [103] for the study of the limit dynamics as α goes to zero). A second possibility is the quadratic function $g(x,s) = \alpha s(s-1)$, $\alpha > 0$; in that case, has applications in biology [42, 104] and, more precisely, models wound healing and tumor growth [88]. A third possibility, with applications in biology and more specifically in tumor growth [5], is the function $g(x,s) = \frac{\alpha}{2}(s+1) - \beta(1-s)^2(1+s)^2 + s(x,t)$, where α and β are the death and growth coefficients, respectively. A fourth possibility is the function $g(x,u) = 1_{\Omega \setminus D}(x)u$ (where $D \subset\subset \Omega$). In that case (5.2) has application in image inpainting (see [16, 17, 25, 38] ; see also [20, 39], where singular nonlinear terms are considered).

Our aim in this article is to discuss the Cahn-Hilliard equation with mass source. First, we consider the equation endowed with Neumann boundary conditions and study the asymptotic behavior of the problem. In that case, we take $g(x,s) = \sum_{j=0}^{2q-1} b_j s^j$, $b_{2q-1} > 0$. The odd degree of g allows to obtain the dissipativity of the order parameter u. In the case when g has even degree, e.g., $g(s) = \alpha s(s-1)$, $\alpha > 0$, the solution can blow up in finite time (see, e.g., [42]). Furthermore, we consider the equation endowed with Dirichlet boundary conditions. Here, the assumptions on the mass source g are more general and we do not have blow up in finite time.

We denote by $\|.\|$ the usual L^2-norm (with associated scalar product $((.,.)))$ and set $\|.\|_{-1} = \|(-\Delta)^{-\frac{1}{2}}.\|$, where $(-\Delta)^{-1}$ denotes in section 5.2 the inverse minus Laplace operator associated with Neumann boundary conditions and acting on functions with null spatial average and in section 5.3 the one associated with Dirichlet boundary conditions. More generally, $\|.\|_X$ denotes the norm in the Banach space X.

Throughout this paper, the same letter c (and, sometimes, c' and c'') denotes constants which may vary from line to line, or even in a same line. Similarly, the same letter Q denotes monotone increasing (with respect to each argument) functions which may vary from line to line, or even in a same line.

5.2 Neumann boundary conditions

In this part, we consider the following initial and boundary value problem :

$$\frac{\partial u}{\partial t} + \Delta^2 u - \Delta f(u) + g(u) = 0, \tag{5.3}$$

$$\frac{\partial u}{\partial \nu} = \frac{\partial \Delta u}{\partial \nu} = 0 \qquad \text{on } \Gamma, \tag{5.4}$$

$$u|_{t=0} = u_0, \tag{5.5}$$

in a bounded and regular domain $\Omega \subset \mathbb{R}^n$, $n = 1,\ 2,$ or 3, with boundary Γ.

As mentioned in the introduction, we may not have global existence for problem (5.3)–(5.5) with a function g having an even degree (see, e.g., [88, 42]). Consequently, we define g in this section as follows :

$$g : \mathbb{R} \to \mathbb{R}, \qquad s \to g(s) = \sum_{j=0}^{2q-1} b_j s^j, \quad b_{2q-1} > 0,\ q \geq 1.$$

As far as the nonlinear terms f is considered, we assume that f is defined as follows :

$$f(s) = \sum_{i=0}^{2p-1} c_i s^i, \quad c_{2p-1} > 0.$$

Since b_{2q-1} and c_{2p-1} are strictly positive constants, it is easy to conclude that there exist constants ξ_1, ξ_2, ξ_3, and ξ_4 such that

$$\frac{c_{2p-1}}{2p-2} s^{2p-2} - \xi_1 \leq f'(s) \leq \frac{3c_{2p-1}}{2p-2} s^{2p-2} + \xi_1, \quad \forall s \in \mathbb{R}, \tag{5.6}$$

$$\frac{b_{2q-1}}{2} s^{2q} - \xi_2 \leq g(s)s \leq \frac{3b_{2q-1}}{2} s^{2q} + \xi_2, \quad \forall s \in \mathbb{R}, \tag{5.7}$$

$$|g(s)| \leq 2q\varepsilon b_{2q-1} s^{2q} + \xi_3(\varepsilon), \quad \forall s \in \mathbb{R},\ \forall \varepsilon > 0, \tag{5.8}$$

$$g'(s) \leq \frac{3b_{2p-1}}{2q} s^{2q-2} + \xi_4, \quad \forall s \in \mathbb{R}. \tag{5.9}$$

We introduce the following spaces :

$$H = L^2(\Omega), \quad V = H^1(\Omega),$$

and

$$W = \left\{ v \in H^2(\Omega), \ \frac{\partial v}{\partial \nu} = 0 \text{ on } \Gamma \right\}.$$

We denote by $\langle \phi \rangle$ the spatial average of a function ϕ in $L^1(\Omega)$,

$$\langle \phi \rangle = \frac{1}{Vol(\Omega)} \int_\Omega \phi(x) dx.$$

We also introduce the following spaces :

$$\dot{H}^{-1}(\Omega) = \{ \phi \in H^{-1}(\Omega), \ \langle \phi, 1 \rangle_{H^{-1}(\Omega), H^1(\Omega)} = 0 \},$$

$$\dot{H} = \{ \phi \in H, \ \langle \phi \rangle = 0 \},$$

$$\dot{V} = \{ \phi \in V, \ \langle \phi \rangle = 0 \},$$

and

$$\dot{W} = \{ \phi \in W, \ \langle \phi \rangle = 0 \}.$$

Let

$$A = -\Delta : D(A) \subset \dot{H} \to \dot{H}$$

with $D(A) = \dot{W}$. The operator A is a strictly positive self-adjoint linear operator with compact inverse A^{-1}.

Integrating (5.3) over Ω, we obtain

$$\frac{d\langle u \rangle}{dt} + \langle g(u) \rangle = 0. \tag{5.10}$$

We set

$$v = u - \langle u \rangle.$$

We can rewrite (5.3) in the form

$$\frac{\partial v}{\partial t} + A^2 u + A f(u) + g(u) - \langle g(u) \rangle = 0. \tag{5.11}$$

Finally, we can reformulate the problem as follows :

$$A^{-1} \frac{\partial v}{\partial t} + Av + f(v + \langle u \rangle) - \langle f(u) \rangle + A^{-1}(g(u) - \langle g(u) \rangle) = 0, \tag{5.12}$$

$$\frac{\partial v}{\partial \nu} = 0 \qquad \text{on } \Gamma, \tag{5.13}$$

$$v|_{t=0} = v_0. \tag{5.14}$$

We note that

$$\left(\|A^{-\frac{1}{2}}(\varphi - \langle \varphi \rangle)\|^2 + \langle \varphi \rangle^2 \right)^{\frac{1}{2}},$$

$$\left(\|\varphi - \langle\varphi\rangle\|^2 + \langle\varphi\rangle^2\right)^{\frac{1}{2}},$$

$$\left(\|A^{\frac{1}{2}}\varphi\|^2 + \langle\varphi\rangle^2\right)^{\frac{1}{2}},$$

and

$$\left(\|A\varphi\|^2 + \langle\varphi\rangle^2\right)^{\frac{1}{2}},$$

are norms in $H^{-1}(\Omega)$, $L^2(\Omega)$, $H^1(\Omega)$, and $H^2(\Omega)$, respectively, which are equivalent to the usual ones.

5.2.1 A priori estimates

We multiply (5.10) by $\langle u\rangle$ to have

$$\frac{1}{2}\frac{d}{dt}\langle u\rangle^2 + \langle g(u)\rangle\langle u\rangle = 0, \tag{5.15}$$

hence

$$\frac{1}{2}\frac{d}{dt}\langle u\rangle^2 \le |\langle g(u)\rangle|\|\langle u\rangle|.$$

It thus follows from (5.8) and Hölder's inequality that

$$\frac{1}{2}\frac{d}{dt}\langle u\rangle^2 \le c\|u\|(\varepsilon\|u\|^{2q}_{L^{2q}(\Omega)} + c(\varepsilon)), \tag{5.16}$$

which yields

$$\frac{d}{dt}\langle u\rangle^2 \le \varepsilon\|u\|^{4q}_{L^{2q}(\Omega)} + c. \tag{5.17}$$

We multiply (5.3) by u and have

$$\frac{1}{2}\frac{d}{dt}\|u\|^2 + \|Au\|^2 + ((f'(u)A^{\frac{1}{2}}u, A^{\frac{1}{2}}u)) + ((g(u), u)) = 0. \tag{5.18}$$

Using the facts that

$$((f'(u)A^{\frac{1}{2}}u, A^{\frac{1}{2}}u)) \ge -\xi_1\|A^{\frac{1}{2}}u\|^2$$

and

$$((g(u), u)) \ge \frac{b_{2q-1}}{2}\|u\|^{2q}_{L^{2q}(\Omega)} - \xi_2 Vol(\Omega),$$

we find

$$\frac{1}{2}\frac{d}{dt}\|u\|^2 + \|Au\|^2 + \langle u\rangle^2 + \frac{b_{2q-1}}{2}\|u\|^{2q}_{L^{2q}(\Omega)} \le c(\|A^{\frac{1}{2}}u\|^2 + \langle u\rangle^2) + \xi_2 Vol(\Omega). \tag{5.19}$$

It thus follows from (5.19) and the interpolation inequality $\|u\|^2_{H^1(\Omega)} \le c\|u\|\|u\|_{H^2(\Omega)}$ that

$$\frac{d}{dt}\|u\|^2 + \|u\|^2_{H^2(\Omega)} + \frac{b_{2q-1}}{2}\|u\|^{2q}_{L^{2q}(\Omega)} \le c, \qquad \forall q > 1. \tag{5.20}$$

Noting that, for $q = 1$, we can proceed as in [38] to obtain

$$\frac{d}{dt}(\|v\|_{-1}^2 + \delta\|v\|^2) + c\Big(\|Au\|^2 + \int_\Omega (v^4 + v^2\langle u\rangle^2)dx\Big) \le c', \quad \forall t \ge 0,\ q = 1, \tag{5.21}$$

where $\delta > 0$ is small enough, and

$$|\langle u\rangle| \le Q(\|v\| + |\langle u_0\rangle|)e^{-ct} + c', \quad c > 0, \quad \forall t \ge 0,\ q = 1, \tag{5.22}$$

we finally deduce from (5.20), (5.21), (5.22) and Gronwall's lemma that

$$\|u(t)\|^2 \le Q(\|u_0\|)e^{-ct} + c', \quad c > 0, \quad \forall t \ge 0,\ \forall q \ge 1. \tag{5.23}$$

We multiply (5.3) by A^2u and have

$$\frac{1}{2}\frac{d}{dt}\|Au\|^2 + \|A^2u\|^2 + ((Af(u), A^2u)) + ((g(u), A^2u)) = 0. \tag{5.24}$$

We note that, since $H^2(\Omega)$ is continuously embedded in $C(\overline{\Omega})$,

$$\begin{aligned} |((g(u), A^2u))| &\le \|g(u)\|\|A^2u\| \\ &\le c\|g(u)\|^2 + \frac{1}{4}\|A^2u\|^2 \\ &\le Q(\|u\|_{H^2(\Omega)}) + \frac{1}{4}\|A^2u\|^2 \end{aligned}$$

and, owing to the continuous embedding $H^1(\Omega)$ in $L^4(\Omega)$, we have

$$\begin{aligned} ((Af(u), A^2u)) &\le c\|Af(u)\|^2 + \frac{1}{4}\|A^2u\|^2 \\ &\le \|f''(u)|A^{\frac{1}{2}}u|^2 + f'(u)Au\|^2 + \frac{1}{4}\|A^2u\|^2 \\ &\le \|f''(u)\|_{L^\infty(\Omega)}^2\|A^{\frac{1}{2}}u\|_{L^4(\Omega)}^4 + \|f'(u)\|_{L^\infty(\Omega)}^2\|Au\|^2 + \frac{1}{4}\|A^2u\|^2 \\ &\le \|f''(u)\|_{L^\infty(\Omega)}^2\|u\|_{H^2(\Omega)}^4 + \|f'(u)\|_{L^\infty(\Omega)}^2\|Au\|^2 + \frac{1}{4}\|A^2u\|^2 \\ &\le Q(\|u\|_{H^2(\Omega)}) + \frac{1}{4}\|A^2u\|^2. \end{aligned}$$

Thus, we infer

$$\frac{d}{dt}\|Au\|^2 + \|A^2u\|^2 \le Q(\|u\|_{H^2(\Omega)}), \tag{5.25}$$

so that

$$\frac{d}{dt}\|Au\|^2 \le Q(\|u\|_{H^2(\Omega)}^2). \tag{5.26}$$

Summing (5.26) and (5.17), we find

$$\frac{d}{dt}\|u\|_{H^2(\Omega)}^2 \le Q(\|u\|_{H^2(\Omega)}^2). \tag{5.27}$$

In particular, setting

$$y = \|u\|^2_{H^2(\Omega)}, \tag{5.28}$$

we deduce from (5.27) an inequation of the form

$$y' \leq Q(y). \tag{5.29}$$

Let z be the solution to the ordinary differential equation

$$z' = Q(z), \qquad z(0) = y(0). \tag{5.30}$$

It follows from the comparison principle that there exists $T_0 = T_0(\|u_0\|_{H^2(\Omega)})$ belonging to, say, $(0, \frac{1}{2})$ such that

$$y(t) \leq z(t), \quad \forall t \in [0, T_0], \tag{5.31}$$

hence

$$\|u(t)\|_{H^2(\Omega)} \leq Q(\|u_0\|_{H^2(\Omega)}), \quad t \leq T_0. \tag{5.32}$$

Now, multiplying (5.12) by $A\frac{\partial v}{\partial t}$, we have, for $t \leq T_0$,

$$\frac{1}{2}\frac{d}{dt}\|Av\|^2 + \left\|\frac{\partial v}{\partial t}\right\|^2 + \left(\left(Af(u), \frac{\partial v}{\partial t}\right)\right) + \left(\left(g(u), \frac{\partial v}{\partial t}\right)\right) = 0. \tag{5.33}$$

Here,

$$\begin{aligned}
\left|\left(\left(g(u), \frac{\partial v}{\partial t}\right)\right)\right| &\leq \|g(u)\|\left\|\frac{\partial v}{\partial t}\right\| \\
&\leq c\|g(u)\|^2 + \frac{1}{4}\left\|\frac{\partial v}{\partial t}\right\|^2 \\
&\leq \text{(thanks to (5.32) and the continuous embedding } H^2(\Omega) \subset C(\overline{\Omega})) \\
&\leq \frac{1}{4}\left\|\frac{\partial v}{\partial t}\right\|^2 + Q(\|u_0\|_{H^2(\Omega)}).
\end{aligned}$$

Similarly,

$$\begin{aligned}
\left|\left(\left(Af(u), \frac{\partial v}{\partial t}\right)\right)\right| &\leq \|A(f(u))\|\left\|\frac{\partial v}{\partial t}\right\| \\
&\leq \frac{1}{4}\left\|\frac{\partial v}{\partial t}\right\|^2 + Q(\|u_0\|_{H^2(\Omega)})
\end{aligned}$$

and, owing to the estimates obtained above, (5.33) yields

$$\frac{d}{dt}\|Av\|^2 + \left\|\frac{\partial v}{\partial t}\right\|^2 \leq Q(\|u_0\|_{H^2(\Omega)}), \quad \forall t \leq T_0. \tag{5.34}$$

Therefore, integrating (5.34) over $(0, T_0)$ and owing to (5.32), we obtain

$$\int_0^{T_0} \left\|\frac{\partial v}{\partial t}\right\|^2 dx \leq Q(\|u_0\|_{H^2(\Omega)}) \tag{5.35}$$

and, also owing to (5.32), we further have

$$\begin{aligned}\left|\left\langle\frac{\partial u}{\partial t}\right\rangle\right| &\le |\langle g(u)\rangle| \\ &\le Q(\|u_0\|_{H^2(\Omega)}).\end{aligned} \tag{5.36}$$

Differentiating (5.3) with respect to time, we rewrite the resulting equation as

$$\frac{\partial \vartheta}{\partial t} + A^2\vartheta + A(f'(u)\vartheta) + g'(u)\vartheta = 0, \tag{5.37}$$

where $\vartheta = \frac{\partial u}{\partial t}$.

We multiply (5.37) by $t\vartheta$ and have, for $t \le T_0$,

$$\frac{1}{2}\frac{d}{dt}(t\|\vartheta\|^2) + t\|A\vartheta\|^2 + t((A(f'(u)\vartheta),\vartheta)) + t((g'(u)\vartheta,\vartheta)) = \frac{1}{2}\|\vartheta\|^2. \tag{5.38}$$

Observe now that

$$\begin{aligned}\left|((g'(u)\vartheta,\vartheta))\right| &\le \|g'(u)\|\|\vartheta\|\|\vartheta\|_{L^\infty(\Omega)} \\ &\le Q(\|u_0\|_{H^2})\|\vartheta\|\|\vartheta\|_{H^2}\end{aligned}$$

and

$$\begin{aligned}&\left|((A(f'(u)\vartheta),\vartheta))\right| \\ &\quad\le \|A(f'(u)\vartheta)\|\|\vartheta\| \\ &\quad\le \|f''(u)Au\vartheta + f'''(u)|A^{\frac{1}{2}}u|^2\vartheta + 2f''(u)A^{\frac{1}{2}}uA^{\frac{1}{2}}\vartheta + f'(u)A\vartheta\|\|\vartheta\| \\ &\quad\le Q(\|u_0\|_{H^2})\|\vartheta\|\|\vartheta\|_{H^2}.\end{aligned}$$

Therefore, we obtain

$$\frac{d}{dt}(t\|\vartheta\|^2) + t\|\vartheta\|_{H^2}^2 \le tQ(\|u_0\|_{H^2})\|\vartheta\|^2 + \|\vartheta\|^2. \tag{5.39}$$

It thus follows from (5.32), (5.35), (5.36), (5.39), and Gronwall's lemma that

$$\|\vartheta\|^2 \le \frac{1}{t}Q(\|u_0\|_{H^2}), \quad 0 < t \le T_0. \tag{5.40}$$

Note that, integrating (5.20) over $(0,t)$, we have

$$\int_0^t \|u\|_{H^2(\Omega)}^2 \le c\|u_0\|^2 + c't + c''. \tag{5.41}$$

We then multiply (5.37) by ϑ and proceed as above to obtain

$$\frac{d}{dt}(\|\vartheta\|^2) + \|A\vartheta\|^2 \le Q(\|u\|_{H^2})\|\vartheta\|^2. \tag{5.42}$$

By exploiting (5.40) and (5.41), on account of (5.42), and using Gronwall's lemma we infer

$$\|\vartheta\|^2 \le e^{ct}Q(\|u_0\|_{H^2}), \quad c > 0, \ \ t \ge T_0. \tag{5.43}$$

We then rewrite, for $t \geq T_0$ fixed, (5.3) in the form

$$A^2 u + Af(u) + g(u) = -\vartheta, \quad \frac{\partial u}{\partial \nu} = 0 \quad \text{on } \Gamma. \tag{5.44}$$

We multiply (5.44) by u and have

$$\|Au\|^2 + ((f'(u)A^{\frac{1}{2}}u, A^{\frac{1}{2}}u)) + ((g(u), u)) \leq \|\vartheta\|\|u\|. \tag{5.45}$$

Then, owing to (5.6), (5.7), and (5.43), we obtain

$$\|Au\|^2 + \frac{b_{2q-1}}{2}\|u\|^{2q}_{L^{2q}(\Omega)} \leq e^{ct}Q(\|u_0\|_{H^2(\Omega)}) + \|u\|^2 + \xi_1\|A^{\frac{1}{2}}u\|^2, \tag{5.46}$$

which yields, owing to the interpolation inequality $\|A^{\frac{1}{2}}u\|^2 \leq c\|u\|\|u\|_{H^2(\Omega)}$,

$$(\|Au\|^2 + \langle u\rangle^2) + \frac{b_{2q-1}}{2}\|u\|^{2q}_{L^{2q}(\Omega)} \leq e^{ct}Q(\|u_0\|_{H^2(\Omega)}) + c\|u\|^2 + \varepsilon\|u\|^2_{H^2(\Omega)}, \quad \forall \varepsilon > 0. \tag{5.47}$$

This yields

$$(1-\varepsilon)\|u\|^2_{H^2(\Omega)} + c\|u\|^{2q}_{L^{2q}(\Omega)} \leq e^{c't}Q(\|u_0\|_{H^2(\Omega)}), \quad c,\ c' > 0,\ \ \forall \varepsilon > 0. \tag{5.48}$$

Consequently, we find

$$\|u\|^2_{H^2(\Omega)} \leq e^{ct}Q(\|u_0\|_{H^2(\Omega)}) \quad c > 0, \quad t \geq T_0. \tag{5.49}$$

Finally, we deduce from (5.32) and (5.49) that

$$\|u\|^2_{H^2(\Omega)} \leq e^{c't}Q(\|u_0\|_{H^2}) + c'', \quad c > 0, \quad t \geq 0. \tag{5.50}$$

We now deduce from (5.20), (5.21), and (5.22) that

$$\int_0^1 \|u\|^2_{H^2(\Omega)} \leq c\|u_0\|^2 + c', \tag{5.51}$$

so that there exists some $T \in (0,1)$ such that

$$\|u(T)\|^2_{H^2(\Omega)} \leq c\|u_0\|^2 + c'. \tag{5.52}$$

Actually, repeating the above estimates, starting from $t = T$ instead of $t = 0$, we have the smoothing property

$$\|u(1)\|^2_{H^2(\Omega)} \leq c\|u_0\|^2 + c', \quad c \geq 0. \tag{5.53}$$

We note that, owing to (5.20), (5.21), and (5.22) ,

$$\int_t^{t+1} \|u(t)\|^2_{H^2(\Omega)} ds \leq e^{-ct}Q(\|u_0\|^2) + c', \quad c > 0, \ \ t \geq 0, \tag{5.54}$$

hence, for every $t \geq 1$, there exists a time $t_1 \in [t-1, t]$ such that

$$\|u(t_1)\|^2_{H^2(\Omega)} \leq e^{-ct}Q(\|u_0\|^2) + c', \tag{5.55}$$

which yields, for $t_2 \in [0,1]$ such that $t = t_1 + t_2$ and owing to (5.50) and (5.55),

$$\begin{aligned}\|u(t)\|^2_{H^2(\Omega)} = \|u(t_1+t_2)\|^2_{H^2(\Omega)} &\le e^{ct_2} Q(\|u(t_1)\|_{H^2(\Omega)}) + c' \\ &\le c e^{-c't_2} Q(\|u(t_1)\|_{H^2(\Omega)}) + c'' \\ &\le c e^{-c't_2} Q(e^{-c''t} Q'(\|u_0\|^2) + c''') + c'''' \\ &\le e^{-ct} Q(\|u_0\|^2_{H^2(\Omega)}) + c'.\end{aligned}$$

Finally, we deduce that

$$\|u(t)\|_{H^2(\Omega)} \le e^{-ct} Q(\|u_0\|_{H^2(\Omega)}) + c', \quad c > 0, \ \ t \ge 0. \tag{5.56}$$

On account of (5.42) and (5.56), and using Gronwall's lemma, we have

$$\left\|\frac{\partial u}{\partial t}\right\|^2 \le e^{ct} Q(\|u_0\|_{H^2(\Omega)}) + c', \quad c > 0, \ \ t \ge T_0. \tag{5.57}$$

We now rewrite (5.3) in the form

$$A^2 u = \varsigma_u, \quad \frac{\partial u}{\partial \nu} = 0 \ \text{ on } \Gamma, \tag{5.58}$$

where

$$\varsigma_u = -\frac{\partial u}{\partial t} + A f(u) - g(u) \tag{5.59}$$

satisfies, for $t \ge T_0$,

$$\|\varsigma_u\| \le e^{ct} Q(\|u_0\|_{H^2}), \quad c > 0. \tag{5.60}$$

We multiply (5.58) by $A^2 u$ and have

$$\|A^2 u\|^2 \le \|\varsigma_u\| \|A^2 u\|. \tag{5.61}$$

It then follows from (5.17), (5.60), and (5.61) that

$$\|u\|_{H^4(\Omega)} \le e^{ct} Q(\|u_0\|_{H^2}), \quad t \ge T_0. \tag{5.62}$$

We multiply (5.37) by $A\vartheta$ and have, for $t \ge T_0$,

$$\begin{aligned}\frac{1}{2}\frac{d}{dt}\|A^{\frac{1}{2}}\vartheta\|^2 + \|A^{\frac{3}{2}}\vartheta\|^2 \le &\left|((A(f'(u)\vartheta), A\vartheta))\right| \\ &+ \left|((g'(u)\vartheta, A\vartheta))\right|.\end{aligned} \tag{5.63}$$

Here,

$$\left|((g'(u)\vartheta, A\vartheta))\right| \le Q(\|u_0\|_{H^2}) \|\vartheta\| \|A\vartheta\|.$$

Furthermore,

$$\begin{aligned}\left|((A(f'(u)\vartheta), A\vartheta))\right| &= \left|((A^{\frac{1}{2}}(f'(u)\vartheta), A^{\frac{3}{2}}\vartheta))\right| \\ &\le \|A^{\frac{1}{2}}(f'(u)\vartheta)\| \|A^{\frac{3}{2}}\vartheta\|\end{aligned}$$

and, owing to (5.62),

$$\begin{aligned}\|A^{\frac{1}{2}}(f'(u)\vartheta)\| &= \|f''(u)\vartheta A^{\frac{1}{2}}u + f'(u)A^{\frac{1}{2}}\vartheta\| \\ &\le Q(\|u_0\|_{H^2})(\|\vartheta\| + \|A^{\frac{1}{2}}\vartheta\|),\end{aligned}$$

which yields

$$\frac{d}{dt}\|A^{\frac{1}{2}}\vartheta\|^2 + \|A^{\frac{3}{2}}\vartheta\|^2 \le Q(\|u_0\|_{H^2})(\|\vartheta\|^2 + \|A^{\frac{1}{2}}\vartheta\|^2 + \|A\vartheta\|^2). \tag{5.64}$$

We note that, integrating (5.57)over $(t-1, t)$, we have, for $t \ge T_0$,

$$\int_{t-1}^{t} \|A\vartheta\|^2 ds \le Q(\|u_0\|_{H^2}). \tag{5.65}$$

It thus follows from (5.65), (5.64), and the uniform Gronwall's lemma that

$$\left\|A^{\frac{1}{2}}\frac{\partial u}{\partial t}\right\|^2 \le Q(\|u_0\|_{H^2}), \quad \forall t \ge T_0 + 1. \tag{5.66}$$

5.2.2 The dissipative semigroup

We have the

Theorem 4. *We assume that $u_0 \in H^2(\Omega)$. Then, (5.3)–(5.5) possesses a unique solution u such that $u(t) \in H^2(\Omega)$, $\forall t \ge 0$.*

Proof. *The proof of existence is based on (5.56) and, e.g., a standard Galerkin scheme. Let now u_1 and u_2 be two solutions to (5.3)–(5.5) with initial data $u_{0,1}$ and $u_{0,2}$, respectively. We set $u = u_1 - u_2$ and $u_0 = u_{0,1} - u_{0,2}$ and have*

$$\frac{\partial u}{\partial t} + A^2 u + A(f(u_1) - f(u_2)) + g(u_1) - g(u_2) = 0, \tag{5.67}$$

$$\frac{\partial u}{\partial \nu} = \frac{\partial \Delta u}{\partial \nu} = 0 \qquad on\ \Gamma, \tag{5.68}$$

$$u|_{t=0} = u_0. \tag{5.69}$$

Integrating (5.67) over Ω, we obtain

$$\frac{d\langle u\rangle}{dt} + \langle g(u_1) - g(u_2)\rangle = 0, \tag{5.70}$$

hence

$$\frac{\partial v}{\partial t} + A^2 v + A(f(u_1) - f(u_2)) + g(u_1) - g(u_2) - \langle g(u_1) - g(u_2)\rangle = 0, \tag{5.71}$$

which yields

$$\begin{aligned}&A^{-1}\frac{\partial v}{\partial t} + Av + f(u_1) - f(u_2) - \langle f(u_1) - f(u_2)\rangle \\ &+ A^{-1}(g(u_1) - g(u_2) - \langle g(u_1) - g(u_2)\rangle) = 0.\end{aligned} \tag{5.72}$$

We multiply (5.72) by v and have

$$\frac{1}{2}\frac{d}{dt}\|A^{-\frac{1}{2}}v\|^2 + \|A^{\frac{1}{2}}v\|^2 + ((f(u_1)-f(u_2),u)) - ((f(u_1)-f(u_2),\langle u\rangle)) + ((A^{-1}(g(u_1)-g(u_2)-\langle g(u_1)-g(u_2)\rangle),v)) = 0. \tag{5.73}$$

We note that

$$\begin{aligned}
&\Big|((A^{-1}(g(u_1)-g(u_2)-\langle g(u_1)-g(u_2)\rangle),v))\Big| \\
&\quad= \Big|((g(u_1)-g(u_2)-\langle g(u_1)-g(u_2)\rangle,A^{-1}v))\Big| \\
&\quad= \Big|((g(u_1)-g(u_2),A^{-1}v))\Big| \\
&\quad\le \int_\Omega |A^{-1}v||u|\int_0^1 |g'(su_1+(1-s)u_2)|dsdx \\
&\quad\le (\textit{thanks to (5.9) and the continuous embedding } H^2(\Omega)\subset C(\overline{\Omega})) \\
&\quad\le Q(\|u_{0,1}\|_{H^2(\Omega)},\|u_{0,2}\|_{H^2(\Omega)})\|A^{-1}v\|_{L^\infty(\Omega)}\|u\| \\
&\quad\le Q(\|u_{0,1}\|_{H^2(\Omega)},\|u_{0,2}\|_{H^2(\Omega)})(\|v\|^2+\langle u\rangle^2).
\end{aligned}$$

Furthermore, owing to (5.6),

$$((f(u_1)-f(u_2),u)) \ge -\xi_1\|u\|^2 \ge -\xi_1(\|v\|^2+\langle u\rangle^2)$$

and

$$\begin{aligned}
&\Big|((f(u_1)-f(u_2),\langle u\rangle))\Big| \\
&\le |\langle u\rangle|\Big|\int_\Omega u\int_0^1 f'(su_1+(1-s)u_2)dsdx\Big| \\
&\le (\textit{thanks to (5.6) and the continuous embedding } H^2(\Omega)\subset C(\overline{\Omega})) \\
&\le Q(\|u_{0,1}\|_{H^2(\Omega)},\|u_{0,2}\|_{H^2(\Omega)})(\|v\|^2+\langle u\rangle^2),
\end{aligned}$$

which yields

$$\frac{1}{2}\frac{d}{dt}\|A^{-\frac{1}{2}}v\|^2 + \|A^{\frac{1}{2}}v\|^2 \le Q(\|u_{0,1}\|_{H^2(\Omega)},\|u_{0,2}\|_{H^2(\Omega)})(\|v\|^2+\langle u\rangle^2). \tag{5.74}$$

Now multiplying (5.70) *by* $\langle u\rangle$*, we have*

$$\begin{aligned}
\frac{1}{2}\frac{d}{dt}\langle u\rangle^2 &\le |\langle g(u_1)-g(u_2)\rangle||\langle u\rangle| \\
&\le |\langle u\rangle|\int_\Omega |u|\int_0^1 |g'(su_1+(1-s)u_2|dsdx \\
&\le (\textit{thanks to (5.9) and the continuous embedding } H^2(\Omega)\subset L^\infty(\Omega)) \\
&\le Q(\|u_{0,1}\|_{H^2(\Omega)},\|u_{0,2}\|_{H^2(\Omega)})\|u\||\langle u\rangle| \\
&\le Q(\|u_{0,1}\|_{H^2(\Omega)},\|u_{0,2}\|_{H^2(\Omega)})(\|v\|^2+\langle u\rangle^2).
\end{aligned} \tag{5.75}$$

Summing (5.75) and (5.74) and employing the interpolation inequality

$$\|v\|^2 \le \|A^{-\frac{1}{2}}v\|\|A^{\frac{1}{2}}v\|,$$

we obtain

$$\frac{d}{dt}\|u\|^2_{H^{-1}(\Omega)} + \|A^{\frac{1}{2}}v\|^2 \leq Q(\|u_{0,1}\|_{H^2(\Omega)}, \|u_{0,2}\|_{H^2(\Omega)})\|u\|^2_{H^{-1}(\Omega)}. \tag{5.76}$$

We finally deduce from (5.76) and Gronwall's lemma that

$$\|u_1(t) - u_2(t)\|_{H^{-1}(\Omega)} \leq e^{ct}Q(\|u_{0,1}\|_{H^2(\Omega)}, \|u_{0,2}\|_{H^2(\Omega)})\|u_{0,1} - u_{0,2}\|_{H^{-1}(\Omega)}, \quad c > 0, \quad t \geq 0, \tag{5.77}$$

hence the uniqueness, as well as the continuous dependence with respect to the initial data in the H^{-1}–norm. □

It follows Theorem 2.1 that we have the continuous (with respect to the H^{-1}–norm) semigroup

$$S(t) : H^2(\Omega) \to H^2(\Omega), \qquad u_0 \mapsto u(t), \quad t \geq 0$$

(i.e., $S(0) = I$, $S(t+s) = S(t) \circ S(s)$, t, $s \geq 0$). We then deduce from (5.56) the

Theorem 5. *The semigroup $S(t)$ is dissipative in $H^2(\Omega)$, i.e., there exists a bounded set $\mathcal{B}_1 \subset H^2(\Omega)$ (called absorbing set) such that, for every bounded set $B \subset H^2(\Omega)$, there exists $t_0 = t_0(B) \geq 0$ such that $t \geq t_0$ implies $S(t)B \subset \mathcal{B}_1$.*

Remark 5.2.1. *It is easy to see that we can assume, without loss of generality, that $\mathcal{B}_1$ is positively invariant by $S(t)$, i.e., $S(t)\mathcal{B}_1 \subset \mathcal{B}_1$, $\forall t \geq 0$.*

5.2.3 Existence of exponential attractors

Let u_1 and u_2 be two solutions to (5.3)–(5.5) with initial data $u_{0,1}$ and $u_{0,2}$, respectively. We again set $u = u_1 - u_2$ and $u_0 = u_{0,1} - u_{0,2}$ and have

$$\frac{\partial u}{\partial t} + \Delta^2 u - \Delta(f(u_1) - f(u_2)) + g(u_1) - g(u_2) = 0, \tag{5.78}$$

$$\frac{\partial u}{\partial \nu} = \frac{\partial \Delta u}{\partial \nu} = 0 \quad \text{on } \Gamma, \tag{5.79}$$

$$u|_{t=0} = u_0. \tag{5.80}$$

Furthermore, it is sufficient here to take initial data belonging to the bounded absorbing set $\mathcal{B}_1$ defined in the previous section.

We rewrite (5.78) as

$$\begin{aligned}\frac{\partial}{\partial t}A^{-1}v - \Delta u + f(u_1) - f(u_2) - \langle f(u_1) - f(u_2)\rangle \\ + A^{-1}\Big(g(u_1) - g(u_2) - \langle g(u_1) - g(u_2)\rangle\Big) = 0.\end{aligned} \tag{5.81}$$

Multiplying (5.81) by $t\frac{\partial v}{\partial t}$, we have

$$\begin{aligned}\frac{1}{2}\frac{d}{dt}(t\|A^{\frac{1}{2}}u\|^2) + t\left\|A^{-\frac{1}{2}}\frac{\partial v}{\partial t}\right\|^2 + t\left(\left(f(u_1) - f(u_2), \frac{\partial v}{\partial t}\right)\right) \\ + t\left(\left(A^{-1}\Big(g(u_1) - g(u_2) - \langle g(u_1) - g(u_2)\rangle\Big), \frac{\partial v}{\partial t}\right)\right) = \frac{1}{2}\|A^{\frac{1}{2}}u\|^2.\end{aligned} \tag{5.82}$$

Here,

$$\begin{aligned}
&\left|\left(\left(A^{-1}\big(g(u_1)-g(u_2)-\langle g(u_1)-g(u_2)\rangle\big),\frac{\partial v}{\partial t}\right)\right|\\
&=\left|\left(\left(g(u_1)-g(u_2),A^{-1}\frac{\partial v}{\partial t}\right)\right|\\
&\le\int_\Omega|u|\left|A^{-1}\frac{\partial v}{\partial t}\right|\int_0^1|g'(u_1+s(u_2-u_1))|dsdx\\
&\le c\int_\Omega(1+|u_1|^{2q-2}+|u_2|^{2q-2})|u|\left|A^{-1}\frac{\partial v}{\partial t}\right|dx\\
&\le\text{(thanks to (5.56) and to the continuous embedding } H^2(\Omega)\subset C(\overline{\Omega}))\\
&\le c\|u\|\left\|A^{-\frac12}\frac{\partial v}{\partial t}\right\|,
\end{aligned}$$

where the constant c only depends on $\mathcal{B}_1$. Furthermore,

$$\begin{aligned}
\left|\left(\left(f(u_1)-f(u_2),\frac{\partial v}{\partial t}\right)\right)\right|&\le c\|A^{\frac12}(f(u_1)-f(u_2))\|\left\|A^{-\frac12}\frac{\partial v}{\partial t}\right\|\\
&\le c\left\|A^{\frac12}\Big(\int_0^1 f'(u_1+s(u_2-u_1))dsu\Big)\right\|\left\|A^{-\frac12}\frac{\partial v}{\partial t}\right\|\\
&\le c\left\|\int_0^1 f'(u_1+s(u_2-u_1))dsA^{\frac12}u\right\|\left\|A^{-\frac12}\frac{\partial v}{\partial t}\right\|\\
&\quad+c\left\|u\int_0^1 f''(u_1+s(u_2-u_1))(A^{\frac12}u_1+s(A^{\frac12}u_2-A^{\frac12}u_1))ds\right\|\left\|A^{-\frac12}\frac{\partial v}{\partial t}\right\|\\
&\le c(\|A^{\frac12}u\|+\|uA^{\frac12}u_1\|+\|uA^{\frac12}u_2\|)\left\|A^{-\frac12}\frac{\partial v}{\partial t}\right\|\\
&\le c(\|A^{\frac12}u\|+\|u\|_{L^4(\Omega)}\|A^{\frac12}u_1\|_{L^4(\Omega)}+\|u\|_{L^4(\Omega)}\|A^{\frac12}u_2\|_{L^4(\Omega)})\left\|A^{-\frac12}\frac{\partial v}{\partial t}\right\|\\
&\le c(\|A^{\frac12}u\|+c\|u\|_{L^4(\Omega)}(\|u_1\|_{H^2(\Omega)}+\|u_2\|_{H^2(\Omega)})\left\|A^{-\frac12}\frac{\partial v}{\partial t}\right\|\\
&\le\text{(thanks to (5.56) and to the continuous embedding } H^2(\Omega)\subset C(\overline{\Omega}))\\
&\le c(\|A^{\frac12}u\|+\|u\|_{L^4(\Omega)})\left\|\frac{\partial v}{\partial t}\right\|_{-1}\\
&\le\text{(thanks to the continuous embedding } H^1(\Omega)\subset L^4(\Omega))\\
&\le c\|u\|_{H^1(\Omega)}\left\|\frac{\partial v}{\partial t}\right\|_{-1},
\end{aligned}$$

where the constant c only depends on $\mathcal{B}_1$, which yields

$$t\frac{d}{dt}\|A^{\frac12}u\|^2+ct\left\|A^{-\frac12}\frac{\partial v}{\partial t}\right\|^2\le c't\|u\|^2_{H^1(\Omega)}+\frac12\|A^{\frac12}u\|^2. \tag{5.83}$$

By the estimates obtained above (in particular, (5.70)) we infer

$$\begin{aligned}
\frac{d}{dt}(t\|A^{\frac12}u\|^2+t\langle u(t)\rangle^2)+ct\left\|A^{-\frac12}\frac{\partial v}{\partial t}\right\|^2&\le c't(\|u\|^2_{H^1(\Omega)}\\
&\quad+\langle u(t)\rangle^2)+c''(\|A^{\frac12}u\|^2+\langle u(t)\rangle^2)
\end{aligned}$$

and

$$\frac{d}{dt}(t(\|A^{\frac{1}{2}}u\|^2+\langle u(t)\rangle^2))+ct\left\|A^{-\frac{1}{2}}\frac{\partial v}{\partial t}\right\|^2\leq c't(\|A^{\frac{1}{2}}u\|^2+\langle u(t)\rangle^2)\\ +c''(\|A^{\frac{1}{2}}u\|^2+\langle u(t)\rangle^2). \tag{5.84}$$

We note that, integrating (5.76) over $(0,t)$ and owing to (5.77), we have

$$\int_0^t\|A^{\frac{1}{2}}u\|^2ds\leq ce^{c't}\|u_{0,1}-u_{0,2}\|^2_{H^{-1}(\Omega)}, \tag{5.85}$$

where c and c' only depend on $\mathcal{B}_1$, hence

$$\int_0^t\|u\|^2_{H^1(\Omega)}ds\leq ce^{c't}\|u_{0,1}-u_{0,2}\|^2_{H^{-1}(\Omega)}. \tag{5.86}$$

We then deduce from (5.84), (5.86), and Gronwall's lemma that

$$\|u_1-u_2\|^2_{H^1(\Omega)}\leq\frac{c}{t}e^{c't}\|u_{0,1}-u_{0,2}\|^2_{H^{-1}(\Omega)}\quad\forall t>0. \tag{5.87}$$

Now multiplying (5.81) by $\frac{\partial v}{\partial t}$, we obtain, proceeding as above,

$$\frac{d}{dt}(\|A^{\frac{1}{2}}u\|^2+\langle u\rangle^2)+\left\|A^{-\frac{1}{2}}\frac{\partial v}{\partial t}\right\|^2\leq c(\|A^{\frac{1}{2}}u\|^2+\langle u\rangle^2), \tag{5.88}$$

where the constant c only depends on $\mathcal{B}_1$. Therefore, integrating (5.88) over $(1,t)$ and owing to (5.86) and (5.87) (for t = 1), we have

$$\int_1^t\left\|\frac{\partial v}{\partial t}\right\|^2_{H^{-1}(\Omega)}d\tau\leq ce^{c't}\|u_{0,1}-u_{0,2}\|^2_{H^{-1}(\Omega)}, \tag{5.89}$$

where c and c' only depend on $\mathcal{B}_1$.

We note that, integrating (5.78) over $(0,t)$, we easily obtain

$$\int_0^t\langle\frac{\partial u}{\partial t}\rangle^2d\tau\leq ce^{c't}\|u_{0,1}-u_{0,2}\|^2_{H^{-1}(\Omega)}, \tag{5.90}$$

where the constant c only depends on $\mathcal{B}_1$.

Differentiating (5.81) with respect to time, we find

$$\frac{\partial}{\partial t}A^{-1}\theta+A\theta+\zeta(t)\frac{\partial u}{\partial t}+\zeta'(t)u-\langle\frac{\partial}{\partial t}\zeta(t)u\rangle\\ +A^{-1}\Big((\eta(t)\frac{\partial u}{\partial t}+\eta'(t)u)-\langle\frac{\partial}{\partial t}\eta(t)u\rangle\Big)=0, \tag{5.91}$$

where $\zeta(t)=\int_0^1 f'(u_1+s(u_2-u_1))ds$, $\eta(t)=\int_0^1 g'(u_1+s(u_2-u_1))ds$, and $\theta=\frac{\partial v}{\partial t}$.

We multiply (5.91) by $(t-1)\theta$ and have

$$\frac{1}{2}\frac{d}{dt}((t-1)\|A^{-\frac{1}{2}}\theta\|^2)+(t-1)\|A^{\frac{1}{2}}\theta\|^2+(t-1)((\zeta(t)\frac{\partial u}{\partial t},\theta))+(t-1)((\zeta'(t)u,\theta))\\ +(t-1)((A^{-1}\Big((\eta(t)\frac{\partial u}{\partial t}+\eta'(t)u)-\langle\frac{\partial}{\partial t}\eta(t)u\rangle\Big),\theta))=\frac{1}{2}\|A^{-\frac{1}{2}}\theta\|^2. \tag{5.92}$$

Here,

$$\begin{aligned}
&\left|((A^{-1}\Big((\eta(t)\frac{\partial u}{\partial t}+\eta'(t)u)-\langle\frac{\partial}{\partial t}\eta(t)u\rangle\Big),\theta))\right| \\
&\quad=\left|(((\eta(t)\frac{\partial u}{\partial t}+\eta'(t)u),A^{-1}\theta))\right| \\
&\quad\le\Big(\|\eta\|_{L^\infty(\Omega)}\Big\|\frac{\partial u}{\partial t}\Big\|+\|\eta'\|_{L^4(\Omega)}\|u\|_{L^4(\Omega)}\Big)\|\theta\|_{-1} \\
&\quad\le\text{(thanks to (5.62), (5.66), (5.87) and the continuous embedding } H^2(\Omega)\subset C(\overline{\Omega}))\\
&\quad\le c\Big(\|\theta\|^2+\langle\frac{\partial u}{\partial t}\rangle^2+\|u\|^2_{H^1(\Omega)}\Big)+c'\|\theta\|^2_{-1} \\
&\quad\le c\Big(\|\theta\|^2_{-1}+\langle\frac{\partial u}{\partial t}\rangle^2+\|u\|^2_{H^1(\Omega)}\Big)+\frac{1}{4}\|\nabla\theta\|^2,
\end{aligned}$$

owing to the above estimates and a proper interpolation inequality. Furthermore, owing to (5.59),

$$\begin{aligned}
\left|((\zeta(t)\frac{\partial u}{\partial t},\theta))\right|&\le c\left\|A^{\frac12}\Big(\zeta(t)\frac{\partial u}{\partial t}\Big)\right\|\|\theta\|_{-1}\\
&\le c(\|\zeta\|_{L^\infty(\Omega)}+\|A^{\frac12}\zeta\|_{L^4(\Omega)})\Big\|\frac{\partial u}{\partial t}\Big\|_{H^1(\Omega)}\|\theta\|_{-1}\\
&\le c\Big(\|A^{\frac12}\theta\|^2+\langle\frac{\partial u}{\partial t}\rangle^2\Big)^{\frac12}\|\theta\|_{-1}
\end{aligned}$$

and, owing to (5.43) and (5.66),

$$\begin{aligned}
\|\zeta'(t)u\|&=\|\int_0^1 f''(u_1+s(u_2-u_1))(\frac{\partial u_1}{\partial t}+s(\frac{\partial u_2}{\partial t}-\frac{\partial u_1}{\partial t}))dsu\|\\
&\le c(\|\frac{\partial u_1}{\partial t}\|_{L^4(\Omega)}+\|\frac{\partial u_2}{\partial t}\|_{L^4(\Omega)})\|u\|_{L^4(\Omega)}\\
&\le c(\|\frac{\partial u_1}{\partial t}\|_{H^1(\Omega)}+\|\frac{\partial u_2}{\partial t}\|_{H^1(\Omega)})\|u\|_{H^1(\Omega)}\\
&\le c\|u\|_{H^1(\Omega)},
\end{aligned}$$

which yields

$$\begin{aligned}
\frac{d}{dt}((t-1)(\|\theta\|^2_{-1}+\langle\frac{\partial u}{\partial t}\rangle^2))+(t-1)\|\theta\|^2_{H^1(\Omega)}\le c(t-1)(\|\theta\|^2_{-1}+\\
\langle\frac{\partial u}{\partial t}\rangle^2)+\|\theta\|^2_{-1}+\langle\frac{\partial u}{\partial t}\rangle^2+c'(t-1)\|u\|^2_{H^1(\Omega)}.
\end{aligned}\tag{5.93}$$

We thus deduce from (5.86), (5.87), (5.89), (5.90), and Gronwall's lemma that

$$\|\theta(t)\|^2_{H^{-1}(\Omega)}\le\frac{c}{t-1}e^{c't}\|u_0\|^2_{H^{-1}(\Omega)},\qquad\forall t>1.\tag{5.94}$$

We finally rewrite (5.81) in the form

$$-\Delta u=\varrho_u,\quad\frac{\partial u}{\partial\nu}=0\quad\text{on }\Gamma,\tag{5.95}$$

where

$$\begin{aligned}\varrho_u = -A^{-1}\Big(\frac{\partial v}{\partial t}\Big) - (f(u_1) - f(u_2)) + \langle f(u_1) - f(u_2)\rangle \\ - A^{-1}\Big(g(u_1) - g(u_2) - \langle g(u_1) - g(u_2)\rangle\Big)\end{aligned} \tag{5.96}$$

satisfies

$$\begin{aligned}\|\varrho_u\| \leq & c\Big(\Big\|\frac{\partial v}{\partial t}\Big\|_{-1} + \|f(u_1) - f(u_2)\| + |\langle f(u_1) - f(u_2)\rangle| \\ & + \|g(u_1) - g(u_2)\| + |\langle g(u_1) - g(u_2)\rangle|\Big) \\ \leq & c\Big(\Big\|\frac{\partial v}{\partial t}\Big\|_{-1} + \|u\int_0^1 f'(su_1 + (1-s)u_2)ds\| + |\langle u\int_0^1 f'(su_1 + (1-s)u_2)ds\rangle| \\ & + \|u\int_0^1 g'(su_1 + (1-s)u_2)ds\| + |\langle u\int_0^1 g'(su_1 + (1-s)u_2)ds\rangle|\Big) \\ \leq & c\Big(\Big\|\frac{\partial v}{\partial t}\Big\|_{-1} + \|u\|\Big) \\ \leq & c\Big(\Big\|\frac{\partial v}{\partial t}\Big\|_{-1} + \|u\|_{H^1(\Omega)}\Big),\end{aligned} \tag{5.97}$$

where the constant c only depends on $\mathcal{B}_1$. It then follows from (5.87), (5.94), (5.97), and standard elliptic regularity results that

$$\|u_1(t) - u_2(t)\|_{H^2(\Omega)} \leq \frac{c}{\sqrt{t-1}} e^{c't}\|u_{0,1} - u_{0,2}\|_{H^{-1}(\Omega)}, \quad c, c' \geq 0, \ \ t > 1, \tag{5.98}$$

where the constant c only depends on $\mathcal{B}_1$.

Next, we derive a Hölder (both with respect to space and time) estimate. Actually, owing to (5.77), it suffices to prove the Hölder continuity with respect to time. We have

$$\begin{aligned}\|u(t_1) - u(t_2)\|_{H^{-1}(\Omega)} = & \Big\|\int_{t_1}^{t_2}\frac{\partial u}{\partial t}d\tau\Big\|_{H^{-1}(\Omega)} \leq \Big|\int_{t_1}^{t_2}\Big\|\frac{\partial u}{\partial t}\Big\|_{H^{-1}(\Omega)}d\tau\Big| \\ & \leq |t_1 - t_2|^{\frac{1}{2}}\Big|\int_{t_1}^{t_2}\Big\|\frac{\partial u}{\partial t}\Big\|^2_{H^{-1}(\Omega)}d\tau\Big|^{\frac{1}{2}},\end{aligned} \tag{5.99}$$

where u is solution to (5.3)–(5.5).

By using (5.34) and (5.57), it easy to show that

$$\Big|\int_{t_1}^{t_2}\Big\|\frac{\partial v}{\partial t}\Big\|^2_{H^{-1}(\Omega)}d\tau\Big| \leq c, \tag{5.100}$$

where the constant c only depends on $\mathcal{B}_1$ and T such that $t_1, t_2 \in [0, T]$, so that

$$\|u(t_1) - u(t_2)\|_{H^{-1}(\Omega)} \leq c|t_1 - t_2|^{\frac{1}{2}}, \tag{5.101}$$

where the constant c only depends on $\mathcal{B}_1$ and T such that $t_1, t_2 \in [0, T]$.

We finally deduce from (5.77), (5.98), and (5.101) the following result (see, e.g., [52, 53]).

Theorem 6. *The semigroup $S(t)$ possesses an exponential attractor $\mathcal{M} \subset \mathcal{B}_1$, i.e.*

(i) $\mathcal{M}$ is compact in $H^{-1}(\Omega)$;

(ii) $\mathcal{M}$ is positively invariant, $S(t)\mathcal{M} \subset \mathcal{M}$, $\forall t \geq 0$;

(iii) $\mathcal{M}$ has finite fractal dimension in $H^{-1}(\Omega)$;

(iv) $\mathcal{M}$ attracts exponentially fast the bounded subsets of $H^2(\Omega)$,

$$\forall B \subset H^2(\Omega) \text{ bounded}, \quad dist_{H^{-1}(\Omega)}(S(t)B, \mathcal{M}) \leq Q(\|B\|_{H^2(\Omega)})e^{-ct}, \quad c > 0, \ \ t \geq 0,$$

where the constant c is independent of B and $dist_{H^{-1}(\Omega)}$ denotes the Hausdorff semidistance between sets defined by

$$dist_{H^{-1}(\Omega)}(A, B) = \sup_{a \in A} \inf_{b \in B} \|a - b\|_{H^{-1}(\Omega)}.$$

Remark 5.2.2. *Setting $\tilde{\mathcal{M}} = S(1)\mathcal{M}$, we can prove that $\tilde{\mathcal{M}}$ is an exponential attractor for $S(t)$, but now in the topology of $H^2(\Omega)$ (see, e.g., [54]).*

Since $\mathcal{M}$ (or $\tilde{\mathcal{M}}$) is a compact attracting set, we deduce from Theorem 6 the following corollary.

Corollary 2. *The semigroup $S(t)$ possesses the finite-dimensional global attractor $\mathcal{A} \subset \mathcal{B}_1$.*

Remark 5.2.3. *We recall that $f(s) = \sum_{i=0}^{2p-1} c_i s^i, \quad c_{2p-1} > 0$. We studied in this section the case when the mass source is defined by $g(s) = \sum_{j=0}^{2q-1} b_j s^j, \quad b_{2q-1} > 0, \ q \geq 1$. Note that we can obtain the same results in the case when the mass source is defined by $g(x, s) = h(x)L(s)$, where $h \in L^\infty(\Omega)$ and $L(s) = \sum_{j=0}^{2q-1} b_j s^j, \quad b_{2q-1} > 0, \ q > 1$, such that $p = 2q - 1$ and*

$$\langle g(x, u)\rangle\langle u\rangle \geq \xi_8 \langle u^{2q-1}\rangle\langle u\rangle + c\langle u\rangle, \qquad \xi_8 > 0. \tag{5.102}$$

We note that (see [42], Remark 2.11)

$$((f(v + \langle u\rangle) - \langle f(u)\rangle, v)) \geq \alpha \int_\Omega \sum_{k=0}^{p-1} v^{2p-2k}\langle u\rangle^{2k} dx, \quad \alpha > 0. \tag{5.103}$$

Actually, we need a new estimate on the spatial average. Indeed, we multiply (5.10) by $\langle u\rangle$ and have

$$\frac{d}{dt}\langle u\rangle^2 + \langle g(x, u)\rangle\langle u\rangle = 0,$$

so that from (5.102) we immediatly get

$$\frac{1}{2}\frac{d}{dt}\langle u\rangle^2 + \xi_8\langle u^{2q-1}\rangle\langle u\rangle \leq c\langle u\rangle.$$

Besides we have that

$$\begin{aligned}\langle u^{2q-1}\rangle\langle u\rangle &= \langle (v + \langle u\rangle)^{2q-1}\rangle\langle u\rangle \\ &= \sum_{k=0}^{2q-1} C_{2q-1}^k \langle v^k\rangle\langle u\rangle^{2q-k} \\ &\geq \varepsilon\langle u\rangle^{2q} - c\|v\|^{2q}_{L^{2q}(\Omega)},\end{aligned}$$

where $c > 0$. By using Young's lemma we infer

$$\frac{d}{dt}\langle u\rangle^2 + \langle u\rangle^{2q} \le c\|v\|^{2q}_{L^{2q}(\Omega)} + \langle u\rangle^2 + c', \quad c > 0, \tag{5.104}$$

owing to Young's inequality.

In order to estimate the mass source term we observe that

$$\begin{aligned} L(v + \langle u\rangle) - L(\langle u\rangle) &= \sum_{j=0}^{2q-1} b_j((v + \langle u\rangle)^j - \langle u\rangle^j) \\ &= \sum_{j=1}^{2q-1} b_j \sum_{k=1}^{j-1} C_j^k v^{j-k}\langle u\rangle^k \\ &= \sum_{s=0}^{2q-2} b_{s+1} \sum_{k=0}^{s} C_{s+1}^k v^{s+1-k}\langle u\rangle^k \end{aligned}$$

and

$$|L(v + \langle u\rangle) - L(\langle u\rangle)| \le c \sum_{k=0}^{2q-2} |v|^{2q-1-k}\langle u\rangle^k,$$

so that

$$\begin{aligned} \|g(x, v + \langle u\rangle) - g(x, \langle u\rangle)\|^2 &\le \|h\|^2_{L^\infty(\Omega)}\|L(v + \langle u\rangle) - L(\langle u\rangle)\|^2 \\ &\le c\|h\|^2_{L^\infty(\Omega)} \int_\Omega \sum_{k=0}^{2q-2} |v|^{4q-2-2k}\langle u\rangle^{2k} dx \\ &\le c\|h\|^2_{L^\infty(\Omega)} \int_\Omega \sum_{k=0}^{p-1} |v|^{2p-2k}\langle u\rangle^{2k} dx, \end{aligned} \tag{5.105}$$

since $p = 2q - 1$. Moreover, we have

$$((g(x, v + \langle u\rangle) - g(x, \langle u\rangle), A^{-1}v)) \le \varepsilon\|g(x, v + \langle u\rangle) - g(x, \langle u\rangle)\|^2 + c\|v\|^2_{-1}.$$

Therefore, owing to (5.102)*,* (5.103)*, and* (5.105)*, it is easy to obtain the same results as above in the case when $g(x, s) = h(x)L(s)$, where $h \in L^\infty(\Omega)$ and $L(s) = \sum_{j=0}^{2q-1} b_j s^j, \quad b_{2q-1} > 0,\ q \ge 1.$*

5.3 Dirichlet boundary conditions

We consider the following initial and boundary value problem :

$$\frac{\partial u}{\partial t} + \Delta^2 u - \Delta f(u) + g(x, u) = 0, \tag{5.106}$$

$$u = \Delta u = 0 \qquad \text{on } \Gamma, \tag{5.107}$$

$$u|_{t=0} = u_0, \tag{5.108}$$

in a bounded and regular domain $\Omega \subset \mathbb{R}^n$, $n = 1,\ 2$, or 3, with boundary Γ.

We make the following assumptions :

$$f \in C^2(\mathbb{R}),\ f(0) = 0,\ \ g \in L^2(\Omega), \tag{5.109}$$

$$f'(s) \geq -c_0,\ \ c_0 \geq 0,\ \ s \in \mathbb{R}, \tag{5.110}$$

$$f(s)s \geq c_1 F(s) - c_2, F(s) \geq -c_3,\ \ c_1 > 0,\ \ c_2, c_3 \geq 0,\ \ s \in \mathbb{R}, \tag{5.111}$$

where $F(s) = \int_0^s f(\tau)d\tau$,

$$g \text{ is of class } C^1 \ \text{ with respect to } u, \tag{5.112}$$

$$\begin{gathered} \|u\| \int_\Omega |g(x,u)|dx \leq \varepsilon \int_\Omega F(u)dx + c_\varepsilon,\ \ \forall u \in L^2(\Omega) \\ \text{such that } \int_\Omega F(u)dx < +\infty,\ \ \varepsilon > 0, \end{gathered} \tag{5.113}$$

$$\begin{gathered} g(x,u)u \leq cF(u) + c',\ \ \forall x \in \Omega,\ \ \forall u \in L^2(\Omega) \\ \text{such that } \int_\Omega F(u)dx < +\infty,\ \ \varepsilon > 0,\ \ c \geq 0. \end{gathered} \tag{5.114}$$

Remark 5.3.1. *In particular, these assumptions are satisfied by polynomials of degree* $2p+1$ *and* $2p$*, respectively,* $p \geq 1$*, of the form* $f(s) = \sum_{i=1}^{2p+1} a_i s^i,\ a_{2p+1} > 0$ *and* $g(s) = \sum_{i=0}^{2p} b_i s^i$ *(e.g., when* f *has degree three and* g *has degree two).*

We multiply (5.106) by $(-\Delta)^{-1}u$ and have, integrating over Ω and by parts,

$$\frac{1}{2}\frac{d}{dt}\|u\|_{-1}^2 + \|\nabla u\|^2 + ((f(u),u)) + (((-\Delta)^{-1}g(x,u),u)) = 0. \tag{5.115}$$

We note that, since $H^2(\Omega)$ is continuously embedded in $L^\infty(\Omega)$,

$$\begin{aligned} |(((-\Delta)^{-1}g(x,u),u))| &= |((g(x,u),(-\Delta)^{-1}u))| \\ &\leq \int_\Omega |g(x,u)||(-\Delta)^{-1}u|dx \\ &\leq \|(-\Delta)^{-1}u\|_{L^\infty(\Omega)} \int_\Omega |g(x,u)|dx \\ &\leq \|u\| \int_\Omega |g(x,u)|dx \\ &\leq \text{(thanks to (5.113))} \\ &\leq \varepsilon \int_\Omega F(u)dx + c_\varepsilon, \end{aligned}$$

then, owing to (5.111), we have

$$\frac{d}{dt}\|u\|_{-1}^2 + c\Big(\|u\|_{H^1(\Omega)}^2 + \int_\Omega F(u)dx\Big) \leq \frac{c}{2}\int_\Omega F(u)dx + c', \quad c > 0, \tag{5.116}$$

which gives

$$\frac{d}{dt}\|u\|_{-1}^2 + c\Big(\|u\|_{H^1(\Omega)}^2 + \int_\Omega F(u)dx\Big) \leq c', \quad c > 0. \tag{5.117}$$

We then multiply (5.106) by u and find

$$\frac{1}{2}\frac{d}{dt}\|u\|^2 + \|\Delta u\|^2 + ((f'(u)\nabla u, \nabla u)) + ((g(x,u),u)) = 0. \tag{5.118}$$

We deduce from (5.110) and (5.114) that

$$\frac{d}{dt}\|u\|^2 + c\|u\|^2_{H^2(\Omega)} \le c'\|\nabla u\|^2 + c''\int_\Omega F(u)dx + c'', \quad c > 0. \tag{5.119}$$

Summing finally (5.117) and δ_1 times (5.119), where $\delta_1 > 0$ is small enough, we obtain

$$\frac{d}{dt}\Big(\|u\|^2_{-1} + \delta_1\|u\|^2\Big) + c\Big(\|u\|^2_{H^2(\Omega)} + \int_\Omega F(u)dx\Big) \le c', \quad c > 0. \tag{5.120}$$

As a consequence to (5.120) and proceeding as in [104], we have the

Theorem 7. *We assume that $u_0 \in H^2(\Omega) \cap H^1_0(\Omega)$. Let u be a solution to (5.106)–(5.108). Then, there exists a constant $c > 0$ such that*

$$\|u(t)\|_{H^2(\Omega)} \le e^{-ct}Q(\|u_0\|_{H^2(\Omega)}) + c', \quad t \ge 0.$$

Furthermore, let u_1 and u_2 be two solutions to (5.106)–(5.108) with initial data $u_{0,1}$ and $u_{0,2}$, respectively. Then,

$$\| u_1(t) - u_2(t) \|^2_{-1} \le e^{ct}Q(\|u_{0,1}\|_{H^2(\Omega)}, \|u_{0,1}\|_{H^2(\Omega)})\|u_{0,1} - u_{0,2}\|^2_{-1}, \quad c > 0, \ \ t \ge 0.$$

Finally, (5.106)–(5.108) possesses a unique solution u such that $u \in H^2(\Omega) \cap H^1_0(\Omega)$, $\forall t \ge 0$.

We set $\Phi = H^2(\Omega) \cap H^1_0(\Omega)$. It follows from Theorem 7 that we have the continuous (with respect to the H^{-1}–norm) semigroup

$$S(t) : \Phi \to \Phi, \qquad u_0 \mapsto u(t), \quad t \ge 0$$

(i.e., $S(0) = I$, $S(t+s) = S(t) \circ S(s)$, t, $s \ge 0$) and the semigroup $S(t)$ is dissipative in Φ, i.e., there exists a bounded absorbing set $\mathcal{B}_0 \subset \Phi$.

We can assume, without loss of generality, that $\mathcal{B}_0$ is positively invariant by $S(t)$, i.e., $S(t)\mathcal{B}_0 \subset \mathcal{B}_0$, $\forall t \ge 0$.

Theorem 8. *The semigroup $S(t)$ possesses an exponential attractor $\mathcal{M} \subset \mathcal{B}_0$, i.e.*

(i) $\mathcal{M}$ is compact in $H^{-1}(\Omega)$;

(ii) $\mathcal{M}$ is positively invariant, $S(t)\mathcal{M} \subset \mathcal{M}$, $\forall t \ge 0$;

(iii) $\mathcal{M}$ has finite fractal dimension in $H^{-1}(\Omega)$;

(iv) $\mathcal{M}$ attracts exponentially fast the bounded subsets of Φ,

$$\forall B \subset \Phi \text{ bounded}, \quad dist_{H^{-1}(\Omega)}(S(t)B, \mathcal{M}) \le Q(\|B\|_{H^2(\Omega)})e^{-ct}, \quad c > 0, \ \ t \ge 0,$$

where the constant c is independent of B.

Proof. *See [104] ; see also the previous section.* □

Remark 5.3.2. *Setting $\tilde{\mathcal{M}} = S(1)\mathcal{M}$, we can prove that $\tilde{\mathcal{M}}$ is an exponential attractor for $S(t)$, but now in the topology of Φ (see, e.g., [104]).*

Corollary 3. *The semigroup $S(t)$ possesses the finite-dimensional global attractor $\mathcal{A} \subset \mathcal{B}_0$.*

Remark 5.3.3. *Note that the system is dissipative even if the degree of g is greater than the one of f. More precisely, in the case when we replace assumptions (5.113) and (5.114) by*

$$g(x,u)u \geq cF(u) + c', \ \ \forall x \in \Omega, \ \ \forall u \in L^2(\Omega), \tag{5.121}$$

the system is also dissipative and we can obtain the same results as above.

Indeed, multiplying (5.106) *by u, we find*

$$\frac{1}{2}\frac{d}{dt}\|u\|^2 + \|\Delta u\|^2 + ((f'(u)\nabla u, \nabla u)) + ((g(x,u),u)) = 0 \tag{5.122}$$

and we deduce from (5.110) and (5.121) that

$$\frac{d}{dt}\|u\|^2 + c\|u\|^2_{H^2(\Omega)} + c' \int_\Omega F(u)dx \leq c''\|\nabla u\|^2 + c''', \quad c, \ c' > 0. \tag{5.123}$$

It thus follows from the interpolation inequality $\|\nabla u\|^2 \leq c\|u\|\|u\|_{H^2(\Omega)}$ and Gronwall's lemma that

$$\|u\|^2 \leq e^{-ct}Q(\|u_0\|) + c', \quad c > 0, \tag{5.124}$$

hence the dissipativity of the solution. We then use (5.123) *and also proceed as in [104] to obtain the same results as above.*

5.4 Numerical simulations

As far as the numerical simulations are concerned, we rewrite the problem in the form

$$\frac{\partial u}{\partial t} + \Delta\mu + g(x,u) = 0 \quad \text{in } \Omega, \tag{5.125}$$

$$\mu = \Delta u - f(u) \quad \text{in } \Omega, \tag{5.126}$$

$$u_{|t=0} = u_0, \tag{5.127}$$

which has the advantage of splitting the fourth-order (in space) equation into a system of two second-order ones (see [55] and [43]). Consequently, we use a P1-finite element for the space discretization, together with an implicit Euler time discretization with Neumann boundary conditions and with a semi-implicit Euler time discretization with Dirichlet ones. The numerical simulations are performed with the software Freefem++ [84].

In the numerical results presented below, Ω is a $(0,5) \times (0,1)$-ellipse. The triangulation is obtained by dividing Ω into 1272 equal triangles.

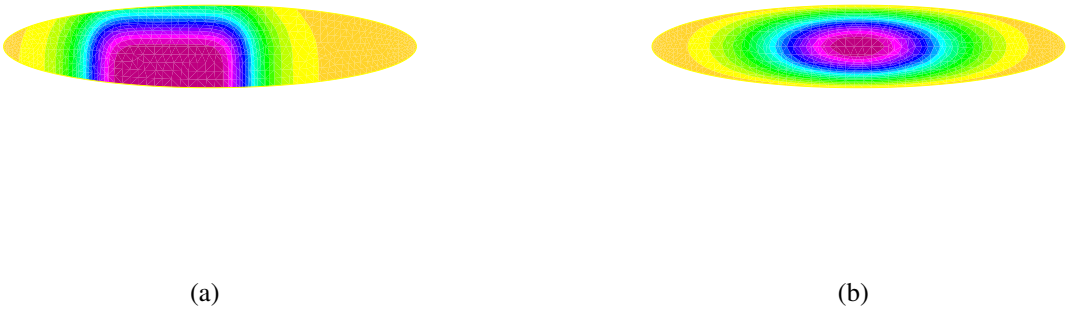

(a) (b)

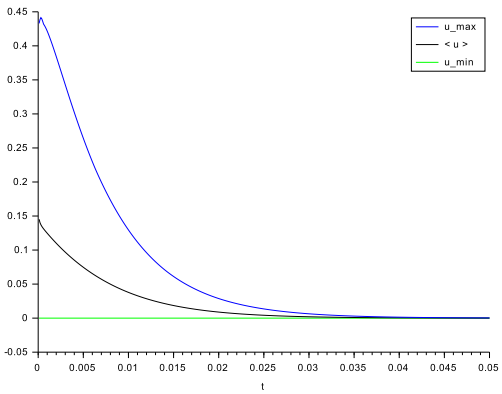

(c)

FIGURE 5.1 – (a) Initial datum at $t = 0$ with a nontrivial growth term $g(x, u) = u^3(u-1)^3$. (b) Solution at $t = 0.02$. At $t = 0.05$, we see in (c) that the solution vanishes, leading to contour lines losing interest. (c) Variations of the order parameter u and the spatial average $\langle u \rangle$.

5.4.1 Dirichlet case

In the first Figure, we take $u_0 = \frac{1}{5(x^6+1)(y^5+\frac{1}{2})} \in [0, 1]$ and $g(u) = u^3(u-1)^3$ with two minimas 0 and 1. In that case, the solution is bounded for all times. The dark red color in Figure 5.1(a) and Figure 5.1(b) correspond to $u_{\max}$ in Figure 5.1(c) and the light orange one in Figure 5.1(a) and Figure 5.1(b) correspond to $u_{\min}$ in Figure 5.1(c). In this example, $f(s) = 4s^3 - 12s^2 + 2s$ and $\Delta t = 0.0001$.

5.4.2 Neumann case

In the second test, we take the same initial datum $u_0 = \frac{1}{5(x^6+1)(y^5+\frac{1}{2})} \in [0, 1]$, $g(u) = u^3(u-1)^3$ with two minimas 0 and 1, $f(s) = 4s^3 - 12s^2 + 2s$, and $\Delta t = 0.0001$, but, now, the problem

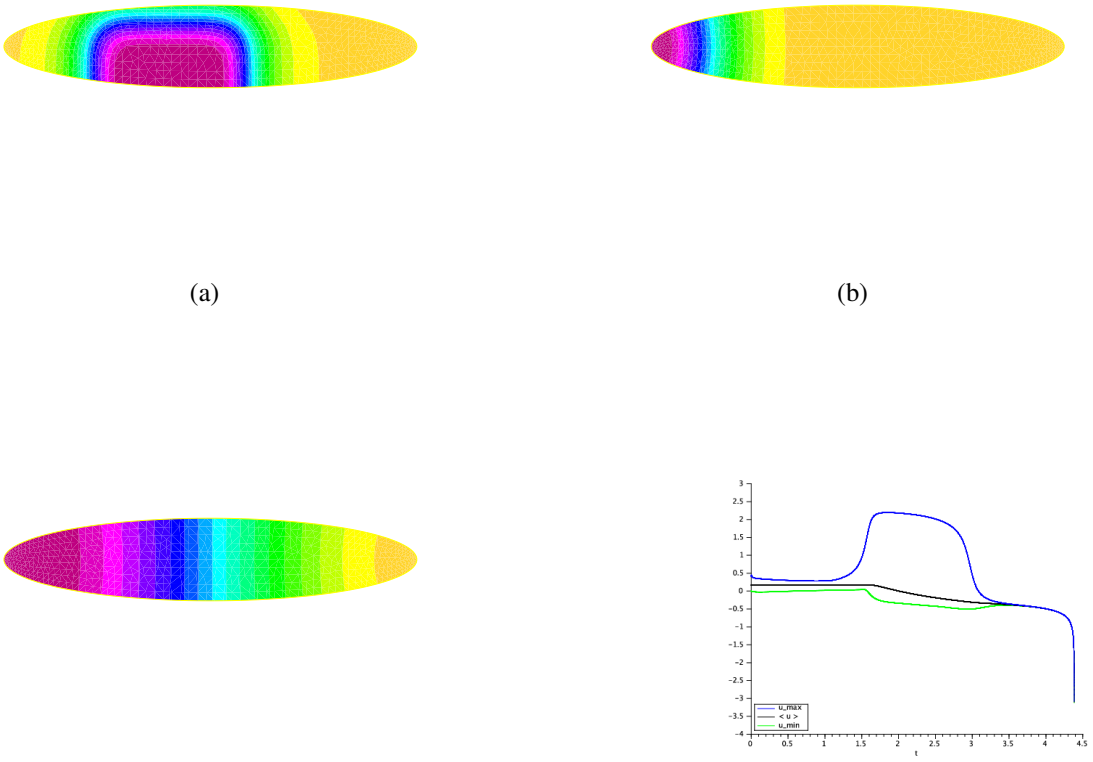

(a) (b)

(c) (d)

FIGURE 5.2 – (a) Initial datum at $t = 0$ with a nontrivial growth term $g(x, u) = u^3(u - 1)^3$. (b) Solution at $t = 2$ (20000 iterations). (c) Solution at $t = 4.3843$ (43843 iterations). (d) Variations of the order parameter u and the spatial average $\langle u \rangle$.

is endowed with Neumann boundary conditions. The dark red color in Figure 5.2(a), Figure 5.2(b), and Figure 5.2(c)correspond to $u_{\max}$ in Figure 5.2(d) and the light orange one in Figure 5.2(a), Figure 5.2(b), and Figure 5.2(c) correspond to $u_{\min}$ in Figure 5.2(d).

Remark 5.4.1. *We gave an example when the solution blows up in finite time with Neumann boundary conditions when the growth term has degree six even if the initial datum u_0 lies between the two minimas of g (in $[0, 1]$). We can also find examples of solutions which blow up when the growth term has degree four, see, e.g., [5] and when the growth term has degree two, see, e.g., [42, 64].*

Acknowledgments : The author would like to thank L. Cherfils and A. Miranville, his supervisors, for many stimulating discussions and useful comments on the subject of the paper. He also wishes to thank the anonymous refree for her/his careful reading of the manuscript and useful suggestions.

Conclusion générale et perspectives

L'objectif de cette thèse a été d'étudier des généralisations de l'équation de Cahn–Hilliard en chimie, biologie et retouche d'images. En particulier, on s'est intéressé à l'étude de l'existence, l'unicité et la régularité, le comportement asymptotique et la convergence vers un état d'équilibre des solutions, ainsi que l'existence d'un attracteur global de dimension finie. On a aussi donné des simulations numériques confirmant les résultats théoriques obtenus.

Les principaux résultats obtenus dans ce mémoire sont :

- Le comportement asymptotique de l'équation de Bertozzi–Esedoglu–Gillette–Cahn–Hilliard, en termes d'un attracteur global de dimension fractale finie.
- Un schéma numérique rapide pour l'équation de Bertozzi–Esedoglu–Gillette–Cahn–Hilliard, appliqué à la retouche d'image ; ce schéma à un pas avec seuil permet de connecter des régions à travers de grands domaines à retoucher.
- L'existence locale de la solution de l'équation Bertozzi–Esedoglu–Gillette–Cahn–Hilliard avec une nonlinéarité singulière de type logarithmique ; on a en outre donné des simulations numériques qui confirment les avantages de ce modèle avec une nonlinéarité de type logarithmique dans la retouche d'images binaires.
- On a proposé un modèle à $n-$composants basé sur le modèle de Bertozzi–Esedoglu–Gillette–Cahn–Hilliard pour la retouche d'images colorées.
- L'existence, l'unicité, et la régularité ainsi que le comportement asymptotique de la solution de ce modèle, en termes d'existence d'un attracteur global de dimension fractale finie.
- La convergence de la solution vers l'état d'équilibre d'une généralisation du modèle proposé dans [141]. En outre, on a démontré que si la moyenne spatiale est bornée alors la solution existe globalement en temps. Finalement, on a démontré que la solution peut exploser en temps fini.
- La convergence de la solution vers l'état d'équilibre d'un cas particulier du modèle proposé dans [5]. En outre, on a démontré que si la moyenne spatiale est bornée alors la solution existe globalement en temps. Finalement, on a démontré que la solution peut exploser en temps fini.
- L'existence, l'unicité, et la régularité ainsi que le comportement asymptotique de la solution d'une généralisation de l'équation de Cahn–Hilliard avec un terme source. Dans ce cas, on considère le modèle à la fois avec des conditions aux limites de type Neumann et de type Dirichlet.

À court terme, nous nous donnons comme perspectives de proposer un modèle basé sur le modèle de Bertozzi–Esedoglu–Gillette–Cahn–Hilliard appliqué à la retouche d'images en niveaux de gris. On note que l'application du modèle de Bertozzi–Esedoglu–Gillette–Cahn–

Hilliard à la retouche d'images en niveaux de gris diffuse les informations de ces images. Dans ce cadre, les auteurs dans [25] ont proposé un modèle basé sur le modèle de Bertozzi–Esedoglu–Gillette–Cahn–Hilliard. Cependant, les applications du modèle proposé dans [25] sont restreintes (dans le sens où la taille du domaine à retoucher est petite) et le modèle n'a pas pu être appliqué à la retouche d'images binaires avec de grands domaines à retoucher. Notre objectif est de proposer un modèle qui conserve les résultats de la retouche d'images binaires qu'on a obtenu et qui s'applique également à la retouche d'images en niveaux de gris. Par ailleurs, le problème de la retouche en $3D$ est très intéressant dans les applications, en particulier dans les images médicales. Dans ce cas, plusieurs simulations on été effectuées par des modèles de la retouche (voir aussi l'annexe D), mais la question importante ici est sur les conditions nécessaires sur le bord du domaine à retoucher pour obtenir des meilleurs résultats en $3D$. En d'autres termes, est-ce que ce sont les conditions aux limites de la retouche proposées dans [15] (l'intensité de l'image et la continuité des lignes isophotes sur le bord du domaine à retoucher) sont également suffisantes en $3D$? De plus, on se propose de nous tester le modèle de Cahn–Hilliard non local dans le problème de retouche. Dans ce cas, la difficulté réside dans les simulations numériques (due à la présence du terme du fidélité) et également dans l'analyse numérique du schéma proposé. D'autre part, on souhaite trouver une bonne stratégie d'adaptation de maillage dans les exemples de la croissance tumorale comme dans [5]. On note que les simulations numériques de la solution qui décrit la croissance tumorale avec le terme de prolifération proposé dans [64] nécessite un maillage très fin ainsi qu'un temps de convergence très long.

Annexe A

Modèles pour la retouche d'images

A.1 Définition et origine de la retouche d'images

La retouche d'images est un processus de remplissage des parties manquantes d'une image endommagée à l'aide d'informations glanées dans les régions voisines. Cette tâche est très importante dans le traitement d'images.

Soit h une fonction qui représente une image donnée dans un domaine Ω. Le problème consiste à reconstituer l'image originale u dans le domaine endommagé $D \Subset \Omega$ qui est appelé domaine à retoucher ou trou ou bien écart. Ceci veut dire que u est connue dans le domaine $\Omega \backslash D$ et on doit chercher la solution u dans D à partir des informations de $u(0)$ (u à l'instant $t = 0$) se trouvant hors du domaine D (comme dans la Figure A.1). La direction des vecteurs isophotes est indiquée dans la Figure A.1.

Dans les modèles de type équations aux dérivées partielles, on s'intéresse plutôt à l'ajout d'un terme, appelé terme de fidélité, au modèle proposé. Ce terme ajouté doit être intégré au sens L^2 sur $\Omega \backslash D$ pour garder la solution u très proche de l'image originale h dans $\Omega \backslash D$ (hors du domaine à retoucher D).

Il est intéressant de noter que la retouche est pertinente dans plusieurs domaines tels que la suppression des rayures dans de vielles photographies et des films [15, 32, 94], la restauration numérique de peintures anciennes (présentant des défauts) [6], l'effacement de textes, comme la suppression des dates, de sous-titres, ou de la publicité d'une photographie [9, 13, 15, 32, 35, 50], des effets tels qu'objets disparus [15, 35], la désocclusion (la récupération des parties cachées des objets dans une image digitale par une interpolation à partir des régions voisines de la zone bouchée) [101], un zoom spatial ou temporel et de super-résolution [9, 32, 140], le masquage d'erreurs [145], la perte de codage perceptive de l'image [32], la suppression de l'effet éblouissant laser [30], et la retouche des sinogrammes en imagerie à rayons X [83].

L'origine de la retouche a été bien décrite dans plusieurs livres ; on cite, par exemple, [144]. A partir des années 1980, quelques méthodes générales pour les retouches ont été largement utilisées. Ces méthodes de retouches stochastiques utilisent les statistiques générales sur des parties de l'image existante afin de trouver les probabilités de ce qui devrait exister dans les régions à retoucher manquantes. Les exemples de ces méthodes sont le recuit simulé ("simulated annealing") et les réseaux neuronaux dans des schémas de retouche ("neural net inpainting schemes"). D'autres méthodes sont axées sur la détection d'arêtes et le filtrage d'échelles d'es-

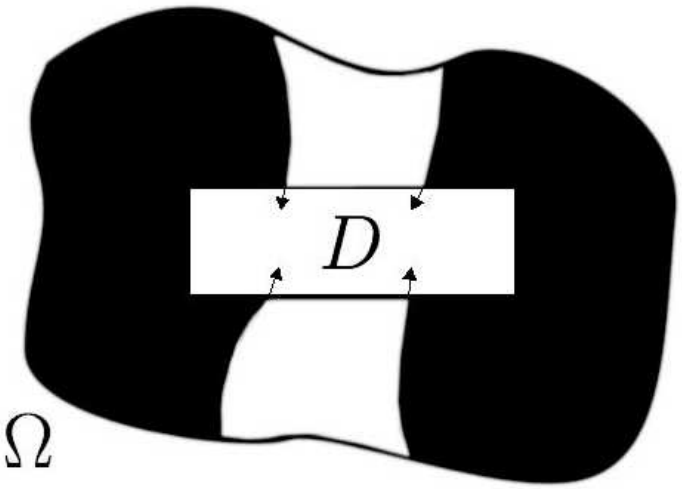

FIGURE A.1 – Problème de la retouche. Figure par [16].

pace. L'exemple principal de ces dernieres méthodes dans les années antérieures à 2000 est la diffusion anisotrope.

En 1984, Geman et Geman dans [73] ont utilisé le recuit simulé pour effectuer la retouche. L'algorithme du recuit simulé fournit un moyen pour chercher une valeur minimale assez bonne d'une fonction de coût. Trouver un minimum global précis peut être extrêmement difficile. Une introduction bien détaillée du recuit simulé peut être trouvée dans Kirkpatrick, Gellatt, et Vecchi [90]. Geman et Geman ont utilisé une fonction de coût statistique qui, lorsqu'elle est utilisée en conjonction avec un recuit simulé, maximise l'état le plus probable de l'image sous une distribution de Gibbs.

En 1992, Perona et Malik [125] ont introduit l'idée de la diffusion anisotrope pour la retouche. Ils ont montré que cette méthode peut être considérée comme une descente de gradient sur une énergie, et qu'elle peut être appliquée à la segmentation d'images multi-échelles. Le point important est le fait qu'ils ont trouvé une façon d'accroitre les échanges intra-zones de régularité, de préférence à interrégions régulières [125]. Les arêtes tranchantes sont laissées en grande partie intactes par leur algorithme. Voir aussi [128, 148].

A.2 Travail pionnier en retouche images

Tout d'abord, la terminologie de la retouche digitale est apparue dans [15]. L'idée de base de ce travail est de propager des informations (l'intensité de l'image) dans la direction des isophotes (les lignes de niveau : ensembles de points de l'image ayant des valeurs de gris constantes) à l'entrée du domaine à retoucher.

Dans [15], les auteurs ont proposé un algorithme conçu pour projeter le gradient de la régularité de l'intensité de l'image dans la direction des isophotes. Le schéma résultant s'écrit sous la forme suivante :

$$\frac{\partial I}{\partial t} = -\nabla^{\perp} I.\nabla\Delta I, \quad \text{dans } D \tag{A.1}$$

$$I = I_0, \quad \text{sur } \partial D \tag{A.2}$$

où I représente l'intensité de l'image, $I_0 = I(0)$, et $\nabla^{\perp}$ est le gradient perpendiculaire (ou orthogonal) ($\nabla^{\perp} := (-\partial y, \partial x)$ dans $\mathbb{R}^2$). Ensuite, pour assurer une évolution correcte du champ de direction, un processus de diffusion est ajouté à la retouche d'images. Les auteurs appliquent quelques itérations de diffusion d'image dans quasiment toutes les étapes. Cette diffusion correspond aux courbes des lignes périodiques pour leur éviter de se couper. Ils utilisent la diffusion anisotrope (voir [125]) afin d'atteindre cet objectif sans perdre le tranchant de la reconstruction. Le modèle final s'écrit alors

$$\frac{\partial I}{\partial t} = \nabla^{\perp} I.\nabla\Delta I + \nu\nabla.(g(|\nabla I|)\nabla I), \tag{A.3}$$

où ν est un terme du viscosité.

L'objectif est de faire évoluer (A.3) vers une solution stationnaire stable, satisfaisant une certaine condition dans la région retouchée. Cette condition stipule que les lignes isophotes, dans le sens de $\nabla^{\perp} I$, doivent être parallèles aux courbes de niveau de la régularité de l'intensité de l'image ΔI, qui devient, pour $\nu = 0$

$$\nabla^{\perp} I.\nabla\Delta I = 0. \tag{A.4}$$

On note que les auteurs de [15] présentent leur méthode basée sur le déplacement de l'intensité de l'image le long des lignes isophotes. L'équation (A.1) est l'équation de transport qui connecte l'intensité de l'image I le long des courbes de niveau de la régularité, ΔI. L'équation (A.1) peut être vue comme équivalente à $DI/Dt = 0$ où D/Dt est la dérivée matérielle $(\partial/\partial t + v.\nabla)$ pour le champ de vitesse ($v = \nabla^{\perp}\Delta I$). En particulier, I est connectée par le champ de vitesse v qui est dans la direction des courbes de niveau de régularité, ΔI.

En général, les conditions de l'obtention de bons résultats de retouche sont :

- La structure de la zone qui entoure le domaine à retoucher est continue dans la zone à retoucher (les courbes de niveau sont dessinées dans le prolongement de celles qui arrivent à la frontière du domaine retouché) ;
- La retouche se fait par la connexion des courbes de niveaux de l'intensité d'image constante en niveaux de gris (isophotes) dans tout le domaine à retoucher.

La Figure A.2 montre une image vandalisée et sa restauration. Elle représente un exemple où le texte doit être supprimé de l'image. C'est un exemple parmi des exemples typiques où les algorithmes de synthèse de texture ne peuvent pas être utilisés puisque le nombre de régions différentes est très grand. Cependant, le résultat présenté dans la Figure A.2 montre l'efficacité du modèle de Bertalmio et al. [15] dans le problème de la retouche.

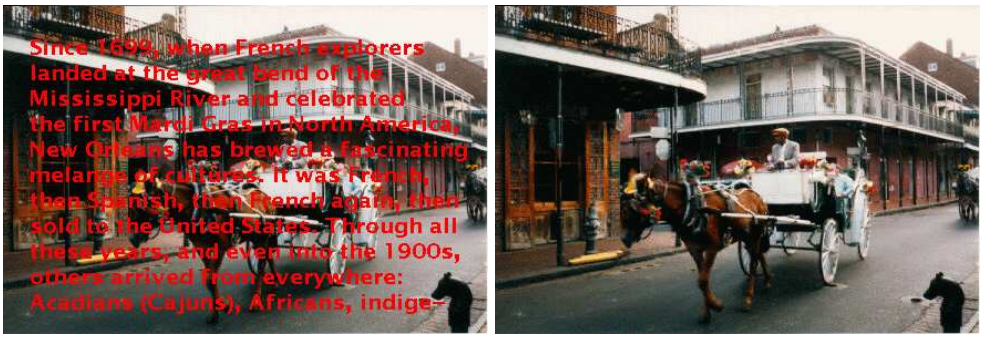

(a) (b)

FIGURE A.2 – (a) Image originale. (b) Résultat final de la retouche d'image obtenu par le modèle de Bertelmio et al.. Figure tirée de [15].

A.3 Quelques modèles appliqués à la retouche d'images

A.3.1 Applications de l'équation de Navier–Stokes à la retouche d'images

Les fluides newtoniens incompressibles sont régis par les équations de Navier–Stokes, qui couplent le champ de vecteur vitesse $\vec{u}$ à une pression scalaire p :

$$\begin{aligned} u_t + u.\nabla u &= -\nabla p + \nu \nabla u, \\ \nabla . v &= 0. \end{aligned} \tag{A.5}$$

Dans l'espace à deux dimensions, la divergence du champ de vitesse libre u possède une fonction de fluide Ψ satisfaisant $\nabla^{\perp}\Psi = u$. En outre, la vorticité, $w = \nabla \times u$, satisfait une équation de diffusion–advection très simple qui peut être calculée en prenant le rotationnel de la première équation dans (A.5) et en utilisant certains faits de base sur la géométrie en deux dimensions d'espace :

$$w_t + u.\nabla w = \nu \Delta w. \tag{A.6}$$

Dans ce cas, on note que la vorticité est une quantité scalaire qui est liée à la fonction d'écoulement à travers l'opérateur de Laplace, $\Delta\Psi = w$. En absence de viscosité ($\nu = 0$), on obtient les équations d'Euler pour l'écoulement non visqueux. Les deux problèmes visqueux et non visqueux, avec des conditions aux limites appropriées, sont globalement bien posés dans deux dimensions d'espace. Des solutions existent pour n'importe quelle condition initiale régulière et dépendant continûment de l'instant initial (t_0).

En termes de la fonction d'écoulement, l'équation (A.6) implique que les écoulements non visqueux à l'état stationnaire doivent satisfaire

$$\nabla^{\perp}\Psi.\nabla\Delta\Psi = 0, \tag{A.7}$$

ce qui signifie que le Laplacien de la fonction d'écoulement, et donc la vorticité, doit avoir des courbes de niveau identiques à la fonction d'écoulement. L'analogie avec la retouche d'images dans le modèle de Bertalmio et al. dans [15] est maintenant claire : la fonction de flux pour les

fluides non visqueux en deux dimensions d'espace satisfait l'équation à l'état stationnaire (A.7) qui est la même que celle donnée par l'intensité de l'image (A.4).

Afin de résoudre le problème de retouche proposé dans [15], on doit chercher la fonction d'écoulement pour l'état stationnaire des équations des fluides non visqueux, qui est un problème possédant une histoire riche et bien développée, voir par exemple, [134], [135] et [136].

Soit D un domaine régulier dans $\mathbb{R}^2$ où D représente le domaine à retoucher à partir des données voisines. On suppose que l'intensité de l'image I_0 est une fonction régulière (avec possibilité de gradients forts) à l'extérieur de D et on connait simultanément I_0 et ΔI_0 sur le bord ∂D. En effet, les paramètres du fluide sont équivalents aux paramètres de la retouche.

Equation de Navier-Stokes	Equation de retouche d'images
Fonction d'écoulement Ψ	Intensité de l'image I
Vitesse du fluide $v = \nabla^{\perp}\Psi$	Direction des isophotes $\nabla^{\perp} I$
Vorticité $w = \Delta\Psi$	Régularité $w = \Delta I$
Viscosité du fluide ν	Diffusion anistrope ν

D'après [15], lorsqu'on utilise une équation aux dérivées partielles pour faire la retouche, une question importante est les conditions aux limites du domaine à retoucher. En effet, les conditions aux bords dans la retouche sont la continuité de l'intensité de l'image I sur le bord du domaine à retoucher et la direction des courbes des niveaux (isophotes) $\nabla^{\perp}$ sur le bord du domaine à retoucher. Ainsi pour le problème de fluide, on a besoin d'une généralisation sans glissement des conditions aux limites qui nécessite une nouvelle formulation de l'équation de Navier–Stokes avec un terme de diffusion anistrope. Le modèle complet proposé dans [9] est

$$\partial w/\partial t + u.\nabla w = \nu\nabla.\Big(g(|\nabla w|)\nabla w\Big), \tag{A.8}$$

où la fonction g représente la diffusion anisotrope de la régularité w. L'intensité de l'image I qui définit le champ de vitesse $u = \nabla^{\perp} I$ dans (A.8) est récupérée en résolvant simultanément le problème de Poisson

$$\begin{aligned} \Delta I &= w, \\ I|_{\partial D} &= I_0. \end{aligned} \tag{A.9}$$

Pour les problèmes de fluides à viscosité faible ν, la dynamique précédente peut prendre un certain temps pour converger vers l'état d'équilibre ; dans ce cas la méthode devient moins pratique. A la place de cette méthode, on utilise des méthodes pseudo-stables qui consistent à remplacer l'équation de Poisson (A.9) par une équation de relaxation dynamique

$$\begin{aligned} I_t - \alpha[\Delta I + w] = 0, \quad \alpha > 0, \\ I|_{\partial D} = I_0. \end{aligned} \tag{A.10}$$

où le paramètre α détermine un taux de relaxation. Dans cette situation, la diffusion peut entraîner une confusion des interfaces tranchantes (les gradients de I) dans la région à retoucher. Par conséquent, il est souvent préférable d'inclure la diffusion anisotrope dans la solution I. Ceci

peut être ajouté directement au problème dynamique (A.10) ou comme une étape supplémentaire en conjonction avec l'équation de Poisson (A.9).

La Figure A.3 montre une image vandalisé et sa restauration. Elle représente un exemple où des parties obscurcissantes existent dans l'image.

(a) (b)

FIGURE A.3 – (a) Image originale. (b) Résultat final de la retouche d'image obtenu par le modèle de Navier–Stokes. Figure tirée de [9].

A.3.2 Retouche d'images par la variation totale de la diffusion anisotrope : diffusion axée sur la courbure

Modèle de Chan et Shen

Les auteurs dans [32] ont utilisé une généralisation d'un modèle bien connu dans le débruitage pour l'appliquer à la retouche d'images. Ils ont supposé que $u^0|_E$ est contaminée par un bruit blanc homogène (modélisé par une distribution gaussienne). Le modèle variationnel de la retouche consiste à trouver une fonction u sur le domaine à retoucher prolongé $E \cup D$ de telle sorte qu'elle minimise une fonctionnelle de régularité appropriée,

$$R[u] := \int_{E\cup D} r(|\nabla u|)dxdy, \tag{A.11}$$

sous la contrainte de débruitage sur E,

$$\frac{1}{\text{Aire}(E)} \int_E |u - u^0|dx = \sigma^2. \tag{A.12}$$

Dans ce cas,

(i) r est une fonction appropriée réelle qui est positive ou nulle pour les entrées non négatives,

(ii) σ est la déviation standard du bruit blanc.

On note que, si D est un ensemble vide, la formulation variationnelle ci-dessus s'apparente à des modèles classiques de débruitage tels que le modèle dans H^1 si $r(s) = s^2$, et la variation totale de Rudin, Osher et Fatemi [129] si $r(s) = s$.

De plus, suivant un pas d'une arête, ∇u est une mesure de Dirac $\delta(x)$ de dimension 1. Ainsi, pour être capable de restaurer un pas d'une arête cassée, il faut exiger que

$$\int_{E\cup D} r(\delta_1)dxdy,$$

soit fini. Cela implique que si

$$r(s) = s^{\alpha} + (\text{termes d'ordre inférieur}),$$

pour la même puissance α lorsque $s \to +\infty$, alors $\alpha \leq 1$. Le meilleur choix de α pour garantir la convexité est $\alpha = 1$ (dans ce cas, on a la variation totale de restauration de Rudin, Osher, et Fatemi dans [129]).

Enfin, le modèle de retouche proposé dans [32] consiste à minimiser l'énergie suivante :

$$J_{\lambda}[u] = \int_{E \cup D} |\nabla u| dxdy + \frac{\lambda}{2} \int_{E} |u - u^0| dxdy, \tag{A.13}$$

où λ joue le rôle d'un multiplicateur de Lagrange pour la contrainte du problème variationnel (A.12), d'où l'équation d'Euler-Lagrange

$$-\nabla.\left(\frac{\nabla u}{|\nabla u|}\right) + \lambda \chi_{\Omega \setminus D}(x)(u - u^0) = 0, \quad \text{dans } E \cup D, \tag{A.14}$$

$$u = u_0, \quad \text{sur } \partial E. \tag{A.15}$$

Ce modèle peut se propager sur les arêtes aigues dans le domaine endommagé. Cependant, cette technique ne peut pas connecter les contours à travers de très grandes distances puisque le terme de régularisation dans ce modèle exige une pénalisation sur la longueur des arêtes. Un autre inconvénient de cette méthode est qu'elle ne garde pas toujours la direction des isophotes continues sur la frontière du domaine à retoucher.

La figure A.4 illustre le lien étroit entre la variation totale de restauration et le problème des surfaces minimales.

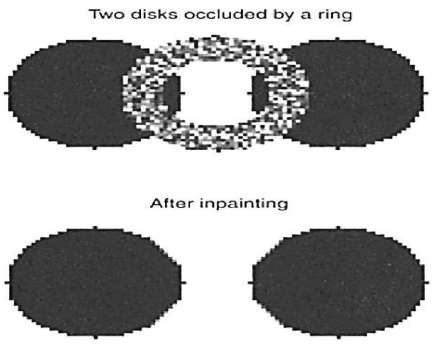

FIGURE A.4 – Retouche d'images avec le modèle de Chan et Shen. Figure tirée de [32]

.

Modèle de Chan, Kang, et Shen

Les auteurs dans [31] ont introduit un nouveau modèle variationnel appliqué à la retouche d'images qui a abordé les insuffisances des modèles basés sur la variation totale. Ce modèle est inspiré du travail de Nitzberg, Mumford, et Shiota [115] et comprend un nouveau terme de

régularisation qui pénalise non seulement la longueur des contours dans une image, mais aussi l'intégrale du carré de la courbure le long des contours des arêtes. L'énergie est donnée par

$$J[u] = \int_D \phi(\kappa)|\nabla u|dx, \kappa \quad = \nabla.\Big[\frac{\nabla u}{|\nabla u|}\Big], \tag{A.16}$$

et l'équation d'Euler-Lagrange résultante est

$$\frac{\partial u}{\partial t} = \nabla.\Big(\phi(\kappa)\frac{\nabla u}{|\nabla u|} - \frac{\vec{t}}{|\nabla u|}\frac{\partial(\phi'(\kappa)\nabla u)}{\partial \vec{t}}\Big), \tag{A.17}$$

où $\frac{\partial}{\partial \vec{t}}$ est la dérivée directionnelle dans la direction du vecteur tangent (isophote) $\vec{t} = \frac{\nabla^{\perp} u}{|\nabla u|}$. Ceci permet de connecter les isophotes sur de grandes distances et leurs directions sont conservées continues sur la frontière de la région à retoucher. L'idée principale de ce modèle est de combiner la diffusion axée sur la courbure du modèle de Chan et Shen dans [32] avec les modèles élastiques d'Euler ("Euler's elastica") Dans ce cadre, voir aussi le travail de Chan et Shen dans [36].

La Figure A.5 est obtenue en utilisant les modèles élastiques d'Euler avec la diffusion axée sur la courbure (modèle (A.17)).

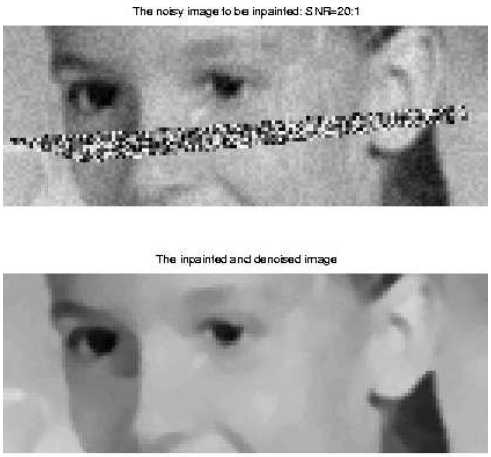

Figure A.5 – Retouche d'image avec le modèle de Chan, Kang, et Shen. Figure tirée de [31].

Modèle de Masnou et Morel

Le modèle de Masnou et Morel proposé dans [101] présente un modèle fonctionnel basé sur la même idée que le modèle précédent de Chan, Kang, et Shen dans [31]. Cela signifie qu'au lieu d'un modèle de courbes élastiques pour les lignes de niveau de l'image (A.11), ils ont réécrit l'énergie de courbes élastiques en termes d'une fonction de l'image u. Ensuite, le terme régularisé est donné par

$$R[u] := \int_{E \cup D} \Big(a + b(\nabla.(\frac{\nabla u}{|\nabla u|}))^2\Big)|\nabla u|dxdy, \tag{A.18}$$

où a et b sont deux constantes positives qui représentent des poids.

Dans la Figure A.6, la figure du dessus représente l'image originale. En outre, la figure en dessous, à gauche, représente les désocclusions effectuées en résolvant $(\nabla.(\frac{\nabla u}{|\nabla u|}))^2 = 0$. Les parties singulières de l'image ne peuvent pas être retouché mais les parties régulières de l'image sont bien récupérées. La figure en dessous, à droite, représente les désocclusions effectuées en résolvant le modèle proposé par Masnou et Morel dans [101]. Dans ce cas, les parties singulières de l'image sont bien récupérées.

FIGURE A.6 – Retouche d'image avec le modèle de Masnou et Morel. Figure tirée de [101]

.

A.3.3 Modèles en retouche basés sur l'énergie de Mumford–Shah

Dans ce paragraphe, on s'intéresse aux modèles proposés par Esedoglu et Shen dans [59]. Ces modèles sont basés sur le modèle de segmentation qui a été proposé par Mumford et Shah en 1989 dans [111]. On rappelle que l'énergie de Mumford–Shah proposée pour le problème de segmentation d'images est donnée par

$$E(u,K) := \int_{\Omega\setminus K} |\nabla u|^2 dx + \alpha \text{ Longueur}(K) + \lambda \int_{\Omega} (h-u)^2 dx, \quad u(x) \in L^2(\Omega), \tag{A.19}$$

où $K \subset \Omega$ est une union de courbes sur le bord et doit être Lipschitzienne.

Le premier modèle proposé dans [59] basé sur l'énergie de Mumford-Shah est un problème variationnel qui approxime une image donnée par une image régulière par morceaux de complexité minimale. Soit $\Omega \subset \mathbb{R}^2$ un domaine borné avec une frontière Lipshitzienne et $h(x) : \Omega \to [0,1]$ une image en niveaux de gris telle que h est une fonction mesurable bornée. Le problème de la retouche s'écrit :

$$\inf_{\substack{u(x) \in L^2(\Omega) \\ K \subset \Omega}} \Big\{ MS(u,K) := \int_{\Omega\setminus K} |\nabla u|^2 dx + \alpha \text{ Longueur}(K) + \lambda \int_{\Omega\setminus D} (h-u)^2 dx \Big\}. \tag{A.20}$$

Ici, l'ensemble K inconnu est supposé être une union de courbes et approche les arêtes de l'image donnée $h(x)$. La fonction $u(x)$, qui est aussi une inconnue du problème, est nécessairement régulière loin de l'ensemble des arêtes K par le terme de régularisation ($|\nabla u|^2$) qui apparaît dans cette énergie. $D \Subset \Omega$ est la région à retoucher. La dernière intégrale dans (A.20) représente le terme de fidélité et la contrainte de la fonction régulière par morceaux $u(x)$ de rester fermée au sens L^2 pour l'image donnée $h(x)$. La seule différence entre (A.20) et (A.19) est que le terme de fidélité est intégré sur $\Omega \backslash D$ au lieu d'être intégré sur tout le domaine Ω.

L'énergie (A.20) est très difficile à minimiser car une partie de la minimisation doit être effectuée sur des ensembles de courbes dans le plan. Ambrosio et Tortorelli ont introduit une énergie elliptique qui approche la fonctionnelle de Mumford-Shah dans le sens de la $\Gamma-$convergence (voir les détails dans [4]), dont le traitement numérique est par conséquent beaucoup plus facile.

Dans [4], l'approximation de $\Gamma-$convergence de l'ensemble des arêtes K est donnée par une fonction "signature" z_ε :

$$z_\varepsilon : \Omega \to [0, 1],$$

qui possède des valeurs proches de 1 presque partout sauf sur une partie (avec une largeur $O(\varepsilon)$) de K, où elle est proche de 0. Ainsi jusqu'à un facteur multiplicatif de normalisation d'ordre $O(1)$,

$$\frac{1}{\varepsilon}|1 - z_\varepsilon|^p, \quad p \geq 1,$$

est une approximation de la mesure de Dirac de $K - \delta_K(x)$:

$$\int_\Omega \delta_K(x) f(x) dx = \int_k f(x(s)) ds,$$

où s est l'abscisse curviligne. Par conséquent,

$$\text{Longueur}(K) = \int_K \delta_K(x) dx = c \int_\Omega \frac{|1 - z_\varepsilon|^p}{\varepsilon} dx,$$

où c est une constante. En fait, dans l'approximation de Ambrosio–Tortorelli, $p = 2$ et $z = z_\varepsilon$, et on peut minimiser (A.19) par

$$E_\varepsilon[z \backslash u] = \int_\Omega z^2 |\nabla u|^2 dx + \alpha \int_\Omega (\varepsilon |\nabla u|^2 + \frac{(1 - z)^2}{4\varepsilon}) dx + \lambda \int_\Omega (h - u)^2 dx$$

(z^2 doit être $z^2 + o(z)$). Par rapport au modèle de débruitage de l'image (A.19), elle est basée sur deux approximations (couplées) (à une constante multiplicative près d'ordre un)

$$\int_{\Omega \backslash K} |\nabla u|^2 dx \simeq \int_\Omega z^2 |\nabla u|^2 dx$$

et

$$\text{Longueur}(K) \simeq \int_\Omega (\varepsilon |\nabla z|^2 + \frac{(1 - z)^2}{4\varepsilon}) dx.$$

L'inconvénient de l'approximation est que les arêtes de l'image sont représentées par des interfaces diffuses, par opposition à celles tranchantes. Comme mentionné ci-dessus, la largeur de bande de transition de l'arête z est d'ordre ε. En outre, l'épaisseur de l'interface diffuse ε

doit être choisie très petite en théorie et la taille de la grille numérique impose une borne inférieure. Par conséquent, numériquement ε conduit à des transitions assez diffuses et augmente l'incertitude des emplacements de bord.

En résumé, l'énergie (A.20) pour la retouche est approximée dans le sens de la $\Gamma-$convergence par

$$MS_\varepsilon(u,z) = \int_\Omega \Big(z^2|\nabla u|^2 + \alpha\Big(\varepsilon|\nabla z|^2 + \frac{(1-z)^2}{4\varepsilon}\Big)\Big)dx + \lambda\int_{\Omega\setminus D}(h-u)^2dx. \tag{A.21}$$

La conséquence est que tout point d'accumulation de minimiseurs de (A.21) doit minimiser (A.20). Ces approximations sont souvent appelées approximations d'interfaces diffuses parce que, pour une valeur fixe de ε, le minimiseur approche le problème d'interface nette dans lequel il y a une interface d'épaisseur d'ordre ε. Les schémas numériques basés sur l'approximation de $\Gamma-$convergence (A.21) sont beaucoup plus simple et convergent rapidement (voir [59])

La Figure A.7 montre une application de la technique d'effacement automatique de texte par le modèle de retouche basé sur l'approximation (A.21). On note aussi que les exemples avec le modèle (A.21) dans [59] ont été comparés avec le modèle de Masnou et Morel dans [101].

Figure A.7 – Retouche d'image avec le modèle généralisé de Mumford-Shah. Figure tirée de [59].

Le deuxième modèle proposé dans [59] est une autre modification de l'énergie de Mumford–Shah obtenue en utilisant la courbe élastique d'Euler

$$e(K) = \int_\Omega(\alpha+\beta\kappa^2)ds = \alpha\,\text{Longueur}(K) + \beta\int_K \kappa^2 ds.$$

Ici, κ désigne la courbure, ds est l'élément de longueur, et α et β sont deux poids positifs (voir aussi les travaux basés sur la courbe élastique d'Euler proposés par Masnou et Morel et Chan, Kang, et Shen détaillés ci-dessus). L'énergie de débruitage de l'image (énergie de Mumford–Shah) (A.19) devient

$$\begin{aligned} E[u,K] &= \int_{\Omega\setminus K}|\nabla u|^2dx + e(K) + \lambda\int_\Omega(h-u)^2dx \\ &= \int_{\Omega\setminus K}|\nabla u|^2dx + \int_K(\alpha+\beta\kappa^2)ds + \lambda\int_\Omega(h-u)^2dx \end{aligned}$$

et celle de la retouche (A.20) devient

$$MSE(u,K) = \int_{\Omega\setminus K}|\nabla u|^2dx + \int_K(\alpha+\beta\kappa^2)dx + \lambda\int_{\Omega\setminus D}(u-h)^2dx. \tag{A.22}$$

L'énergie (A.22) est également difficile à minimiser, comme l'énergie (A.20). En effet, d'après la conjecture de De Giorgi dans [78] et ensuite le travail de Dolcetta, Vita, et March dans [51] on approche le modèle (A.22) par l'approximation de l'interface diffuse par une énergie elliptique sur la "signature" z :

$$E_\varepsilon[z] = \alpha \int_\Omega (\varepsilon|\nabla z|^2) + \frac{1}{\varepsilon}F(z))dx + \frac{\beta}{\varepsilon}\int_\Omega (2\varepsilon\Delta z - \frac{1}{\varepsilon}F'(z))^2 dx + \lambda \int_{\Omega\setminus D}(u-h)^2 dx, \tag{A.23}$$

où

$$F(z) = z^2(z-1)^2.$$

Puis, le modèle d'interface diffuse de (A.22) est décrit par une énergie elliptique sur les signatures u et z :

$$\begin{aligned} MSE_\varepsilon(u,z) = \int_\Omega \Big(z^2|\nabla u|^2 + \alpha\Big[\varepsilon|\nabla z|^2 + \frac{1}{\varepsilon}W(z)\Big] + \frac{\beta}{\varepsilon}\Big[2\varepsilon\Delta z - \frac{1}{\varepsilon}W'(z)\Big]^2\Big)dx \\ + \lambda\int_{\Omega\setminus D}(u-f)^2 dx. \end{aligned} \tag{A.24}$$

Les équations de descente de gradient pour (A.24) par rapport au produit scalaire L^2 sont

$$u_t = \nabla.(z^2\nabla u) + \lambda(f-u), \tag{A.25}$$

et

$$z_t = \Big(\alpha + \frac{\beta}{2\varepsilon^2}W''(z) - 4\beta\Delta\Big)\Big(2\varepsilon\Delta z - \frac{1}{4\varepsilon}W'(z)\Big) - |\nabla u|^2 z. \tag{A.26}$$

A.3.4 Modèles en retouche basés sur l'énergie de Ginzburg–Landau

Tout d'abord, on note que l'application de l'énergie de Ginzburg–Landau dans le problème de la retouche résulte du modèle proposé dans [59] (voir le paragraphe précédent). En particulier, on prend $\alpha = \frac{1}{2}, \beta = 0$ et $\lambda = 0$ dans (A.23) pour obtenir

$$E_\varepsilon[z] = \int_\Omega (\frac{\varepsilon}{2}|\nabla z|^2) + \frac{1}{2\varepsilon}F(z))dx, \tag{A.27}$$

qui est exactement l'énergie de Ginzburg–Landau (introduite dans l'introduction).

Modèle de retouche par l'équation complexe de Ginzburg–Landau

Une approche différente du problème de retouche d'images en niveaux de gris a été proposé par Grossauer et Scherzer en 2003 dans [81]. Ils ont proposé de traiter l'image donnée comme complexe, où la partie réelle est la valeur du point de l'image en niveaux de gris, tandis que la partie imaginaire est la contrainte de placement de la frontière dans un cercle de rayon 1 dans le plan complexe.

L'énergie complexe de Ginzburg–Landau est

$$F(u,\nabla u) = \frac{1}{2}\int_\Omega \Big(|-i\nabla u|^2 + \alpha|u|^2 + \frac{\beta}{2}|u|^4\Big)dx, \tag{A.28}$$

où α et β sont des constantes ($\alpha < 0$, $\beta > 0$). Ensuite, l'équation de descente de Ginzburg–Landau est

$$\frac{\partial u}{\partial t} = \Delta u + \frac{1}{\varepsilon^2}(1 - |u|^2)u. \tag{A.29}$$

La solution de l'équation (A.29) est de la forme $u(x,t) = u_1(x,t) + iu_2(x,t)$, où la valeur initiale de $u_2(x,t)$ est donnée par

$$u_2(x,0) = \sqrt{1 - u_1(x,0)^2}. \tag{A.30}$$

Cela conduit à un système d'équations couplées pour $u_1(x,t)$ et $u_2(x,t)$. Les auteurs dans [81] ont résolu ce système dans le domaine à retoucher D par un schéma numérique explicite en supposant des conditions au bord de type Dirichlet $u(x,t)|_{\partial D} = u(x,0)|_{\partial D}$.

Dans la Figure A.8, les conditions aux limites sont discontinues et il faut prolonger les lignes de niveau d'une manière appropriée dans le domaine à retoucher. Ils sont basés sur l'extrapolation des caractéristiques géométriques de l'image, en particulier le bord, c'est-à-dire que l'on crée des régions à l'intérieur du domaine de retouche.

(a)

(b)

(c)

FIGURE A.8 – (a) Image originale. (b) Retrait d'une partie de l'image. (c) Résultat final de la retouche obtenue par le modèle de Ginzburg–Landau. Figure tirée de [82].

En utilisant la même méthodologie, récemment Belhachmi et al. dans [13] ont proposé une stratégie pour adapter le maillage lors de la résolution de l'équation complexe de Ginzburg–

Landau dans le problème de retouche d'images en niveaux de gris. Soit h_1 une image donnée où $h_1 : \Omega \to [-1, 1]$. On généralise la fonction h_1 par une fonction $h : \Omega \to \mathbb{C}$ telle que $h(x) = h_1(x) + ih_2(x), \ \forall x \in \Omega$, avec $h_2 := \sqrt{1 - h_1^2}$. En outre, pour les images en niveaux de gris, les auteurs ont proposé de minimiser l'énergie de type Ginzburg–Landau sous la forme suivante :

$$\mathcal{E}(u) = \int_\Omega \Big[\frac{\alpha(x)|\nabla u|^2}{2} + \frac{1}{\varepsilon^2}F(u)\Big]dx + \frac{\lambda_0}{2}\int_{\Omega\setminus D}(u-h)^2dx, \tag{A.31}$$

où $F(u) = \frac{1}{4}(1 - |u^2|)^2$. Ainsi le problème évolutif basé sur l'énergie (A.31) s'écrit sous la forme suivante :

$$\frac{\partial u_\alpha}{\partial t} - \nabla.[\alpha(x)\nabla u_\alpha] + \frac{1}{\varepsilon^2}f(u_\alpha) + \lambda_0\chi_{\Omega\setminus D}(x)(u_\alpha - h) = 0, \qquad \text{dans } \Omega, \tag{A.32}$$

$$\alpha(x)(u_\alpha.\vec{n}) = 0, \qquad \text{sur } \partial\Omega, \tag{A.33}$$

$$u_\alpha|_{t=0} = h = h_1 + ih_2, \tag{A.34}$$

où $\vec{n}$ est le vecteur normal unitaire et $f(u_\alpha) = F'(u_\alpha) = (|u_\alpha^2| - 1)u_\alpha$.

Enfin, pour vérifier l'efficacité de ce modèle dans le problème de retouche, les auteurs dans [13] ont utilisé un schéma numérique en utilisant les éléments finis $P1$ pour la discrétisation en espace et une discrétisation d'Euler semi-implicite en temps (voir, par exemple, la Figure A.9).

FIGURE A.9 – Retouche d'image avec le modèle de Belhachmi et al.. Figure tirée de [13].

Modèle de retouche par l'équation de Cahn–Hilliard

Bertozzi, Esedoglu, et Gillette ont introduit dans [16, 17] une généralisation de l'équation de

Cahn–Hilliard pour résoudre le problème de la retouche d'images binaires. Ce modèle a de nombreuses propriétés avantageuses vérifiées par le modèle de Esedoglu et Shen dans [59], mais pour lesquelles il y a des techniques de calcul disponibles très rapides. En particulier, ils ont montré que, dans le cas des images binaires, une légère modification de l'équation de Cahn–Hilliard, permet d'obtenir de très bons résultats de retouche, meilleurs que ceux obtenus dans [59] et également beaucoup plus rapides.

L'équation de Cahn–Hilliard possède certaines caractéristiques qui la rendent intéressante à des fins de retouche. Le fait d'imposer des conditions aux limites à la fois pour la solution $u(x)$ et sa dérivée ∇u est l'un des grands avantages des modèles d'ordre 4. En effet, il permet d'obtenir une information d'image générée par le modèle dans la région à retoucher D pour correspondre aux données d'image originale définies sur $\Omega\backslash D$ non seulement en intensité u, mais aussi dans des directions isophotes $\nabla^{\perp}u$. Cela signifie que le modèle permet de construire les arêtes dans le domaine à retoucher sans introduire de condition supplémentaire à la frontière ∂D. Un modèle de retouche du quatrième ordre basé sur l'équation de Cahn–Hilliard résoud le problème de continuité des isophotes et permet la retouche d'images dans de grands domaines à retoucher.

L'équation de Bertozzi–Esedoglu–Gillette–Cahn–Hilliard s'écrit

$$\frac{\partial u}{\partial t} + \varepsilon\Delta^2 u - \frac{1}{\varepsilon}\Delta f(u) + \lambda_0\chi_{\Omega\backslash D}(x)(u-h) = 0, \qquad \text{dans } \Omega, \tag{A.35}$$

où $f(s) = F'(s)$ avec $F(s) = s^2(1-s)^2$. L'équation (A.35) est associée aux conditions aux limites de type Neumann

$$\frac{\partial u}{\partial \nu} = \frac{\partial \Delta u}{\partial \nu} = 0, \qquad \text{sur } \partial\Omega. \tag{A.36}$$

Les simulations dans [16, 17] sont données par un schéma numérique basé sur la décomposition convexe de l'énergie. Ce schéma en deux étapes sur l'épaisseur de l'interface diffuse ε ; plus précisément, le bord du domaine à retoucher se connecte avec une grande épaisseur ε et on obtient le résultat final de retouche avec une valeur de l'épaisseur ε très petite.

La figure A.10 montre l'efficacité du modèle de Bertozzi, Esedoglu, et Gillette basé sur l'équation de Cahn–Hillard pour la retouche d'images binaires. On remarque que les bords du domaine à retoucher (en gris dans la figure à gauche) restent continues dans le résultat final de la retouche.

Plusieurs résultats numériques sont effectués sur ce modèle, voir par exemple [87, 20]. Les résultats dans [87] sont toujours effectués avec un potentiel F régulier de type polynomial, tandis que les auteurs de [20] considèrent un potentiel F non régulier à double obstacle. Dans ce cas, les résultats obtenus sont meilleurs que ceux considérés avec le potentiel régulier de type polynomial.

Enfin, Burger, He, et Schönlieb dans [25] ont proposé une généralisation de l'application de l'équation de Cahn–Hilliard avec une variation totale dans H^{-1}. Cette variation totale est obtenue en utilisant le résultat de $\Gamma-$convergence de l'énergie de Cahn–Hilliard. On note que l'énergie de Cahn–Hilliard converge dans le sens de la $\Gamma-$convergence pour ε tendant vers 0 vers

$$\mathcal{E}(u) = \begin{cases} C_0 \displaystyle\int_\Omega |Du| & \text{si } u = 1_\Sigma, \text{ pour tout } \Sigma \in BV(\Omega) \\ +\infty & \text{ailleurs,} \end{cases}$$

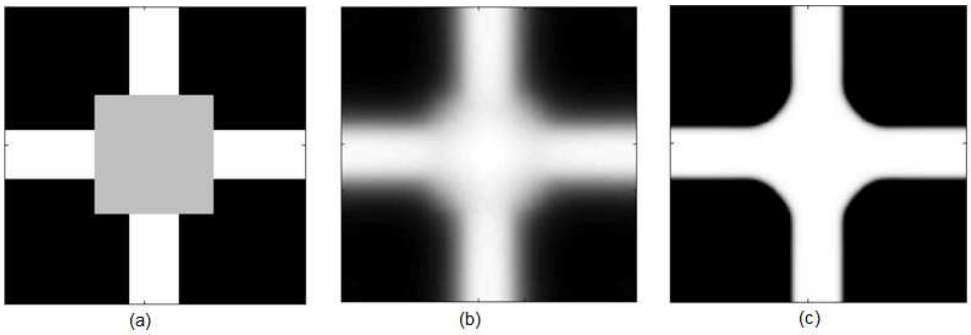

FIGURE A.10 – Retouche d'image binaire avec l'équation de Bertozzi–Esedoglu–Gillette–Cahn–Hilliard. Figure tirée de [16].

où 1_Σ représente la fonction caractéristique de Σ. La variation totale H^{-1} de la retouche est

$$\frac{\partial u}{\partial t} - \Delta p + \lambda_0 \chi_{\Omega\setminus D}(x)(u-h) = 0, \quad p \in \partial E(u),$$

où h représente toujours l'image originale ($h \in L^2(\Omega)$).

On note qu'un élément $p \in \partial E(u)$ avec $|u(x)| \leq 1$ pour tout $x \in \Omega$ satisfait les trois équations suivantes :

$$p = -\nabla.\Big(\frac{\nabla u}{|\nabla u|}\Big) \quad p.p.\ \text{sur supp}(\{|u| < 1\}),$$

$$p = -\nabla.\Big(\frac{\nabla u}{|\nabla u|}\Big) + \tilde{p}, \ \ \tilde{p} \leq 0 \quad p.p.\ \text{sur supp}(\{|u| = -1\}),$$

$$p = -\nabla.\Big(\frac{\nabla u}{|\nabla u|}\Big) + \tilde{p}, \ \ \tilde{p} \geq 0 \quad p.p.\ \text{sur supp}(\{|u| = 1\}),$$

où $\tilde{p} \in \partial 1_{\{|u|\leq 1\}}(u)$.

Les simulations dans [25] sont données par un schéma numérique basé sur la décomposition convexe de l'énergie. Dans ce schéma, les auteurs utilisent la régularisation par la racine carrée, c'est-à-dire

$$|\nabla u| \approx \sqrt{|\nabla u|^2 + \delta^2}$$

et le résultat final de retouche est obtenu pour δ assez petit.

La figure A.11 montre l'efficacité du modèle de variation totale H^{-1} basé sur l'énergie de Cahn–Hillard pour la retouche d'images digitales (images en niveaux de gris).

Modèle de retouche par l'équation de Ginzburg–Landau ondelette

On définit le Laplacien ondelette Δ_w pour une base d'ondelettes orthonormale $\{\Psi_{j,k}\}$ et pour toute fonction $v \in L^2(\Omega)$ par

$$\Delta_w v := -\sum_{j=1}^{\infty} 2^{2j}((v, \Psi_{j,k}))\Psi_{j,k}.$$

La fonctionnelle d'énergie pondérée qui minimise l'équation

$$\frac{\partial u}{\partial t} = \Delta_w u$$

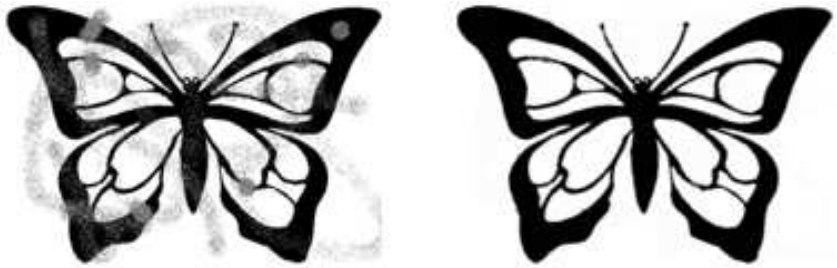

FIGURE A.11 – Retouche d'image avec la vartiation totale H^{-1}. Figure tirée de [25].

est donnée par

$$\mathcal{E}_w(u) := \frac{1}{2}\sum_{j=1}^{\infty} |2^{2j}((u, \Psi_{j,k}))|^2.$$

Les auteurs dans [50] ont alors proposé l'énergie de type Ginzburg–Landau suivante pour résoudre le problème de la retouche :

$$\mathcal{E}(u) = \frac{\varepsilon}{2}\mathcal{E}_w(u) + \frac{1}{4\varepsilon}F(u) + \frac{\lambda_0}{2}\int_{\Omega\setminus D}(u-h)^2 dx.$$

L'équation de descente de gradient correspondant est

$$\frac{\partial u}{\partial t} - \varepsilon\Delta_w u - \frac{1}{\varepsilon}f(u) + \lambda_0\chi_{\Omega\setminus D}(x)(u-h) = 0,$$

où $f = F'$ et h l'image originale dans $L^2(\Omega)$.

Pour généraliser la solution de ce modèle afin de l'appliquer à la retouche d'images en niveaux de gris, on utilise l'approximation suivante :

$$u(x) \approx \sum_{i=0}^{K-1} u_i(x)2^{-i},$$

où u_i désigne la i-ème composante dans la représentation binaire du signal et $u_i(x) \in \{0, 1\}$ pour tout x. Le problème se réduit à K problèmes dyadiques de retouche, où chaque terme de fidélité est obtenu comme étant une composante respective de la partie connue de l'image (voir la Figure A.12).

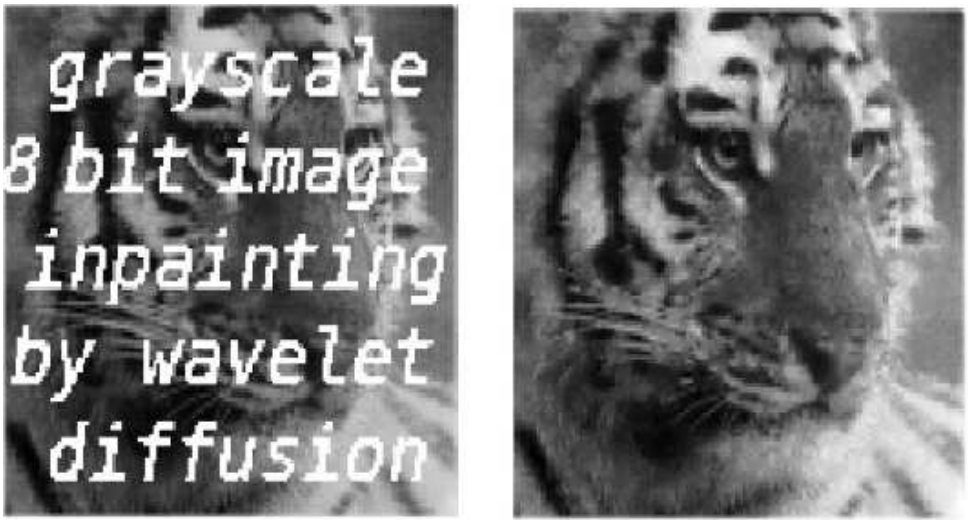

FIGURE A.12 – Retouche d'image avec le Laplacien ondelette. Figure tirée de [50].

Annexe B

The Cahn–Hilliard equation as a gradient flow

B.1 Some definitions and properties of the dual of H^1 with Neumann boundary conditions

We start by introducing negative norms and the spaces $H^{-m}(\Omega)$ following [149], Appendix, Distributions and Sobolev spaces, page 1055. Let $m \in \mathbb{N}$, $\mathcal{D}(\Omega) = C_0^\infty(\Omega)$ and $\mathcal{D}'(\Omega)$ be the space of distributions with the usual topology (cf. e.g. [147], Section 1.4). Then for $U \in \mathcal{D}'(\Omega)$ we define the negative norm ($\| \, . \, \|_m = \| \, . \, \|_{H^m(\Omega)}$)

$$\|U\|_{-m} := \sup_{\varphi \in \mathcal{D}(\Omega)} \frac{\|U(\varphi)\|}{\|\varphi\|_m}$$

Definition B.1.1. *The space $H^{-m}(\Omega)$ is defined as follow*

$$H^{-m}(\Omega) := \{U \in \mathcal{D}'(\Omega) : \|U\|_{-m} < \infty\}$$

Theorem B.1.2.

$$H^{-m} = [H_0^m]' = \mathcal{L}(H_0^m, \mathbb{R})$$

Proof. *Let $U \in [H_0^m]'$ be given, i.e., U be a continuous linear functional on $H_0^m(\Omega)$ with norm $\|U\|_{\mathcal{L}(H_0^m,\mathbb{R})} = \sup_{\varphi \in H_0^m(\Omega)} \frac{\|U(\varphi)\|}{\|U\|_m}$. Since $\mathcal{D}(\Omega) \subset H_0^m(\Omega)$, we have*

$$\|U(\varphi)\| \leq \|U\|_{-m} \|\varphi\|_m \quad \textit{for all } \varphi \in \mathcal{D}(\Omega).$$

Since $\mathcal{D}(\Omega)$ is dense in $H_0^m(\Omega)$, by the Hahn-Banach Theorem, U can be uniquely extended to a linear continuous functional $\tilde{U}$ on $H_0^m(\Omega)$ with the same norm, i.e.,

$$\|\tilde{U}\|_{\mathcal{L}(H_0^m(\Omega),\mathbb{R})} = \|U\|_{-m}$$

□

Concerning the elements of $H^{-m}(\Omega)$ we have the following representation theorem :

Theorem B.1.3. *Let $u_\alpha \in L^2(\Omega)$, for all α, $|\alpha| \leq m$, be given. We set*

$$U(\varphi) := \sum_{|\alpha|\leq m} (u_\alpha, \mathcal{D}^\alpha \varphi)_0, \quad \varphi \in \mathcal{D}(\Omega). \tag{B.1}$$

Then $U \in H^{-m}(\Omega)$, and conversely, each $U \in H^{-m}(\Omega)$ can be represented in the form (B.1)

Proof. *The first assertion is obvious because $\|U(\varphi)\| \leq \left(\sum_{|\alpha|\leq m} \|u_\alpha\|_0^2\right)^{\frac{1}{2}} \|\varphi\|_m$. To obtain the form (B.1) for $U \in H^{-m}(\Omega)$ we apply Theorem B.1.2 and the Riesz Representation Theorem.* □

By the last theorem we may now view $H^{-m}(\Omega)$ as the cross product between $X_{|\alpha|\leq m}$ and $L^2(\Omega)$, where

$$X_{|\alpha|\leq m} = \{\mathcal{D}^\alpha \varphi, \ \ \forall |\alpha| \leq m, \ \ \forall \phi \in \mathcal{D}(\Omega)\}.$$

In this sense, we have

$$\ldots \subset H^2(\Omega) \subset H^1(\Omega) \subset L^2(\Omega) \subset H^{-1}(\Omega) \subset \ldots$$

This motivates the notation "H^{-m}". In particular, we can give the

Definition B.1.4. *The space $\dot{H}^{-1}(\Omega)$ is defined as follows :*

$$\dot{H}^{-1}(\Omega) := \left\{ v \in H^{-1}(\Omega) / \int_\Omega v dx = 0 \right\} \subset H^{-1}(\Omega).$$

We observe that $v \in \dot{H}^{-1}(\Omega)$ if and only if the Neumann boundary value problem

$$\begin{cases} -\Delta \Phi = v & \text{in } \Omega \\ \dfrac{\partial \Phi}{\partial \nu} = 0 & \text{on } \partial\Omega \end{cases} \tag{B.2}$$

has a unique solution $\Phi = \Phi_v(x)$ in $H^1(\Omega)$ and satisfying $\int_\Omega \Phi(x) dx = 0$. Following this equation, for any $v \in \dot{H}^{-1}(\Omega)$ there is a unique Φ_v with the above proprieties.

Lemma B.1.5. *The space $\dot{H}^{-1}(\Omega)$ endowed with*

$$(v_1, v_2)_{\dot{H}^{-1}(\Omega)} := \left(\nabla \Phi_{v_1}, \nabla \Phi_{v_2}\right)_0$$

is a Hilbert space. Furthermore, $\|v\|_{-1}$ and $\|v\|_{\dot{H}^{-1}(\Omega)} = \|\nabla \Phi_v\|_0$ are equivalent norms on $\dot{H}^{-1}(\Omega)$.

Proof. *By the representation given in Theorem B.1.2 any $v \in L^2(\Omega)$ defines a distribution $T_v \in H^{-1}(\Omega) \subset \mathcal{D}'(\Omega)$*

$$T_v(\varphi) := \int_\Omega v\varphi dx, \quad \varphi \in \mathcal{D}(\Omega),$$

and by definition

$$\|v\|_{-1} = \|T_v\|_{-1} = \sup_{\varphi \in \mathcal{D}(\Omega)} \frac{(v, \varphi)_0}{\|\varphi\|_1}.$$

Now $\mathcal{D}(\Omega) \subset H_0^1(\Omega)$ and on $H_0^1(\Omega)$ it is known that $\|\varphi\|_1$ and $\|\nabla\varphi\|_0$ are equivalent norms. Hence $\|T_v\|_{-1}$ is equivalent to

$$\begin{aligned}\|T_v\|_{\dot{H}^{-1}(\Omega)} :&= \sup_{\varphi\in\mathcal{D}(\Omega)} \frac{(v,\varphi)_0}{\|\nabla\varphi\|_0} = \sup_{\varphi\in\mathcal{D}(\Omega)} \frac{(-\Delta\Phi_v,\varphi)_0}{\|\Delta\phi\|_0} \\ &= \sup_{\varphi\in\mathcal{D}(\Omega)} \frac{(\nabla\Phi_v,\varphi)_0}{(\nabla\varphi,\nabla\varphi)_0^{\frac{1}{2}}} = \|\nabla\Phi_v\|_0,\end{aligned}$$

and the Lemma is proved. □

B.2 Gradient Flow in $\dot{H}^{-1}(\Omega)$

We first define the mathematical concept of gradient flows as defined in [106, 118].

Definition B.2.1 (Gradient flow)**.** *Let V a Banach space, H a Hilbert space and $S(t),\ t \geq 0$, on V a semiflow. We say that the semiflow S is a gradient flow on H if there exist $E : V \to \mathbb{R}$ and $h : V \to H$ such that, for every $T > 0$ and $\varphi_0 \in V$, we have*

$$E(S(.)\varphi_0) \in H^1(0,T), \qquad \frac{\partial S(.)\varphi_0}{\partial t},\ h(S(.)\varphi_0) \in L^2(0,T,H), \tag{B.3}$$

$$\frac{d}{dt}E(S(.)\varphi_0) = \left\langle h(S(.)\varphi_0), \frac{\partial S(.)\varphi_0}{\partial t}\right\rangle_H \qquad in L^2(0,T), \tag{B.4}$$

$$\frac{\partial S(.)\varphi_0}{\partial t} = -h(S(.)\varphi_0) \qquad in L^2(0,T,H), \tag{B.5}$$

where $h(S(.)\varphi_0)$ is called the gradient of E at $S(t)\varphi_0$ in H and is denoted by $grad_H E(S(t)\varphi_0)$. We then have the evolution law

$$\frac{\partial S(t)\varphi_0}{\partial t} = -grad_H E(S(t)\varphi_0) \qquad in L^2(0,T,H). \tag{B.6}$$

This equation says that $S(t)\varphi_0$ evolves in the direction opposite to the gradient of E. This is a way, for the system, to dissipate its energy. Indeed, by (B.4)*,* (B.5)*,*

$$\frac{d}{dt}E(S(t)\varphi_0) = -\|grad_H E(S(t)\varphi_0)\|_H^2 \leq 0. \tag{B.7}$$

Moreover, this dissipation is optimal for gradient flows in the sense that, for a given velocity, the decay rate of the energy is maximal for smooth gradient flows. More precisely, let $u : [0,T] \to V$ be a smooth trajectory starting from φ_0. Let us assume that

$$\frac{d}{dt}E(u(t))|_{t=0} = \left\langle grad_H E(u(0)), \frac{\partial u}{\partial t}(0)\right\rangle_H$$

and $\|\frac{\partial u}{\partial t}(0)\|_H = \|\frac{\partial S(.)\varphi_0}{\partial t}(0)\|_H$. Then, in view of (B.6)*,* (B.7)*,*

$$\frac{d}{dt}E(u(t))|_{t=0} \geq -\|grad_H E(S(t)\varphi_0)\|_H\|\frac{\partial u}{\partial t}(0)\|_H = \frac{d}{dt}E(S(t)\varphi_0)|_{t=0}.$$

We now intend to define a gradient flow for the energy

$$E(u) = E_\varepsilon(u) = \int_\Omega \Big(\frac{\varepsilon^2}{2}|\nabla u|^2 + W(u)\Big)dx.$$

This is mainly along the lines of Fife [65]. In order to find the evolution in $M_{\tilde{v}} = \langle u\rangle + M_0$ $\Big(M$ is a Hilbert space, $M_0 \subset M$, $\langle u\rangle = \frac{1}{|\Omega|}\int_\Omega u(t,x)dx$ and $M_0 = \{u \in M/\int_\Omega u dx = 0\}\Big)$, we need to define $\nabla E(u) \in \{w \in L^2(\Omega)/\int_\Omega w = 0\}$ such that

$$\frac{d}{dt}E(u + t.v)|_{t=0} = (\nabla E(u), v)_H \quad \text{for all } v \in M_0,$$

where we intend to use the scalar product in $H = \dot{H}^{-1}(\Omega)$. We choose $T = M_0$ and hence $S = cl_H(T) = \dot{H}^{-1}(\Omega)$. Since $v \in M_0 \subset \{w \in L^2(\Omega)/\int_\Omega w = 0\}$, we can choose a unique $\Phi = \Phi_v$. Then

$$\begin{aligned}\frac{d}{dt}E(u + t.v)|_{t=0} &= \frac{d}{dt}E(u - t\Delta\Phi_v)|_{t=0}\\ &= \int_\Omega [-\varepsilon^2\Delta u - W'(u)](-\Delta\Phi_v)dx.\end{aligned}$$

An integration by parts yields

$$\frac{d}{dt}E(u + t.v)|_{t=0} = \int_\Omega \nabla(-[\varepsilon^2\Delta u - W'(u)])(\nabla\Phi_v)dx,$$

where the boundary term vanishes in view of the Neumann boundary conditions for Φ_v. We need

$$\frac{\partial}{\partial\nu}(\varepsilon^2\Delta u + W'(u)) = 0 \quad \text{on } \partial\Omega,$$

such that $\Phi_{\tilde{v}} = -(\varepsilon^2\Delta u + W'(u) + c)$ (for a suitable c) is the unique solution for the Neumann Problem for $\tilde{v} := -\Delta\Phi_{\tilde{v}} = \Delta(\varepsilon^2\Delta u + W'(u))$. Hence

$$\frac{\partial}{\partial t}E(u + t.v)|_{t=0} = (\nabla\Phi_{\tilde{v}}, \nabla\Phi_v)_0 = (\tilde{v}, v)_{\dot{H}^{-1}(\Omega)} \quad \text{for all } v \in M_0.$$

Using

$$\frac{\partial}{\partial t}E(u(t))|_{t=0} = (w_0, \frac{\partial u}{\partial t}(0))_{\mathbb{R}^n},$$

we thus choose

$$\nabla_{\dot{H}^{-1}(\Omega)}E(u) := \Delta(\varepsilon^2\Delta u + W'(u)).$$

The corresponding evolution equation for $t \geq 0$ is exactly the Cahn-Hilliard equation

$$\begin{cases} u_t = -\Delta(\varepsilon^2\Delta u + W'(u)), & \text{in } \Omega,\\ 0 = \dfrac{\partial u}{\partial\nu} = \dfrac{\partial}{\partial\nu}(\varepsilon^2\Delta u + W'(u)), & \text{on } \partial\Omega \end{cases} \tag{B.8}$$

Corollary 8. *The solutions $u = u(t, x)$ of (B.8) are mass preserving, i.e.,*

$$\langle u \rangle := \int_\Omega u(t, x) dx \in \mathbb{R}$$

is a constant in time. Furthermore, $E = E_\varepsilon$ is a Lyapunov functional for these solutions

$$\frac{d}{dt} E(u(t)) = -\left\| \frac{d}{dt} u(t) \right\|^2_{\dot{H}^{-1}(\Omega)} \leq 0.$$

Annexe C

Full proofs of Theorems 7 and 8 in Chapter 5

We recall that the initial and boundary value problem is written as

$$\frac{\partial u}{\partial t} + \Delta^2 u - \Delta f(u) + g(x,u) = 0, \tag{C.1}$$

$$u = \Delta u = 0 \qquad \text{on } \Gamma, \tag{C.2}$$

$$u|_{t=0} = u_0, \tag{C.3}$$

in a bounded and regular domain $\Omega \subset \mathbb{R}^n$, $n = 1,\ 2$, or 3, with boundary Γ.

We make the following assumptions :

$$f \in C^2(\mathbb{R}),\ f(0) = 0,\ \ g \in L^2(\Omega), \tag{C.4}$$

$$f'(s) \geq -c_0,\ \ c_0 \geq 0,\ \ s \in \mathbb{R}, \tag{C.5}$$

$$f(s)s \geq c_1 F(s) - c_2, F(s) \geq -c_3,\ \ c_1 > 0,\ \ c_2, c_3 \geq 0,\ \ s \in \mathbb{R}, \tag{C.6}$$

where $F(s) = \int_0^s f(\tau)d\tau$,

$$g \text{ is of class } C^1 \ \text{ with respect to } u, \tag{C.7}$$

$$\begin{gathered} \|u\| \int_\Omega |g(x,u)|dx \leq \varepsilon \int_\Omega F(u)dx + c_\varepsilon,\ \ \forall u \in L^2(\Omega) \\ \text{such that } \int_\Omega F(u)dx < +\infty,\ \ \varepsilon > 0, \end{gathered} \tag{C.8}$$

$$\begin{gathered} g(x,u)u \leq cF(u) + c',\ \ \forall x \in \Omega,\ \ \forall u \in L^2(\Omega) \\ \text{such that } \int_\Omega F(u)dx < +\infty,\ \ \varepsilon > 0,\ \ c \geq 0. \end{gathered} \tag{C.9}$$

Remark C.0.2. *In particular, these assumptions are satisfied by polynomials of degree $2p+1$ and $2p$, respectively, $p \geq 1$, of the form $f(s) = \sum_{i=1}^{2p+1} a_i s^i$, $a_{2p+1} > 0$ and $g(s) = \sum_{i=0}^{2p} b_i s^i$ (e.g., when f has degree three and g has degree two).*

We denote by $\|.\|$ the usual L^2-norm (with associated scalar product $((.,.)))$ and set $\|.\|_{-1} = \|(-\Delta)^{-\frac{1}{2}}.\|$, where $-\Delta$ denotes the minus Laplace operator with Dirichlet boundary conditions. More generally, $\|.\|_X$ denotes the norm in the Banach space X.

Throughout this paper, the same letter c (and, sometimes, c' and c'') denotes constants which may vary from line to line, or even in a same line. Similarly, the same letter Q denotes monotone increasing (with respect to each argument) functions which may vary from line to line, or even in a same line.

C.1 A priori estimates

In what follows, the Poincaré, Hölder and Young inequalities are extensively used, without further referring to them. We rewrite (C.1) in the equivalent form

$$(-\Delta)^{-1}\frac{\partial u}{\partial t} - \Delta u + f(u) + (-\Delta)^{-1}g(x,u) = 0. \tag{C.10}$$

We multiply (C.10) by u and have, integrating over Ω and by parts,

$$\frac{1}{2}\frac{d}{dt}\|u\|_{-1}^2 + \|\nabla u\|^2 + ((f(u),u)) + (((-\Delta)^{-1}g(x,u),u)) = 0. \tag{C.11}$$

Using the fact that

$$\begin{aligned}
|(((-\Delta)^{-1}g(x,u),u))| &= |((g(x,u),(-\Delta)^{-1}u))| \\
&\leq \int_\Omega |g(x,u)||(-\Delta)^{-1}u|dx \\
&\leq \|(-\Delta)^{-1}u\|_{L^\infty(\Omega)}\int_\Omega |g(x,u)|dx \\
&\leq \|u\|\int_\Omega |g(x,u)|dx \\
&\leq \text{(thanks to } (C.8)) \\
&\leq \varepsilon\int_\Omega F(u)dx + c_\varepsilon,
\end{aligned}$$

owing to the continuous embedding $H^2(\Omega)\subset L^\infty(\Omega)$, we find, owing to (C.6),

$$\frac{d}{dt}\|u\|_{-1}^2 + c\Big(\|u\|_{H^1(\Omega)}^2 + \int_\Omega F(u)dx\Big) \leq \frac{c}{2}\int_\Omega F(u)dx + c', \quad c>0, \tag{C.12}$$

hence

$$\frac{d}{dt}\|u\|_{-1}^2 + c\Big(\|u\|_{H^1(\Omega)}^2 + \int_\Omega F(u)dx\Big) \leq c', \quad c>0. \tag{C.13}$$

We then multiply (C.10) by Δu and find

$$\frac{1}{2}\frac{d}{dt}\|u\|^2 + \|\Delta u\|^2 + ((f'(u)\nabla u,\nabla u)) + ((g(x,u),u)) = 0. \tag{C.14}$$

We deduce from (C.5) and (C.9) that

$$\frac{d}{dt}\|u\|^2 + c\|u\|^2_{H^2(\Omega)} \le c'\|\nabla u\|^2 + c'' \int_\Omega F(u)dx + c'', \quad c > 0. \tag{C.15}$$

Summing finally (C.13) and δ_1 times (C.15), where $\delta_1 > 0$ is small enough, we obtain

$$\frac{d}{dt}\Big(\|u\|^2_{-1} + \delta_1\|u\|^2\Big) + c\Big(\|u\|^2_{H^2(\Omega)} + \int_\Omega F(u)dx\Big) \le c', \quad c > 0. \tag{C.16}$$

We now multiply (C.1) by $\Delta^2 u$ and have

$$\frac{1}{2}\frac{d}{dt}\|\Delta u\|^2 + \|\Delta^2 u\|^2 - ((\Delta f(u), \Delta^2 u)) + ((g(x,u), \Delta^2 u)) = 0. \tag{C.17}$$

Here,

$$\begin{aligned}\Big|((g(x,u), \Delta^2 u))\Big| &\le \|g(.,u)\|\|\Delta^2 u\| \\ &\le c\|g(.,u)\|^2 + \frac{1}{4}\|\Delta^2 u\|^2.\end{aligned}$$

Furthermore,

$$\Big|((\Delta f(u), \Delta^2 u))\Big| \le c\|f(u)\|^2_{H^2(\Omega)} + \frac{1}{4}\|\Delta^2 u\|^2,$$

which yields

$$\frac{d}{dt}\|\Delta u\|^2 + \|\Delta^2 u\|^2 \le c\Big(\|f(u)\|^2_{H^2(\Omega)} + \|g(.,u)\|^2 + 1\Big). \tag{C.18}$$

We note that, owing to (C.7) and $H^2(\Omega) \subset C(\overline{\Omega})$ with continuous injection,

$$\|f(u)\|^2_{H^2(\Omega)} + \|g(.,u)\|^2 + 1 \le Q(\|u\|_{H^2(\Omega)}), \tag{C.19}$$

hence

$$\frac{d}{dt}\|\Delta u\|^2 \le Q(\|\Delta u\|^2). \tag{C.20}$$

In particular, setting

$$y = \|\Delta u\|^2, \tag{C.21}$$

we deduce from (C.20) an inequation of the form

$$y' \le Q(y). \tag{C.22}$$

Let z be the solution to the ordinary differential equation

$$z' = Q(z), \qquad z(0) = y(0). \tag{C.23}$$

It follows from the comparison principle that there exists $T_0 = T_0(\|u_0\|_{H^2(\Omega)})$ belonging to, say, $(0, \frac{1}{2})$ such that

$$y(t) \le z(t), \quad \forall t \in [0, T_0], \tag{C.24}$$

hence

$$\|u(t)\|_{H^2(\Omega)} \le Q(\|u_0\|_{H^2(\Omega)}), \quad t \le T_0. \tag{C.25}$$

We now multiply (C.1) by $(-\Delta)^{-1}\frac{\partial u}{\partial t}$ and have

$$\frac{1}{2}\frac{d}{dt}\|\nabla u\|^2 + \left\|\frac{\partial u}{\partial t}\right\|_{-1}^2 + \left(\left(f(u), \frac{\partial u}{\partial t}\right)\right) + \left(\left(g(x,u), (-\Delta)^{-1}\frac{\partial u}{\partial t}\right)\right) = 0, \tag{C.26}$$

which yields, owing to (C.25) and (C.7),

$$\begin{aligned}\frac{d}{dt}\|\nabla u\|^2 + \left\|\frac{\partial u}{\partial t}\right\|_{-1}^2 &\leq c(\|f(u)\|_{H^1(\Omega)}^2 + \|g(.,u)\|^2) \\ &\leq Q(\|u_0\|_{H^2(\Omega)}), \quad t \leq T_0.\end{aligned} \tag{C.27}$$

It thus follows from (C.27) that

$$\int_0^{T_0} \left\|\frac{\partial u}{\partial t}\right\|_{-1}^2 dt \leq Q(\|u_0\|_{H^2(\Omega)}). \tag{C.28}$$

We then differentiate (C.1) with respect to time and rewrite the resulting equation as

$$(-\Delta)^{-1}\frac{\partial \theta}{\partial t} - \Delta\theta + f'(u)\theta + (-\Delta)^{-1}\Big(g_x'(u)\theta\Big) = 0, \tag{C.29}$$

where $\theta = \frac{\partial u}{\partial t}$.

We multiply (C.29) by $t\theta$ and have, for $t \leq T_0$,

$$\frac{t}{2}\frac{d}{dt}\|\theta\|_{-1}^2 + t\|\nabla\theta\|^2 \leq t|((f'(u)\theta,\theta))| + t|(((-\Delta)^{-1}(g_x'(u)\theta),\theta))|.$$

Here,

$$\begin{aligned}|(((-\Delta)^{-1}(g_x'(u)\theta),\theta))| &\leq |((g_x'(u)\theta, (-\Delta)^{-1}\theta))| \\ &\leq \int_\Omega |g_x'(u)||\theta||(-\Delta)^{-1}\theta|dx \\ &\leq \|g_x'(u)\|\|\theta\|\|(-\Delta)^{-1}\theta\|_{L^\infty(\Omega)} \\ &\leq \text{(thanks (C.7) and the continuous embedding} H^2(\Omega) \subset C(\overline{\Omega})) \\ &\leq Q(\|u_0\|_{H^2(\Omega)})\|\theta\|^2.\end{aligned}$$

Furthermore,

$$((f'(u)\theta,\theta)) \geq -c_0\|\theta\|^2,$$

owing to (C.5), which yields

$$\frac{1}{2}\frac{d}{dt}(t\|\theta\|_{-1}^2) + t\|\nabla\theta\|^2 \leq Q(\|u_0\|_{H^2(\Omega)})(t\|\theta\|^2) + \frac{1}{2}\|\theta\|_{-1}^2. \tag{C.30}$$

Noting that

$$\|\theta\|^2 \leq c\|\theta\|_{-1}\|\nabla\theta\|,$$

we find

$$\frac{d}{dt}(t\|\theta\|_{-1}^2) \leq Q(\|u_0\|_{H^2(\Omega)})(t\|\theta\|_{-1}^2) + \|\theta\|_{-1}^2, \tag{C.31}$$

hence, owing to (C.28) and Gronwall's lemma, we have

$$\left\|\frac{\partial u}{\partial t}\right\|_{-1}^2 \le \frac{1}{t} Q(\|u_0\|_{H^2(\Omega)}), \quad 0 < t \le T_0. \tag{C.32}$$

We now multiply (C.29) by θ and obtain, owing to (C.5),

$$\frac{1}{2}\frac{d}{dt}\left\|\frac{\partial u}{\partial t}\right\|_{-1}^2 + \left\|\nabla \frac{\partial u}{\partial t}(t)\right\|^2 \le c_0 \left\|\frac{\partial u}{\partial t}\right\|^2 + \left|\left(\left((-\Delta)^{-1}\left(g_x'(u)\frac{\partial u}{\partial t}\right), \frac{\partial u}{\partial t}\right)\right)\right|. \tag{C.33}$$

We note that, since $H^2(\Omega) \subset L^\infty(\Omega)$ with continuous injection,

$$\begin{aligned}
\left|\left(\left((-\Delta)^{-1}\left(g_x'(u)\frac{\partial u}{\partial t}\right), \frac{\partial u}{\partial t}\right)\right)\right| &= \left|\left(\left(\left(g_x'(u)\frac{\partial u}{\partial t}\right), (-\Delta)^{-1}\frac{\partial u}{\partial t}\right)\right)\right| \\
&\le \int_\Omega |g_x'(u)| \left|\frac{\partial u}{\partial t}\right| \left|(-\Delta)^{-1}\frac{\partial u}{\partial t}\right| dx \\
&\le \|g_x'(u)\| \left\|\frac{\partial u}{\partial t}\right\| \left\|(-\Delta)^{-1}\frac{\partial u}{\partial t}\right\|_{L^\infty(\Omega)} \\
&\le c\|g_x'(u)\| \left\|\frac{\partial u}{\partial t}\right\|^2
\end{aligned}$$

and we thus deduce from (C.7), (C.33) and a proper interpolation inequality (see above) that

$$\frac{d}{dt}\left\|\frac{\partial u}{\partial t}\right\|_{-1}^2 + \left\|\nabla \frac{\partial u}{\partial t}\right\|^2 \le Q(\|u\|_{H^2(\Omega)}) \left\|\frac{\partial u}{\partial t}\right\|_{-1}^2. \tag{C.34}$$

Noting that it follows from (C.16) that

$$\int_0^t \|u\|_{H^2(\Omega)} ds \le c\|u_0\|^2 + c't + c'', \tag{C.35}$$

(C.34), (C.35) and Gronwall's lemma yield

$$\left\|\frac{\partial u}{\partial t}(t)\right\|_{-1}^2 \le e^{ct} Q(\|u_0\|_{H^2(\Omega)}) \left\|\frac{\partial u}{\partial t}(T_0)\right\|_{-1}^2, \quad t \ge T_0,$$

and it finally follows from (C.32) that

$$\left\|\frac{\partial u}{\partial t}(t)\right\|_{-1}^2 \le e^{ct} Q(\|u_0\|_{H^2(\Omega)}), \quad c \ge 0, \ \ t \ge T_0. \tag{C.36}$$

We then rewrite, for $t \ge T_0$ fixed, (C.10) in the form

$$-\Delta u + f(u) + (-\Delta)^{-1} g(x, u) = h_u, \quad u = 0 \quad \text{on } \Gamma, \tag{C.37}$$

where

$$h_u = -(-\Delta)^{-1}\frac{\partial u}{\partial t} \tag{C.38}$$

satisfies, owing (C.36),

$$\|h_u\| \le e^{ct} Q(\|u_0\|_{H^2(\Omega)}), \quad t \ge T_0. \tag{C.39}$$

We multiply (C.37) by u and have

$$\|\nabla u\|^2 + ((f(u), u)) \leq \|h_u\|\|u\| + \|u\| \int_\Omega |g(., u)|dx,$$

which yields, owing to (C.6), (C.8), (C.16) and (C.39),

$$\|\nabla u\|^2 + c \int_\Omega F(u)dx \leq e^{c't} Q(\|u_0\|_{H^2(\Omega)}) + c'', \quad c > 0. \tag{C.40}$$

Then multiplying (C.37) by $-\Delta u$, we obtain

$$\|\Delta u\|^2 + ((f'(u)\nabla u, \nabla u)) \leq \|h_u\|\|\Delta u\| + |((g(x, u), u))|$$

and it follows from (C.5) and (C.9) that

$$\|\Delta u\|^2 \leq \|h_u\|^2 + c\|\nabla u\|^2 + c' \int_\Omega F(u)dx + c''. \tag{C.41}$$

Summing finally (C.40) and δ_2 times (C.41), where $\delta_2 > 0$ is small enough, we find

$$\|u(t)\|_{H^2(\Omega)} \leq e^{ct} Q(\|u_0\|_{H^2(\Omega)}) + c', \quad c \geq 0, \ \ t \geq T_0. \tag{C.42}$$

Finally, we deduce from (C.25) and (C.42) that

$$\|u(t)\|_{H^2(\Omega)} \leq e^{ct} Q(\|u_0\|_{H^2(\Omega)}) + c', \quad c \geq 0, \ \ t \geq 0. \tag{C.43}$$

We now deduce from (C.16) that

$$\int_0^1 \|u(t)\|^2_{H^2(\Omega)} dt \leq c\|u_0\|^2 + c', \tag{C.44}$$

so that there exists a $T \in (0, 1)$ such that

$$\|u(T)\|^2_{H^2(\Omega)} \leq c\|u_0\|^2 + c'. \tag{C.45}$$

Actually, repeating the above estimates, starting from $t = T$ instead of $t = 0$, we have the smoothing proprety

$$\|u(1)\|^2_{H^2(\Omega)} \leq c\|u_0\|^2 + c', \quad c \geq 0. \tag{C.46}$$

We note that, integrating (C.16) over $(t, t + 1)$,

$$\int_t^{t+1} \|u(t)\|^2_{H^2(\Omega)} ds \leq e^{-ct} Q(\|u_0\|^2) + c', \quad c > 0, \ \ t \geq 0, \tag{C.47}$$

hence, for every $t \geq 1$, there exists a time $t_1 \in [t - 1, t]$ such that

$$\|u(t_1)\|^2_{H^2(\Omega)} \leq e^{-ct} Q(\|u_0\|^2) + c', \tag{C.48}$$

which yields, for $t_2 \in [0, 1]$ such that $t = t_1 + t_2$ and owing to (C.43) and (C.46),

$$\begin{aligned} \|u(t)\|^2_{H^2(\Omega)} = \|u(t_1 + t_2)\|^2_{H^2(\Omega)} &\leq e^{ct_2} Q(\|u(t_1)\|_{H^2(\Omega)}) + c' \\ &\leq ce^{-c't_2} Q(\|u(t_1)\|_{H^2(\Omega)}) + c'' \\ &\leq cQ(e^{-c't}\|u_0\|^2) + c'') + c'' \\ &\leq e^{-ct} Q(\|u_0\|^2_{H^2(\Omega)}) + c'. \end{aligned}$$

Finally, we deduce that

$$\|u(t)\|_{H^2(\Omega)} \leq e^{-ct} Q(\|u_0\|_{H^2(\Omega)}) + c', \quad c > 0, \ \ t \geq 0, \tag{C.49}$$

C.2 The dissipative semigroup

We have the

Theorem C.2.1. *We assume that $u_0 \in H^2(\Omega) \cap H_0^1(\Omega)$. Then, (C.1)–(C.3) possesses a unique solution u such that $u \in H^2(\Omega) \cap H_0^1(\Omega)$, $\forall t \geq 0$.*

Démonstration. The proof of existence is based on (C.49) and, e.g., a standard Galerkin scheme.

Let now u_1 and u_2 be two solutions to (C.1)–(C.2) with initial data $u_{0,1}$ and $u_{0,2}$, respectively. We set $u = u_1 - u_2$ and $u_0 = u_{0,1} - u_{0,2}$. We have

$$\frac{\partial u}{\partial t} + \Delta^2 u - \Delta(f(u_1) - f(u_2)) + g(x, u_1) - g(x, u_2) = 0, \tag{C.50}$$

$$u = \Delta u = 0 \quad \text{on } \Gamma, \tag{C.51}$$

$$u|_{t=0} = u_0. \tag{C.52}$$

We multiply (C.50) by $(-\Delta)^{-1}u$ and have

$$\begin{aligned} \frac{1}{2}\frac{d}{dt}\|u\|_{-1}^2 + \|\nabla u\|^2 \leq\ & |((f(u_1) - f(u_2), u))| \\ & + |((g(., u_1) - g(., u_2), (-\Delta)^{-1}u))|. \end{aligned} \tag{C.53}$$

Here,

$$\begin{aligned} &|((g(x, u_1) - g(x, u_2), (-\Delta)^{-1}u))| \\ &\leq \int_\Omega |g(x, u_1) - g(x, u_2)||(-\Delta)^{-1}u| \\ &\leq \int_\Omega |u||(-\Delta)^{-1}u|dx \int_0^1 |g_x'(u_1 + s(u_2 - u_1)|ds \\ &\leq \|u\|\|(-\Delta)^{-1}u\|_{L^\infty(\Omega)}\Big(\int_0^1 \|g_x'(u_1 + s(u_2 - u_1)\|ds\Big) \\ &\leq \text{(thanks to (C.7) and the continuous embedding } H^2(\Omega) \subset C(\overline{\Omega})) \\ &\leq Q(\|u_{0,1}\|_{H^2(\Omega)}, \|u_{0,2}\|_{H^2(\Omega)})\|u\|^2 \\ &\leq Q(\|u_{0,1}\|_{H^2(\Omega)}, \|u_{0,2}\|_{H^2(\Omega)})\|u\|_{-1}\|\nabla u\|, \end{aligned}$$

owing to interpolation inequality $\|u\|^2 \leq \|u\|_{-1}\|\nabla u\|$. Furthermore,

$$|((f(u_1) - f(u_2), u))| \leq \|\nabla(f(u_1) - f(u_2))\|\|u\|_{-1}$$

and owing to (C.49),

$$\begin{aligned} \|\nabla(f(u_1) - f(u_2))\| \leq & \Big\|\nabla\Big(\int_0^1 f'(su_2 + (1 - s)u_1)dsu\Big)\Big\| \\ \leq & \Big\| \int_0^1 f'(su_2 + (1 - s)u_1)ds\nabla u\Big\| \\ & + \Big\|u \int_0^1 f''(su_2 + (1 - s)u_1)(s\nabla u_2 + (1 - s)\nabla u_1)ds\Big\| \\ \leq & Q(\|u_{0,1}\|_{H^2(\Omega)}, \|u_{0,2}\|_{H^2(\Omega)})(\|\nabla u\| + \|\|u\|\nabla u_1\|\| + \|\|u\|\nabla u_2\|\|) \\ \leq & Q(\|u_{0,1}\|_{H^2(\Omega)}, \|u_{0,2}\|_{H^2(\Omega)})\|\nabla u\|, \end{aligned}$$

which yields

$$\frac{d}{dt}\|u\|_{-1}^2 + \|\nabla u\|^2 \leq Q(\|u_{0,1}\|_{H^2(\Omega)}, \|u_{0,2}\|_{H^2(\Omega)})\|u\|_{-1}^2. \tag{C.54}$$

We deduce from (C.54) and Gronwall's lemma that

$$\begin{aligned}\|u_1(t) - u_2(t)\|_{-1}^2 \leq e^{ct} Q(\|u_{0,1}\|_{H^2(\Omega)}, \|u_{0,2}\|_{H^2(\Omega)}) \\ \|u_{0,1} - u_{0,2}\|_{-1}^2, \quad c \geq 0, \ \ t \geq 0,\end{aligned} \tag{C.55}$$

hence the uniqueness, as well as the continuous depending with respect to the initial data in the H^{-1}-topology. □

We set $\Phi = H^2(\Omega) \cap H_0^1(\Omega)$. It follows Theorem C.2.1 that we have the continuous (with respect to the H^{-1}-norm) semigroup

$$S(t) : \Phi \to \Phi, \qquad u_0 \mapsto u(t), \quad t \geq 0$$

(i.e., $S(0) = I$, $S(t+s) = S(t) \circ S(s)$, t, $s \geq 0$). We then deduce from (C.49) the

Theorem C.2.2. *The semigroup $S(t)$ is dissipative in Φ, i.e., there exists a bounded set $\mathcal{B}_0 \subset \Phi$ (called absorbing set) such that, for every bounded set $B \subset \Phi$, there exists $t_0 = t_0(B) \geq 0$ such that $t \geq t_0$ implies $S(t)B \subset \mathcal{B}_0$.*

Remark C.2.3. *It is easy to see that we can assume, without loss of generality, that $\mathcal{B}_0$ is positively invariant by $S(t)$, i.e., $S(t)\mathcal{B}_0 \subset \mathcal{B}_0$, $\forall t \geq 0$.*

C.3 Existence of exponential attractors

We first derive a smoothing property on the difference of two solutions which is one of the key tools to construct exponential attractors (see [53] ; see also [54, 107, 108] for generalizations).

Let u_1 and u_2 be two solutions to (C.1)–(C.2) with initial data $u_{0,1}$ and $u_{0,2}$, respectively. We note that it sufficient here to take the initial data in the bounded absorbing set $\mathcal{B}_0$ constructed in the previous section. We again set $u = u_1 - u_2$ and $u_0 = u_{0,1} - u_{0,2}$ and have

$$\frac{\partial u}{\partial t} + \Delta^2 u - \Delta(f(u_1) - f(u_2)) + g(x, u_1) - g(x, u_2) = 0, \tag{C.56}$$

$$u = \Delta u = 0 \quad \text{on } \Gamma, \tag{C.57}$$

$$u|_{t=0} = u_0. \tag{C.58}$$

We first deduce from (C.54) that

$$\int_0^t \|\nabla u\|^2 d\tau \leq c e^{c't} \|u_0\|_{-1}^2, \quad c, c' \geq 0, \ \ t \geq 0, \tag{C.59}$$

where the constants only depend on $\mathcal{B}_0$.

Multiplying (C.56) by $t(-\Delta)^{-1}\frac{\partial u}{\partial t}$, we have

$$\begin{aligned}\frac{1}{2}\frac{d}{dt}(t\|\nabla u\|^2)+t\left\|\frac{\partial u}{\partial t}\right\|_{-1}^2 \le -\frac{1}{2}\|\nabla u\|^2+t\left|\left(\left(f(u_1)-f(u_2),\frac{\partial u}{\partial t}\right)\right)\right| \\ +t\left|\left(\left(g(x,u_1)-g(x,u_2),(-\Delta)^{-1}\frac{\partial u}{\partial t}\right)\right)\right|,\end{aligned} \tag{C.60}$$

hence,

$$\frac{d}{dt}(t\|\nabla u\|^2)+t\left\|\frac{\partial u}{\partial t}\right\|_{-1}^2 \le ct\|\nabla u\|^2+\|\nabla u\|^2, \tag{C.61}$$

where the constant c depends only on $\mathcal{B}_0$. We thus deduce from (C.59), (C.61) and Gronwall's lemma that

$$\|\nabla u\|^2 \le c\frac{1}{t}e^{c't}\|u_0\|_{-1}^2, \qquad c'\ge 0,\ t>0, \tag{C.62}$$

where the constants depend only on $\mathcal{B}_0$. In particular, we have

$$\|\nabla u\|^2 \le ce^{c't}\|u_0\|_{-1}^2, \qquad c,c'\ge 0,\ t\ge 1, \tag{C.63}$$

where the constants depend only on $\mathcal{B}_0$. Furthermore, it also follows from (C.61) that

$$\int_1^t \left\|\frac{\partial u}{\partial t}\right\|_{-1}^2 \le ce^{c't}\|u_0\|_{-1}^2, \qquad c,c'\ge 0,\ t\ge 1, \tag{C.64}$$

where the constants depend only on $\mathcal{B}_0$.

We now differentiate (C.56) with respect to time and have

$$\begin{aligned}(-\Delta)^{-1}\frac{\partial}{\partial t}\frac{\partial u}{\partial t}-\Delta\frac{\partial u}{\partial t}+f'(u_1)\frac{\partial u}{\partial t}+(f'(u_1)-f'(u_2))\frac{\partial u_2}{\partial t} \\ +(-\Delta)^{-1}\left(g_x'(u_1)\frac{\partial u}{\partial t}\right)+(-\Delta)^{-1}\left((g_x'(u_1)-g_x'(u_2))\frac{\partial u_2}{\partial t}\right)=0.\end{aligned} \tag{C.65}$$

We multiply (C.65) by $(t-1)\frac{\partial u}{\partial t}$ and obtain, owing to (C.5),

$$\begin{aligned}\frac{1}{2}\frac{d}{dt}\left((t-1)\left\|\frac{\partial u}{\partial t}\right\|_{-1}^2\right)+(t-1)\left\|\nabla\frac{\partial u}{\partial t}\right\|^2 \le +\frac{1}{2}\left\|\frac{\partial u}{\partial t}\right\|_{-1}^2+c(t-1)\left\|\frac{\partial u}{\partial t}\right\|^2+(t-1) \\ \left|\left(\left((f'(u_1)-f'(u_2))\frac{\partial u_2}{\partial t},\frac{\partial u}{\partial t}\right)\right)\right|+(t-1)\left|\left(\left((-\Delta)^{-1}\left(g_x'(u_1)\frac{\partial u}{\partial t}\right),\frac{\partial u}{\partial t}\right)\right)\right| \\ +\left|(t-1)\left(\left((-\Delta)^{-1}\left((g_x'(u_1)-g_x'(u_2))\frac{\partial u_2}{\partial t}\right),\frac{\partial u}{\partial t}\right)\right)\right|.\end{aligned}$$

Here,

$$\begin{aligned}\left|\left(\left((f'(u_1)-f'(u_2))\frac{\partial u_2}{\partial t},\frac{\partial u}{\partial t}\right)\right)\right| &\le \int_\Omega |f'(u_1)-f'(u_2)|\left|\frac{\partial u}{\partial t}\right|\left|\frac{\partial u_2}{\partial t}\right|dx \\ &\le c\int_\Omega |u|\left|\frac{\partial u}{\partial t}\right|\left|\frac{\partial u_2}{\partial t}\right|dx \\ &\le c\|\nabla u\|\left\|\nabla\frac{\partial u}{\partial t}\right\|\left\|\frac{\partial u_2}{\partial t}\right\|.\end{aligned}$$

Furthermore,

$$\begin{aligned}\left|\left(\left((-\Delta)^{-1}\Big(g_x'(u_1)\frac{\partial u}{\partial t}\Big),\frac{\partial u}{\partial t}\right)\right)\right| &= \left|\left(\left(g_x'(u_1)\frac{\partial u}{\partial t},(-\Delta)^{-1}\frac{\partial u}{\partial t}\right)\right)\right|\\ &\le \int_\Omega |g_x'(u_1)|\left|\frac{\partial u}{\partial t}\right|\left|(-\Delta)^{-1}\frac{\partial u}{\partial t}\right|dx\\ &\le \|g_x'(u_1)\|\left\|\frac{\partial u}{\partial t}\right\|\left\|(-\Delta)^{-1}\frac{\partial u}{\partial t}\right\|_{L^\infty(\Omega)}\\ &\le c\left\|\frac{\partial u}{\partial t}\right\|^2\\ &\le c\left\|\nabla\frac{\partial u}{\partial t}\right\|\left\|\frac{\partial u}{\partial t}\right\|_{-1},\end{aligned}$$

owing to the continuous embedding $H^2(\Omega)\subset C(\overline{\Omega})$ and

$$\begin{aligned}&\left|\left(\left((-\Delta)^{-1}\Big((g_x'(u_1)-g_x'(u_2))\frac{\partial u_2}{\partial t}\Big),\frac{\partial u}{\partial t}\right)\right)\right|\\ &\quad=\left(\left((g_x'(u_1)-g_x'(u_2))\frac{\partial u_2}{\partial t},(-\Delta)^{-1}\frac{\partial u}{\partial t}\right)\right)\Big|\\ &\quad\le\int_\Omega|g_x'(u_1)-g_x'(u_2)|\left|\frac{\partial u_2}{\partial t}\right|\left|(-\Delta)^{-1}\frac{\partial u}{\partial t}\right|dx\\ &\quad\le c\|g_x'(u_1)-g_x'(u_2)\|\left\|\frac{\partial u_2}{\partial t}\right\|\left\|\frac{\partial u}{\partial t}\right\|\\ &\quad\le c\left\|\int_0^1 g_x''(u_1+s(u_2-u_1))dsu\right\|\left\|\frac{\partial u_2}{\partial t}\right\|\left\|\frac{\partial u}{\partial t}\right\|\\ &\quad\le c\|u\|\left\|\frac{\partial u_2}{\partial t}\right\|\left\|\frac{\partial u}{\partial t}\right\|,\end{aligned}$$

where the constant c depends only on $\mathcal{B}_0$, which yields

$$\begin{aligned}\frac{d}{dt}\Big((t-1)\left\|\frac{\partial u}{\partial t}\right\|_{-1}^2\Big)+(t-1)\left\|\nabla\frac{\partial u}{\partial t}\right\|^2 &\le c(t-1)\left\|\frac{\partial u}{\partial t}\right\|_{-1}^2\\ &\quad+c(t-1)\|\nabla u\|^2\left\|\frac{\partial u_2}{\partial t}\right\|^2+\left\|\frac{\partial u}{\partial t}\right\|_{-1}^2,\end{aligned}\tag{C.66}$$

We thus deduce from (C.34), (C.35), (C.36) (for $u=u_2$; note that $T_0\le 1$), (C.63), (C.64) and Gronwall's lemma that

$$\left\|\frac{\partial u}{\partial t}\right\|_{-1}^2\le ce^{c't}\|u_0\|_{-1}^2,\qquad c,c'\ge 0,\ t\ge 2,\tag{C.67}$$

where the constants only depend on $\mathcal{B}_0$.

We rewrite (C.56) in the form

$$-\Delta u=\tilde{h}_u(t),\quad u=0\text{ on }\Gamma,\tag{C.68}$$

for $t\ge 0$ fixed, where

$$\tilde{h}_u(t)=-(-\Delta)^{-1}\frac{\partial u}{\partial t}-(f(u_1)-f(u_2))-(-\Delta)^{-1}(g(x,u_1)-g(x,u_2))\tag{C.69}$$

satisfies, owing to (C.63) and (C.67),

$$\|\tilde{h}_u(t)\| \le ce^{c't}\|u_0\|_{-1}, \qquad t \ge 2, \tag{C.70}$$

where the constants only depend on $\mathcal{B}_0$. Multiplying (C.68) by $-\Delta u$, we have

$$\|\Delta u\| \le \|\tilde{h}_u(t)\|,$$

hence,

$$\|u_1(t) - u_2(t)\|_{H^2(\Omega)} \le ce^{c't}\|u_{0,1} - u_{0,2}\|_{-1}, \qquad t \ge 2, \tag{C.71}$$

where the constants only depends on $\mathcal{B}_0$.

Next, we derive a Hölder (both with respect to space and time) estimate. Actually, owing to (C.55), it suffices to prove the Hölder continuity with respect to time. We have

$$\begin{aligned} \|u(t_1) - u(t_2)\|_{-1} &= \left\| \int_{t_1}^{t_2} \frac{\partial u}{\partial t} d\tau \right\|_{-1} \\ &\le \left| \int_{t_1}^{t_2} \left\| \frac{\partial u}{\partial t} \right\|_{-1} d\tau \right| \\ &\le |t_1 - t_2|^{\frac{1}{2}} \left| \int_{t_1}^{t_2} \left\| \frac{\partial u}{\partial t} \right\|_{-1}^2 d\tau \right|^{\frac{1}{2}}. \end{aligned} \tag{C.72}$$

Then, multiplying (C.1) by $(-\Delta)^{-1}\frac{\partial u}{\partial t}$, we obtain, proceeding as above,

$$\frac{d}{dt}\|\nabla u\|^2 + \left\| \frac{\partial u}{\partial t} \right\|_{-1}^2 \le c\|\nabla u\|^2, \tag{C.73}$$

where the constants c depends only on $\mathcal{B}_0$. Therefore, owing to (C.13),

$$\left| \int_{t_1}^{t_2} \left\| \frac{\partial u}{\partial t} \right\|_{-1}^2 d\tau \right| \le c, \tag{C.74}$$

where the constants c depends only on $\mathcal{B}_0$ and $T \ge 0$ such that $t_1,\ t_2 \in [0,\ T]$, so that

$$\|u(t_1) - u(t_2)\|_{-1} \le c|t_1 - t_2|^{\frac{1}{2}}, \tag{C.75}$$

where the constants c depends only on $\mathcal{B}_0$ and $T \ge 0$ such that $t_1,\ t_2 \in [0,\ T]$.

We finally deduce from (C.55), (C.71) and (C.75) the following result (see [52, 53])

Theorem C.3.1. *The semigroup $S(t)$ possesses an exponential attractor $\mathcal{M} \subset \mathcal{B}_0$, i.e.*

(i) $\mathcal{M}$ is compact in $H^{-1}(\Omega)$;

(ii) $\mathcal{M}$ is positively invariant, $S(t)\mathcal{M} \subset \mathcal{M}$, $\forall t \ge 0$;

(iii) $\mathcal{M}$ has finite fractal dimension in $H^{-1}(\Omega)$;

(iv) $\mathcal{M}$ attracts exponentially fast the bounded subsets of Φ,

$$\forall B \subset \Phi \text{ bounded}, \quad dist_{H^{-1}(\Omega)}(S(t)B, \mathcal{M}) \le Q(\|B\|_{H^2(\Omega)})e^{-ct}, \qquad c > 0,\ \ t \ge 0,$$

where the constant c is independent of B and $dist_{H^1(\Omega)}$ denotes the Hausdorff semidistance between sets defined by

$$dist_{H^{-1}(\Omega)}(A, B) = \sup_{a \in A} \inf_{b \in B} \|a - b\|_{H^{-1}(\Omega)}.$$

Since $\mathcal{M}$ (or $\tilde{\mathcal{M}}$) is a compact attracting set, we deduce from Theorem C.3.1 and standard results (see, e.g., [7, 108, 137] the following corollary.

Corollary 9. *The semigroup $S(t)$ possesses the finite-dimensional global attractor $\mathcal{A} \subset \mathcal{B}_0$.*

C.4 More regular exponential attractors

Multiplying (C.1) by $\frac{\partial u}{\partial t}$, we have

$$\left\|\frac{\partial u}{\partial t}\right\|^2 + \frac{1}{2}\frac{d}{dt}\|\Delta u\|^2 \leq \left|\left(\left(\Delta f(u), \frac{\partial u}{\partial t}\right)\right)\right| + \left|\left(\left(g(x,u), \frac{\partial u}{\partial t}\right)\right)\right|. \tag{C.76}$$

Here,

$$\begin{aligned}\left|\left(\left(g(x,u), \frac{\partial u}{\partial t}\right)\right)\right| &\leq \|g_x(u)\|\left\|\frac{\partial u}{\partial t}\right\| \\ &\leq c\|g_x(u)\|^2 + \frac{1}{4}\left\|\frac{\partial u}{\partial t}\right\|^2.\end{aligned}$$

Furthermore,

$$\begin{aligned}\left|\left(\left(\Delta f(u), \frac{\partial u}{\partial t}\right)\right)\right| &\leq \|\Delta f(u)\|\left\|\frac{\partial u}{\partial t}\right\| \\ &\leq c\|f(u)\|^2_{H^2(\Omega)} + \frac{1}{4}\left\|\frac{\partial u}{\partial t}\right\|^2,\end{aligned}$$

which yields, owing to (C.7) and (C.49),

$$\frac{d}{dt}\|\Delta u\|^2 + \left\|\frac{\partial u}{\partial t}\right\|^2 \leq e^{-ct}Q(\|u_0\|_{H^2(\Omega)}) + c', \quad \forall t \geq 0,$$

and deduce that

$$\int_t^{t+r}\left\|\frac{\partial u}{\partial t}\right\|^2 d\tau \leq e^{-ct}Q(\|u_0\|_{H^2(\Omega)}) + c', \quad t \geq 0,\ r > 0. \tag{C.77}$$

Differentiating (C.1) with respect to time, we rewrite the resulting equation as, setting $\theta = \frac{\partial u}{\partial t}$,

$$\frac{\partial \theta}{\partial t} + \Delta^2\theta - \Delta\Big(f'(u)\theta\Big) + g'_x(u)\theta = 0. \tag{C.78}$$

We multiply (C.78) by θ and have

$$\frac{1}{2}\frac{d}{dt}\|\theta\|^2 + \|\Delta\theta\|^2 \leq \left|((f'(u)\theta, \Delta\theta))\right| + \left|((g'_x(u)\theta, \theta))\right|. \tag{C.79}$$

Here,

$$\begin{aligned}\left|((g'_x(u)\theta, \theta))\right| &\leq \int_\Omega |g'_x(u)||\theta|^2 dx \\ &\leq \|g'_x(u)\|\|\theta\|\|\theta\|_{L^\infty(\Omega)} \\ &\leq \text{(thanks to the continuous embedding } H^2(\Omega) \subset L^\infty(\Omega)) \\ &\leq c\|g'_x(u)\|^2\|\theta\|^2 + \frac{1}{4}\|\Delta\theta\|^2 \\ &\leq \text{(thanks to (C.7))} \\ &\leq Q(\|u\|_{H^2(\Omega)})\|\theta\|^2 + \frac{1}{4}\|\Delta\theta\|^2.\end{aligned}$$

Furthermore,

$$\begin{aligned}\left|\left(\left(f'(u)\theta, \Delta\theta\right)\right)\right| &\le \left\|f'(u)\theta\right\|\|\Delta\theta\| \\ &\le \text{(thanks to (C.49) and the continuous embedding} \\ &\qquad H^2(\Omega) \subset C(\bar{\Omega})) \\ &\le Q(\|u\|_{H^2(\Omega)})\|\theta\|^2 + \frac{1}{4}\|\Delta\theta\|^2\end{aligned}$$

which yields

$$\frac{d}{dt}\|\theta\|^2 + \|\Delta\theta\|^2 \le Q(\|u\|_{H^2(\Omega)})\|\theta\|^2, \quad \forall t \ge 0. \tag{C.80}$$

Thus, by (C.35), (C.49), (C.77), (C.80), and uniform Gronwall's lemma,

$$\left\|\frac{\partial u}{\partial t}\right\|^2 \le c, \qquad \forall t \ge r, \tag{C.81}$$

where $0 < r < 1$.

We now rewrite (C.1) in the form

$$\Delta^2 u = \hat{h}_u, \quad u = \Delta u = 0 \quad \text{on } \Gamma, \tag{C.82}$$

where

$$\hat{h}_u = -\frac{\partial u}{\partial t} + \Delta f(u) - g(x, u) \tag{C.83}$$

satisfies, for $t \ge t_0 + 1$,

$$\|\hat{h}_u\| \le c. \tag{C.84}$$

We multiply (C.82) by $\Delta^2 u$ and have,

$$\|\Delta^2 u\|^2 = ((\hat{h}_u, \Delta^2 u))$$

It then follows from (C.84) that

$$\|u\|^2_{H^4(\Omega)} \le c, \qquad \forall t \ge 1, \tag{C.85}$$

where u be a solution to (C.1)-(C.3).

We multiply (C.50) by $\frac{\partial u}{\partial t}$ (here $u = u_1 - u_2$, u_1 and u_2 be two solutions to (C.56)-(C.58)) and have

$$\frac{1}{2}\frac{d}{dt}\|\Delta u\|^2 + \left\|\frac{\partial u}{\partial t}\right\|^2 \le \left|\left(\left(\Delta(f(u_1) - f(u_2)), \frac{\partial u}{\partial t}\right)\right)\right| + \left|\left(\left(g(x, u_1) - g(x, u_2), \frac{\partial u}{\partial t}\right)\right)\right|. \tag{C.86}$$

Here,

$$\begin{aligned}
&\left|\left(\left(g(x,u_1)-g(x,u_2),\frac{\partial u}{\partial t}\right)\right)\right| \\
&\leq \|g(x,u_1)-g(x,u_2)\|\left\|\frac{\partial u}{\partial t}\right\| \\
&\leq \left\|\int_0^1 \frac{\partial g}{\partial u}(x,su_2+(1-s)u_1)uds\right\|\left\|\frac{\partial u}{\partial t}\right\| \\
&\leq \text{(thanks to the continuous embedding } H^2(\Omega)\subset L^\infty(\Omega)) \\
&\leq \|\Delta u\|\left\|\frac{\partial u}{\partial t}\right\|\Big(\int_0^1 \|g'_x(su_2+(1-s)u_1)\|ds\Big) \\
&\leq \text{(thanks to (C.7))} \\
&\leq Q(\|u_{0,1}\|_{H^2(\Omega)},\|u_{0,2}\|_{H^2(\Omega)})\|\Delta u\|\left\|\frac{\partial u}{\partial t}\right\|.
\end{aligned}$$

Furthermore,

$$\left|\left(\left(\Delta(f(u_1)-f(u_2)),\frac{\partial u}{\partial t}\right)\right)\right| \leq \|\Delta(f(u_1)-f(u_2))\|\left\|\frac{\partial u}{\partial t}\right\|$$

and owing to (C.49),

$$\begin{aligned}
\|\Delta(f(u_1)-f(u_2))\| \leq& \left\|\Delta\Big(\int_0^1 f'(su_2+(1-s)u_1)dsu\Big)\right\| \\
\leq& \left\|\int_0^1 f'(su_2+(1-s)u_1)ds\Delta u\right\| \\
&+2\left\|\nabla u\int_0^1 f''(su_2+(1-s)u_1)(s\nabla u_2+(1-s)\nabla u_1)ds\right\| \\
&+\left\|u\int_0^1 f'''(su_2+(1-s)u_1)(s\nabla u_2+(1-s)\nabla u_1)^2ds\right\| \\
&+\left\|u\int_0^1 f''(su_2+(1-s)u_1)(s\Delta u_2+(1-s)\Delta u_1)ds\right\| \\
\leq& Q(\|u_{0,1}\|_{H^2(\Omega)},\|u_{0,2}\|_{H^2(\Omega)})(\|\Delta u\|+\|\|\nabla u\|\nabla u_1\|+\|\|\nabla u\|\nabla u_2\| \\
&+\|\|u\|\nabla u_1|^2\|+\|\|u\|\nabla u_2|^2\|+\|\|u\|\Delta u_1\|+\|\|u\|\Delta u_2\|) \\
\leq& Q(\|u_{0,1}\|_{H^2(\Omega)},\|u_{0,2}\|_{H^2(\Omega)})\|\Delta u\|,
\end{aligned}$$

which yields

$$\frac{d}{dt}\|\Delta u\|^2+\left\|\frac{\partial u}{\partial t}\right\|^2 \leq Q(\|u_{0,1}\|_{H^2(\Omega)},\|u_{0,2}\|_{H^2(\Omega)})\|\Delta u\|^2. \tag{C.87}$$

We deduce from (C.87) and Gronwall's lemma that

$$\begin{aligned}
\|u_1(t)-u_2(t)\|^2_{H^2(\Omega)} \leq e^{ct}Q(\|u_{0,1}\|_{H^2(\Omega)},\|u_{0,2}\|_{H^2(\Omega)}) \\
\|u_{0,1}-u_{0,2}\|^2_{H^2(\Omega)},\quad c\geq 0,\ \ t\geq 0.
\end{aligned} \tag{C.88}$$

We then deduce from (C.85) the

Theorem C.4.1. *The semigroup $S(t)$ possesses a bounded set $\mathcal{B}_1 \subset H^4(\Omega)$ (called absorbing set) such that, for every bounded set $B \subset \Phi$, there exists $t_1 = t_1(B) \geq 0$ such that $t \geq t_1$ implies $S(t)B \subset \mathcal{B}_1$.*

Remark C.4.2. *It is easy to see that we can assume, without loss of generality, that $\mathcal{B}_1$ is positively invariant by $S(t)$, i.e., $S(t)\mathcal{B}_1 \subset \mathcal{B}_1$, $\forall t \geq 0$.*

It sufficient here and below to take the initial data in the bounded absorbing set $\mathcal{B}_1$ (which is positively invariant by $S(t)$).

We now differentiate (C.56) with respect to time and have

$$\begin{aligned}\frac{\partial}{\partial t}\frac{\partial u}{\partial t} + \Delta^2\frac{\partial u}{\partial t} - \Delta\Big(f'(u_1)\frac{\partial u}{\partial t}\Big) - \Delta\Big((f'(u_1) - f'(u_2))\frac{\partial u_2}{\partial t}\Big) \\ + g_x'(u_1)\frac{\partial u}{\partial t} + (g_x'(u_1) - g_x'(u_2))\frac{\partial u_2}{\partial t} = 0.\end{aligned} \tag{C.89}$$

We multiply (C.89) by $(t-1)\frac{\partial u}{\partial t}$ and obtain, owing to (C.5),

$$\begin{aligned}&\frac{1}{2}\frac{d}{dt}\Big((t-1)\Big\|\frac{\partial u}{\partial t}\Big\|^2\Big) + (t-1)\Big\|\Delta\frac{\partial u}{\partial t}\Big\|^2 \leq (t-1)\Big|\Big(\Big(\Delta(f'(u_1)\frac{\partial u}{\partial t}), \frac{\partial u}{\partial t}\Big)\Big)\Big| \\ &+ (t-1)\Big|\Big(\Big(\Delta\Big((f'(u_1) - f'(u_2))\frac{\partial u_2}{\partial t}\Big), \frac{\partial u}{\partial t}\Big)\Big)\Big| + (t-1)\Big|\Big(\Big(g_x'(u_1)\frac{\partial u}{\partial t}, \frac{\partial u}{\partial t}\Big)\Big)\Big| \\ &+ (t-1)\Big|\Big(\Big((g_x'(u_1) - g_x'(u_2))\frac{\partial u_2}{\partial t}, \frac{\partial u}{\partial t}\Big)\Big)\Big| + \frac{1}{2}\Big\|\frac{\partial u}{\partial t}\Big\|^2.\end{aligned}$$

Here,

$$\begin{aligned}\Big|\Big(\Big(\Delta((f'(u_1) - f'(u_2))\frac{\partial u_2}{\partial t}), \frac{\partial u}{\partial t}\Big)\Big)\Big| &= \Big|\Big(\Big((f'(u_1) - f'(u_2))\frac{\partial u_2}{\partial t}, \Delta\frac{\partial u}{\partial t}\Big)\Big)\Big| \\ &\leq \int_\Omega |f'(u_1) - f'(u_2)|\Big|\Delta\frac{\partial u}{\partial t}\Big|\Big|\frac{\partial u_2}{\partial t}\Big|dx \\ &\leq c\int_\Omega |u|\Big|\Delta\frac{\partial u}{\partial t}\Big|\Big|\frac{\partial u_2}{\partial t}\Big|dx \\ &\leq c\|\Delta u\|\Big\|\Delta\frac{\partial u}{\partial t}\Big\|\Big\|\frac{\partial u_2}{\partial t}\Big\|.\end{aligned}$$

Furthermore,

$$\begin{aligned}\Big|\Big(\Big(g_x'(u_1)\frac{\partial u}{\partial t}, \frac{\partial u}{\partial t}\Big)\Big)\Big| &\leq \int_\Omega |g_x'(u_1)|\Big\|\frac{\partial u}{\partial t}\Big\|\Big|\frac{\partial u}{\partial t}\Big|dx \\ &\leq \|g_x'(u_1)\|\Big\|\frac{\partial u}{\partial t}\Big\|\Big\|\frac{\partial u}{\partial t}\Big\|_{L^\infty(\Omega)} \\ &\leq c\Big\|\frac{\partial u}{\partial t}\Big\|\Big\|\Delta\frac{\partial u}{\partial t}\Big\|,\end{aligned}$$

owing to the continuous embedding $H^2(\Omega) \subset L^\infty(\Omega)$ and

$$\begin{aligned}\Big|\Big(\Big((g_x'(u_1) - g_x'(u_2))\frac{\partial u_2}{\partial t}, \frac{\partial u}{\partial t}\Big)\Big)\Big| &\leq \int_\Omega |g_x'(u_1) - g_x'(u_2)|\Big\|\frac{\partial u_2}{\partial t}\Big\|\Big|\frac{\partial u}{\partial t}\Big|dx \\ &\leq c\Big\|\int_0^1 g_x''(u_1 + s(u_2 - u_1))ds u\Big\|\Big\|\frac{\partial u_2}{\partial t}\Big\|\Big\|\Delta\frac{\partial u}{\partial t}\Big\| \\ &\leq c\|u\|\Big\|\frac{\partial u_2}{\partial t}\Big\|\Big\|\Delta\frac{\partial u}{\partial t}\Big\|,\end{aligned}$$

where the constant c depends only in $\mathcal{B}_1$, which yields

$$\begin{aligned}\frac{d}{dt}\left((t-1)\left\|\frac{\partial u}{\partial t}\right\|^2\right)+(t-1)\left\|\Delta\frac{\partial u}{\partial t}\right\|^2 &\le c(t-1)\left\|\frac{\partial u}{\partial t}\right\|^2\\ &+c(t-1)\|\Delta u\|^2\left\|\frac{\partial u_2}{\partial t}\right\|^2+\left\|\frac{\partial u}{\partial t}\right\|^2,\end{aligned}\tag{C.90}$$

where the constant c depends only in $\mathcal{B}_1$.

We note that, integrating (C.87) over $(0,t)$, we obtain owing to (C.88) that

$$\int_0^t\left\|\frac{\partial u}{\partial t}\right\|^2 d\tau\le ce^{c't}\|u_0\|^2_{H^2(\Omega)},\tag{C.91}$$

where the constant c depends only in $\mathcal{B}_1$. We thus deduce from (C.77), (C.90), (C.91) and Gronwall's lemma that

$$\left\|\frac{\partial u}{\partial t}\right\|^2\le ce^{c't}\|u_0\|^2_{H^2(\Omega)},\qquad t\ge 2,\tag{C.92}$$

where the constants only depend on $\mathcal{B}_1$.

We rewrite (C.56) in the form

$$\Delta^2 u=\check{h}_u(t),\quad u=0\quad\text{on }\Gamma,\tag{C.93}$$

for $t\ge 2$ fixed, where

$$\check{h}_u(t)=-\frac{\partial u}{\partial t}+\Delta(f(u_1)-f(u_2))-(g(x,u_1)-g(x,u_2))\tag{C.94}$$

satisfies, owing to (C.88) and (C.92),

$$\|\check{h}_u(t)\|\le ce^{c't}\|u_0\|_{H^2(\Omega)},\qquad t\ge 2,\tag{C.95}$$

where the constants only depend on $\mathcal{B}_1$. Multiplying (C.93) by $\Delta^2 u$, we have

$$\|\Delta^2 u\|\le\|\check{h}_u(t)\|,\qquad t\ge 2,$$

hence,

$$\|u(t)\|_{H^4(\Omega)}\le ce^{c't}\|u_0\|_{H^2(\Omega)},\qquad t\ge 2,\tag{C.96}$$

where the constants only depends on $\mathcal{B}_1$.

Next, we derive a Hölder (both with respect to space and time) estimate. Actually, owing to (C.88), it suffices to prove the Hölder continuity with respect to time. We have

$$\begin{aligned}\|u(t_1)-u(t_2)\|_{H^2(\Omega)}&\le c\|\Delta(u(t_1)-u(t_2))\|\\ &\le c\left\|\int_{t_1}^{t_2}\Delta\frac{\partial u}{\partial t}d\tau\right\|\\ &\le c|t_1-t_2|^{\frac12}\left|\int_{t_1}^{t_2}\left\|\Delta\frac{\partial u}{\partial t}\right\|^2 d\tau\right|^{\frac12}.\end{aligned}\tag{C.97}$$

Multiplying (C.1) by $\Delta^2 \frac{\partial u}{\partial t}$, we obtain, proceeding as above,

$$\frac{d}{dt}\|\Delta^2 u\|^2 + \left\|\Delta \frac{\partial u}{\partial t}\right\|^2 \leq c\|\Delta^2 u\|^2,$$

where the constant c depends only on $\mathcal{B}_1$. Therfore, owing to (C.85),

$$\left| \int_{t_1}^{t_2} \left\|\Delta \frac{\partial u}{\partial t}\right\|^2 d\tau \right| \leq c, \tag{C.98}$$

where the constant c depends only on $\mathcal{B}_1$ and T such that $t_1,\ t_2 \in [0,\ T]$, so that

$$\|u(t_1) - u(t_2)\|_{H^2(\Omega)} \leq c|t_1 - t_2|^{\frac{1}{2}}, \tag{C.99}$$

where the constant c depends only on $\mathcal{B}_1$ and T such that $t_1,\ t_2 \in [0,\ T]$. We finally deduce from (C.88), (C.96) and (C.99) the following result (see [52, 53])

Theorem C.4.3. *The semigroup $S(t)$ possesses an exponential attractor $\breve{\mathcal{M}} \subset \mathcal{B}_1$, i.e.*

(i) $\breve{\mathcal{M}}$ is compact in $H^2(\Omega)$;

(ii) $\breve{\mathcal{M}}$ is positively invariant, $S(t)\breve{\mathcal{M}} \subset \breve{\mathcal{M}}$, $\forall t \geq 0$;

(iii) $\breve{\mathcal{M}}$ has finite fractal dimension in $H^2(\Omega)$;

(iv) $\breve{\mathcal{M}}$ attracts exponentially fast the bounded subsets of Φ,

$$\forall B \subset \Phi \text{ bounded}, \quad dist_{H^2(\Omega)}(S(t)B, \mathcal{M}) \leq Q(\|B\|_\Phi)e^{-ct},$$
$$c > 0, \quad t \geq 0,$$

where the constant c is independent of B.

Annexe D

Numerical Algorithms and results in image inpainting

D.1 Operator splitting scheme with threshold

We rewrite the problem in the form

$$\frac{\partial u}{\partial t} - \Delta\mu + \lambda_0\chi_{\Omega\setminus D}(x)(u-h) = 0 \quad \text{in } \Omega, \tag{D.1}$$

$$\mu = -\varepsilon\Delta u + \frac{1}{\varepsilon}f(u) \quad \text{in } \Omega, \tag{D.2}$$

$$\frac{\partial u}{\partial \nu} = \frac{\partial \mu}{\partial \nu} = 0 \quad \text{on } \Gamma, \tag{D.3}$$

$$u_{|t=0} = u_0 \quad \text{in } \Omega, \tag{D.4}$$

which has the advantage of splitting the fourth-order (in space) equation into a system of two second-order ones (see [55], [80], [86], and [43]).

Therefore, the variational formulation associated with this problem reads

$$((\frac{\partial u}{\partial t}, \phi)) = -((\nabla\mu, \nabla\phi)) + ((\lambda(x)(h-u), \phi)), \tag{D.5}$$

$$((\mu, \psi)) = \frac{1}{\varepsilon}((f(u), \psi)) + \varepsilon((\nabla u, \nabla\psi)), \tag{D.6}$$

for all $\phi,\ \psi \in H^1(\Omega)$.

As far as the space discretization is concerned, we consider a quasiuniform family of decompositions $\{\Omega^h\}$ of Ω into d-simplices, so that $\{\Omega^h\}$ is also a triangulation of $\overline{\Omega}$. The triangulation Ω^h of $\overline{\Omega}$ induces a triangulation Γ^h of Γ into $d-1$-simplices in a natural way. For a given triangulation $\Omega^h = \cup_{T\in\Omega^h} T$, we define V^h as the usual $P1$ conforming finite element space,

$$V^h = \{v^h = (v_i^h)_i \in C^0(\overline{\Omega}),\ v^h|_T \text{ is affine},\ \forall T \in \Omega^h\}.$$

The discrete version of this problem reads : Find $(u^h, \mu^h) : [0,T] \to V^h \times V^h$ such that

$$((\frac{\partial u^h}{\partial t}, \phi)) = -((\nabla\mu^h, \nabla\phi)) + \lambda_0((\chi_{\Omega\setminus D}(x)(h-u^h), \phi)), \tag{D.7}$$

$$((\mu^h, \psi)) = \frac{1}{\varepsilon}(f(u^h), \psi)) + \varepsilon((\nabla u^h, \nabla\psi)), \tag{D.8}$$

for all $\phi,\ \psi \in V^h$.

As far as the time discretization of the problem is concerned, we consider here the semi-implict Euler scheme applied to the space semidiscrete scheme. The time step $\delta t > 0$ is fixed. The scheme (Scheme 1) reads : Let $u_{0h} \in V^h$; for $n = 1, 2, ...$, find $(u_h^n, \mu_h^n) \in V^h \times V^h$ such that

$$\begin{aligned}\frac{1}{\delta}((u_h^{n+1}, \phi)) + ((\nabla\mu_h^{n+1}, \nabla\phi)) + \lambda_0((\chi_{\Omega\setminus D}(x)u_h^{n+1}, \phi))\\ = \frac{1}{\delta}((u_h^n, \phi)) + \lambda_0((\chi_{\Omega\setminus D}(x)h, \phi)),\end{aligned} \tag{D.9}$$

$$((\mu_h^{n+1}, \psi)) - \varepsilon((\nabla u_h^{n+1}, \nabla\psi)) = \frac{1}{\varepsilon}((f(u_h^n), \psi)), \tag{D.10}$$

for all $\phi,\ \psi \in V^h$.

We proposed a numerical algorithm based on this scheme in [38, 39] to obtain a good inpainting results which has a dynamic of one step with threshold method involving the diffuse interface thickness ε. Here, the idea is to look for an intermediate value of ε which is sufficient to obtain good results. This one step algorithm is not always applicable (see Chapter 1 and Chapter 2). The thresholding consists in replacing $u(t) \geq \frac{1}{2}$ by 1 and $u(t) < \frac{1}{2}$ by 0 at every point $(x, y) \in \Omega$ (more generally, at every point $(x, y, z) \in \Omega$).

In [40] (Chapter 3), we also use a scheme based on operator splitting with threshold method for color image inpainting. In this case, the thresholding consists in replacing $\max_{i=1,...,n} c_i$ by 1 and $c_j \neq \max_{i=1,...,n} c_i$ by 0 for all j and at every point $(x, y) \in \Omega$ (more generally, at every point $(x, y, z) \in \Omega$) ; this means that we replace the dominant phase (color) by 1 at every point of Ω and the other phases (colors) by 0 to obtain the final inpainting result. The scheme (Scheme 2) is given as

$$\begin{aligned}\frac{1}{\delta}((c_{ih}^{m+1}, \phi_i)) + ((\nabla\mu_{ih}^{m+1}, \nabla\phi_i)) + \lambda_0((\chi_{\Omega\setminus D}(x)c_{ih}^{m+1}, \phi_i))\\ = \frac{1}{\delta}((c_{ih}^m, \phi_i)) + \lambda_0((\chi_{\Omega\setminus D}(x)h_i, \phi_i)),\end{aligned} \tag{D.11}$$

$$((\mu_{ih}^{m+1}, \psi)) - \varepsilon^2((\nabla u_{ih}^{m+1}, \nabla\psi_i)) = ((f_i(c_h^n), \psi_i)), \tag{D.12}$$

$i = 1, ..., n$, for all $(\phi_i)_i,\ (\psi_i)_i \in (V^h)^n \cap S$, n being the number of color in original image, and $f_i(c) = \frac{2}{n}[c_i(1 - c_i)^2 - c_i^2(1 - c_i)] - \frac{1}{n}\sum_{i=1}^{n}\frac{\partial F(c)}{\partial c_i}$, $i = 1, ..., n$. Here, $F(c) = \frac{1}{n}\sum_{i=1}^{n} c_i^2(1 - c_i)^2$ and $S = \{\varphi = (\varphi_i)_i \in \mathbb{R}^n$ such that $\sum_{i=1}^n \varphi_i = 1\}$.

D.2 Convexity splitting scheme

The author in [60, 61] proposed the convexity splitting scheme for gradient flow-derived equations which allows an unconditionally gradient stable time-discretization scheme. Then, it means that the scheme is stable for any arbitrarily large time steps, see [60, 61] and see also [142]. Here, the idea consists in dividing the energy functionals into two parts, a convex plus a concave one. Then, the convex part is treated implicitly while the concave part is treated

explicitly. In particular, this scheme has been used as a specific fast solver of the Bertozzi-Esedoglu–Gillette–Cahn–Hilliard equation ; see, e.g., [16, 17, 77, 25, 20].

The Bertozzi-Esedoglu–Gillette–Cahn–Hilliard equation is not a gradient flow. However, the Bertozzi-Esedoglu–Gillette–Cahn–Hilliard equation is the sum of a gradient descent with respect to the $H^{-1}-$inner product for the original Cahn–Hilliard energy and a gradient descent with respect to the L^2-inner product for the additional fidelity energy. We recall that the original Cahn–Hilliard energy is given by

$$\mathcal{E}(u) = \int_\Omega \Big(\frac{\varepsilon}{2}|\nabla u|^2 + \frac{1}{\varepsilon}F(u)\Big)dx$$

and the additional fidelity energy

$$\mathcal{F}(u) = \frac{\lambda_0}{2}\int_{\Omega\setminus D}(u-h)^2 dx.$$

In this way, we split $\mathcal{E}(u) = \mathcal{E}_1(u) - \mathcal{E}_2(u)$ and $\mathcal{F}(u) = \mathcal{F}_1(u) - \mathcal{F}_2(u)$, where

$$\mathcal{E}_1(u) = \int_\Omega \Big(\frac{\varepsilon}{2}|\nabla u|^2 + \frac{c_1}{2}|u|^2\Big)dx,$$

$$\mathcal{E}_2(u) = \int_\Omega \Big(-\frac{1}{\varepsilon}F(u) + \frac{c_1}{2}|u|^2\Big)dx,$$

$$\mathcal{F}_1(u) = \int_\Omega \frac{c_2}{2}|u|^2 dx,$$

and

$$\mathcal{F}_2(u) = \int_\Omega \Big(-\frac{\lambda}{2}(u-h)^2 + \frac{c_2}{2}|u|^2\Big)dx,$$

such that c_1 et c_2 are nonnegative constants and need to be chosen large enough such that the energies $\mathcal{E}_1(u)$, $\mathcal{E}_2(u)$, $\mathcal{F}_1(u)$, and $\mathcal{F}_2(u)$ are convex.

As far as the backward Euler discretization for the time of this problem is concerned. The time step $\delta t > 0$ is fixed. The resulting time-stepping scheme is :

$$\frac{u_h^{n+1}-u_h^n}{\delta t} = -\nabla_{H^{-1}}(\mathcal{E}_1(u_h^{n+1}) - \mathcal{E}_2(u_h^n)) - \nabla_{L^2}(\mathcal{F}_1(u_h^{n+1}) - \mathcal{F}_2(u_h^n)),$$

where $\nabla_{H^{-1}}$ and ∇_{L^2} represent the gradient descent with to the $H^{-1}-$ and the L^2-inner product, respectively. This translates to a numerical scheme of the form

$$\frac{u_h^{n+1}-u_h^n}{\delta t} + \varepsilon\Delta^2 u_h^{n+1} - c_1\Delta u_h^{n+1} + c_2 u_h^{n+1} = \frac{1}{\varepsilon}\Delta f(u_h^n) + \lambda_0(\chi_{\Omega\setminus D}(x)(h-u_h^n)) - c_1\Delta u_h^n + c_2 u_h^n.$$

Therefore, using the operator splitting (see [55], [80], [86], and [43]), we obtain the final resulting scheme (Scheme 3) in the form

$$\begin{aligned}\frac{1}{\delta t}((u_h^{n+1},\phi)) + ((\nabla\mu_h^{n+1},\nabla\phi)) + c_1((\nabla u_h^{n+1},\nabla\phi)) + c_2((u_h^{n+1},\phi))\\ = \frac{1}{\delta t}((u_h^n,\phi)) + \lambda_0((\chi_{\Omega\setminus D}(x)(h(x)-u_h^n),\phi))\\ + c_1((\nabla u_h^n,\nabla\phi)) + c_2((u_h^n,\phi)), \quad \forall\phi\in V^h,\end{aligned}$$

$$((\mu_h^{n+1},\psi)) - \varepsilon((\nabla u_h^{n+1},\nabla\psi)) = \frac{1}{\varepsilon}((f(u_h^n),\psi)), \quad \forall\psi\in V^h.$$

Note that, Scheme 3 is unconditionally stable provided $c_1 > \frac{1}{\varepsilon}$ and $c_2 > \lambda_0$ (see [131]).

Under this convexity splitting, the authors of [16, 17] proposed a numerical algorithm to obtain a good inpainting results which has dynamic of two-step involving the diffuse interface thickness ε. It seems that the edges in the image will be connected with a large value of the diffuse interface thickness ε and together switch the interface diffuse thickness ε by a small value (which depends on the mesh discretization) to obtain the final inpainting result.

D.3 Comparison between Scheme 1 and Scheme 3

In all this manuscript, the numerical simulations are performed with the software FreeFem++ (see [67, 84]). Here, in this section, for the numerical results presented below, Ω is a $(0, 0.5)\times(0, 0.5)$-square. The triangulation is obtained by dividing Ω into 120×120 rectangles and by dividing each rectangle along the same diagonal.

In Figure D.1 and Figure D.2, we compare the inpainting results obtained with Scheme 1 and Scheme 3. The gray region in Figure D.1(a) corresponds to the inpainting region. We run the modified Cahn–Hilliard equation (Scheme 1) with $f(s) = 4s^3 - 6s^2 + 2s$ and $\varepsilon = 0.03$ (intermediate value). We are close to a steady state at $t = 1$, as shown in Figure D.1(b), and we replace all values larger than $\frac{1}{2}$ by 1 and all those smaller than $\frac{1}{2}$ by 0 to obtain the final inpainting in Figure D.1(c). Here, $\lambda = 900000$ and $\Delta t = 0.05$

Then, we run again the modified Cahn–Hilliard equation (Scheme 3) with the same $f(s) = 4s^3 - 6s^2 + 2s$ and the same initial datum, but we now take $\varepsilon = 0.1$ (larger value). We are close to a first steady state at $t = 1765$, as shown in Figure D.1(d). We then take Figure D.1(d) as initial datum and run again the modified Cahn–Hilliard equation (Scheme 3) but, we now take $\varepsilon = 4\times 10^{-5}$ (small value). We are close to a second steady state at $t = 4515$, as shown in Figure D.1(e). In this test, $\lambda = 5\times 10^6$, $\Delta t = 1$, $c_1 = \frac{3}{\varepsilon}$ and $c_2 = 3\lambda_0$.

The gray region in Figure D.2(a) corresponds to the inpainting region. We run the modified Cahn–Hilliard equation (Scheme 1) with $f(s) = 4s^3 - 6s^2 + 2s$ and $\varepsilon = 0.05$ (intermediate value). We are close to a steady state at $t = 1.25$, as shown in Figure D.2(b), and we replace all values larger than $\frac{1}{2}$ by 1 and all those smaller than $\frac{1}{2}$ by 0 to obtain the final inpainting in Figure D.2(c). Here, $\lambda = 900000$ and $\Delta t = 0.05$

Furthermore, we run again the modified Cahn–Hilliard equation (Scheme 3) with the same $f(s) = 4s^3 - 6s^2 + 2s$ and the same initial datum, but we now take $\varepsilon = 0.1$ (larger value). We are close to a steady state at $t = 15852$, as shown in Figure D.2(d). Then, We run again the modified Cahn–Hilliard equation (Scheme 3) with the initial datum obtained in Figure D.2(d) and $\varepsilon = 4\times 10^{-5}$. We obtained the final inpainting result in Figure D.2(e) at $t = 33804$. The parameters in this example are $\lambda = 500000$, $\Delta t = 1$, $c_1 = \frac{3}{\varepsilon}$ and $c_2 = 3\lambda_0$. Note that, the results with Scheme 3 were not satisfying when use the interface thickness larger than the mesh size, but surprisingly, we obtained better results with a smaller interface thickness. We further note that, the constants c_1 and c_2 added to the functionals energy give the unconditionally stability of Scheme 3 but they increase the convergence time of the scheme as shown in Figure D.1 and Figure D.2.

(a)

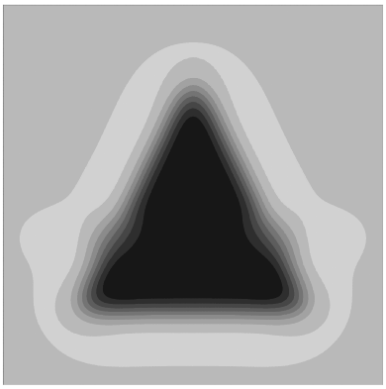

(b)

(c)

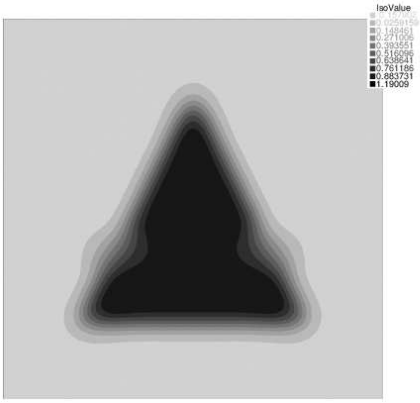

(d)

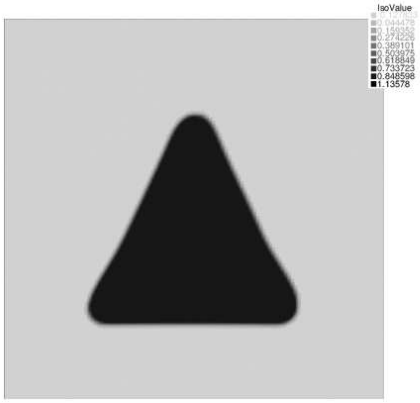

(e)

FIGURE D.1 – (a) Inpainting region in gray. Scheme 1 : (b) Solution at $t = 1$, $\varepsilon = 0.03$. (c) Replacing the values larger than $\frac{1}{2}$ by 1 and those smaller than $\frac{1}{2}$ by 0. Scheme 3 : (d) Solution at $t = 1765$, $\varepsilon = 0.1$. (e) Solution at $t = 4515$, $\varepsilon = 4 \times 10^{-5}$.

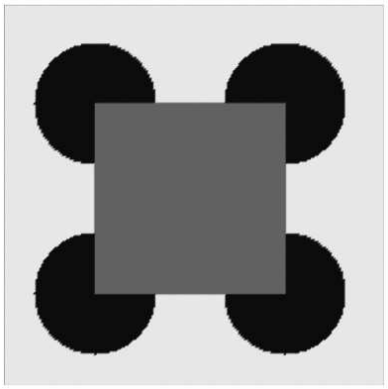

(a)

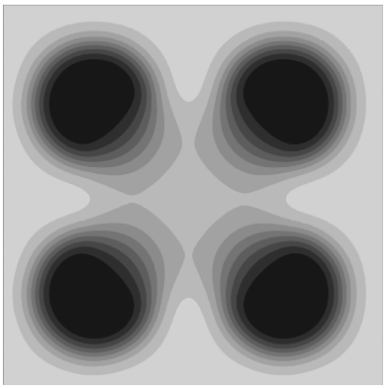

(b)

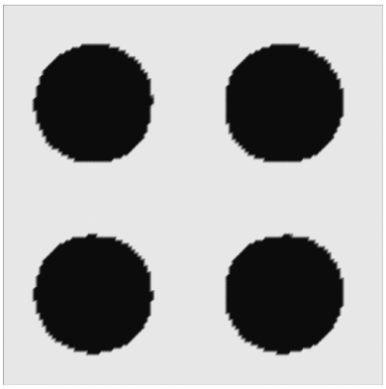

(c)

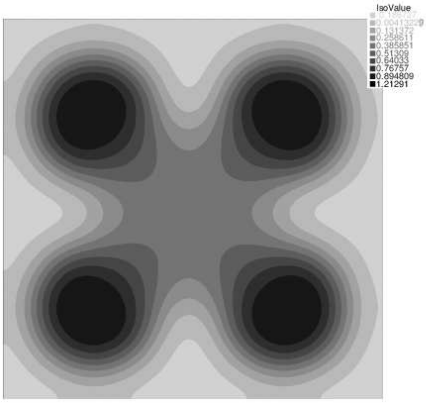

(d)

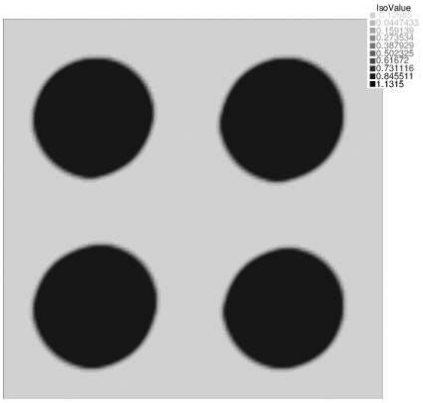

(e)

FIGURE D.2 – (a) Inpainting region in gray. Scheme 1 : (b) Solution at $t = 1.25$, $\varepsilon = 0.05$. (c) Replacing the values larger than $\frac{1}{2}$ by 1 and those smaller than $\frac{1}{2}$ by 0. Scheme 3 : (d) Solution at $t = 15852$, $\varepsilon = 0.1$. (e) Solution at $t = 33804$, $\varepsilon = 4 \times 10^{-5}$.

– **Scheme 1 :** Advantages :

1. Fast numerical results (By the inpainting results shown in Figure D.1 and Figure D.2, we might think that the results obtained with Scheme 1 are very fast than the ones obtained with Scheme 3) ;
2. Algorithm with one step involving ε.

Inconveniences :

1. No stability result for this scheme ;
2. This algorithm is not always applicable (intermediate ε).

– **Scheme 3 :** Advantages :

1. The time-stepping scheme is unconditionally stable provided that $c_1 > \frac{1}{\varepsilon}$ and $c_2 > \lambda_0$;
2. It can connect edges ever when the inpainting area is large.

Inconveniences :

1. Slow numerical results ;
2. algorithm with two steps involving ε.

D.4 Comparison between regular nonlinearities and singular nonlinearities

Here, we use scheme 1 to compare inpainting results obtained by polynomial nonlinear term and logarithmic nonlinear one. Furthermore, the numerical results presented below, Ω is a $(0, 0.5) \times (0, 0.5)-$square. The triangulation is obtained by dividing Ω into 200×200 rectangles and by dividing each rectangle along the same diagonal. In order to have comparable inpainting results, we take the initial datum between 0 and 0.5 with logarithmic nonlinear term and between 0 and 1 with polynomial nonlinear one to obtain better inpainting results, as far as the convergence time is concerned (it is also possible to obtain the inpainting results to take the initial datum in $(-1, 1)$ with logarithmic nonlinear term and in $(0, 0.5)$ with polynomial nonlinear one but, the results obtained here are less good than obtained above, as far as the convergence time is concerned). Furthermore, the parameter λ_0 may be change from test to another one in the same example to give the better inpainting results in each case.

Inpainting of a double Strings

The gray region in Figure D.3(a) corresponds to the inpainting region. We run again the modified Cahn–Hilliard equation with the same initial datum, $\epsilon = 0.05$, $\Delta t = 0.05$ and $\lambda_0 = 4 \times 10^6$, but we now take $f(s) = -2\ln(3)s + \ln\left(\frac{1+s}{1-s}\right)$ (note that f vanishes at -0.5 and 0.5). We observe that the solution remains in $(-1, 1)$ when considering an intermediate value of the diffuse interface thickness ϵ. We are close to a steady state at $t = 0.3$, as shown in Figure D.3(b), and we replace all values larger than $\frac{1}{4}$ by $\frac{1}{2}$ and all those smaller than $\frac{1}{4}$ by 0 to obtain the final inpainting in Figure D.3(c).

Then, we run again the modified Cahn–Hilliard equation with the same $\epsilon = 0.05$, $\Delta t = 0.05$ and $\lambda_0 = 4 \times 10^6$, but we now take $f(s) = 4s^3 - 6s^2 + 2s$ and the initial datum in $[0, 1]$ instead

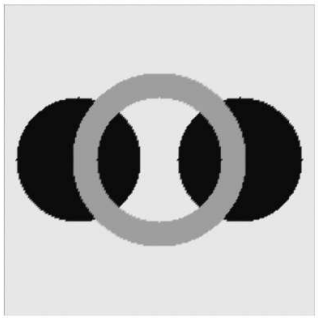

(a)

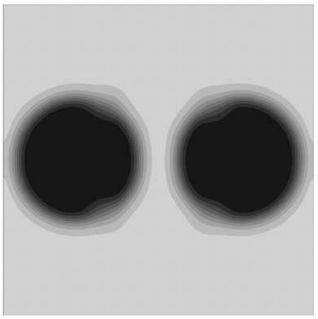

(b)

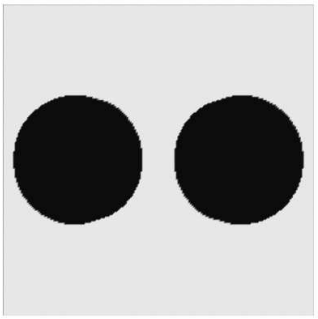

(c)

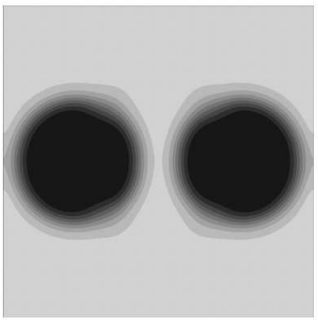

(d)

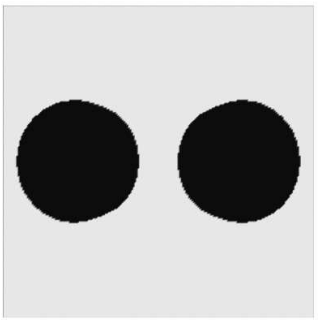

(e)

FIGURE D.3 – (a) Inpainting region in gray, random initial datum between 0 and 0.5 in inpainting region, $\varepsilon = 0.05$. (b) Solution at $t = 0.3$, $f(s) = -2\ln(3)s + \ln\left(\frac{1+s}{1-s}\right)$. (c) Replacing the values larger than $\frac{1}{4}$ by $\frac{1}{2}$ and those smaller than $\frac{1}{4}$ by 0. (d) Solution at $t = 1$, $f(s) = 4s^3 - 6s^2 + 2s$. (e) Replacing the values larger than $\frac{1}{2}$ by 1 and those smaller than $\frac{1}{2}$ by 0.

of $[0, 0.5]$ in order to have comparable inpainting results (note that the solution does not remain in the relevant interval $[0, 1]$). We are close to a steady state at $t = 1$, as shown in Figure D.3(d), and we replace all values larger than $\frac{1}{2}$ by 1 and all those smaller than $\frac{1}{2}$ by 0 to obtain the final inpainting in Figure D.3(e).

Inpainting of a cross

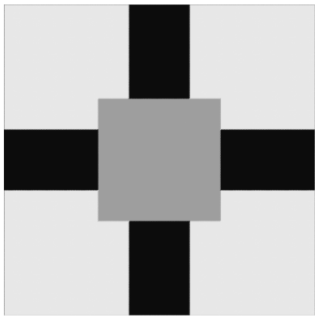

(a)

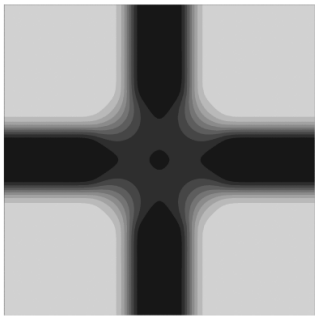

(b)

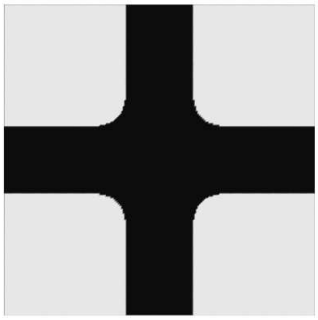

(c)

(d)

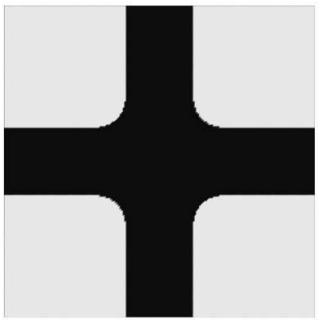

(e)

FIGURE D.4 – (a) Inpainting region in gray, random initial datum between 0 and 0.5 in inpainting region, $\varepsilon = 0.05$. (b) Solution at $t = 0.35$, $f(s) = -2\ln(3)s + \ln\left(\frac{1+s}{1-s}\right)$. (c) Replacing the values larger than $\frac{1}{4}$ by $\frac{1}{2}$ and those smaller than $\frac{1}{4}$ by 0. (d) Solution at $t = 1.2$, $f(s) = 4s^3 - 6s^2 + 2s$. (e) Replacing the values larger than $\frac{1}{2}$ by 1 and those smaller than $\frac{1}{2}$ by 0.

The gray region in Figure D.4(a) corresponds to the inpainting region. We run again the modified Cahn–Hilliard equation with the same initial datum, $\epsilon = 0.05$, $\Delta t = 0.05$ and $\lambda_0 = 4 \times 10^6$, but we now take $f(s) = -2\ln(3)s + \ln\left(\frac{1+s}{1-s}\right)$ (note that f vanishes at -0.5 and 0.5). We observe that the solution remains in $(-1, 1)$ when considering an intermediate value of the

diffuse interface thickness ϵ. We are close to a steady state at $t = 0.35$, as shown in Figure D.4(b), and we replace all values larger than $\frac{1}{4}$ by $\frac{1}{2}$ and all those smaller than $\frac{1}{4}$ by 0 to obtain the final inpainting in Figure D.4(c).

Furthermore, we run again the modified Cahn–Hilliard equation with the same $\epsilon = 0.05$, $\Delta t = 0.05$ and $\lambda_0 = 4 \times 10^6$, but we now take $f(s) = 4s^3 - 6s^2 + 2s$ and the initial datum in $[0, 1]$ instead of $[0, 0.5]$ in order to have comparable inpainting results (note that the solution does not remain in the relevant interval $[0, 1]$). We are close to a steady state at $t = 1.2$, as shown in Figure D.4(d), and we replace all values larger than $\frac{1}{2}$ by 1 and all those smaller than $\frac{1}{2}$ by 0 to obtain the final inpainting in Figure D.4(e).

Inpainting of a circle

The gray region in Figure D.5(a) corresponds to the inpainting region. We run again the modified Cahn–Hilliard equation with the same initial datum, $\epsilon = 0.04$, $\Delta t = 0.05$ and $\lambda_0 = 900000$, but we now take $f(s) = -2\ln(3)s + \ln\left(\frac{1+s}{1-s}\right)$ (note that f vanishes at -0.5 and 0.5). We observe that the solution remains in $(-1, 1)$ when considering an intermediate value of the diffuse interface thickness ϵ. We are close to a steady state at $t = 0.25$, as shown in Figure D.5(b), and we replace all values larger than $\frac{1}{4}$ by $\frac{1}{2}$ and all those smaller than $\frac{1}{4}$ by 0 to obtain the final inpainting in Figure D.5(c).

Then, we run again the modified Cahn–Hilliard equation with the same $\epsilon = 0.04$, $\Delta t = 0.05$ and $\lambda_0 = 900000$, but we now take $f(s) = 4s^3 - 6s^2 + 2s$ and the initial datum in $[0, 1]$ instead of $[0, 0.5]$ in order to have comparable inpainting results (note that the solution does not remain in the relevant interval $[0, 1]$). We are close to a steady state at $t = 0.25$, as shown in Figure D.5(d), and we replace all values larger than $\frac{1}{2}$ by 1 and all those smaller than $\frac{1}{2}$ by 0 to obtain the final inpainting in Figure D.5(e)

D.5 Dynamics of solutions with different values of λ_0

We show in Figure D.6 a numerical example represents the effect of different values of λ_0 on the dynamics of the solution. In Figure D.6(a), the gray region denotes the region to be inpainted. We run the modified Cahn–Hilliard equation with $f(s) = 4s^3 - 6s^2 + 2s$ with $\lambda_0 = 100000$, $\Delta t = 0.05$, and $\varepsilon = 0.05$, we are close to the steady state at $t = 1.95$, as shown in Figure D.6(b). Then, we run again the modified Cahn–Hilliard equation with the same initial data, $f(s) = 4s^3 - 6s^2 + 2s$, $\Delta t = 0.05$, and $\varepsilon = 0.05$, but we now take $\lambda_0 = 500000$ (resp. $\lambda_0 = 5 \times 10^6$) and we are close to the steady state in Figure D.6(c) (resp. Figure D.6(d)) at $t = 1.45$ (resp. at $t = 1.15$). Finally, We run the modified Cahn–Hilliard equation with the same parameters taken above, but we now take $\lambda_0 = 5 \times 10^7$ and we are close to the steady state in Figure D.6(e) at $t = 1.15$. We note that, the choice of λ_0 is crucial and problematic in numerical simulations which is contrary to the theoretical results. Recalling that, in theoretical results (see [16]), the inpainting results are obtained when λ_0 goes to ∞. On the contrary, in numerical simulations (see Figure D.6), the inpainting results does not necessarily improve when we increase the value of λ_0.

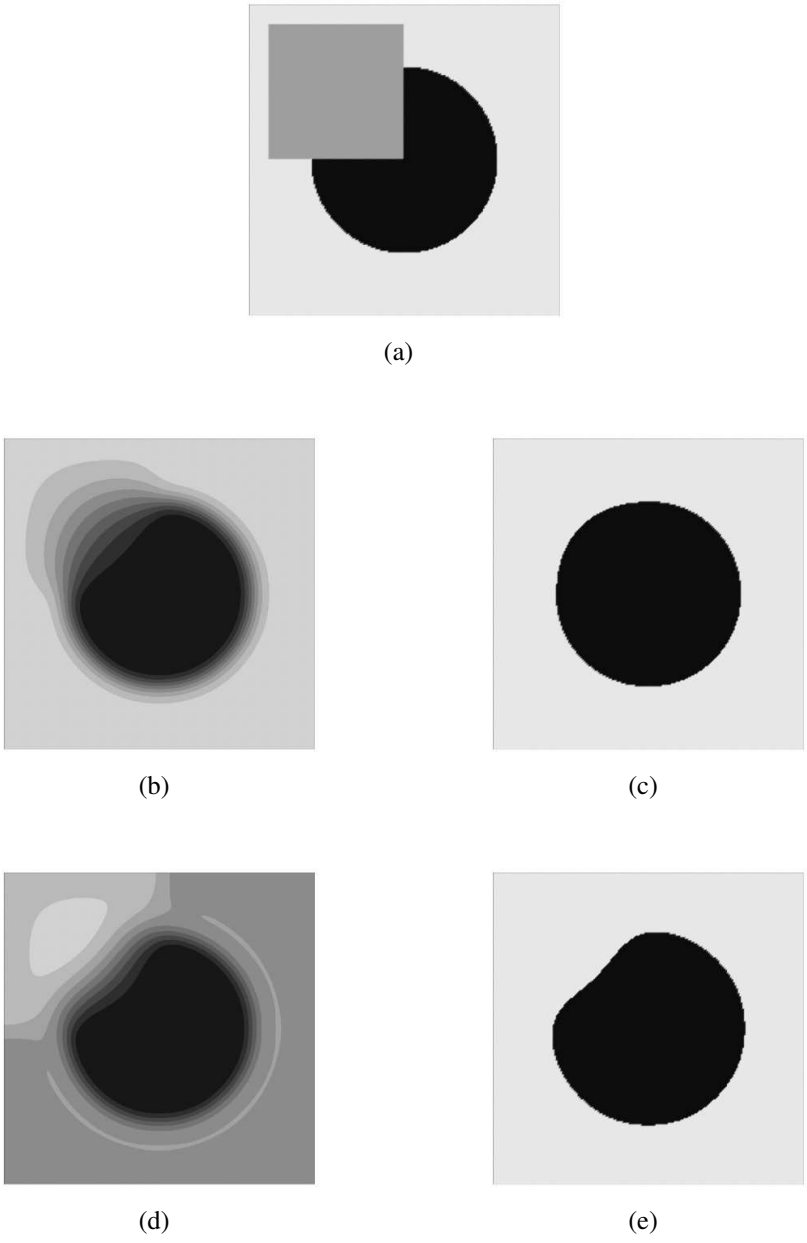

(a)

(b)

(c)

(d)

(e)

FIGURE D.5 – (a) Inpainting region in gray, random initial datum between 0 and 0.5 in inpainting region, $\varepsilon = 0.04$. (b) Solution at $t = 0.25$, $f(s) = -2\ln(3)s + \ln\left(\frac{1+s}{1-s}\right)$. (c) Replacing the values larger than $\frac{1}{4}$ by $\frac{1}{2}$ and those smaller than $\frac{1}{4}$ by 0. (d) Solution at $t = 0.25$, $f(s) = 4s^3 - 6s^2 + 2s$. (e) Replacing the values larger than $\frac{1}{2}$ by 1 and those smaller than $\frac{1}{2}$ by 0.

D.6 Inpainting in 3D with scheme 1

We perform inpainting 3D on a damaged image contained in sphere as shown in Figure D.7(a). In Figure D.7(b), the black region denotes the region to be inpainted. We run the three dimensional Bertozzi–Esedoglu–Gillette–Cahn–Hilliard equation with $f(s) = 4s^3 - 6s^2 + 2s$

with $\lambda_0 = 10^6$, $\Delta t = 0.05$, and $\varepsilon = 1.8$, we are close to the steady state at $t = 0.2$, as shown in Figure D.7(c).

D.7 Comparison between binary inpainting results with Scheme 1 and Scheme 2 ($n = 2$)

We saw in Chapter 3 that the Scheme 2 is efficient in the context of multi-color inpainting. Furthermore, the proposed model is consistent with the diphasic one. Then, an interesting way to see what happened in the binary inpainting results with the system $n = 2$. Is our proposed model for $n = 2$ also efficient in the context of binary inpainting as the Bertozzi–Esedoglu–Gillette–Cahn–Hilliard equation ? A positive answer of this question was obtained based on the construction of the model in Chapter 3. Furthermore, a numerical answer in this way can be shown in Figure D.8. In Figure D.8(b), the gray region denotes the region to be inpainted. We run the Cahn–Hilliard system ($n = 2$) with $f(s) = 4s^3 - 6s^2 + 2s$ with $\lambda_0 = 500000$, $\Delta t = 0.05$, and $\varepsilon = 0.03$, we are close to the steady state at $t = 0.2$, and we replace all values larger than $\frac{1}{2}$ by 1 and all those smaller than $\frac{1}{2}$ by 0 to obtain the final inpainting in Figure D.8(b). Then, we run again the Bertozzi–Esedoglu–Gillette–Cahn–Hilliard equation with the same initial data, $f(s) = 4s^3 - 6s^2 + 2s$, $\Delta t = 0.05$, $\varepsilon = 0.03$, and $\lambda_0 = 500000$ but with Scheme 1 and we are close to the steady state at $t = 3.2$, and we replace all values larger than $\frac{1}{2}$ by 1 and all those smaller than $\frac{1}{2}$ by 0 to obtain the final inpainting in Figure D.8(c). We remark that the inpainting results obtained in Figure D.8(b) are better than the inpainting ones obtained in Figure D.8(c), as far as the singular points in $\Omega \backslash D$. The fact of obtaining better inpainting results in Figure D.8(b) due to the diffuse interface thickness in Scheme 2 is ε^2. Moreover, we can also obtain the same inpainting result with Scheme 1, if we decrease the value of the diffuse interface thickness ε in this case.

D.8 Binary inpainting image applications with Scheme 2 ($n = 2$)

In Figures D.9 and D.10, we use Scheme 2 ($n = 2$). Figure D.9(a) and Figure D.9(b) correspond to vandalized image and masked image, respectively. We run the modified Cahn–Hilliard system ($n = 2$) with $\varepsilon = 0.03$. Then, when we are close to a steady state at $t = 0.15$, we replace the dominant color by 1 and the other colors by 0 to obtain the final inpainting in Figure D.9(c). Here, $\lambda_0 = 10^8$ and $\Delta t = 0.05$.

Furthermore, in Figure D.10, we give an example of remove text in image. Figure D.10(a) and Figure D.10(b) correspond to original image and masked image, respectively. We run the modified Cahn–Hilliard system ($n = 2$) with $\varepsilon = 0.03$. Then, when we are close to a steady state at $t = 0.15$, we replace the dominant color by 1 and the other colors by 0 to obtain the final inpainting in Figure D.10(c). In this case, $\lambda_0 = 10^7$ and $\Delta t = 0.05$.

D.9 Numerical results with mesh adaptation for color image inpainting

Here, we use scheme 2 for the Bertozzi–Esedoglu–Gillette–Cahn–Hilliard system to give more numerical results than those given in Chapter 3. Furthermore, the numerical results presented below, Ω is a $(0, 0.5) \times (0, 0.5)-$square.

Figure D.11(a) corresponds to the mesh adaptation. The light blue region in Figure D.11(b) corresponds to the inpainting region. We run the modified Cahn–Hilliard system ($n = 3$) with $\varepsilon = 0.05$, $\Delta t = 0.05$, and $\lambda_0 = 5 \times 10^6$. We are close to a steady state at $t = 0.15$ and we replace the dominant color by 1 and the other colors by 0 to obtain the final inpainting in Figure D.11(c).

Figure D.12(a) corresponds to the mesh adaptation. The light blue region in Figure D.12(b) corresponds to the inpainting region. We run the modified Cahn–Hilliard system ($n = 9$) with $\varepsilon = 0.005$, $\Delta t = 0.05$, and $\lambda_0 = 10^6$. We are close to a steady state at $t = 0.65$ and we replace the dominant color by 1 and the other colors by 0 to obtain the final inpainting in Figure D.12(c).

D.10 Consistency with three and four phase-model examples

The goal of this section is to give more consistency examples more than the consistency results with the two-phase model ; more precisely, the consistency of the model with the k-phase model, $k < n$, but we do not have a theoretical results in this context.Furthermore, the numerical results presented below, Ω is a $(0, 0.5)\times(0, 0.5)-$square. The triangulation is obtained by dividing Ω into 100×100 rectangles and by dividing each rectangle along the same diagonal.

We first take the same example in Figure D.9 without mesh adaptation. Furthermore, we take $c_1 = h_1 = c_4 = h_4 = 0$. The light green region in Figure D.13(a) corresponds to the inpainting region. We run the modified Cahn–Hilliard system ($n = 5$) with $\varepsilon = 0.05$, $\Delta t = 0.05$, and $\lambda_0 = 5 \times 10^6$. We are close to a steady state at $t = 0.65$ and we replace the dominant color by 1 and the other colors by 0 to obtain the final inpainting in Figure D.13(b). Note that $|c_i| < 10^{-2}, \forall t \geq 0, i = 1, 4$.

As a next step, we take the same example in Figure D.10 without mesh adaptation. Furthermore, we take $c_i = h_i = 0, \forall i \in 1, 2, 3, 5, 6, 7$. The light green region in Figure D.14(a) corresponds to the inpainting region. We run the modified Cahn–Hilliard system ($n = 9$) with $\varepsilon = 0.03$, $\Delta t = 0.05$, and $\lambda_0 = 9 \times 10^6$. We are close to a steady state at $t = 0.65$ and we replace the dominant color by 1 and the other colors by 0 to obtain the final inpainting in Figure D.14(b). Note that $|c_i| < 10^{-2}, \forall t \geq 0, i = 1, 2, 3, 5, 6, 7$.

Finally, in order to give a four-phase model consistence, we also take the same example in Figure D.10 without mesh adaptation. Furthermore, we take $c_i = h_i = 0, \forall i \in 1, 2, 5, 6, 7$. The light green region in Figure D.15(a) corresponds to the inpainting region. We run the modified Cahn–Hilliard system ($n = 9$) with $\varepsilon = 0.03$, $\Delta t = 0.05$, and $\lambda_0 = 9 \times 10^6$. We are close to a steady state at $t = 0.65$ and we replace the dominant color by 1 and the other colors by 0 to obtain the final inpainting in Figure D.15(b). Note that $|c_i| < 10^{-2}, \forall t \geq 0, i = 1, 2, 5, 6, 7$.

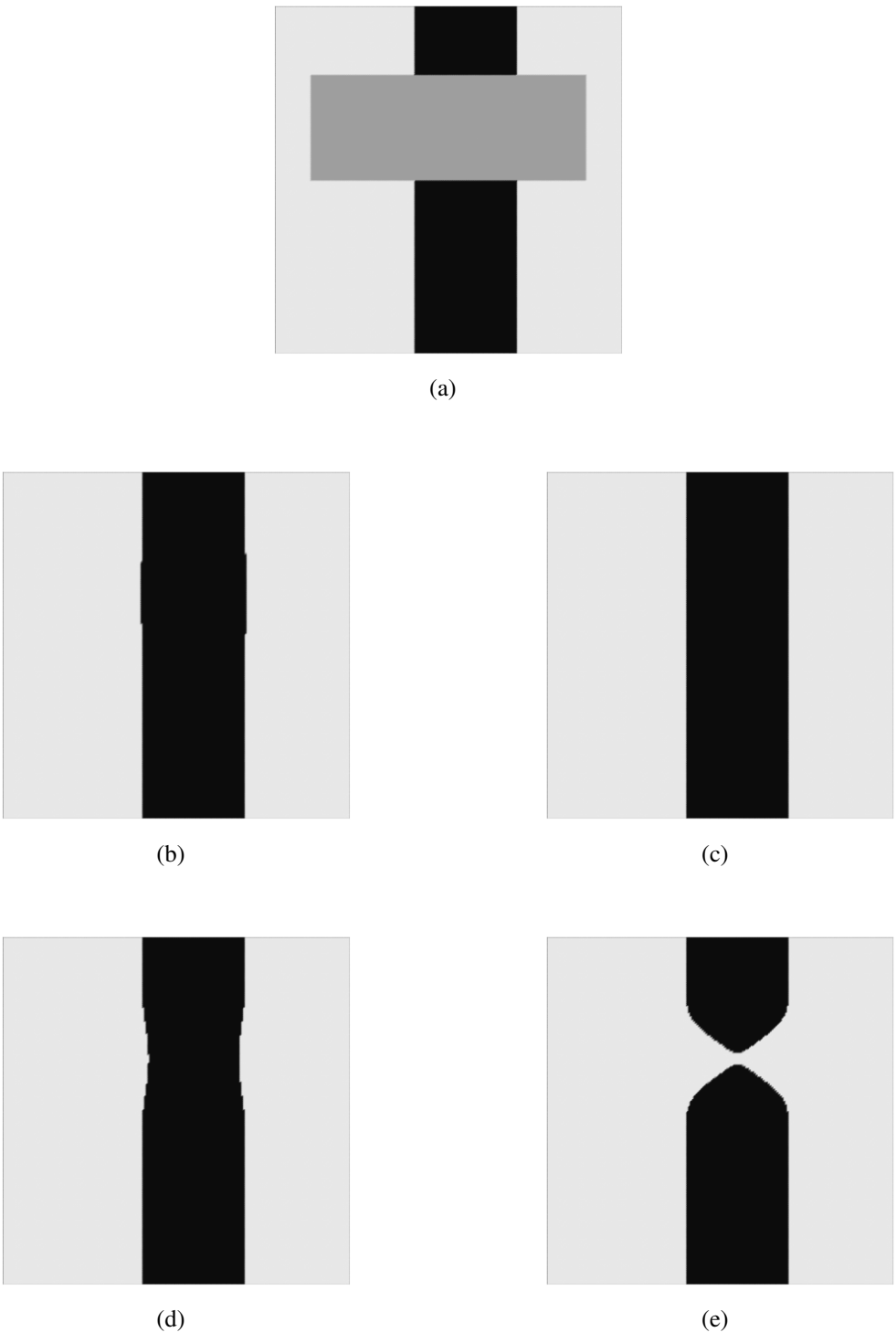

(a)

(b)

(c)

(d)

(e)

FIGURE D.6 – (a) Inpainting region in gray, random initial datum between 0 and 1 in inpainting region. Here, $\varepsilon = 0.05$ and $\Delta t = 0.05$. (b) Solution at $t = 1.95$, $\lambda_0 = 100000$. (c) Solution at $t = 1.45$, $\lambda_0 = 500000$. (d) Solution at $t = 1.15$, $\lambda_0 = 5 \times 10^6$. (e) Solution at $t = 1.15$, $\lambda_0 = 5 \times 10^7$.

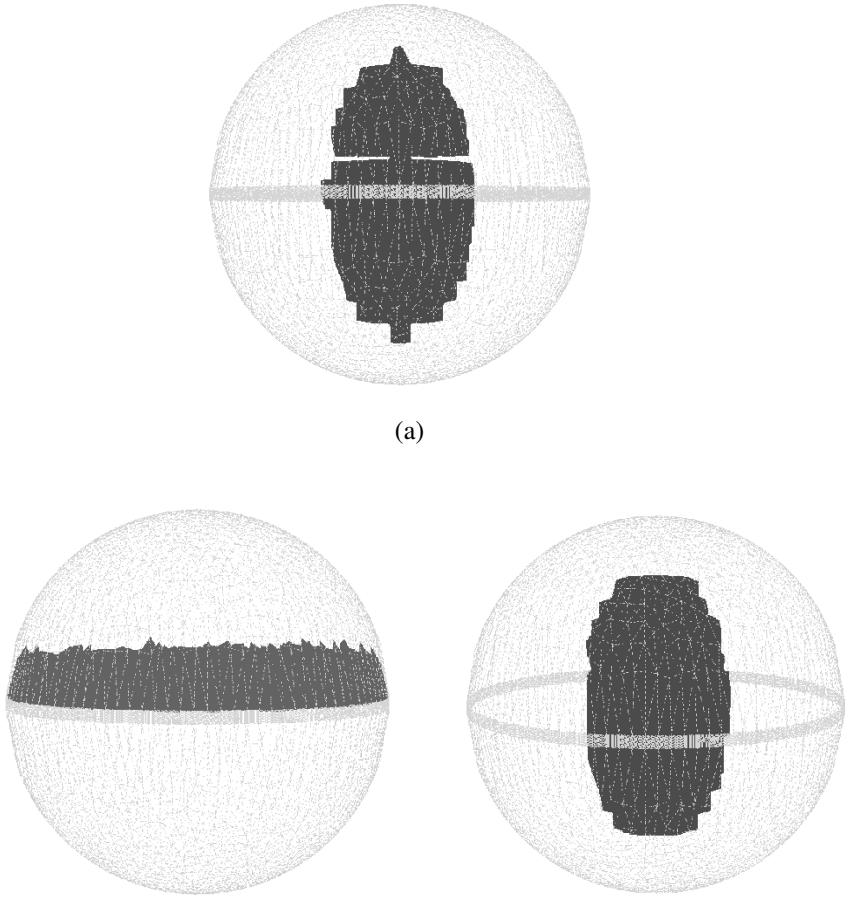

(a)

(b) (c)

FIGURE D.7 – Modified Cahn–Hilliard equation for 3D inpainting

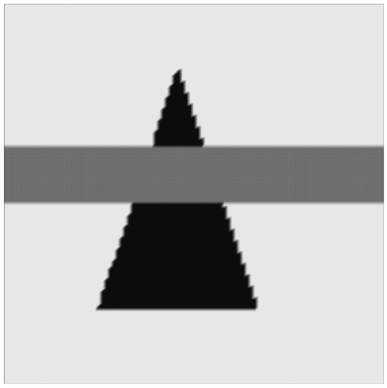

(a)

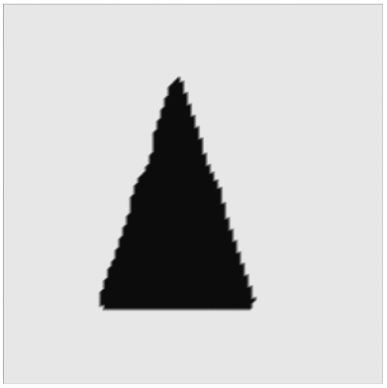

(b)

(c)

FIGURE D.8 – (a) Inpainting region in gray, random initial datum between 0 and 1 in inpainting region. Here, $\varepsilon = 0.03$ and $\Delta t = 0.05$. (b) Solution at $t = 0.2$ with Scheme 2 ($n = 2$). (c) Solution at $t = 3.2$ with Scheme 1.

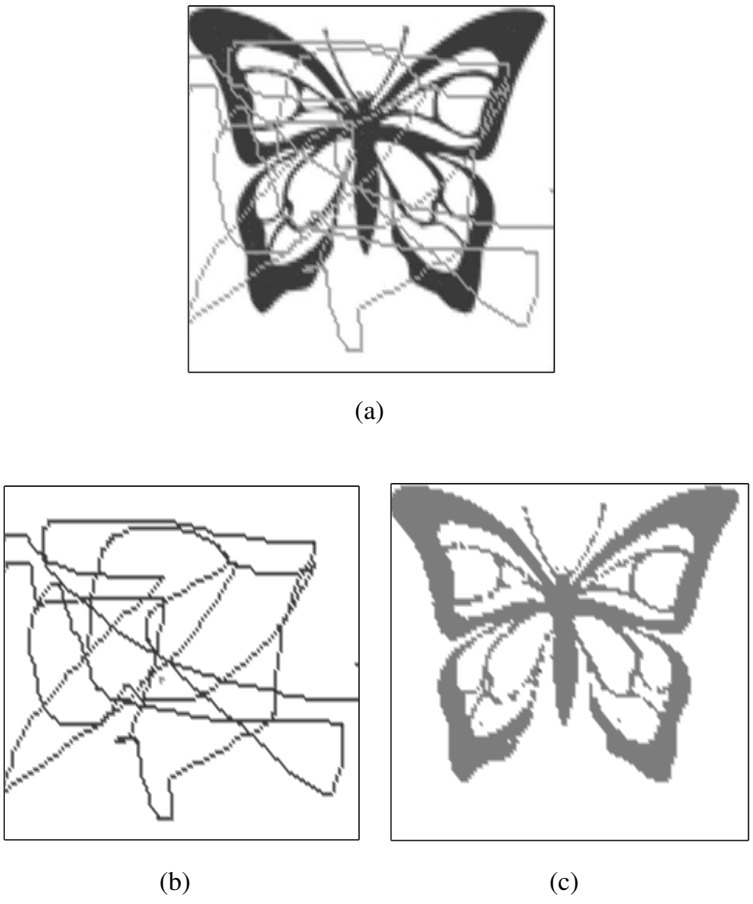

(a)

(b) (c)

FIGURE D.9 – (a) vandalized image. (b) masked image. (c) Inpainting results.

(a)

(b)

(c)

FIGURE D.10 – (a) Damaged image. (b) masked image. (c) Inpainting results.

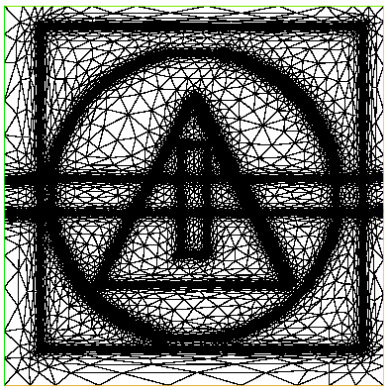

(a)

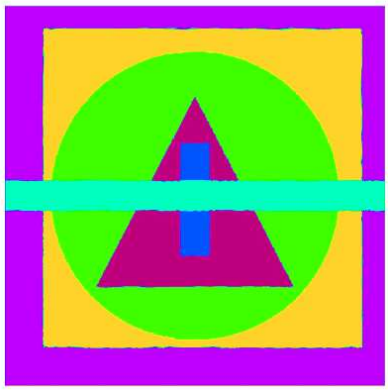

(b)

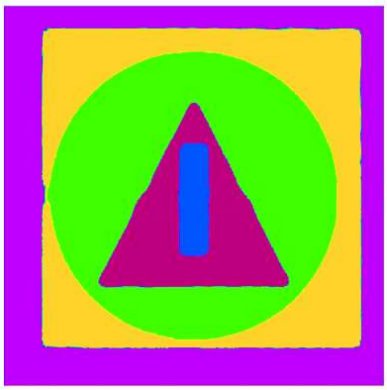

(c)

FIGURE D.11 – (a) Mesh adaptation. (b) Inpainting region in light blue, random initial datum between 0 and 1 in inpainting region, $\varepsilon = 0.05$. (b) Solution at $t = 0.15$; replacing the dominant color by 1 and the other colors by 0.

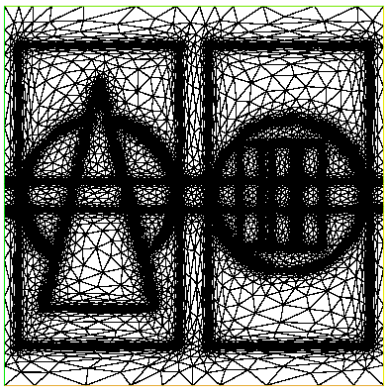

(a)

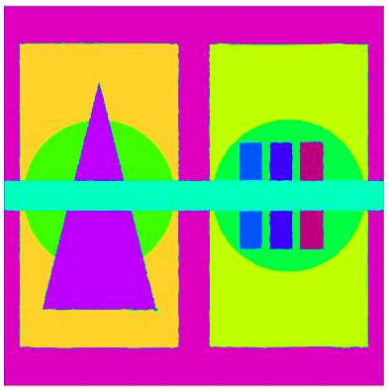

(b)

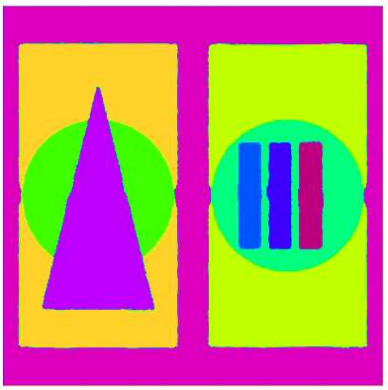

(c)

FIGURE D.12 – (a) Mesh adaptation. (b) Inpainting region in light blue, random initial datum between 0 and 1 in inpainting region, $\varepsilon = 0.05$. (b) Solution at $t = 0.15$; replacing the dominant color by 1 and the other colors by 0.

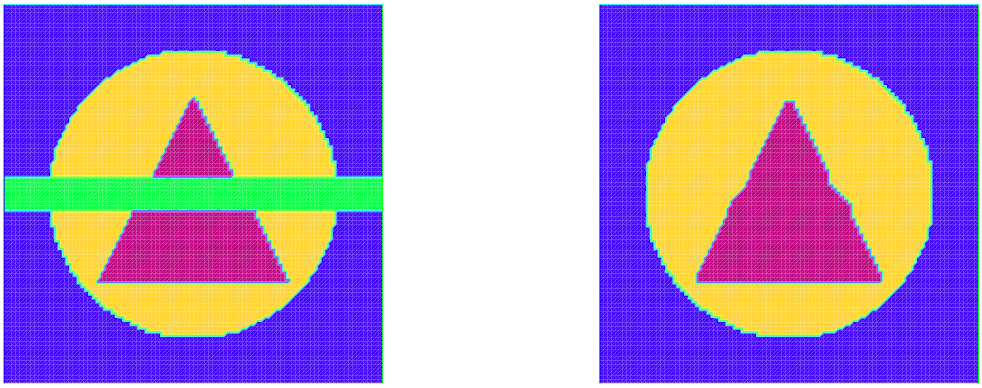

(a) (b)

FIGURE D.13 – (a) Inpainting region in light green, random initial datum between 0 and 1 in inpainting region, $\varepsilon = 0.05$. (b) Solution at $t = 0.15$; replacing the dominant color by 1 and the other colors by 0.

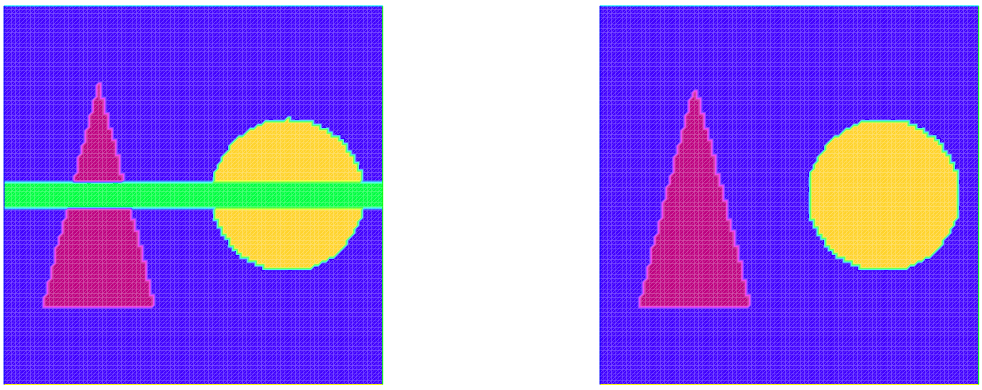

(a) (b)

FIGURE D.14 – (a) Inpainting region in light green, random initial datum between 0 and 1 in inpainting region, $\varepsilon = 0.05$. (b) Solution at $t = 0.2$; replacing the dominant color by 1 and the other colors by 0.

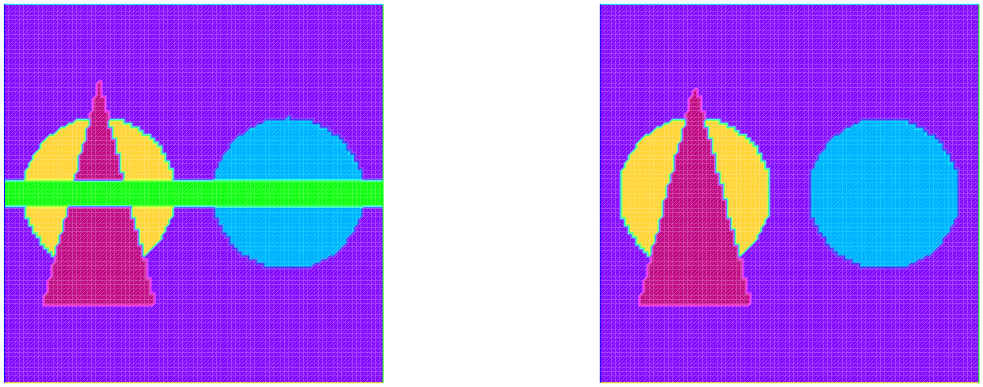

(a) (b)

FIGURE D.15 – (a) Inpainting region in light green, random initial datum between 0 and 1 in inpainting region, $\varepsilon = 0.05$. (b) Solution at $t = 0.2$; replacing the dominant color by 1 and the other colors by 0.

Bibliographie

[1] H. Abels and M. Wilke, Convergence to equilibrium for the Cahn–Hilliard equation with a logarithmic free energy, Nonlinear Anal. TMA 67 (2007), 3176–3193.

[2] N.D. Akikakos, P.W. Bates, and X. Chen, Convergence of the Cahn–Hilliard eqaution to the Hele-Shaw model, Arch, Rational Mech. Anal. 128 (1994), 165–205.

[3] S.M. Allen and J.W. Cahn, A macroscopic theory for antiphase boundary motion and its application to antiphase domain coarsening, Ada Metall 27 (1979), 1085–1095.

[4] L. Ambrosio and V.M. Tortorelli, Approximation of functionals depending on jumps by elliptic functionals via Gamma convergence, Commun. Pure Appl. Math. 43 (1990), 999–1036.

[5] A.C. Aristotelous, O.A. Karakashian, and S.M. Wise, Adaptive, second order in time, primitive-variable discontinuous Galerkin schemes for a Cahn–Hilliard equation with a mass source, IMA J. Numer. Anal 35(2015), 1167–1198.

[6] W. Baatz, M. Fornasier, P. Markowich, C.-B. Schöilieb, Inpainting of ancient Austrian frescoes, Conference Proceedings of Bridges 2008, Leeuwarden, Vol 6, 150–156, 2008.

[7] A.V. Babin and M.I. Vishik, Attractors of Evolution Equations, North-Holland, Amsterdam, 1992.

[8] F. Bai, C.M. Elliott, A. Gardiner, A. Spence, and A.M. Stuart, A. The viscous Cahn–Hilliard equation. Part I : Computations, Nonlinearity 8 (1995), 131.

[9] C. Ballester, M. Bertalmio, V. Caselles, G. Sapiro, and J. Verdera, Fillingin by joint interpolation of vector fields and grey levels, IEEE Transactions on Image Processing 10 (2001), 1200–1211.

[10] T. Bárta, R. Chill, and E. Fašangovà, Every ordinary differential equation with a strict Lyapunov function is a gradient system, Monatshefte für Mathematik 166 (2012), 57–72.

[11] P.W. Bates and P.C. Fife, The dynamics of nucleation for the Cahn–Hilliard equation, SIAM J. Appl. Math. 53 (1993), 990–1008.

[12] P.W. Bates and J. Han, The Dirichlet boundary problem for a nonlocal Cahn ?Hilliard equation, J. Math. Anal. Appl. 311 (2005), 289–312.

[13] Z. Belhachmi, M. Kallel , M. Moakher, and A. Theljani, Weighted Harmonic and Ginzburg-Landau equations in image inpainting, preprint.

[14] M. Bertalmio, A. Bertozzi, and G. Sapiro, Navier-Stokes, fluid dynamics, and image and video inpainting, in Proceedings of the IEEE computer Vision and Pattern Recognition, Vol. 1, 335–362, 2001.

[15] M. Bertalmio, G. Sapiro, V. Casselles, and C. Ballester, Image inpainting, in Siggraph 2000, Computer Graphics Proceedings, K. Akeley, ed., ACM Press/Addison-Wesley, NewYork, 417–424, 2000.

[16] A. Bertozzi, S. Esedoglu, and A. Gillette, Analysis of a two-scale Cahn–Hilliard model for binary image inpainting, Multiscale Model. Simul. 6 (2007), 913–936.

[17] A. Bertozzi, S. Esedoglu, and A. Gillette, Inpainting of binary images using the Cahn-Hilliard equation, IEEE Trans. Image Proc. (2007), 285–291.

[18] F.J. Blowey and C.M. Elliott, The Cahn–Hilliard gradient theory for phase separation with non-smooth free energy part i : mathematical analysis, Euro. J. of Appl. Math. 2 (1991), 233–280.

[19] F.J. Blowey and C.M. Elliott, The Cahn–Hilliard gradient theory for phase separation with non-smooth free energy part ii : mathematical analysis, Euro. J. of Appl. Math. 3 (1992), 147–179.

[20] J. Bosch, D. Kay, M. Stoll, and A.J. Wathen, Fast solvers for Cahn–Hilliard inpainting, SIAM J. Imag. Sci. 7 (2013), 67–97.

[21] J. Bosch and M. Stoll, A fractional inpainting model based on the vector-valued Cahn–Hilliard equation, SIAM J. Imag. Sci., to appear.

[22] F. Boyer and C. Lapuerta, Study of a three component Cahn–Hilliard flow model, M2AN, Mod. Math. Anal. Num. 40 (2006), 653–687.

[23] A. Braides, Γ-convergence for beiginners, Oxford University press, New York, 2000.

[24] C. Braverman, Photoshop retouching handbook, IDG Books Worldwide, 1998.

[25] M. Burger, L. He, and C.-B. Schönlieb, Cahn–Hilliard inpainting and a generalization for grayvalue images, SIAM J. Imag. Sci. 3 (2009), 1129–1167.

[26] J.W. Cahn, On spinodal decomposition, Acta Metall. 9 (1961), 795–801.

[27] J.W. Cahn and J.E. Hilliard, Free energy of a nonuniform system I. Interfacial free energy, J. Chem. Phys. 28 (1958), 258–267.

[28] T. Callaghan, E. Khain, L.M. Sander, and R.M. Ziff, A stochastic model for wound healing, Journal of statistical physics 122 (2006), 909–924.

[29] V. Chalupecki, Numerical studies of Cahn–Hilliard equations and applications in image processing, Proceedings of Gzech-Japanese Seminar in Applied Mathematics, 4-7 August, 2004, Czech Technical University in Prague, 2004.

[30] L. Chanas, J.P. Cocquerez, and J. Blanc-Talon, Simultaneous inpainting and motion estimation of highly degraded video-sequences, Lecture Notes in Computer Science 2749 (2003), 11–23.

[31] T.F. Chan, S.H. Kang, and J. Shen, Euler's elastica and cuvature-based inpainting, SIAM J. Appl. Math. 63 (2002), 564–592.

[32] T.F. Chan and J. Shen, Mathematical models of local nontexture inpaintings, SIAM J. Appl. Math. 62 (2002), 1019–1043.

[33] T.F. Chan and J. Shen, Variationnal image inpainting, Commun. Pure Appl. Math. 58 (2005), 579–619.

[34] T.F. Chan and J. Shen, Variationnal restoration of nonflaat image features : Models and algorithms, SIAM J. Appl. Math. 61 (2001), 1338–1361.

[35] T.F. Chan and J. Shen, Non-texture inpainting by curvature driven diffusions (CDD), J. Visual Comm. Image Rep. 62 (2001), 1019–1043.

[36]] T.F. Chan, and J. Shen, Morphologically invariant PDE inpaintings, CAM report 01-15, 2001.

[37] T.F. Chan J. Shen, and H.M. Zhou, Total variation wavelet inpainting, J. Math. Imag. Vis. 25 (2006), 107–125.

[38] L. Cherfils, H. Fakih, and A. Miranville, Finite-dimensional attractors for the Bertozzi-Esedoglu-Gillette-Cahn–Hilliard equation in image inpainting, Inv. Prob. Imag. 9 (2015), 105–125.

[39] L. Cherfils, H. Fakih, and A. Miranville, On the Bertozzi–Esedoglu–Gillette–Cahn–Hilliard equation with logarithmic nonlinear terms, SIAM J. Imag. Sci 8 (2015), 1123–1140.

[40] L. Cherfils, H. Fakih, A. Miranville, A Cahn–Hilliard system with a fidelity term for color image inpainting, J. Math. Imag. Vision, to appear.

[41] L. Cherfils, A. Miranville and S. Zelik, The Cahn–Hilliard equation with logarithmic potentials, Milan J. Math. 79 (2011), 561–596.

[42] L. Cherfils, A. Miranville, and S. Zelik, On a generalized Cahn–Hilliard equation with biological applications, Discrete Cont. Dyn. Systems B 19 (2014), 2013–2026.

[43] L. Cherfils, M. Petcu, and M. Pierre, A numerical analysis of the Cahn–Hilliard equation with dynamic boundary conditions, Discrete Cont. Dyn. Systems 27 (2010), 1511–1533.

[44] R. Chill, E. Fašangovà, and J. Prüss, Convergence to steady states of solutions of the Cahn–Hilliard equation with dynamic boundary conditions, Math. Nachr. 279 (2006), 1448–1462.

[45] D. Cohen and J.M. Murray, A generalized diffusion model for growth and dispersion in a population, J. Math. Biol. 12 (1981), 237–248.

[46] M. Conti, S. Gatti and A. Miranville, Multi-component Cahn-Hilliard systems with dynamic boundary conditions, Nonlinear Anal. Ser. B 25 (2015), 137–166.

[47] P. Constantin, C. Foias, B. Nicolaenko, and R. Temam, Integral manifolds and inertial manifolds for dissipative partial differential equations, Applied Mathematical Sciences, Vol. 70, Springer-Verlag, New York, 1989.

[48] A. Debussche and L. Dettori, On the Cahn–Hilliard equation with a logarithmic free energy, Nonlinear Anal. TMA 24 (1995), 1491–1514.

[49] F. Della Porta and M. Grasselli, Convective nonlocal Cahn–Hilliard equations with reaction terms, Discrete Cont. Dyn. Systems B 20 (2015), 1529–1553.

[50] J.A. Dobrosotskaya and A. Bertozzi, A Wavelet-Laplace variational thechnique for image deconvolution and inpainting, Trans. Imag. Proc. 17 (2008), 657–663.

[51] I.C. Dolcetta, S.F. Vita, and R. March, Area-preserving curve-shortening flows : From phase separation to image processing, Interfaces Free Bound. 4 (2002), 325–343.

[52] A. Eden, C. Foias, B. Nicolaenko, and R. Temam, Exponential Attractors for Dissipative Evolution Equations, Research in Applied Mathematics, Vol. 37, John-Wiley, New York, 1994.

[53] M. Efendiev, A. Miranville, and S. Zelik, Exponential attractors for a nonlinear reaction–diffusion system in $\mathbb{R}^3$, C.R. Acad. Sci. Paris Série I Math. 330 (2000), 713–718.

[54] M. Efendiev, A. Miranville, and S. Zelik, Exponential attractors for a singularly perturbed Cahn–Hilliard system, Math. Nach. 272 (2004), 11–31.

[55] C.M. Elliott, D.A. French and F.A. Milner, A second order splitting method for the Cahn–Hilliard equation, Numer. Math. 54 (1989), 575–590.

[56] C. M. Elliott, The Cahn–Hilliard model for the kinetics of phase separation, in Mathematical models for phase change problems, Birkhäuser Basel 35–73,1989.

[57] C. M. Elliott and S. Luckhaus, A generalised diffusion equation for phase separation of a multicomponent mixture with interfacial free energy, SFB256 University Bonn, Preprint 195, 1991.

[58] G. Emile-Male, The restorer's handbook of easel painting, Van Nostrand Reinold.

[59] S. Esedoglu and J. Shen, Digital inpainting based on the Mumford–Shah–Euler image model, Eur. J. Appl. Math. 13 (2002), 353–370.

[60] D.J. Eyre, An unconditionally stable one-step scheme for gradient systems, tech. report, Department of Mathematics, University of Utah, Salt Lake City, Utah, USA, 1997.

[61] D.J. Eyre, Unconditionally gradient stable time marching the Cahn–Hilliard equation, Mater. Res. Soc. Symp. Proceedings, Vol. 529, J.W. Bullard, L.Q. Chen, R.K. Kalia, and A.M. Stoneham, eds., Cambridge University Press, 39–46, 1998.

[62] D.J. Eyre, Systems of Cahn-Hilliard equations, SIAM J. Appl. Math. 53 (1993), 1686–1712.

[63] H. Fakih, Asymptotic behavior of a generalized Cahn-Hilliard equation with a mass source, Applicable Analysis, to appear.

[64] H. Fakih, A Cahn–Hilliard equation with a proliferation term for biological and chemical applications, Asymptotic Analysis 94 (2015), 71–104.

[65] P.C. Fife, Models for phase separation and their mathematics, Electronic J. of Differential Equations 48 (2000), 1–26.

[66] R.A. Fisher, The wave of advance of advantageous genes, Annals of Eugenics 7 (1937), 355–369.

[67] FreeFem++ is freely avalaible at *http ://www.freefem.org/ff++*.

[68] S. Frigeri and M. Grasselli, Nonlocal Cahn–Hilliard–Navier–Stokes systems with singular potentials, Dyn. PDE 9 (2012), 273–304.

[69] C.G. Gal, A Cahn–Hilliard model in bounded domains with permeable walls, Math. Methods Appl. Sci. 29 (2006), 2009–2036.

[70] H. Gajewski and K. Zacharias, On a nonlocal phase separation model, J. Math. Anal. Appl. 286 (2003), 11–31.

[71] J. García-Ojalvo, A.M. Lacasta, J.M. Sancho, and R. Toral, Phase separation driven by external fluctuations, Europhysics Letters 42 (1998), 125.

[72] H. Garcke, B. Nestler, and B. Stoth, On anisotropic order parameter models for multiphase systems and their sharp interface limits, Phys. D 115 (1998), 87–108.

[73] S. Geman and D. Geman, stochastic Relaxation Gibbs distrubition, and the Bayesian Restoration of image, IEEE Transactions patt. Anal. band Machine Intell. 20 (1984), 721–741.

[74] G. Giacomin and J.L. Lebowitz, Phase segregation dynamics in particle systems with long range interaction I. Macroscopic limits, J. Statist. Phys. 87 (1997), 37–61.

[75] G. Giacomin and J.L. Lebowitz, Phase segregation dynamics in particle systems with long range interaction II. Interface motion, SIAM J. Appl. Math. 58 (1998), 1707–1729.

[76] G. Gianni, A. Miranville, and G. Schimperna, On the Cahn-Hilliard equation with irregular potentials and dynamic boundary conditions, Commun. Pure Appl. Anal. 8 (2009), 881–912.

[77] A. Gillette, Image inpainting using a modified Cahn-Hilliard equation, PhD thesis, University of California, Los Angeles, 2006.

[78] E. De Giorgi, Some remarks on Gamma-convergence and least squares methods, in Proceedings of Composite Media and Homogenization Theory, G. Dal Maso and G.F Dell Antonion eds., Birkhauser, 135–142, 1991.

[79] K. Glasner, A diffuse interface approach to Hele-Shaw flow, Nonlinearity 16 (2003), 49–66.

[80] M. Grasselli and M. Pierre, A splitting method for the Cahn–Hilliard equation with inertial term, Math. Models Methods Appl. Sci. 20 (2010), 1–28.

[81] H. Grossauer and O. Scherzer, Using the Complex Ginzburg–Landau Equation for Digital Inpainting in $2D$ and $3D$, Scale Space Methods in Computer Vision, Lecture Notes in Computer Science 2695 (2003), 225–236.

[82] H. Grossauer, A combined pde and texture synthesis approach to inpainting, In Computer Vision-ECCV, Springer Berlin Heidelberg, 214–224, 2004.

[83] J.W. Gu, L. Zhang, G.Q. Yu, Y.X. Xing, and Z.Q. Chen, X-ray CT metal artifacts reduction through curvature based sinogram inpainting, J. of X-Ray Sci. and Technol. 14 (2006), 73–82.

[84] F. Hecht, New development in FreeFem++, J. Numer. Math. 20 (2012), 251–265.

[85] J. Hilliard, Spinodal decomposition, Phase transformations, edited by H. I. Aronson (American Society for Metals, Metals Park, Ohio), 18 (1970), 497–560.

[86] S. Injrou and M. Pierre, Stable discretizations of the Cahn–Hilliard–Gurtin equations, Discrete Cont. Dyn. Systems 22 (2008), 1065–1080.

[87] D. Jeong, Y. Li, H.G. Lee, and J.S. Kim, Fast and automatic inpainting of binary images using a phase-field model, J. KSIAM 13 (2009), 225–236.

[88] E. Khain and L.M. Sander, A generalized Cahn–Hilliard equation for biological applications, Phys. Rev. E 77 (2008), 051129.

[89] D. King, The Commissar vanishes, Henry Holt and Company, 1997.

[90] S. Kirkpatrick, C.D. Gellatt, and M.P. Vecchi, Optimization by simulated annealing, IBM Thomas J. Watson Research Center, Yorktown Heights, NY, 1982.

[91] I. Klapper and J. Dockery, Role of cohesion in the material description of biofilms, Phys. Rev. E 74 (2006), 0319021.

[92] R.V. Kohn and F. Otto, Upper bounds for coarsening rates, Commun. Math. Phys. 229 (2002), 375–395.

[93] A.C. Kokaram, Motion Picture Restoration : Digital Algorithms for Artefact Suppression in Degraded Motion Picture Film and Video, Springer Verlag, 1998.

[94] A.C. Kokaram, R.D. Morris, W.J. Fitzgerald, and P.J.W. Rayner, Interpolation of missing data in image sequences II, IEEE Trans. Image Process. 11 (1995), 1509–1519.

[95] L.D. Landau and I.M. Khalatnikov, On the theory of superconductivity, Collected Papers of L.D. Landau (ed. D. Ter Haar) Pergamon, Oxford, 546–568, 1965.

[96] J.S. Langer, Theory of spinodal decomposition in alloys, Ann. Phys. 65 (1975), 53–86.

[97] D. Li and C. Zhong, Global attractor for the Cahn–Hilliard system with fast growing nonlinearity, J. Diff. Eqns. 149 (1998), 191–210.

[98] Q.-X. Liu, A. Doelman, V. Rottschäfer, M. de Jager, P.M.J. Herman, M. Rietkerk and J. van de Koppel, Phase separation explains a new class of self-organized spatial patterns in ecological systems, Proceedings Nation. Acad. Sci., available online at http ://www.pnas.org/cgi/doi/10.1073/pnas.1222339110.

[99] S. Maier-Paape and T. Wanner, Spinodal decomposition for the Cahn–Hilliard equation in higher dimensions. Part I : Probability and wavelength estimate, Commun. Math. Phys. 195 (1998), 435–464.

[100] S. Maier-Paape and T. Wanner, Spinodal decomposition for the Cahn–Hilliard equation in higher dimensions : Nonlinear dynamics, Arch. Ration. Mech. Anal. 151 (2000), 187–219.

[101] S. Masnou and J.M. Morel, Level lines based disocclution, in Proceedings of the 5th IEEE International Conference on Image Processing, Vol. 3, 259-263, 1998.

[102] S. Melchionna and E. Rocca, On a nonlocal Cahn–Hilliard equation with a reaction term, Adv. Math. Sci. Appl. 24 (2014), 461–497..

[103] A. Miranville, Asymptotic behavior of the Cahn–Hilliard–Oono equation, J. Appl. Anal. Comp. 1 (2011), 523–536.

[104] A. Miranville, Asymptotic behavior of a generalized Cahn–Hilliard equation with a proliferation term, Appl. Anal. 92 (2013), 1308–1321.

[105] A. Miranville, A generalized Cahn-Hilliard equation with logarithmic potentials, in Continuous and Distributed Systems II, Springer, 137–148, 2015

[106] A. Miranville and A. Rougirel, Local and asymptotic analysis of the flow generated by the Cahn–Hilliard–Gurtin equations, Zeitschrift für angewandte Mathematik und Physik ZAMP, 57(2006), 244–268.

[107] A. Miranville and S. Zelik, Robust exponential attractors for Cahn–Hilliard type equations with singular potentials, Math. Methods Appl. Sci. 27 (2004), 545–582.

[108] A. Miranville and S. Zelik, Attractors for dissipative partial differential equations in bounded and unbounded domains, in Handbook of Differential Equations, Evolutionary Partial Differential Equations, Vol. 4, C.M. Dafermos and M. Pokorny, eds., Elsevier, Amsterdam, 103–200, 2008.

[109] A. Miranville and S. Zelik, The Cahn–Hilliard equation with singular potentials and dynamic boundary conditions, Discrete Cont. Dyn. Systems 28 (2010), 275–310.

[110] A. Miranville and S. Zelik, Exponential attractors for the Cahn–Hilliard equation with dynamic boundary conditions, Math. Methods Appl. Sci. 28 (2005), 709–735.

[111] D. Mumford and J. Shah, Optimal approximations by piecewise smooth functions and associated variational problems, Commun. Pure Appl. Math. 42(1989), 577–685.

[112] L. Modica and S. Mortolla, Un esempio di Γ-convergenza, Boll, Un. Mat. B5 14 (1977), 285–299.

[113] B. Nicolaenko and B. Scheurer, Low-dimensional behavior of the pattern formation Cahn–Hilliard equation, in Trends in the theory and practice of nonlinear analysis, North-Holland Math. Stud., Vol. 110, North-Holland, Amsterdam, 1985.

[114] B. Nicolaenko, B. Scheurer, and R. Temam, Some global dynamical properties of a class of pattern formation equations, Commun. Diff. Eqns. 14 (1989), 245–297.

[115] M. Nitzberg, D. Mimford, and T. Shiota, Filtering, Segmentation, and Depth, Lecture Notes in Comput. Sci. 662, Springer-verlag, Berlin, 1993.

[116] A. Novick–Cohen, The Cahn–Hilliard equation : Mathematical and modeling perspectives, Adv. Math. Sci. Appl. 8 (1998), 965–985.

[117] A. Novick-Cohen, The Cahn–Hilliard equation, in Handbook of Differential Equations, Evolutionary Partial Differential Equations, Vol. 4, C.M. Dafermos and M. Pokorny eds., Elsevier, Amsterdam, 201–228, 2008.

[118] A. Novick-Cohen, On the viscous Cahn–Hilliard equation. Material instabilities in continuum mechanics (Edinburgh, 1985-1986), Oxford Sci. Publ., Oxford Univ. Press, 329–342, 1988.

[119] A. Novick-Cohen, L.A. Segel, Nonlinear aspects of the Cahn–Hilliard equation. Phys. D 10 (1984), 277–298.

[120] Y. Oono and S. Puri, Study of phase-separation dynamics by use of cell dynamical systems. I. Modeling, Physical Review A 38(1988), 434–453.

[121] Y. Oono and S. Puri, Study of phase-separation dynamics by use of cell dynamical systems. II. Two-dimensional demonstration, Physical Review A 38(1988), 1542-1565.

[122] Y. Oono and S. Puri, Computationally efficient modeling of ordering of quenched phases, Phys. Rev. Lett. 58 (1987), 836–839.

[123] A. Oron, S.H. Davis, and S.G. Bankoff, Long-scale evolution of thin liquid films, Rev. Mod. Phys. 69 (1997), 931–980.

[124] R. Pego, Front migration in the nonlinear Cahn–Hilliard equation, Proc. Roy. Soc. London Ser. A 422 (1989), 261–278.

[125] P. Perona and J. Malik, Scale-space and edge detection using anistropic diffusion, IEEE Trans. Pattern Anal. Mach. Intell. 12 (1990), 629–639.

[126] J. Prüss, R. Racke and S. Zheng, Maximal regularity and asymptotic behavior of solutions for the Cahn–Hilliard equation with dynamic boundary conditions, Ann. Mat. Pura Appl. 185 (2006), 627–648.

[127] R. Racke and S. Zheng, The Cahn–Hilliard equation with dynamic boundary conditions, Adv. Diff. Eqns. 8 (2003), 83–110.

[128] A. Rosenfled and M. Thurston, Edge and curve detection for visual scene analysis, IEEE Trans. Comput. 20 (1971), 562–569.

[129] L. Rudin, S. Osher, and E. Fatemi, Nonlinear total variation based noise removal algorithms, Phys. D 60 (1992), 259–268.

[130] L. Rudin and S. Osher, Total variation based image restoration with free local constraints, in Proceedings 1st IEEE ICIP, Vol 1, 259–268, 1994.

[131] C.-B. Schönlieb and A. Bertozzi, Unconditionally stable schemes for higher order inpainting, Commun. Math. Sci. 9 (2011), 413–457.

[132] B. Saoud, Attracteurs pour des systèmes dissipatifs non autonomes, PhD thesis, Université de Poitiers, 2011.

[133] J.E. Taylor and J.W. Cahn, Linking anisotropic sharp and diffuse surface motion laws via gradient flows, J. Statist. Phys. 77 (1994), 183–197.

[134] R. Temam, Navier-Stokes Equations, North-Holland publishing company, Ansterdam, second edition, 1986.

[135] R. Temam, Navier-Stokes equations : theory and numerical analysis, Vol. 343, American Mathematical Soc., 2001.

[136] R. Temam, Navier-Stokes equations and nonlinear functional analysis, Vol. 66, Siam, 1995.

[137] R. Temam, Infinite-Dimensional Dynamical Systems in Mechanics and Physics, 2nd ed., Springer-Verlag, New York, 1997.

[138] U. Thiele and E. Knobloch, Thin liquid films on a slightly inclined heated plate, Phys. D 190 (2004), 213–248.

[139] S. Tremaine, On the origin of irregular structure in Saturn's rings, Astron. J. 125 (2003), 894–901.

[140] A. Tsai, J.A. Yezzi, and A.S. Willsky, Curve evolution implementation of the Mumford–Shah functional for image segmentation, denoising, interpolation, and magnification, Trans. Imag. Proc. 10 (2001), 1169–1186.

[141] J. Verdasca, P. Borckmans, and G. Dewel, Chemically frozen phase separation in an adsorbed layer, Phys. Review E 52 (1995), 4616–4619.

[142] B.P. Vollmayr-Lee and A.D. Rutenberg, Fast and accurate coarsening simulation with an unconditionally stable time step, Phys. Rev. E, 68 (2003).

[143] S. Villain-Guillot, Phases modulées et dynamique de Cahn–Hilliard, Habilitation thesis, Université Bordeaux 1, 2010.

[144] S. Walden, The Ravished Image : an introduction to the art of picture restoration and its risks, Gibson Square, London, 2004.

[145] Y. Wang, and Q.F. Zhu, Error control and concealment for video communication, Proc. IEEE, Vol. 86, 1998, 974–997.

[146] H. Wu and S. Zheng, Convergence to equilibrium for the Cahn–Hilliard equation with dynamic boundary conditions, J. Diff. Eqns. 204 (2004), 511–531.

[147] J. Wloka, Partialle Differential gleichunge, Teubner, Stuttgant, 1982.

[148] A. Yuille and T. Poggio, Scaling theorems for zero crossings, IEEE Trans. Pattern Anal. Mach. Intellig. 8 (1986), 15–25.

[149] E. Zeidler, Nonlinear Functional Analysis, Volume IIb. Springer, New york, 1988.